

## **SFR Site Investigation**

# **Evaluation of selected interference tests and pressure responses during drilling at SFR**

Ellen Walger, Jan-Erik Ludvigson, Bengt Gentschein  
Geosigma AB

October 2010

**Svensk Kärnbränslehantering AB**

Swedish Nuclear Fuel  
and Waste Management Co

Box 250, SE-101 24 Stockholm  
Phone +46 8 459 84 00



## **SFR Site Investigation**

# **Evaluation of selected interference tests and pressure responses during drilling at SFR**

Ellen Walger, Jan-Erik Ludvigson, Bengt Gentschein  
Geosigma AB

October 2010

*Keywords:* P-report SKBdoc 1263493, Review statement SKBdoc 1263499, HFR101, HFR102, HFR106, KFR102A, KFR105, KFR106, KFR27, Pumping test, Injection test, Hydraulic interference test, Hydraulic parameters, Response analysis, Drilling responses, AP SFR-10-008, Project SFR extension.

This report concerns a study which was conducted for SKB. The conclusions and viewpoints presented in the report are those of the authors. SKB may draw modified conclusions, based on additional literature sources and/or expert opinions.

Data in SKB's database can be changed for different reasons. Minor changes in SKB's database will not necessarily result in a revised report. Data revisions may also be presented as supplements, available at [www.skb.se](http://www.skb.se).

A pdf version of this document can be downloaded from [www.skb.se](http://www.skb.se).

# Abstract

In this activity, evaluation of selected hydraulic interference tests and drilling activities within the SFR area performed during 2008–2010 has been made. During the selected interference tests, pumping (or injection) was carried out in boreholes KFR105, HFR101 (both pumping and injection) and HFR102 during the time period from May, 2008 to March, 2010. Groundwater head measurements were performed in all existing SFR-boreholes at the time of testing during the entire test periods as well as during different drilling periods of boreholes HFR102, KFR27, KFR102A, KFR105, HFR106 and KFR106.

The activity involves identification and evaluation of potential pressure responses in all instrumented SFR-boreholes from three interference tests and drilling of six boreholes. A fourth interference test (in HFR102), for which no responses were detected by the preliminary analysis, was also included for more detailed evaluation.

For the four interference test, quantitative evaluation of hydraulic parameters and response indices of the responding observation sections was made when possible. Finally, a resulting response matrix was prepared for the interference tests. The drilling responses were classified by diagnostic analysis and response index 1, which is based on the response time lag. The hydraulic diffusivity T/S of the responding observation sections was estimated from the response time lags during drilling. For the drilling responses, a response matrix based on the diagnostic analysis and probable depth of response was prepared as well as a resulting response matrix based on response index 1.

The pressure responses in the observation boreholes during the interference tests in KFR105 and HFR101 were generally rather slow and weak and in many cases significantly delayed, both at start and stop of pumping/injection respectively. According to the response analysis, the most distinct and fastest responses were found in borehole sections KFR104:1-2 during the interference pumping test in HFR101 and section KFR27:2 during the interference pumping test in KFR105.

A strong but more delayed response occurred in section KFR02:4 during the interference pumping test in HFR101. The weakest and most delayed responses occurred in sections KFR104:1-2 during the interference test in KFR105. Very delayed but relatively strong responses occurred in sections KFR104:3 and KFR02:2-3 during the interference pumping test in HFR101. No pressure responses were detected during the interference injection test in HFR102.

Transient evaluation was made for 27 responding observation sections during the interference tests in KFR105 and HFR101 by standard methods. The transmissivity of the observation sections ranged from  $c 5 \cdot 10^{-6}$  to  $5 \cdot 10^{-5}$  m<sup>2</sup>/s while the storativity ranged from  $c 2 \cdot 10^{-5}$  to  $2 \cdot 10^{-3}$ . These values represent an equivalent homogeneous medium and constitute average values for a large volume of rock within the influence area of the test. They may thus not be representative for the specific hydraulic connection between the pumping borehole and the observation sections. The estimated hydraulic diffusivity T/S is assumed to better reflect the hydraulic connection between the boreholes.

The estimated hydraulic diffusivity T/S of the observation sections ranged from  $c 0.01$  to  $0.5$  m<sup>2</sup>/s. The hydraulic diffusivity, estimated from the transient test evaluation and the response time lags respectively generally showed good agreement.

The drilling responses showed a few distinct responses but mostly weak and delayed responses. A total of 59 responses, strong enough to determine Index 1, were found during the 6 drilling activities.

## Sammanfattning

I denna aktivitet gjordes tolkning av utvalda hydrauliska interferenstester och borrhållaktiviteter i SFR-området som utfördes under 2008–2010. Under de utvalda interferenstesterna utfördes pumpning (eller injektion) i borrhålen KFR105, HFR101 (både pump- och injektionstester) och HFR102 under tidsperioden från maj 2008 till mars 2010. Grundvattentryckmätningar utfördes i alla existerande borrhål vid tiden för testningen under hela testperioderna såväl som under olika borrhållperioder för borrhålen HFR102, KFR27, KFR102A, KFR105, HFR106 och KFR106.

Aktiviteten omfattar identifiering och tolkning av potentiella tryckresponser i alla instrumenterade SFR-borrhål från tre interferenstester och borrhåll av sex borrhål. En fjärde interferenstest (i HFR102), för vilken inga responser upptäckts vid den preliminära analysen, inkluderades också för mer detaljerad tolkning.

För de fyra interferenstesterna gjordes kvantitativ tolkning av hydrauliska parametrar och responsindex för responderande observationssektioner om möjligt. Slutligen framtogs en resulterande responsmatrix för interferenstesterna. Borresponserna klassificerades genom diagnostisk analys och responsindex 1 som är baserad på responstiden. Den hydrauliska diffusiviteten  $T/S$  för de responderande observationssektionerna skattades från responstiden. För borresponserna framtogs en responsmatrix baserad på den diagnostiska analysen och förmodat djup för responserna och en resulterande responsmatrix baserad på responsindex 1.

Tryckresponserna i observationsborrhålen under interferenstesterna i KFR105 och HFR101 var vanligen ganska fördröjda och svaga och i många fall avsevärt fördröjda, både vid start och stopp av pumpningen/injektionen. Enligt responsanalysen fanns de mest distinkta och snabbaste responserna i borrhållssektionerna KFR104:1-2 under interferenspumpstesten i HFR101 och i sektion KFR27:2 under interferenspumpstesten i KFR105.

En stark men mer fördröjd respons skedde i sektion KFR02:4 under interferenspumpstesten i HFR101. De svagaste och mest fördröjda responserna skedde i KFR104:1-2 under interferenstesten i KFR105. Mycket fördröjda men relativt starka responser skedde i sektionerna KFR104:3 och KFR02:2-3 under interferenspumpstesten i HFR101. Inga tryckresponser upptäcktes under interferenstesten i HFR102.

Transient tolkning gjordes för 27 responderande observationssektioner under interferenstesterna i KFR105 och HFR101 med standardmetoder. Transmissiviteten för observationssektionerna varierade från ca  $5 \cdot 10^{-6}$  till  $5 \cdot 10^{-5}$   $\text{m}^2/\text{s}$  medan magasin-koefficienten varierade från ca  $2 \cdot 10^{-5}$  till  $2 \cdot 10^{-3}$ . Dessa värden representerar ett ekvivalent homogent medium och utgör medelvärden för en stor bergvolym inom influensområdet för testen. De behöver därför inte vara representativa för den specifika hydrauliska förbindelsen mellan pumpborrhålet och observationssektionerna. Den skattade hydrauliska diffusiviteten  $T/S$  antas bättre avspegla den hydrauliska förbindelsen mellan borrhålen.

Den skattade hydrauliska diffusiviteten för observationssektionerna varierade från ca 0.01 till 0.5  $\text{m}^2/\text{s}$ . Den hydrauliska diffusiviteten, skattad från den transienta testtolkningen och baserad på responstiden, visade vanligen god överensstämmelse.

Borresponserna visade några distinkta responser men för det mesta svaga och fördröjda responser. Totalt 59 responser, starka nog för att beräkna responsindex 1, detekterades under de 6 borrhållaktiviteterna.

# Contents

<b>1</b>	<b>Introduction</b>	7
<b>2</b>	<b>Objective and scope of work</b>	9
<b>3</b>	<b>Methodology and evaluation</b>	11
3.1	Hydraulic interference tests	11
3.1.1	Test evaluation	11
3.1.2	Response analysis and estimation of hydraulic diffusivity	12
3.2	Drilling responses	14
3.2.1	Evaluation of pressure responses	14
3.2.2	Response analysis and estimation of hydraulic diffusivity	14
<b>4</b>	<b>Evaluation of hydraulic interference tests</b>	15
4.1	Interference pumping test in KFR105	15
4.1.1	Test evaluation	15
4.1.2	Response analysis	17
4.2	Interference pumping test in HFR101	18
4.2.1	Test evaluation	18
4.2.2	Response analysis	20
4.3	Interference injection test in HFR101	20
4.3.1	Test evaluation	20
4.3.2	Response analysis	21
4.4	Interference injection test in HFR102	22
<b>5</b>	<b>Evaluation of drilling responses</b>	23
5.1	Percussion drilling of HFR102	23
5.2	Percussion drilling of HFR106	23
5.3	Core drilling of KFR27	24
5.4	Core drilling of KFR102A	24
5.5	Core drilling of KFR105	25
5.6	Core drilling of KFR106	25
<b>6</b>	<b>Summary of results</b>	27
6.1	Hydraulic interference tests	27
6.2	Drilling responses	32
6.2.1	Drilling responses	32
6.2.2	Response analysis	38
<b>7</b>	<b>References</b>	43
<b>Appendix 1</b>	Drawdown responses and spherical distance to all observation borehole sections in the interference tests.	45
<b>Appendix 2</b>	Linear plots of hydraulic head versus time for responding observation sections together with precipitation, barometric pressure and sea level data.	47
<b>Appendix 3</b>	Hydraulic interference test diagrams	57
<b>Appendix 4</b>	Response index 1 and spherical distance ( $r_s$ ) to all observation borehole sections during drilling	85
<b>Appendix 5</b>	Linear plots of hydraulic head versus time for responding sections during drilling together with precipitation, barometric pressure and sea level data.	91

# 1 Introduction

This document reports the results from analysis of selected hydraulic interference tests and drilling activities in the SFR area. The interference tests and drilling activities were performed previously. All of the work was carried out in accordance with activity plan AP SFR-10-008. In Table 1-1 controlling documents for performing this activity are listed. The activity plan and the method descriptions are SKB's internal controlling documents. The data obtained from the activity are reported to the Sicada database, where they are traceable by the activity plan number. A map of the investigation area at SFR with borehole locations is shown in Figure 1.

**Table 1-1. Controlling documents for performance of the activity.**

Activity plan	Number	Version
Utvärdering av interferenstester och borresponser i SFR	AP SFR-10-008	1.0
Method descriptions	Number	Version
Metodinstruktion för analys av injektions- och enhåls-pumptester	SKB MD 320.004	1.0
Metodbeskrivning för interferenstester	SKB MD 330.003	1.0

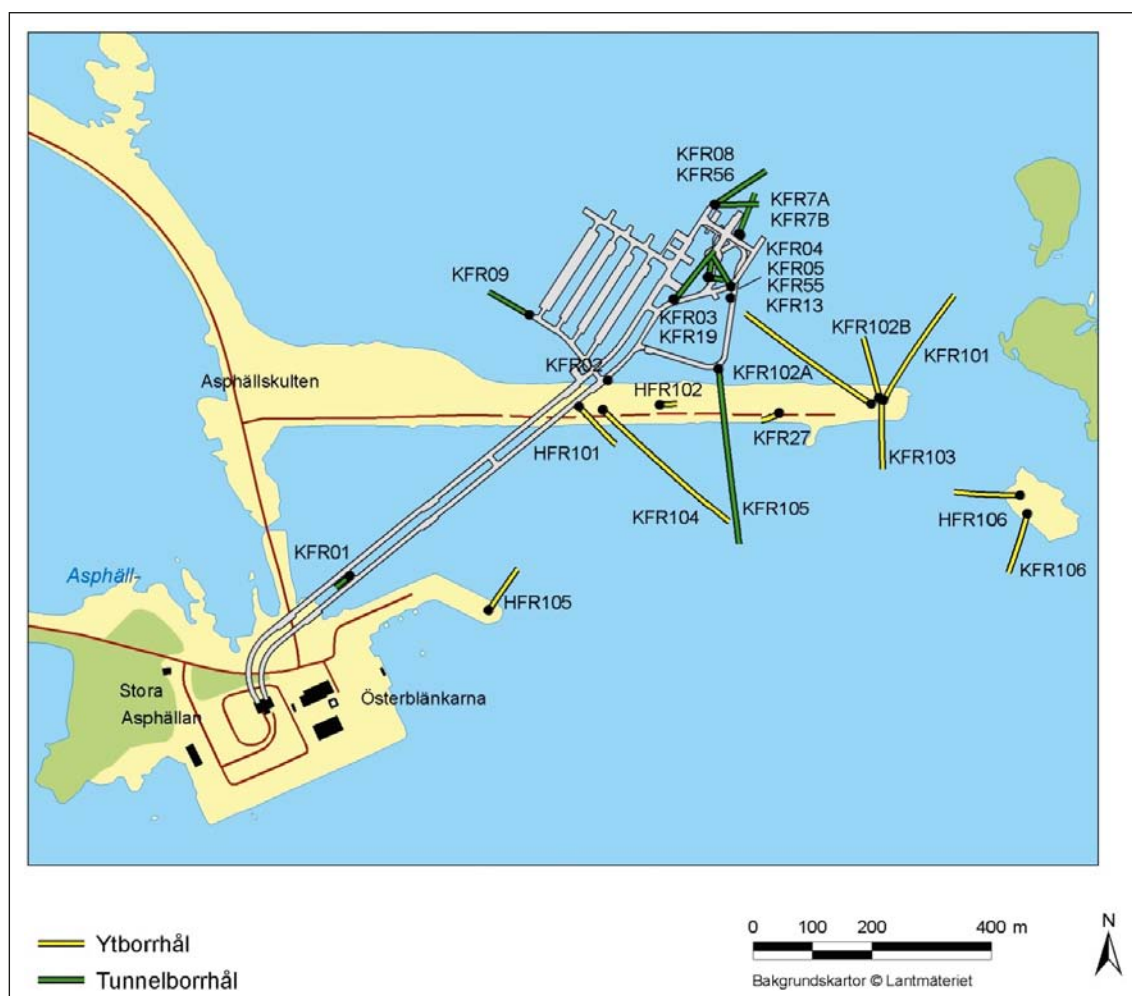


*Figure 1-1. The SFR area and the boreholes involved in the tests.*

## 2 Objective and scope of work

The primary objectives of this work were to identify and quantify pressure responses in boreholes during selected hydraulic interference test and drilling activities at SFR. A preliminary identification of pressure responses was made by SKB prior to this study, see Table 2-1.

According to the Activity Plan, the activity involves identification and evaluation of potential pressure responses in all instrumented SFR-boreholes from drilling of six boreholes and from 3 interference pumping/injection tests, see Table 2-1. A fourth interference test (in HFR102), for which no responses were detected by the preliminary analysis, was also included. Quantitative evaluation of hydraulic parameters and response indices should be made when possible. Finally, a resulting response matrix should be prepared for the interference tests and drilling activities respectively. Input data are collected from HMS, DMS and Sicada. If possible, official data deliveries from Sicada should be used.

The aim is to prepare input data to the description of mainly the interpreted deterministic hydraulic structures regarding their hydraulic and geometric properties. The tests may also provide information of the hydraulic properties of the rock blocks. In addition, interference tests also provide information of hydraulic connectivity and hydraulic boundary conditions of the tested area. Finally, the tests provide a basis for calibration of numerical models of the area.

Table 2-1. Preliminary identified pressure interferences by SKB. From AP SFR-10-008.

Disturbance (borehole section/activity)	Observation (borehole section/modelled HCD)																
	KFR02:4 (43–80 m)	KFR04:1-3 (28–101 m) (H2)	KFR05:2 (80–96) (H2)	KFR7B:1 (9–21 m) (H2)	KFR13:1-3 (4–77 m) (H2)	KFR55:3 (22–39 m) (2–4) (H2 mod i s1?)	KFR27:2 (47–109 m) (:1)	KFR27:3 (0–46 m)	HFR102:1 (28–55 m)	HFR106:1 (c. 50–209 m)	KFR101:1 (280–342 m)	KFR101:2 (91–279 m)	KFR102A:7-8 (0–184 m)	KFR102B:1-2 (128–180 m)	KFR103:1 (178–201 m)	KFR103:2 (79–177 m)	KFR104:2 (98–332 m) (1–3)
HFR102 Drilling, injection test																	
KFR27 193–198 m Drilling, loss of returned drilling water										Smaller than in :2		More direct response than the H2-holes					
KFR102A 207 m Drilling																	
KFR102A c 280 m Drilling																	
HFR101 Pumping																	
KFR105 133 m Drilling						May be a very weak response also in :1	Smaller and delayed com- pared to :2						Response delayed 1–2 d				Response delayed 3-4 d
HFR106 c 40 m Drilling																	
HFR106 c 104 m Drilling																	
HFR106 c 140 m Drilling																	
HFR106 177–181 m Drilling																	
KFR106 c 70 m Drilling																	
KFR106 c 155 m Drilling																	
KFR105 Opening all section simulta- neously 2010-03-03/04						May be a very weak response also in :1	Smaller and delayed com- pared to :2										? Uncertain



## 3 Methodology and evaluation

### 3.1 Hydraulic interference tests

#### 3.1.1 Test evaluation

##### *General*

Standard methods for constant flow rate interference tests in an equivalent porous medium were used for evaluation of the responses in the observation borehole sections in accordance with the methodology description for interference tests (SKB MD 330.003 v2.0) and for single-hole tests in the pumping borehole according to the Instruction for analysis of hydraulic injection and single-hole pumping tests (SKB MD 320.004 v.2.0).

The quantitative transient analysis was performed using the software AQTESOLV Pro v. 4.0 that enables both manual and automatic type curve matching. The transient evaluation was carried out as an iterative process of manual type curve matching and by employing automatic non-linear regression. The quantitative, transient interpretation of the hydraulic parameters of the observation sections (mainly transmissivity and storativity) is normally based on the identified pseudo-radial flow regime and associated flow regimes during the tests.

All pressure data from the observation boreholes presented in this report have, prior to evaluation, been corrected automatically in HMS for atmospheric pressure changes by subtracting the latter pressure from the measured (absolute) pressure. No other corrections of the measured drawdown due to e.g. precipitation, drought periods, tidal effects have been made.

##### *Observation boreholes*

In the primary diagnostic analysis, data from all observation borehole sections included in the interference tests were studied in linear pressure versus time (HMS)-diagrams to identify responding sections. Corresponding diagrams of air pressure, precipitation and sea water level fluctuations were also used in the diagnostic analysis. Diagnostic analysis of responses in linear diagrams was made for all core-drilled and percussion-drilled boreholes in rock in the SFR area, monitored in the HMS system.

The evaluation of the dominating transient flow regimes, i.e. pseudo-linear- (PLF), pseudo-radial- (PRF) and pseudo-spherical flow (PSF) and outer boundary conditions was mainly based on the drawdown responses in logarithmic diagrams. In particular, pseudo-radial flow is reflected by a constant (horizontal) derivative in such diagrams, whereas apparent no-flow- (NFB) and constant head boundaries (CHB) are characterized by a rapid increase and decrease of the derivative, respectively. Based on the diagnostic analysis, relevant models were selected for the transient evaluation of the responses.

In the transient evaluation, sections with clear responses were analysed with standard transient methods, mainly regarding transmissivity and storativity /Kruseman and de Ridder 1991/. In addition, the hydraulic diffusivity  $T/S$  of the observation sections was calculated from the tests. Observation borehole sections with a very weak and/or uncertain response were only analysed qualitatively. Such borehole sections are not included in the response analysis. The classification of responses in the observation borehole sections are presented in Table 3-1.

##### *Pumping/injection borehole*

The evaluation of the single-hole pumping test was made according to the instruction SKB MD 320.004. The transmissivity and the skin factor were obtained by type curve matching. The storativity,  $S$  [-] was estimated according to Equation 3-1 where the transmissivity,  $T$  has the unit [ $m^2/s$ ].

$$S=0.0007 \cdot T^{0.5} \qquad \text{Equation 3-1}$$

In addition to the transient analysis, interpretation of transmissivity based on the assumption of stationary conditions in the pumping borehole was performed.

The wellbore storage coefficient, CWBS (m<sup>3</sup>/Pa), in an isolated pumping/injection borehole section can be obtained by assuming a fictive casing radius, r(c) [m], in an equivalent open test system according to Equation 3-2.

$$C_{wBS} = \frac{\pi \cdot r(c)^2}{\rho \cdot g} \quad \text{Equation 3-2}$$

The radius of influence at a certain time during the test may be estimated from Jacob's approximation of the Theis' well function according to Equation 3-3.

$$r_i = \sqrt{\frac{2.25 \cdot T \cdot t}{S}} \quad \text{Equation 3-3}$$

Where r<sub>i</sub> [L] is the radius of influence at time t after start of pumping, usually at stop of pumping/injection.

Furthermore, r<sub>i</sub>-index (-1, 0 or 1) is defined to characterize the hydraulic conditions by the end of the test as shown below. It is assumed that a certain time interval of PRF can be identified between t<sub>1</sub> and t<sub>2</sub> during the tests.

- r<sub>i</sub>-index = 0: The transient response indicates that the size of the hydraulic feature tested is greater than the radius of influence based on the actual test time (t<sub>2</sub>=t<sub>p</sub>), i.e. the PRF is continuing at stop of the test. This fact is reflected by a flat derivative at this time.
- r<sub>i</sub>-index = 1: The transient response indicates that the hydraulic feature tested is connected to a hydraulic feature with lower transmissivity or an apparent barrier boundary (NFB). This fact is reflected by an increase of the derivative. The size of the hydraulic feature tested is estimated as the radius of influence based on t<sub>2</sub>.
- r<sub>i</sub>-index = -1: The transient response indicates that the hydraulic feature tested is connected to a hydraulic feature with higher transmissivity or an apparent constant head boundary (CHB). This fact is reflected by a decrease of the derivative. The size of the hydraulic feature tested is estimated as the radius of influence based on t<sub>2</sub>.

If a certain time interval of PRF cannot be identified during the test, the r<sub>i</sub>-indices -1 and 1 are defined as above. In such cases the radius of influence is estimated using the flow time t<sub>p</sub> in Equation 3-3 using a value of S estimated from Equation 3-1.

### 3.1.2 Response analysis and estimation of hydraulic diffusivity

In responding observation sections the response indices 1 and 2-new and the hydraulic diffusivity based on the estimated response time were calculated. The maximal drawdown, s<sub>p</sub>, occurred in several observation sections long times after stop of pumping/injection. The response time, dt<sub>L</sub>, is defined as the time lag after start of pumping/injection until a drawdown response of 0.1 m is observed in the actual observation section. This criterion was used both for calculating the response indices and estimating the hydraulic diffusivity.

The pumping flow rate, Q<sub>p</sub> [m<sup>3</sup>/s], was used in combination with the response time (dt<sub>L</sub>), spherical distance (r<sub>s</sub>) and maximal drawdown (s<sub>p</sub>) to calculate the response indices 1 and 2-new, which represent the speed of propagation and strength of the response, respectively which in turn are assumed to characterize the hydraulic connection between the pumping and the observed sections. Index 1 is directly related to the hydraulic diffusivity (T/S) of the formation. The spherical distance is calculated from the midpoints of the pumping borehole and the observation sections.

The response indices were calculated according to Equation 3-4 and Equation 3-5 as follows:

**Index 1** [m<sup>2</sup>/s]:

Normalised spherical distance ( $r_s$ ) with respect to the response time  $dt_L$  ( $s = 0.1$ m).

$$Index\ 1 = \frac{r_s^2}{dt_L} \quad \text{Equation 3-4}$$

**Index 2 new** [s/m<sup>2</sup>]:

Normalised maximal drawdown ( $s_p$ ) with respect to the pumping rate by the end of the flow period ( $Q_p$ ), also considering the distance ( $r_s$ ) assuming  $r_0=1$  m (fictive borehole radius).

$$Index\ 2\ new = \frac{s_p}{Q_p} \cdot \ln\left(\frac{r_s}{r_0}\right) \quad \text{Equation 3-5}$$

The classification of the response indices is given in Table 3-1 below.

The head data in the observation borehole sections are influenced by natural fluctuations of the groundwater level such as tidal effects, sea water level fluctuations and possibly, by long term trends. These background variations of pressure may sometimes make it difficult to deduce whether the observation sections are affected by the pumping/injection and if so, estimate the response time lag in the observation sections. The pressure changes due to tidal effects and other natural fluctuations are generally different for the observation boreholes and sections.

The calculation of the hydraulic diffusivity T/S from the lag times is based on radial flow according to /Streltsova 1988/ and may be estimated according to Equation 3-6.

$$\frac{T}{S} = \frac{r_s^2}{4 \cdot dt_L \cdot \left(1 + \frac{dt_L}{t_p}\right) \cdot \ln\left(1 + \frac{t_p}{dt_L}\right)} \quad \text{Equation 3-6}$$

The time lag  $dt_L$  is in this case defined as the time when the pressure response in an observation section is 0.1 m. The pumping time is included as  $t_p$ . The estimates of the hydraulic diffusivity from the lag times could be compared with the hydraulic diffusivity T/S from the transient evaluation of the observation sections.

**Table 3-1. Classification of response indices.**

	Limits	Classification	Colour code
Index 1 $r_s^2/dt_L$	$r_s^2/dt_L > 100$ m <sup>2</sup> /s	Excellent	Red
	$10 < r_s^2/dt_L \leq 100$ m <sup>2</sup> /s	High	Yellow
	$1 < r_s^2/dt_L \leq 10$ m <sup>2</sup> /s	Medium	Green
	$r_s^2/dt_L \leq 1$ m <sup>2</sup> /s	Low	Blue
	$s_p < 0.1$ m	No response	Grey
Index 2 new $s_p/Q_p \cdot \ln(r_s/r_0)$	$(s_p/Q_p) \cdot \ln(r_s/r_0) > 5 \cdot 10^5$ s/m <sup>2</sup>	Excellent	Red
	$5 \cdot 10^4 < (s_p/Q_p) \cdot \ln(r_s/r_0) \leq 5 \cdot 10^5$ s/m <sup>2</sup>	High	Yellow
	$5 \cdot 10^3 < (s_p/Q_p) \cdot \ln(r_s/r_0) \leq 5 \cdot 10^4$ s/m <sup>2</sup>	Medium	Green
	$(s_p/Q_p) \cdot \ln(r_s/r_0) \leq 5 \cdot 10^3$ s/m <sup>2</sup>	Low	Blue
	$s_p < 0.1$ m	No response	Grey

## 3.2 Drilling responses

### 3.2.1 Evaluation of pressure responses

In the diagnostic analysis, data from all observation borehole sections included in the drilling activities were studied in linear (HMS) pressure versus time diagrams to identify responding sections. Corresponding diagrams of precipitation, barometric pressure and sea level fluctuations were also used. Diagnostic analysis of responses in linear diagrams was made for all core-drilled and percussion-drilled boreholes in rock in the SFR area monitored in the HMS system. A qualitative classification of the strength of the responses in the observation sections was made.

Drilling may result in different responses as increasing, decreasing and fluctuating pressure variations in the surrounding boreholes, depending on where the transmitting fracture is located, at which depth the drilling has reached and how fast the response is.

When possible, the depth in the drilling borehole at which the response in the observation borehole started to show up is determined. Since the response often is delayed it is sometimes hard to decide exactly at which fracture and at which depth the response comes from. BIPS logging of the drilling boreholes has been used in order to identify possible fractures giving responses.

No pressure in the drilling borehole or depth of the drill bit has been automatically registered during drilling of the actual boreholes. Therefore, the position of the drill bit has been taken from the drilling log records. The information about loss of returned drilling water is also used in the evaluation.

The head data in the observation borehole sections are influenced by natural fluctuations of the groundwater level such as tidal effects, sea water level fluctuations and possibly and by long term trends. These background variations of pressure may sometimes make it difficult to deduce whether the observation sections are affected by the drilling and if so, estimate the response time lag in the observation sections. The pressure changes due to tidal effects and other natural fluctuations are generally different for the observation boreholes and sections.

The pressures in the observation boreholes are also influenced by other activities in the SFR area than the actual drilling. The Sicada system has been used in order to detect these disturbing activities but not all activities are recorded in the Sicada database.

All pressure data from the observation boreholes presented in this report have, prior to evaluation, been corrected automatically in HMS for atmospheric pressure changes by subtracting the latter pressure from the measured (absolute) pressure. No other corrections of the measured pressure due to e.g. precipitation, drought periods, tidal effects have been made.

### 3.2.2 Response analysis and estimation of hydraulic diffusivity

In responding observation sections the response index 1 and the hydraulic diffusivity based on the estimated response time were calculated according to Equation 3-4 and Equation 3-6. The classification of the response indices are made according to Table 3-1.

The response time,  $dt_L$ , is for the interference tests defined as the time lag after start of pumping/injection until a drawdown response of 0.1 m is observed in the actual observation section. However, for the drilling response analysis  $dt_L$  is defined as the time lag after start of the Nitrogen lifting (pumping) until a drawdown response of 0.1 m is observed in the actual observation section. When no nitrogen lifting was performed, either a pumping shortly after drilling or an opening of valve was used. During drilling of KFR105 a certain distinct fracture with a clear response was used for calculation the time lag until a drawdown response of 0.1 m is observed in the actual observation section after penetrating this fracture.

For the drilling activities,  $t_p$  is defined as the actual drilling period. The estimates of the hydraulic diffusivity according to Equation 3-6 should be seen as approximate. Because of disturbances, e.g. oscillating head or responses to other activities in the area it was sometimes difficult to determine the exact time lag for a drawdown of 0.1 m. The estimated time lag for some of the responding observation sections must therefore be regarded as rough estimates.

## 4 Evaluation of hydraulic interference tests

The location of the boreholes in the SFR area, including the pumping borehole KFR105, is shown in Figure 1-1. In Appendix 1, all observation sections included in the interference tests are listed together with the spherical distances to the actual pumping/injection borehole. Measurements of air pressure, precipitation and sea water level at SFR together with the observed groundwater head in the pumping boreholes and all responding observation borehole sections during the interference test periods are shown in linear (HMS)-diagrams in Appendix 2. In several of the observation sections the head showed an oscillating behaviour. This behaviour is caused by so called tidal fluctuations or earth tides in combination with changes in the sea water level. These phenomena have, to some extent, been investigated previously at Forsmark in /Ludvigson et al. 2004/. Transient evaluation was made in all responding observation sections with a drawdown response greater than 0.1 m. Test diagrams of the transient evaluation of the responding sections are shown in Appendix 3.

### 4.1 Interference pumping test in KFR105

#### 4.1.1 Test evaluation

The flow period of the interference pumping test in KFR105 lasted from 2010-03-03 10:05 to 2010-03-04 09:44. The test was performed by flowing all four borehole sections simultaneously. The duration of the flow period was 1,419 min. The total flow rate from the borehole sections was c 11.4 L/min by the end of the flow period. The pressure was measured in all borehole sections in the pumping borehole KFR105 and in surrounding boreholes. In KFR105 the drawdown varied between c 80–105 m in the different sections. The subsequent recovery period was also recorded in all borehole sections. The beginning of the recovery period was used to deduce if the actual observation section responded to the pumping in KFR105 or not in the diagnostic analysis, particularly in weakly responding sections.

The air pressure, precipitation and sea water level at SFR during the interference test period in KFR105 are shown in Figure A2-1 in Appendix 2. According to Figure A2-1, none or little precipitation occurred during the test period in KFR105. Linear diagrams of the groundwater head versus time (HMS diagrams) in all responding observation borehole sections are presented in Figures A2-3 to A2-7. A significant response was detected in borehole section KFR27:2 while weaker responses occurred in boreholes HFR102, KFR102A, KFR103 and KFR104.

However, there was a leakage between section 3 and 8 in KFR102A during the time of the test. Therefore these sections were hydraulically connected and the responses in these sections can not be separated.

Figure A2-5 indicates that the groundwater head in most sections in borehole KFR102A is strongly correlated to the sea water level at this time scale. However, a more detailed time scale is likely to reveal phase shifts between the head and sea water level, cf /Jönsson and Ludvigson 2004/. The same behaviour can be expected in other boreholes and also during the other interference tests.

In some observation sections located relatively close to the pumping borehole KFR105, e.g. in KFR27, a temporarily increasing head trend of c 0.1 m was observed shortly after start of pumping, see Figure 4-1. The reason to this effect is not known but it may have to do with the procedures at start of pumping in KFR105. However, the actual scan time interval for pressure in KFR105 at start of pumping was not sufficient to confirm this behaviour. The temporary head increase resulted initially in a negative drawdown in the observation sections, see Figure 4-2.

In the transient analysis of the responses in the observation sections, start of pumping ( $t=0$ ) and initial head ( $s=0$ ) is defined at the real start time of pumping and the actual head in the observation sections at this time, respectively. The initial head increase most likely also caused slightly delayed response times after start of pumping (at  $s=0.1$  m) in these sections (see below). However, the influence of this effect is considered to be negligible on the estimated hydraulic parameters from the transient evaluation and on the response analysis. The estimated response times were rather similar during the flow and recovery periods, respectively.

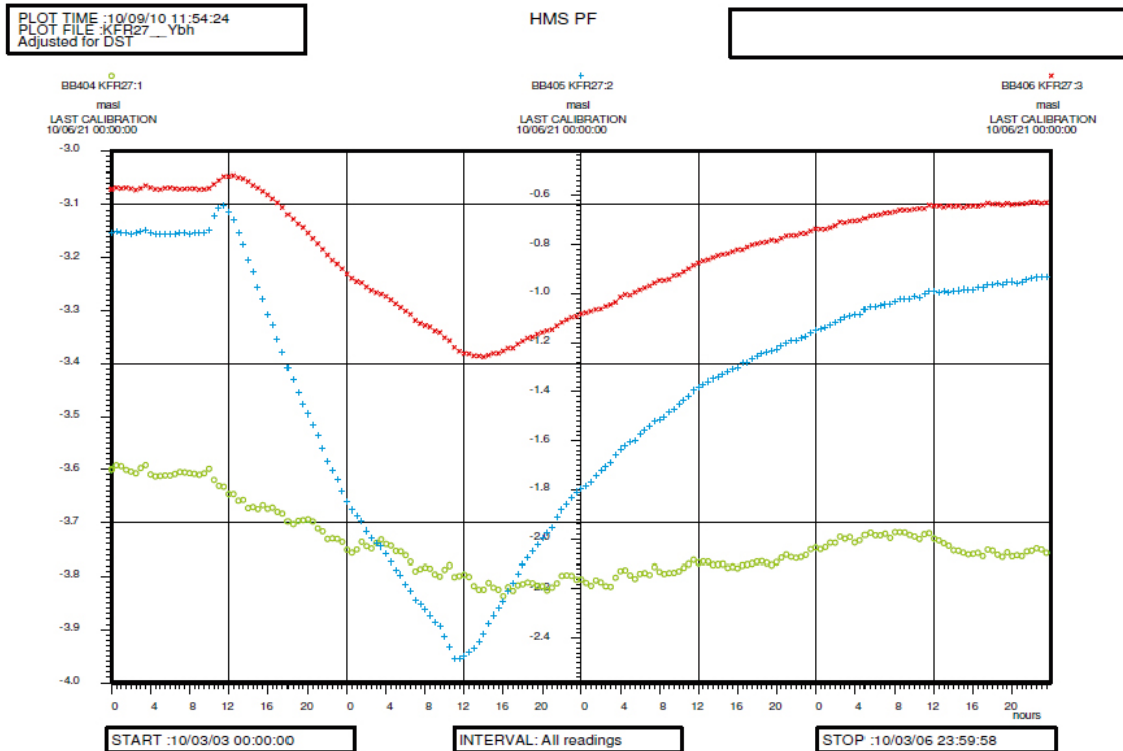


Figure 4-1. Linear plot of observed head versus time in the observation borehole KFR27 during the interference pumping test in KFR105.

Interference test in KFR105, observation borehole section KFR27:2

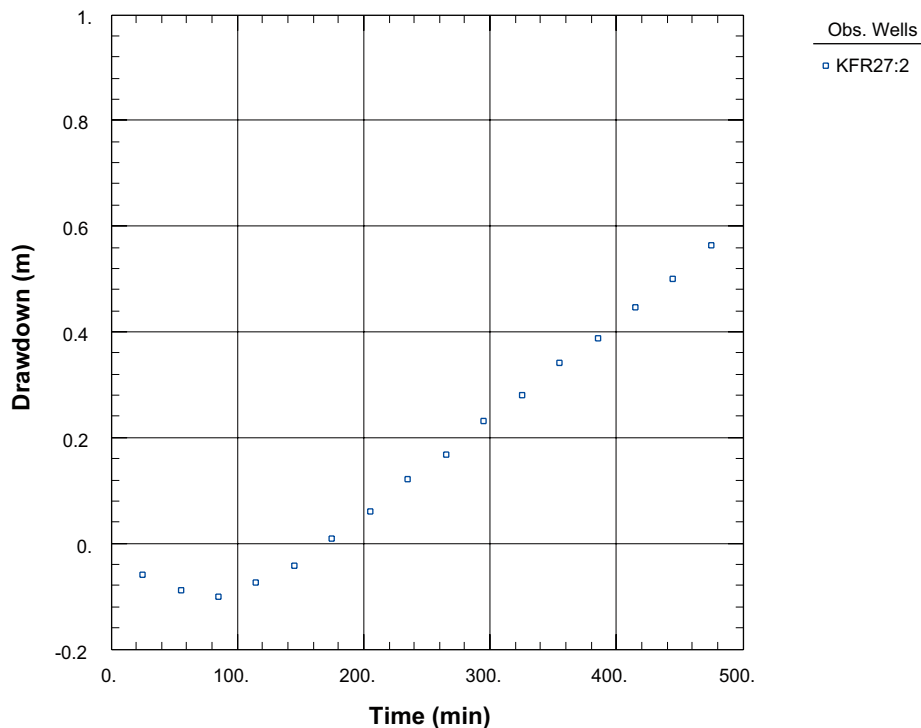


Figure 4-2. Example of early drawdown behaviour in observation borehole section KFR27:2 showing slightly negative drawdown after start of pumping in KFR105 due to a temporary head increase. The spherical distance from KFR105 to KFR27:2 is 128 m.

Another observation made during the interference test in KFR105 was the significantly delayed response times in most observation sections that occurred both after start and stop of pumping respectively. This fact caused that the pressure drawdown in most sections was still ongoing long times after stop of pumping until the maximal drawdown was reached. An example is shown in Figure 4-3. In this observation section, the maximal drawdown occurred at c 2,800 min after start of pumping which is more than 1,400 min (c 24 h) after stop of pumping. For this reason it was decided to perform the transient evaluation on the flow and recovery period in one sequence in this case. The delayed responses are assumed to reflect the (weak) hydraulic connection between the pumping borehole and the observation sections which, in turn, is assumed to correspond to the estimated hydraulic diffusivity (T/S) of the sections, cf Chapter 6.

Since the drawdown derivative indicated (transition to) pseudo-radial flow in most sections without any effects of apparent hydraulic boundaries, This method was used by the transient evaluation. As mentioned above, the flow and recovery period were analysed in one sequence. The estimated transmissivity T, storativity S and hydraulic diffusivity T/S of the observation sections are listed in Table 6-1 in Chapter 6. The estimated hydraulic diffusivity is assumed to reflect the hydraulic connection between the pumping borehole KFR105 and the observation sections.

#### 4.1.2 Response analysis

Response analysis was made for the interference test in KFR105 according to the method description for interference tests. All responding sections are included in the response analysis. The lag times ( $dt_L$ ) were derived from the response during the flow period at a drawdown of 0.1 m in the observation borehole sections. The drawdown  $s_p$  corresponds in this case to the maximal drawdown which generally occurred long time after stop of pumping as discussed above. The flow rate  $Q_p$  corresponds in this case to the final flow rate at stop of pumping. The estimated response parameters together with the numerical values of the response indices and their classification, as defined in Section 3.1.2, are presented in Table 6-1 in Chapter 6.

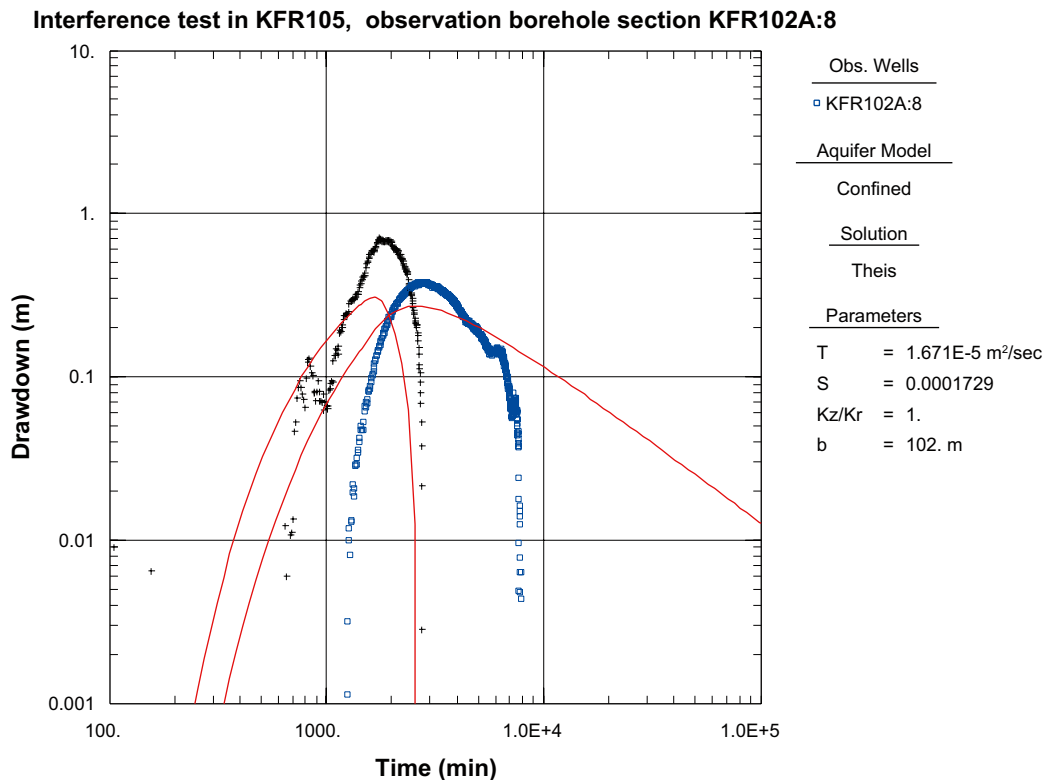


**Figure 4-3.** Log-log plot of drawdown (□) and drawdown derivative,  $ds/d(\ln t)$  (+), versus time in KFR102A:8 during the interference test in KFR105 showing the delay of the drawdown response after stop of pumping. The spherical distance to section KFR102A:8 from KFR105 is 199 m.

Due to the temporary increase of head after start of pumping, as discussed in the previous section, the estimated time lags in these sections will probably be slightly overestimated

(delayed) using the standard procedures for defining the initial head at the observation sections and time of start of pumping, respectively. An alternative procedure would be to redefine the initial head in these sections as the actual head value just before the onset of the real response due to pumping, while maintaining the actual start time for the pumping in KFR105. However, the latter approach has not been applied in this study.

Because of disturbances, e.g. oscillating head or responses to other activities in the area it was sometimes difficult to determine the exact time lag for a drawdown of 0.1 m. The estimated time lag for some of the responding observation sections during the interference tests must therefore be regarded as rough estimates.

The hydraulic diffusivity  $T/S$  of the responding observation sections was estimated from the response time lag  $dt_L$  according to Section 3.1.2. The estimated values of hydraulic diffusivity from the lag times are shown in Table 6-1. For comparison, the ratio of the estimated transmissivity and storativity,  $T_0/S_0$ , from the transient evaluation in these sections are also presented.

## **4.2 Interference pumping test in HFR101**

### **4.2.1 Test evaluation**

The flow period of the interference pumping test in HFR101 lasted from 2009-04-06 11:38 to 2009-04-09 12:51. The test was performed by pumping in the open borehole. The duration of the flow period was 4,393 min. The flow rate from the borehole varied in the beginning but stabilised at c 10 L/min by the end of the flow period. The pressure was measured in the pumping borehole HFR101 and in surrounding boreholes. In HFR101 the drawdown was c 15.6 m by the end of the flow period. The subsequent recovery period was also recorded in all borehole sections. The beginning of the recovery period was in some cases used to deduce if the actual observation section responded to the pumping in HFR101 or not in the diagnostic analysis, particularly in weakly responding sections.

In Appendix 1, all observation sections included in the interference pumping test in HFR101 are listed together with the spherical distances to the actual pumping/injection borehole. The air pressure, precipitation and sea water level at SFR during the interference test period in HFR101 are shown in Figure A2-8 in Appendix 2. Linear diagrams of the groundwater head versus time (HMS diagrams) in all responding observation borehole sections are presented in Figures A2-10 to A2-12. Significant responses were detected in boreholes KFR02 and KFR104. In borehole HFR105 weak responses are identified, see Figure A2-12. The head in the borehole sections seems to be well correlated to the sea water level on this time scale.

Transient evaluation was made in all responding observation sections with a drawdown response greater than 0.1 m. The test diagrams showing the transient evaluation for the responding sections are shown in Appendix 3.

As also was observed during the previous interference pumping test in KFR105, significantly delayed response times occurred in most observation sections after start and stop of pumping respectively. This fact caused that the pressure drawdown in most sections was still ongoing long times after stop of pumping until the maximal drawdown was reached. For this reason it was decided to analyse the flow and recovery period in one sequence by the transient evaluation. This behaviour is assumed to reflect the hydraulic connection between the pumping borehole and the observation sections which, in turn, is assumed to be reflected by the estimated hydraulic diffusivity ( $T/S$ ) of the sections.

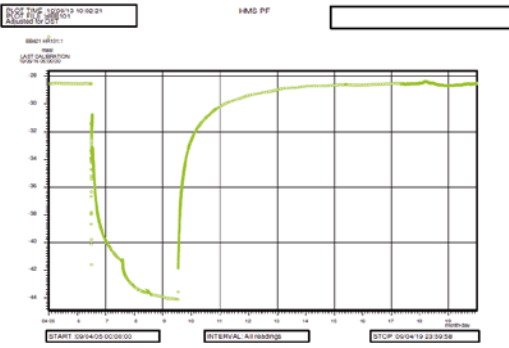
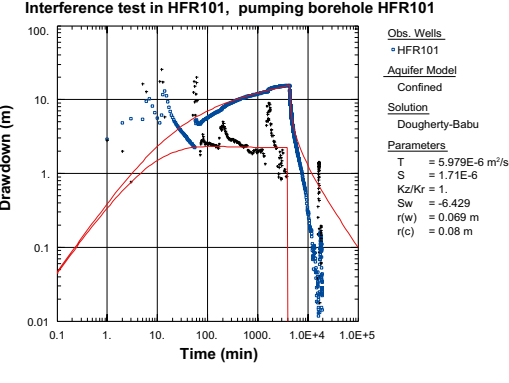
Since the drawdown derivative indicated (transition to) pseudo-radial flow in most sections without any effects of apparent no-flow boundaries, This method was used by the transient evaluation of the observation sections. The estimated transmissivity  $T$ , storativity  $S$  and hydraulic diffusivity  $T/S$  of the observation sections are listed in Table 6-1 in Chapter 6.



## Pumping borehole HFR101

An approximate transient evaluation was also made of the pressure in the pumping borehole HFR101 considering wellbore storage and skin. The response in the pumping borehole HFR101 during the flow period indicated approximate pseudo-radial flow without any effects of apparent NFB's. Test data from the pumping borehole HFR101 together with the estimated transmissivity and other parameters from HFR101 are shown in Table 4-1.

**Table 4-1. Test Summary Sheet for the pumping borehole HFR101.**

Test Summary Sheet – Pumping borehole HFR101			
Project:	SFR	Test type:	1B
Area:	Forsmark	Test no:	1
Borehole ID:	HFR101	Test start:	2009-04-06 11:38
Test section (m):	8.04–209.3	Responsible for test execution:	SKB field crew
Section diameter, 2·r <sub>w</sub> (m):	0.138	Responsible for test evaluation:	GEO SIGMA AB Jan-Erik Ludvigson
Linear plot Q and p		Flow period	
		Recovery period	
		Indata	
		p <sub>0</sub> (kPa)	
		h <sub>i</sub> (m)	–28.53
		h <sub>p</sub> (m)	–44.12
		Q <sub>p</sub> (m <sup>3</sup> /s)	1.67·10 <sup>–4</sup>
		t <sub>p</sub> (min)	4,393
		S* (–)	1.7·10 <sup>–6</sup>
		EC <sub>w</sub> (mS/m)	
		Te <sub>w</sub> (°C)	
		Derivative factor	0.1
		r (m)	
		Indata	
		h <sub>F</sub> (m)	–28.52
		t <sub>F</sub> (min)	
		S* (–)	
		Derivative fact.	
		r (m)	
Log-Log plot incl. derivatives- flow and recovery period		Results	
<p>Interference test in HFR101, pumping borehole HFR101</p>  <p>Obs. Wells = HFR101</p> <p>Aquifer Model Confined</p> <p>Solution Dougherty-Babu</p> <p>Parameters T = 5.979E-6 m<sup>2</sup>/sec S = 1.71E-6 Kz/Kr = 1. Sw = -6.429 r(w) = 0.069 m r(c) = 0.08 m</p>		Results	
		Q/s (m <sup>2</sup> /s)	1.1·10 <sup>–5</sup>
		T <sub>M</sub> (m <sup>2</sup> /s)	1.4·10 <sup>–5</sup>
		Flow regime:	→ PRF
		dt <sub>1</sub> (min)	
		dt <sub>2</sub> (min)	
		T (m <sup>2</sup> /s)	6.0·10 <sup>–6</sup>
		S (–)	
		K <sub>s</sub> (m/s)	
		S <sub>s</sub> (1/m)	
		C (m <sup>3</sup> /Pa)	2.1·10 <sup>–6</sup>
		C <sub>D</sub> (–)	
		x (–)	–6.4
		T <sub>GRF</sub> (m <sup>2</sup> /s)	
		S <sub>GRF</sub> (–)	
		D <sub>GRF</sub> (–)	
		Flow regime:	
		dt <sub>1</sub> (min)	
		dt <sub>2</sub> (min)	
		T (m <sup>2</sup> /s)	
		S (–)	
		K <sub>s</sub> (m/s)	
		S <sub>s</sub> (1/m)	
		C (m <sup>3</sup> /Pa)	
		C <sub>D</sub> (–)	
		x (–)	
		T <sub>GRF</sub> (m <sup>2</sup> /s)	
		S <sub>GRF</sub> (–)	
		D <sub>GRF</sub> (–)	
Selected representative parameters.			
dt <sub>1</sub> (min)		C (m <sup>3</sup> /Pa)	2.1·10 <sup>–6</sup>
dt <sub>2</sub> (min)		C <sub>D</sub> (–)	
T <sub>T</sub> (m <sup>2</sup> /s)		x (–)	–6.4
S* (–)			
K <sub>s</sub> (m/s)			
S <sub>s</sub> (1/m)			
Comments:			
The flow rate varied significantly in the beginning but was relatively constant during the later phase of the flow period.			
The flow and recovery period were analysed in one sequence. The early response can not be evaluated due to the varying flow rate but approximate pseudo-radial flow is assumed to occur by the end of the flow period.			

## 4.2.2 Response analysis

The response analysis was made according to the method description for interference tests for the interference pumping test in HFR101. All responding sections are included in the response analysis. The lag times ( $dt_L$ ) were derived from the response during the flow period at a drawdown of 0.1 m in the observation borehole sections. The drawdown  $s_p$  corresponds in this case to the maximal drawdown which generally occurred long time after stop of pumping as discussed above. The flow rate  $Q_p$  corresponds in this case to the final flow rate at stop of pumping. The estimated response parameters together with the numerical values of the response indices and their classification, as defined in Section 3.1.2, are presented in Table 6-1 in Chapter 6.

Because of disturbances, e.g. oscillating head or responses to other activities in the area it was sometimes difficult to determine the exact time lag for a drawdown of 0.1 m. The estimated time lag for some of the responding observation sections must therefore be regarded as rough estimates. The hydraulic diffusivity  $T/S$  of the responding observation sections was estimated from the response time lag  $dt_L$  according to Section 3.1.2. The estimated values of hydraulic diffusivity from the lag times are shown in Table 6-1. For comparison, the ratio of the estimated transmissivity and storativity,  $T_0/S_0$ , from the transient evaluation in these sections are also presented.

## 4.3 Interference injection test in HFR101

### 4.3.1 Test evaluation

A short interference test was made by injecting water in the open borehole HFR101. The flow (injection) period of the injection test in HFR101 lasted from 2008-05-23 09:53 to 2008-05-23 15:57. A decreasing pressure trend was ongoing in some boreholes before start of the injection test due to pumping and water sampling in HFR101 the day before the injection test, see /Jönsson et al. 2008/. The duration of the injection period was 364 min. The injection rate from the borehole decreased from c 32.2 L/min in the beginning but stabilised at c 22.4 L/min by the end of the injection period.

The pressure responses were measured in HFR101 and in surrounding boreholes. The results of the single-hole injection test in HFR101 are reported in /Jönsson et al. 2008/. In HFR101, the head increase was c 22.7 m by the end of the injection period. The subsequent recovery period was also recorded in the borehole sections. The beginning of the recovery period was in some cases used to deduce if the actual observation section responded to the injection in HFR101 or not in the diagnostic analysis, particularly in weakly responding sections.

However, in most sections in borehole KFR02, a long term increasing pressure trend was ongoing, probably due to re-installation of packers in this borehole starting at 2008-03-11, see Figure 4-4. The figure also shows that a clear effect of the injection test (and of the previous pumping test) in HFR101 is seen in section KFR02:4. Due to the ongoing, increasing pressure trend in KFR02 no recovery (pressure decrease) after the injection test is seen in the sections in KFR02. .

The air pressure, precipitation and sea water level at SFR during the interference test period in HFR101 are shown in Figure A2-13 in Appendix 2. Linear diagrams of the groundwater level versus time (HMS diagrams) in all responding observation borehole sections are also presented in Appendix 2. The test diagrams showing the transient evaluation for the responding sections are shown in Appendix 3.

In several of the observation sections the head showed an oscillating behaviour. This behaviour is caused by so called tidal fluctuations or earth tides in combination with changes in the sea water level. In Appendix 1, all observation sections included in the interference injection test in HFR101 are listed together with the spherical distances to the actual pumping/injection borehole.

Visual inspection of the pressure responses in the observation sections in the linear diagrams indicated that presumed response was only registered in borehole section KFR02:4, see Appendix A2-14. Sections KFR02:2-3 may also be slightly affected ( $< 0.1$  m) by the injection test. Transient evaluation of the pressure increase was made in observation sections with a response greater than 0.1 m. It should be noted that both the diagnostic test analysis, transient evaluation as well as the response analysis are uncertain in this case due to the ongoing natural pressure trends together with pressure trends from the previous pumping tests in HFR101 for water sampling.

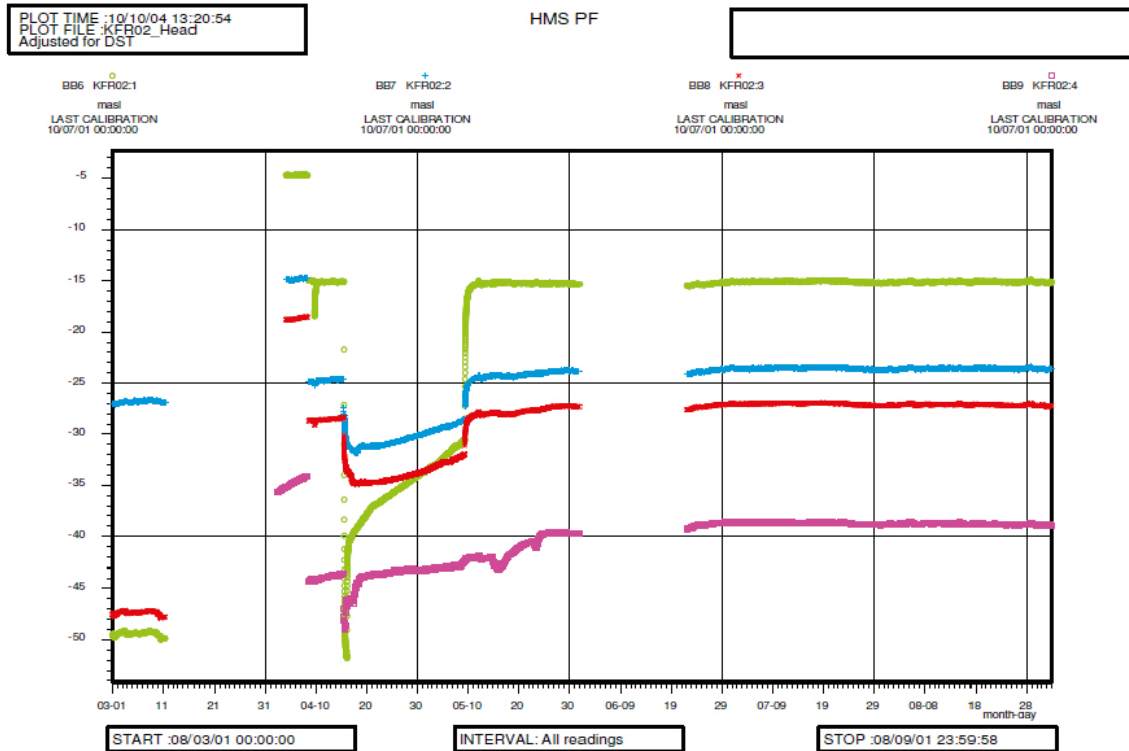


**Figure 4-4.** Linear plot of observed head versus time in the observation borehole KFR02 during the interference injection test in HFR101.

As was observed during the previous interference pumping tests in HFR101, the response time in the responding observation section(s) in KFR02 was rather delayed after start and stop of injection, respectively. As discussed above, the pressure still increased in most sections in KFR02 after stop of injection and then aligned with the long-term pressure trend. The transient evaluation of the responding section KFR02:4 was therefore based on the first c 1,000 min of the test in this case.

Since the drawdown derivative indicated (transition to) pseudo-radial flow in the responding section KFR02:4 without any effects of apparent hydraulic boundaries, Theis method was used by the transient evaluation. The estimated transmissivity  $T$ , storativity  $S$  and hydraulic diffusivity  $T/S$  of the observation sections are listed in Table 6-1 in Chapter 6.

### 4.3.2 Response analysis

The response analysis for the interference injection test in HFR101 was made according to the method description for interference tests. Only one observation section with a clear response to the injection in HFR101 was observed in this case. As for the previous interference tests, the lag time ( $dt_L$ ) was derived from the response during the flow period at a drawdown of 0.1 m in this observation section and the drawdown  $s_p$  corresponds to the maximal head increase which occurred long time after stop of injection. The flow rate  $Q_p$  corresponds to the final injection rate at stop of injection. The estimated response parameters together with the numerical values of the response indices and their classification, as defined in Section 3.1.2, are presented in Table 6-1 in Chapter 6.

The hydraulic diffusivity  $T/S$  of the responding observation sections was estimated from the response time lag  $dt_L$  according to Section 3.1.2. The estimated values of hydraulic diffusivity from the lag times are shown in Table 6-1. For comparison, the ratio of the estimated transmissivity and storativity,  $T_0/S_0$ , from the transient evaluation in these sections are also presented.

#### 4.4 Interference injection test in HFR102

A short interference test was made by injecting water in the open borehole HFR102. The flow period of the injection test in HFR102 lasted from 2008-05-28 13:20 to 2008-05-28 14:20, see /Jönsson et al. 2008/. The duration of the injection period was 60 min. The injection rate from the borehole was 4 L/min by the end of the injection period. In Appendix 1, all observation sections included in the interference injection test in HFR102 are listed together with the spherical distances to the injection borehole.

The pressure responses were measured in HFR102 and in surrounding boreholes. The results of the single-hole injection test in HFR102 are reported in /Jönsson et al. 2008/. In HFR102, the head increase was c 20 m by the end of the injection period. The subsequent recovery period was also recorded in the borehole sections. The beginning of the recovery period was used to deduce if the observation sections responded to the injection in HFR102, or not, in the diagnostic analysis.

The air pressure, precipitation and sea water level at SFR during the interference test period are shown in Figure A2-15. Visual inspection of the head versus time in the observation borehole sections in linear (HMS)-diagrams indicated that no presumed responses ( $>0.1$  m) to the injection test in HFR102 occurred in any of the observation borehole sections listed in Appendix 1. An example is shown in Figure A2-16 for borehole KFR02 which is assumed to be unaffected by the injection test. Thus, no response analysis or transient evaluations were made for the interference test in HFR102.

## 5 Evaluation of drilling responses

The location of the boreholes in the SFR area is shown in Figure 1. In Appendix 4, all observation sections included in the drilling activities are listed together with the spherical distances to the drilling borehole and Index 1. Measurements of air pressure, precipitation and sea water level at SFR together with the observed groundwater head in the responding observation borehole sections during the drilling periods are shown in linear (HMS)-diagrams in Appendix 5.

In several of the observation sections the head showed an oscillating behaviour. This behaviour is caused by so called tidal fluctuations or earth tides in combination with changes in the sea water level. These phenomena have, to some extent, been investigated previously at Forsmark in /Ludvigson et al. 2004/.

Because of disturbances, e.g. oscillating head or responses to other activities in the area it was sometimes difficult to determine the exact time lag for a drawdown of 0.1 m. The estimated time lag for some of the responding observation sections must therefore be regarded as rough estimates. The hydraulic diffusivity  $T/S$  of the responding observation sections was estimated from the response time lag  $dt_L$  according to Section 3.2.2. The estimated values of hydraulic diffusivity from the lag times together with Index 1 are shown in Table 6-10 to Table 6-14.

A qualitative classification of the strength of the responses in the observation sections was made and is presented in Table 6-9 below.

A response matrix of Index 1 for all 6 drillings in this report, including all observation sections investigated is shown in Table 6-15.

### 5.1 Percussion drilling of HFR102

The percussion drilling of HFR102 lasted from 2008-04-29 13:00 to 2008-05-05 15:00 down to the depth of 55.04 m.

No Nitrogen lifting was performed after the drilling.

No responses were detected in any core-drilled or percussion-drilled boreholes in rock in the SFR area monitored in the HMS system.

Since no responses were detected, no response analysis was made.

### 5.2 Percussion drilling of HFR106

The percussion drilling of HFR106 lasted from 2009-06-24 07:45 to 2009-07-02 10:00 and the drilling went down to 190.04 m.

No Nitrogen lifting was performed after the drilling.

In Table 6-3 below the responding sections from the drilling in HFR106 are shown together with information about the depth of the drilling as the response is seen from.

During 2009-06-23 14:26 to 2009-07-01 08:47 a pumping test was performed in KFR105. This pumping can be seen clearly in many observation sections and are not to be mistaken for a drilling response. However, for sections with weak responses these two activities are hard to separate.

KFR103:2 seems to start to respond to the drilling at ca 40 m. At 115 m of drilling a clear response is shown.

KFR103:1 starts to respond to the drilling at ca 92 m. At ca 140 m of drilling a clear response is shown.

Weaker responses occurred in boreholes KFR02, KFR13 and KFR102A. The response in KFR102A is however not strong enough to calculate a response index.

After drilling of HFR106, a pumping test was performed with pumping from 2009-07-07 09:53 to 2009-07-08 10:21. The time lag for this drilling activity was taken from the start of this pumping.

In Table 6-10 below the response parameters together with the estimated values of hydraulic diffusivity from the lag times of the responding sections to the drilling of HFR106 are shown.

### **5.3 Core drilling of KFR27**

The core drilling of KFR27 has been performed in three periods of time. The first one were already 1981-08-06–1981-09-10 down to 146.5 m. This period has not been evaluated in this report. The second and third drilling period were 2008-06-02 09:00–2008-06-10 11:00 down to 148.51 m and 2008-10-02 14:23–2008-10-22 16:51 down to 501.64 m.

The nitrogen lifting in the borehole KFR27 were performed at 2008-06-10 15:49–2008-06-12 15:21 and 2008-06-16 17:45–2008-06-16 17:51 after the second drilling period and 2008-10-27 13:50–2008-10-29 11:24 after the third drilling period.

HFR101 were used as flushing water well during the drilling of KFR27.

Between 2008-10-09 20:26 and 2008-10-09 22:50 a wire line pumping was carried out in KFR27.

After ca 193 m of drilling there was a total loss of returned drilling water.

In Table 6-4 below the responding sections from the drilling in KFR27 are shown together with information about from which depth of drilling as the response is seen from.

Significant responses were detected in borehole sections KFR101:1 and KFR101:2 while weaker responses occurred in boreholes KFR04, KFR05, KFR7B, KFR13 and KFR55.

During drilling of KFR27 some activities not listed in the Sicada database occurred in the SFR area, such as venting of KFR02. These activities are not to be mistaken as drilling responses.

The time lag for the observation sections of this drilling activity is calculated from the nitrogen lifting after the final drilling period of the borehole.

In Table 6-11 below the response parameters together with the estimated values of hydraulic diffusivity from the lag times of the responding sections to the drilling of KFR27 are shown.

For the more uncertain responses in this drilling activity the time lag is very uncertain because of the ongoing decreasing natural trend in the head and also because of the tidal effects during this time.

### **5.4 Core drilling of KFR102A**

The percussion drilling of KFR102A lasted from 2008-11-10 to 2008-11-17 and progressed to 70.42 m and the core drilling was performed from 2008-11-25 15:10 to 2008-12-10 04:57 to 600.83 m.

The nitrogen lifting was performed 2008-12-17 16:33 to 2008-12-18 11:32.

In Table 6-5 below the responding borehole sections from the drilling in KFR102A are shown together with information about from which depth of drilling as the response is seen from.

During 2008-11-23 07:41 and 2008-11-27 07:50 a pumping test was executed in KFR27. This test is seen in many observation boreholes but the recovery from this test starts before the end of the drilling.

Clear responses were detected in borehole section KFR101:1, KFR101:2, KFR102B:1 and KFR102B:2 while weaker responses occurred in boreholes KFR04, KFR05, KFR7B, KFR13, KFR55, KFR102B:3 and KFR103.

The time lag for the observation sections of this drilling activity is calculated from the nitrogen lifting.

In Table 6-12 below, the response parameters together with the estimated values of hydraulic diffusivity from the lag times of the responding sections to the drilling of KFR102A are shown.

## **5.5 Core drilling of KFR105**

There was no percussion drilling of KFR105. The core drilling was performed from 2009-04-21 00:00 to 2009-06-02 00:00 down to 306.81 m.

There was no Nitrogen lifting but the borehole was cleaned by an opening of valves during and after the drilling.

In Table 6-6 below the responding or possibly responding sections from the drilling in KFR105 are shown together with information about from which depth of the drilling the response is seen from.

Relatively strong responses were detected in borehole section KFR102A:3, KFR102A:7 and KFR102A:8 while weaker and more uncertain responses occurred in boreholes HFR101, HFR102, KFR27, KFR102A:4, KFR102A:5 KFR102A:6, KFR103 and KFR104.

In Table 6-13 below the response parameters together with the estimated values of hydraulic diffusivity from the lag times of the responding sections to the drilling of KFR105 are shown.

The time lags for this test are taken from a distinct transmitting fracture at 133 m.

## **5.6 Core drilling of KFR106**

The percussion drilling of KFR106 was drilled during 2009-06-23 and progressed to 9.13 m. The core drilling was performed from 2009-08-19 14:32 to 2009-09-03 01:16 down to 300.13 m.

Between 2009-09-14 11:50 and 2009-09-17 12:06 there was a nitrogen lifting in the drilling borehole KFR106.

In Table 6-7 below the responding borehole sections from the drilling in KFR106 are shown together with information about from which depth of drilling as the response is seen from.

Responses have been detected in observation boreholes HFR106, and KFR103 from the drilling of KFR106. In HFR106 a response was detected in section 1 and section 2, the weakest in section 2.

After drilling but before the nitrogen lifting the packers in HFR106 were removed and the entire borehole is therefore responding to the nitrogen lifting.

The time lag for the observation sections of this drilling activity is calculated from the nitrogen lifting.

In Table 6-14 below the response parameters together with the estimated values of hydraulic diffusivity from the lag times of the responding sections to the drilling of KFR106 are shown.

## 6 Summary of results

### 6.1 Hydraulic interference tests

The estimated transmissivity  $T$ , storativity  $S$  and hydraulic diffusivity  $T/S$  of the observation sections from the interference tests are listed in Table 6-1. In addition, the estimated response parameters from the interference tests together with the numerical values of the response indices and their classification, as defined in Section 3.1.2, are presented in Table 6-1.

Figure 6-1 shows a cross-plot of the estimated apparent transmissivity and storativity from transient evaluation of the responding sections from the interference pumping/injection tests in KFR105 and HFR101. Figure 6-2 shows a comparison of the estimated hydraulic diffusivity of the responding observation sections from the lag times and transient test evaluations, respectively from the interference pumping/injection tests in KFR105 and HFR101. Since the transient evaluation was based on an evaluation model for a homogeneous aquifer, the estimated hydraulic parameters represent average values for a large volume of rock within the influence area of the test in an equivalent homogeneous aquifer. Thus the parameter values may not represent the specific hydraulic connection between the pumping borehole and the observation sections. The estimated hydraulic diffusivity is assumed to better reflect the hydraulic connection between the pumping borehole and the observation sections.

The estimated transmissivity of observation sections assumed to have good hydraulic connection to the pumping borehole should be more representative of the actual pathway between these boreholes. In such cases the estimated transmissivity from the observation sections usually approach the estimated transmissivity of the sections from single-hole tests. Observation sections with potentially good hydraulic connection with the pumping borehole may be identified from the response analysis.

Figure 6-2 shows that there is a fair agreement between the estimated hydraulic diffusivity of the sections based on the response time lags and from the transient evaluation, respectively. This is also the case for observation sections at long distances from the pumping borehole. The estimated hydraulic diffusivity values from the response analysis are consistent with those from the transient evaluation.

Figure 6-3 shows a response diagram for the responding observation sections with  $\text{Log}(\text{Index } 2_{\text{new}})$  versus  $\text{Log}(\text{Index } 1)$  during the interference pumping/injection tests in KFR105 and HFR101. The basic idea with the response diagram is to group the responses according to their strength and time lag respectively. Observation sections represented by data points towards the upper right corner in the diagram generally indicate better connectivity to the pumping borehole and higher hydraulic diffusivities, whereas sections located towards the bottom left corner in the diagram generally represent sections with weak and delayed responses with presumed low connectivity to the pumping borehole.

According to Figure 6-3, the most distinct and fastest responses were found in borehole sections KFR104:1-2 during the interference pumping test in HFR101 and section KFR27:2 during the interference pumping test in KFR105. A strong but more delayed response occurred in section KFR02:4 during the interference pumping test in HFR101. The weakest and most delayed responses occurred in sections KFR104:1-2 during the interference test in KFR105. Very delayed but relatively strong responses occurred in sections KFR104:3 and KFR02:2-3 during the interference pumping test in HFR101. A response matrix of Index 1 and Index 2-new for all interference tests, including all observation sections investigated is shown in Table 6-2. The classification of the response indices is according to Table 3-1.



**Table 6-1. Summary of test data, response indices and estimated hydraulic parameters from the responding observations borehole sections during the interference tests in KFR105 and HFR101 in the SFR area.**

Pumping/ injection	Pumping/ injection test	Observation sektion	secup (m)	seclow (m)	Distance hi (m) (m)	hp (m)	dhp (m)	To (m <sup>2</sup> /s)	So	To/So	dtL (s)	T/S-lag time (m <sup>2</sup> /s)	Index 1 (m <sup>2</sup> /s)	Index 1-class	Index 2-new (s/m <sup>2</sup> )	Index 2-new- class	
KFR105	Pumping	KFR27:1	110.00	501.64	198.7	-3.60	-3.83	0.23	3.95·10 <sup>-05</sup>	1.83·10 <sup>-04</sup>	2.16·10 <sup>-01</sup>	36,000	1.59·10 <sup>-01</sup>	1.10	M	6.41·10 <sup>+03</sup>	M
KFR105	Pumping	KFR27:2	47.00	109.00	128.1	-0.74	-2.48	1.74	1.28·10 <sup>-05</sup>	4.48·10 <sup>-05</sup>	2.86·10 <sup>-01</sup>	13,500	1.32·10 <sup>-01</sup>	1.22	M	4.44·10 <sup>+04</sup>	M
KFR105	Pumping	KFR27:3	0.00	46.00	160.4	-0.57	-1.09	0.52	4.33·10 <sup>-05</sup>	1.47·10 <sup>-04</sup>	2.95·10 <sup>-01</sup>	39,600	9.66·10 <sup>-02</sup>	0.65	L	1.39·10 <sup>+04</sup>	M
KFR105	Pumping	HFR102:1	28.00	55.04	163.2	-1.23	-1.48	0.25	4.58·10 <sup>-05</sup>	3.23·10 <sup>-04</sup>	1.42·10 <sup>-01</sup>	75,000	6.22·10 <sup>-02</sup>	0.36	L	6.70·10 <sup>+03</sup>	M
KFR105	Pumping	KFR102A:8	0.00	102.00	198.7	-1.10	-1.48	0.38	1.67·10 <sup>-05</sup>	1.73·10 <sup>-04</sup>	9.65·10 <sup>-02</sup>	99,000	7.43·10 <sup>-02</sup>	0.40	L	1.06·10 <sup>+04</sup>	M
KFR105	Pumping	KFR102A:7	103.00	184.00	261.5	-1.23	-1.64	0.41	1.66·10 <sup>-05</sup>	8.81·10 <sup>-05</sup>	1.88·10 <sup>-01</sup>	88,800	1.40·10 <sup>-01</sup>	0.77	L	1.19·10 <sup>+04</sup>	M
KFR105	Pumping	KFR102A:6	185.00	213.00	225.8	-3.63	-3.86	0.23	3.15·10 <sup>-05</sup>	1.39·10 <sup>-04</sup>	2.27·10 <sup>-01</sup>	36,000	2.05·10 <sup>-01</sup>	1.42	M	6.56·10 <sup>+03</sup>	M
KFR105	Pumping	KFR102A:5	214.00	219.00	227.7	-3.70	-3.93	0.23	3.16·10 <sup>-05</sup>	1.48·10 <sup>-04</sup>	2.14·10 <sup>-01</sup>	42,300	1.86·10 <sup>-01</sup>	1.23	M	6.57·10 <sup>+03</sup>	M
KFR105	Pumping	KFR102A:4	220.00	254.00	231.7	-3.98	-4.21	0.23	3.01·10 <sup>-05</sup>	1.57·10 <sup>-04</sup>	1.92·10 <sup>-01</sup>	66,000	1.38·10 <sup>-01</sup>	0.81	L	6.59·10 <sup>+03</sup>	M
KFR105	Pumping	KFR102A:3	255.00	422.00	273.5	-5.02	-5.21	0.19	3.14·10 <sup>-05</sup>	1.44·10 <sup>-04</sup>	2.18·10 <sup>-01</sup>	87,000	1.56·10 <sup>-01</sup>	0.86	L	5.61·10 <sup>+03</sup>	M
KFR105	Pumping	KFR102A:2	423.00	443.00	335.9	-5.39	-5.52	0.13	3.34·10 <sup>-05</sup>	1.31·10 <sup>-04</sup>	2.55·10 <sup>-01</sup>	114,000	1.90·10 <sup>-01</sup>	0.99	L	3.98·10 <sup>+03</sup>	L
KFR105	Pumping	KFR102A:1	444.00	600.83	406.8	-5.17	-5.30	0.13	3.29·10 <sup>-05</sup>	8.98·10 <sup>-05</sup>	3.66·10 <sup>-01</sup>	114,000	2.78·10 <sup>-01</sup>	1.45	M	4.11·10 <sup>+03</sup>	L
KFR105	Pumping	KFR103:2	79.00	177.00	261.8	-0.52	-0.87	0.35	4.92·10 <sup>-05</sup>	9.38·10 <sup>-05</sup>	5.25·10 <sup>-01</sup>	60,000	1.90·10 <sup>-01</sup>	1.14	M	1.03·10 <sup>+04</sup>	M
KFR105	Pumping	KFR104:2	98.00	332.00	122.2	-15.13	-15.26	0.13	2.43·10 <sup>-05</sup>	1.35·10 <sup>-03</sup>	1.80·10 <sup>-02</sup>	162,000	1.88·10 <sup>-02</sup>	0.09	N	3.29·10 <sup>+03</sup>	L
KFR105	Pumping	KFR104:1	333.00	454.57	195.6	-14.28	-14.43	0.15	3.09·10 <sup>-05</sup>	6.59·10 <sup>-04</sup>	4.69·10 <sup>-02</sup>	324,000	2.63·10 <sup>-02</sup>	0.12	L	4.17·10 <sup>+03</sup>	L
HFR101	Pumping	KFR02:4	43.24	80.24	91.6	-40.65	-43.79	3.14	5.26·10 <sup>-06</sup>	1.42·10 <sup>-04</sup>	3.70·10 <sup>-02</sup>	27,600	2.92·10 <sup>-02</sup>	0.30	L	8.51·10 <sup>+04</sup>	H
HFR101	Pumping	KFR02:3	81.24	118.24	116.6	-28.36	-29.44	1.08	4.58·10 <sup>-06</sup>	3.71·10 <sup>-04</sup>	1.23·10 <sup>-02</sup>	114,000	1.74·10 <sup>-02</sup>	0.12	L	3.08·10 <sup>+04</sup>	M
HFR101	Pumping	KFR02:2	119.24	136.24	138.8	-24.94	-25.84	0.9	3.72·10 <sup>-06</sup>	3.04·10 <sup>-04</sup>	1.22·10 <sup>-02</sup>	120,000	2.37·10 <sup>-02</sup>	0.16	L	2.66·10 <sup>+04</sup>	M
HFR101	Pumping	KFR02:1	137.24	170.30	161.1	-16.09	-16.58	0.49	9.99·10 <sup>-06</sup>	4.63·10 <sup>-04</sup>	2.16·10 <sup>-02</sup>	90,000	3.93·10 <sup>-02</sup>	0.29	L	1.49·10 <sup>+04</sup>	M
HFR101	Pumping	KFR104:3	0.00	97.00	69.1	-3.39	-4.21	0.82	1.64·10 <sup>-05</sup>	8.58·10 <sup>-04</sup>	1.91·10 <sup>-02</sup>	90,000	7.23·10 <sup>-03</sup>	0.05	N	2.08·10 <sup>+04</sup>	M
HFR101	Pumping	KFR104:2	98.00	332.00	142.5	-13.69	-17.51	3.82	8.14·10 <sup>-06</sup>	2.73·10 <sup>-05</sup>	2.98·10 <sup>-01</sup>	4,200	2.86·10 <sup>-01</sup>	4.83	M	1.14·10 <sup>+05</sup>	H
HFR101	Pumping	KFR104:1	333.00	454.57	315.9	-13.44	-15.26	1.82	7.24·10 <sup>-06</sup>	2.06·10 <sup>-05</sup>	3.51·10 <sup>-01</sup>	28,800	3.37·10 <sup>-01</sup>	3.47	M	6.28·10 <sup>+04</sup>	H
HFR101	Pumping	HFR105:4	0.00	60.00	360.7	-6.02	-6.32	0.30	2.31·10 <sup>-05</sup>	1.30·10 <sup>-04</sup>	1.78·10 <sup>-01</sup>	105,000	1.76·10 <sup>-01</sup>	1.63	M	1.06·10 <sup>+04</sup>	M
HFR101	Pumping	HFR105:3	61.00	106.00	330.6	-6.38	-6.69	0.31	2.44·10 <sup>-05</sup>	1.52·10 <sup>-04</sup>	1.61·10 <sup>-01</sup>	105,000	1.48·10 <sup>-01</sup>	1.37	M	1.08·10 <sup>+04</sup>	M
HFR101	Pumping	HFR105:2	107.00	133.00	314.7	-6.38	-6.70	0.32	2.41·10 <sup>-05</sup>	1.59·10 <sup>-04</sup>	1.52·10 <sup>-01</sup>	105,000	1.34·10 <sup>-01</sup>	1.24	M	1.10·10 <sup>+04</sup>	M
HFR101	Pumping	HFR105:1	134.00	200.50	299.4	-10.96	-11.34	0.38	2.37·10 <sup>-05</sup>	1.54·10 <sup>-04</sup>	1.54·10 <sup>-01</sup>	102,000	1.24·10 <sup>-01</sup>	1.12	M	1.30·10 <sup>+04</sup>	M
HFR101	Injection	KFR02:4	43.24	80.24	91.6	-40.98	-42.23	1.25	3.70·10 <sup>-06</sup>	1.21·10 <sup>-04</sup>	3.06·10 <sup>-02</sup>	22,800	6.70·10 <sup>-02</sup>	0.37	L	1.51·10 <sup>+04</sup>	M

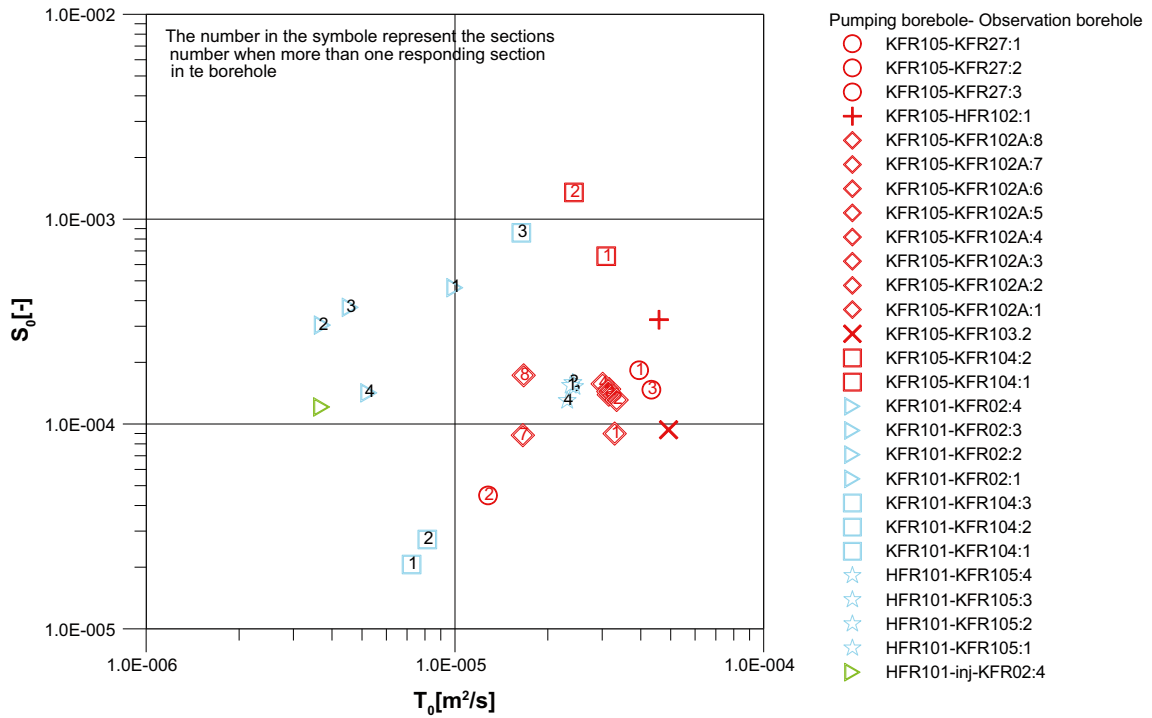


**Figure 6-1.** Estimated transmissivity and storativity from transient evaluation of the responding sections from the interference pumping/injection tests in KFR105 and HFR101. Different colours are used for the pumping boreholes and different symbols for the observation sections. The numbers refer to the section numbers.

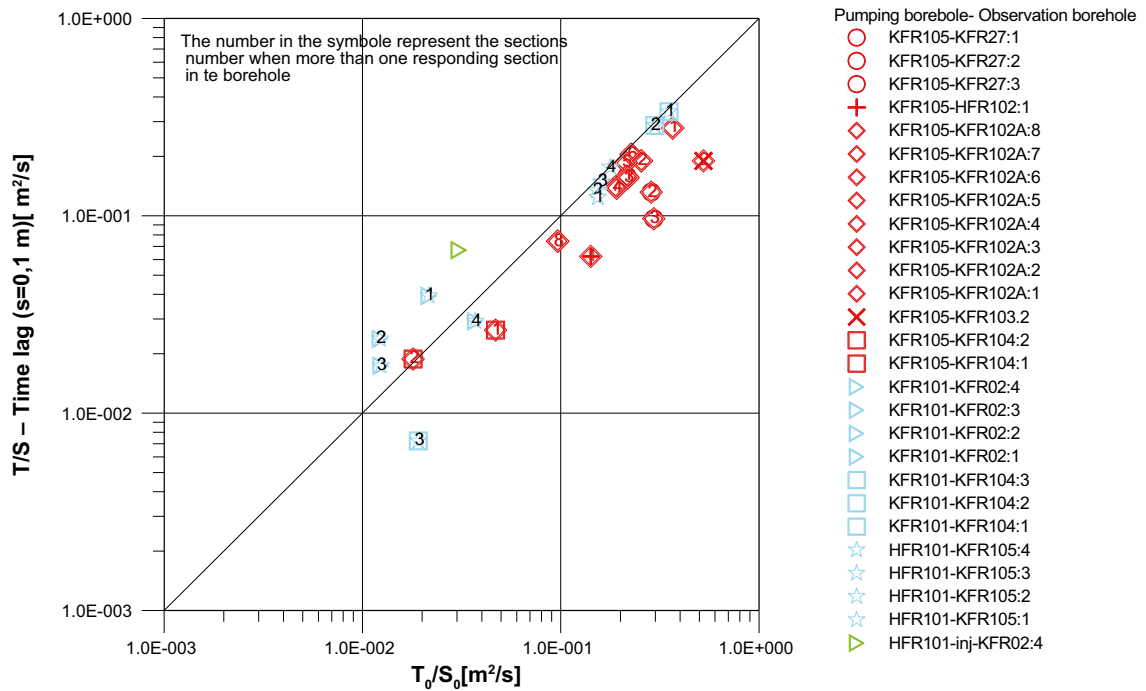


**Figure 6-2.** Comparison of estimated hydraulic diffusivity of the responding observation sections from the lag times and test evaluations, respectively, from the interference pumping/injection tests in KFR105 and HFR101. Different colours are used for the pumping boreholes and different symbols for the observation sections. The numbers refer to the section numbers.

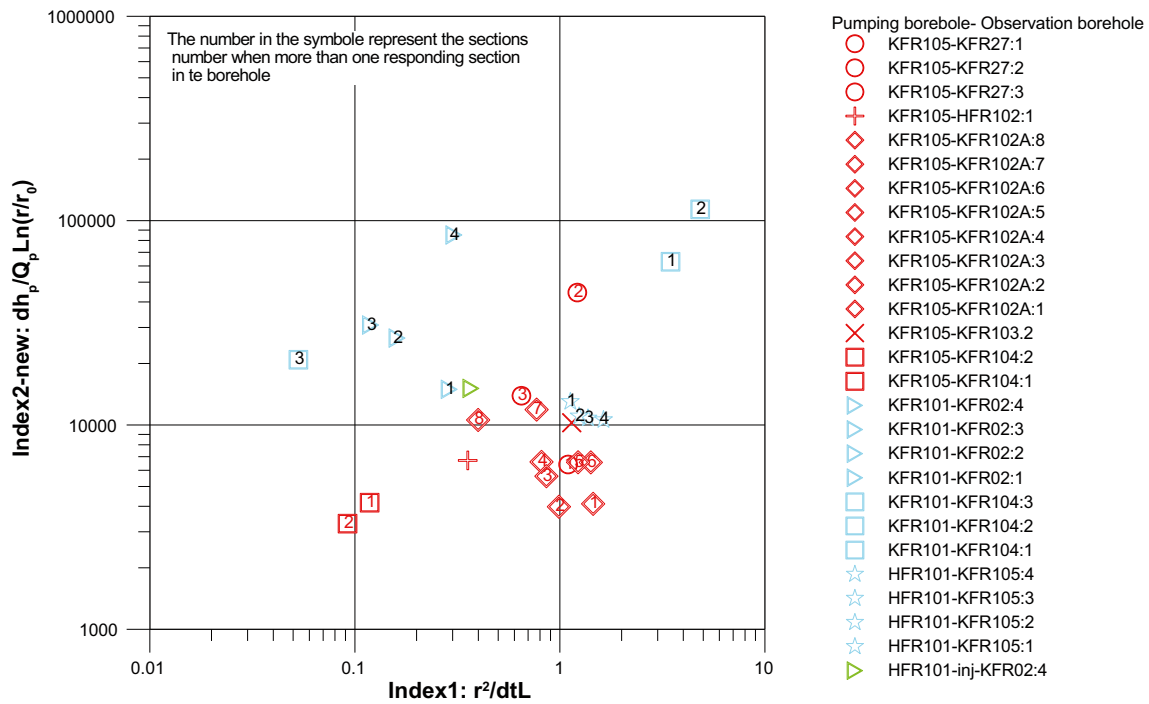


**Figure 6-3.** Response diagram showing responses in responding observation sections during the interference tests in KFR105, HFR101 (pumping test) and HFR101 (injection test). Response Index 2<sub>new</sub> is plotted versus Index 1. The classification of the two indices is shown in Table 3-1. The lag time is based on a drawdown of 0.1 m in the observation sections. Different colours are used for the pumping boreholes and different symbols for the observation sections. The numbers refer to the section numbers.

**Table 6-2. Response matrix with Index 1 and Index 2 new for the interference tests.**

Disturbance borehole	HFR101_inj		HFR101_pump		HFR102		KFR105	
	index 1	Index 2 new	index 1	Index 2 new	index 1	Index 2 new	index 1	Index 2 new
HFR101	Injection	Injection	Pumping	Pumping	No data	No data	N	N
HFR102	N	N	No data	No data	Injection	Injection	No data	No data
HFR102:1	No data	No data	N	N	Injection	Injection	L	M
HFR102:2	No data	No data	N	N	Injection	Injection	N	N
HFR105	N	N	No data	No data	N	N	No data	No data
HFR105:1	No data	No data	M	M	No data	No data	N	N
HFR105:2	No data	No data	M	M	No data	No data	N	N
HFR105:3	No data	No data	M	M	No data	No data	N	N
HFR105:4	No data	No data	M	M	No data	No data	N	N
HFR106:1	No data	No data	No data	No data	No data	No data	N	N
HFR106:2	No data	No data	No data	No data	No data	No data	N	N
HFR106:3	No data	No data	No data	No data	No data	No data	N	N
HFR106:4	No data	No data	No data	No data	No data	No data	N	N
KFR01:1	N	N	N	N	N	N	N	N
KFR01:2	N	N	N	N	N	N	N	N
KFR02:1	N	N	L	M	N	N	N	N
KFR02:2	N	N	L	M	N	N	N	N
KFR02:3	N	N	L	M	N	N	N	N
KFR02:4	L	M	L	H	N	N	N	N
KFR03:1	N	N	N	N	N	N	N	N
KFR03:2	N	N	N	N	N	N	N	N
KFR03:3	N	N	N	N	N	N	N	N
KFR03:4	N	N	N	N	N	N	N	N
KFR04:1	N	N	N	N	N	N	N	N
KFR04:2	N	N	N	N	N	N	N	N

Disturbance borehole	HFR101_inj		HFR101_pump		HFR102		KFR105	
	index 1	Index 2 new	index 1	Index 2 new	index 1	Index 2 new	index 1	Index 2 new
KFR04:3	N	N	N	N	N	N	N	N
KFR04:4	N	N	N	N	N	N	N	N
KFR05:1	N	N	N	N	N	N	N	N
KFR05:2	N	N	N	N	N	N	N	N
KFR05:3	N	N	N	N	N	N	N	N
KFR05:4	N	N	N	N	N	N	N	N
KFR7A:1	N	N	N	N	N	N	N	N
KFR7A:2	N	N	N	N	N	N	N	N
KFR7A:3	N	N	N	N	N	N	N	N
KFR7B:1	N	N	N	N	N	N	N	N
KFR7B:2	N	N	N	N	N	N	N	N
KFR08:1	N	N	N	N	N	N	N	N
KFR08:2	N	N	N	N	N	N	N	N
KFR08:3	N	N	N	N	No data	No data	N	N
KFR09:4	N	N	N	N	N	N	N	N
KFR13:1	N	N	N	N	N	N	N	N
KFR13:2	N	N	N	N	N	N	N	N
KFR13:3	N	N	N	N	N	N	N	N
KFR19:1	N	N	N	N	N	N	N	N
KFR19:2	N	N	N	N	N	N	N	N
KFR19:3	N	N	N	N	N	N	N	N
KFR19:4	N	N	N	N	N	N	N	N
KFR27:1	N	N	N	N	N	N	M	M
KFR27:2	N	N	N	N	No data	No data	M	M
KFR27:3	N	N	N	N	No data	No data	L	M
KFR55:1	N	N	N	N	N	N	N	N
KFR55:2	N	N	N	N	N	N	N	N
KFR55:3	N	N	N	N	N	N	N	N
KFR55:4	N	N	N	N	N	N	N	N
KFR56:1	N	N	N	N	N	N	N	N
KFR101:1	No data	No data	N	N	No data	No data	N	N
KFR101:2	No data	No data	N	N	No data	No data	N	N
KFR101:3	No data	No data	N	N	No data	No data	N	N
KFR102A:1	No data	No data	N	N	No data	No data	M	L
KFR102A:2	No data	No data	N	N	No data	No data	L	L
KFR102A:3*	No data	No data	N	N	No data	No data	L	M
KFR102A:4	No data	No data	N	N	No data	No data	L	M
KFR102A:5	No data	No data	N	N	No data	No data	M	M
KFR102A:6	No data	No data	N	N	No data	No data	M	M
KFR102A:7	No data	No data	N	N	No data	No data	L	M
KFR102A:8*	No data	No data	N	N	No data	No data	L	M
KFR102B:1	No data	No data	N	N	No data	No data	N	N
KFR102B:2	No data	No data	N	N	No data	No data	N	N
KFR102B:3	No data	No data	N	N	No data	No data	N	N
KFR103:1	No data	No data	N	N	No data	No data	N	N
KFR103:2	No data	No data	N	N	No data	No data	M	M
KFR103:3	No data	No data	N	N	No data	No data	N	N
KFR104:1	No data	No data	M	H	No data	No data	L	L
KFR104:2	No data	No data	M	H	No data	No data	N	L
KFR104:3	No data	No data	L	M	No data	No data	N	N
KFR105:1	No data	No data	No data	No data	No data	No data	Pumping	Pumping
KFR105:2	No data	No data	No data	No data	No data	No data	Pumping	Pumping
KFR105:3	No data	No data	No data	No data	No data	No data	Pumping	Pumping
KFR105:4	No data	No data	No data	No data	No data	No data	Pumping	Pumping
KFR105:5	No data	No data	No data	No data	No data	No data	Pumping	Pumping
KFR106:1	No data	No data	No data	No data	No data	No data	N	N
KFR106:2	No data	No data	No data	No data	No data	No data	N	N
KFR106:3	No data	No data	No data	No data	No data	No data	N	N

\* Sections 3 and 8 in KFR102A were hydraulically connected due to a leakage.

## 6.2 Drilling responses

In this section the results of the evaluation of the drilling activities are summarised.

### 6.2.1 Drilling responses

Table 6-3 shows the responding borehole sections during drilling of HFR106 together with information about distances and at which depth of drilling the response first appeared. Sections are only commented when appropriate otherwise it is left blank. In this table all detected responses are reported. There are however sections showing a weak response for which no response indices could be calculated (KFR102A:3, KFR102A:7 and KFR102A:8). These sections are reported in Table 6-3 and in the response matrix in Table 6-9 but not in Table 6-10 or Table 6-15.

**Table 6-3. Sections responding to the drilling of HFR106.**

BH-ID	Secup (m)	Seclow (m)	$r_s$ (m)	Response at depth (m)	Comments
KFR02:1	137.24	170.30	653.3	115	Weak response
KFR02:2	119.24	136.24	648.8	115	Weak response
KFR02:3	81.24	118.24	645.0	115	Weak response
KFR02:4	43.24	80.24	641.9	115	Weak response
KFR13:1	53.75	76.60	530.9	140	Weak response
KFR13:2	33.75	52.75	528.2	140	Weak response
KFR13:3	3.75	32.75	526.2	140	Weak response
KFR102A:3	255.00	422.00	416.1	115	Uncertain response
KFR102A:7	103.00	184.00	286.7	115	Uncertain response
KFR102A:8	0.00	102.00	258.1	115	Uncertain response
KFR103:1	178.00	200.50	161.7	92	Clear response
KFR103:2	79.00	177.00	173.6	40	Clear response

Table 6-4 shows the responding borehole sections to the drilling of KFR27 together with information about distances and at which depth of drilling the response first appeared.

**Table 6-4. Sections responding to the drilling of KFR27.**

BH-ID	Secup (m)	Seclow (m)	$r_s$ (m)	Response at depth (m)	Comments
KFR04:1	84.09	100.50	249.4	193	
KFR04:2	44.09	83.09	257.3	193	
KFR04:3	28.09	43.09	267.7	193	
KFR05:2	80.15	96.15	287.5	193	
KFR7B:1	8.60	21.10	317.5	193	
KFR13:1	53.75	76.60	213.4	193	
KFR13:2	33.75	52.75	214.6	193	
KFR13:3	3.75	32.75	218.6	193	
KFR55:3	21.53	38.53	266.6	193	
KFR55:4	7.53	20.53	252.2	193	Uncertain response
KFR101:1	279.50	341.76	340.6	193	Clear response
KFR101:2	91.00	278.50	263.7	193	Clear response

Table 6-5 shows the responding borehole sections to the drilling of KFR102A together with information about distances and at which depth of drilling the response first appeared. In the table all detected responses are reported. There are however sections that showed a weak response but for which no response indices could be calculated (KFR04:3 and KFR07B:2). These sections are reported in this table and in the response matrix in Table 6-9 but not in Table 6-12 or Table 6-15.

**Table 6-5. Sections responding to the drilling of KFR102A.**

BH-ID	Secup (m)	Seclow (m)	r <sub>s</sub> (m)	Response at depth (m)	Comments
KFR04:1	84.09	100.50	244.8	207	
KFR04:2	44.09	83.09	254.6	207	
KFR04:3	28.09	43.09	266.9	207	Uncertain response
KFR05:2	80.15	96.15	281.3	207	
KFR07B:1	8.60	21.10	288.0	207	
KFR07B:2	3.40	7.60	287.6	207	Uncertain response
KFR13:1	53.75	76.60	212.9	207	
KFR13:2	33.75	52.75	213.8	207	
KFR13:3	3.75	32.75	217.5	207	
KFR55:2	39.53	47.53	270.8	207	
KFR55:3	21.53	38.53	258.8	207	
KFR55:4	7.53	20.53	244.7	207	
KFR101:1	279.50	341.76	236.7	207	Clear response
KFR101:2	91.00	278.50	161.6	207	Clear response
KFR102B:1	146.00	180.08	99.1	207	Clear response
KFR102B:2	128.00	145.00	108.4	207	Clear response
KFR102B:3	0.00	127.00	156.1	207	
KFR103:1	178.00	200.50	181.0	207	Uncertain
KFR103:2	79.00	177.00	169.0	207	

Table 6-6 shows the responding borehole sections to the drilling of KFR105 together with information about distances and at which depth of drilling the response first appeared.

**Table 6-6. Sections responding to the drilling of KFR105.**

BH-ID	Secup (m)	Seclow (m)	r <sub>s</sub> (m)	Response at depth (m)	Comments
HFR101:0	8.04	209.30	224.2	133	Weak and uncertain
HFR102:1	28.00	55.04	149.5	133	Uncertain
HFR102:2	0.00	27.00	174.1	133	Weak and uncertain
KFR27:1	110.00	501.64	196.5	133	
KFR27:2	47.00	109.00	117.7	133	
KFR27:3	0.00	46.00	151.0	133	
KFR102A:3	255.00	422.00	264.7	133	Relatively strong response
KFR102A:4	220.00	254.00	222.5	133	Weak response
KFR102A:5	214.00	219.00	218.7	133	Weak response
KFR102A:6	185.00	213.00	216.9	133	Weak response
KFR102A:7	103.00	184.00	220.8	133	Relatively strong response
KFR102A:8	0.00	102.00	261.5	133	Relatively strong response
KFR103:1	178.00	200.50	265.5	133	Uncertain
KFR103:2	79.00	177.00	262.8	133	
KFR104:1	333.00	454.57	207.6	133	
KFR104:2	98.00	332.00	124.0	133	
KFR104:3	0.00	97.00	212.7	133	

Table 6-7 shows the responding borehole sections to the drilling of KFR106 together with information about distances and at which depth of drilling the response first appeared.

**Table 6-7. Sections responding to the drilling of KFR106.**

BH-ID	Secup (m)	Seclow (m)	r <sub>s</sub> (m)	Response at depth (m)	Comments
HFR106	9.0	190.4	118.8	155	The whole borehole, packers released 2009-09-08.
HFR106:1	50.0	190.4	118.2	155	
HFR106:2	9.03	49.00	147.6	155	Weak response
KFR103:1	178.00	200.50	265.1	155	
KFR103:2	79.00	177.00	289.8	155	
KFR103:3	0.00	78.00	341.4	155	Weak response

A qualitative classification of the strength of the responses in the observation sections was made and presented in Table 6-9 below. The qualitative classification in Table 6-9 and the classification according to index 1 in Table 6-15 do not always agree. For example, there can be a response but not possible to determine index 1 for that response. The response can thus be shown in Table 6-9 as for example “Very small response” (L/T/F) even though it is classified as “no response” in Table 6-15.

The qualitative classification of the drilling responses is given in Table 6-8 below.

**Table 6-8. Qualitative classification of drilling responses.**

Classification	Colour code and denotation
Strong/Fast	S/S
Medium	M
Small/Slow	L/L
Very small/Very slow/Uncertain	L/T/F
No response	I
No data i HMS	No data
Drilling borehole	Drilling

**Table 6-9. Response matrix with qualitative classifications at different depths for the drilling of HFR102, HFR106, KFR27, KFR102A, KFR105 and KFR106.**

Disturbance borehole	HFR102	HFR106	HFR106	HFR106	HFR106	HFR106	HFR106	HFR106	KFR27	KFR102A	KFR102A c	KFR105	KFR106	KFR106
Observation borehole		c 40 m	c 56 m	c 92 m	c 104 m	c 115 m	c 140 m	177–181 m	193–198 m	207 m	280 m	133 m	c 70 m	c 155 m
HFR101	No data	No data	No data	No data	No data	No data	No data	No data	No data			L/L		
HFR102:1	Drilling									No data	No data	L/L		
HFR102:2	Drilling											L/T/F		
HFR105:0		No data	No data	No data	No data	No data	No data	No data	No data	No data	No data	No data	No data	No data
HFR105:1	No data													
HFR105:2	No data													
HFR105:3	No data													
HFR105:4	No data													
HFR106	No data	Drilling	Drilling	Drilling	Drilling	Drilling	Drilling	Drilling	No data	No data	No data	No data		S/S
HFR106:1	No data	Drilling	Drilling	Drilling	Drilling	Drilling	Drilling	Drilling	No data	No data	No data	No data		L/L
HFR106:2	No data	Drilling	Drilling	Drilling	Drilling	Drilling	Drilling	Drilling	No data	No data	No data	No data		L/T/F
KFR01:1														
KFR01:2														
KFR02:1						L/T/F	L/T/F	L/T/F						
KFR02:2						L/T/F	L/T/F	L/T/F						
KFR02:3						L/T/F	L/T/F	L/T/F						
KFR02:4						L/T/F	L/T/F	L/T/F						
KFR03:1														
KFR03:2														
KFR03:3														
KFR03:4														
KFR04:1									L/L	L/L	L/L			
KFR04:2									L/L	L/L	L/L			
KFR04:3									L/T/F	L/T/F	L/T/F			
KFR04:4														
KFR05:1														
KFR05:2									L/L	L/L	L/L			
KFR05:3														
KFR05:4														
KFR7A:1														



Disturbance borehole	HFR102	HFR106 c 40 m	HFR106 c 56 m	HFR106 c 92 m	HFR106 c 104 m	HFR106 c 115 m	HFR106 c 140 m	HFR106 177–181 m	KFR27 193–198 m	KFR102A 207 m	KFR102A c 280 m	KFR105 133 m	KFR106 c 70 m	KFR106 c 155 m
Observation borehole														
KFR7A:2														
KFR7A:3														
KFR07B:1									L/L	L/L	L/L			
KFR07B:2										L/T/F	L/T/F			
KFR08:1														
KFR08:2														
KFR08:3														
KFR09:1														
KFR13:1							L/T/F	L/T/F	L/L	M	M			
KFR13:2							L/T/F	L/T/F	L/L	M	M			
KFR13:3							L/T/F	L/T/F	L/L	M	M			
KFR19:1														
KFR19:2														
KFR19:3														
KFR19:4														
KFR27:0		No data	No data	No data	No data	No data	No data	No data	Drilling	No data	No data	No data	No data	No data
KFR27:1	No data								Drilling	No data	No data	L/L		
KFR27:2	No data								Drilling	No data	No data	M		
KFR27:3	No data								Drilling	No data	No data	M		
KFR55:1														
KFR55:2										M	M			
KFR55:3									L/L	L/L	L/L			
KFR55:4									L/T/F	L/L	L/L			
KFR56														
KFR101:1	No data								S/S	S/S	S/S			
KFR101:2	No data								S/S	S/S	S/S			
KFR101:3	No data													
KFR102A:1	No data								No data	Drilling	Drilling			
KFR102A:2	No data								No data	Drilling	Drilling			
KFR102A:3	No data					L/T/F	L/T/F	L/T/F	No data	Drilling	Drilling	M		
KFR102A:4	No data								No data	Drilling	Drilling	L/L		
KFR102A:5	No data								No data	Drilling	Drilling	L/L		

Disturbance borehole	HFR102	HFR106 c 40 m	HFR106 c 56 m	HFR106 c 92 m	HFR106 c 104 m	HFR106 c 115 m	HFR106 c 140 m	HFR106 177–181 m	KFR27 193–198 m	KFR102A 207 m	KFR102A c 280 m	KFR105 133 m	KFR106 c 70 m	KFR106 c 155 m
Observation borehole														
KFR102A:6	No data								No data	Drilling	Drilling	L/L		
KFR102A:7	No data					L/T/F	L/T/F	L/T/F	No data	Drilling	Drilling	M		
KFR102A:8	No data					L/T/F	L/T/F	L/T/F	No data	Drilling	Drilling	M		
KFR102B:1	No data								No data	S/S	S/S			
KFR102B:2	No data								No data	S/S	S/S			
KFR102B:3	No data								No data	M	M			
KFR103:1	No data			L/L	L/L	L/L	S/S	S/S	No data	L/T/F	L/T/F	L/T/F		M
KFR103:2	No data	L/T/F	L/L	L/L	L/L	M	M	M	No data	L/L	L/L	M		L/L
KFR103:3	No data								No data					L/L
KFR104:1	No data								No data	No data	No data	L/L		
KFR104:2	No data								No data	No data	No data	L/T/F		
KFR104:3	No data								No data	No data	No data	L/T/F		
KFR105:1	No data	No data	No data	No data	No data	No data	No data	No data	No data	No data	No data	Drilling		
KFR105:2	No data	No data	No data	No data	No data	No data	No data	No data	No data	No data	No data	Drilling		
KFR105:3	No data	No data	No data	No data	No data	No data	No data	No data	No data	No data	No data	Drilling		
KFR105:4	No data	No data	No data	No data	No data	No data	No data	No data	No data	No data	No data	Drilling		
KFR105:5	No data	No data	No data	No data	No data	No data	No data	No data	No data	No data	No data	Drilling		
KFR106	No data	No data	No data	No data	No data	No data	No data	No data	No data	No data	No data		Drilling	Drilling

## 6.2.2 Response analysis

In Table 6-10 the response parameters of the borehole sections responding to the drilling of HFR106 is shown.

**Table 6-10. Sections responding to the drilling of HFR106.**

BH-ID	Secup (m)	Seclow (m)	$r_s$ (m)	$dt_L^*$ (s)	Index1 ( $r_s^2/dt_L$ ) ( $m^2/s$ )	Index1 ( $r_s^2/dt_L$ )	T/S ( $m^2/s$ )
KFR02:1	137.24	170.30	653.3	90,420	4.72	M	0.4822
KFR02:2	119.24	136.24	648.8	90,420	4.66	M	0.4755
KFR02:3	81.24	118.24	645.0	94,020	4.42	M	0.4572
KFR02:4	43.24	80.24	641.9	104,820	3.93	M	0.4194
KFR13:1	53.75	76.60	530.9	86,820	3.25	M	0.3277
KFR13:2	33.75	52.75	528.2	83,220	3.35	M	0.3342
KFR13:3	3.75	32.75	526.2	72,420	3.82	M	0.3661
KFR103:1	178.00	200.50	161.7	1,020	25.63	H	0.9797
KFR103:2	79.00	177.00	173.6	19,320	1.56	M	0.1049

In Table 6-11 the response parameters of the borehole sections responding to the drilling of KFR27 is shown.

**Table 6-11. Sections responding to the drilling of KFR27.**

BH-ID	Secup (m)	Seclow (m)	$r_s$ (m)	$dt_L^*$ (s)	Index1 ( $r_s^2/dt_L$ ) ( $m^2/s$ )	Index1 ( $r_s^2/dt_L$ )	T/S ( $m^2/s$ )
KFR04:1	84.09	100.50	249.4	105,000	0.59	L	0.049
KFR04:2	44.09	83.09	257.3	106,800	0.62	L	0.051
KFR04:3	28.09	43.09	267.7	115,800	0.62	L	0.052
KFR05:2	80.15	96.15	287.5	114,000	0.73	L	0.061
KFR7B:1	8.60	21.10	317.5	119,400	0.84	L	0.072
KFR13:1	53.75	76.60	213.4	99,600	0.46	L	0.037
KFR13:2	33.75	52.75	214.6	103,200	0.45	L	0.037
KFR13:3	3.75	32.75	218.6	103,200	0.46	L	0.038
KFR55:3	21.53	38.53	266.6	110,400	0.64	L	0.054
KFR55:4	7.53	20.53	252.2	155,400	0.41	L	0.038
KFR101:1	279.50	341.76	340.6	3,480	33.34	H	1.338
KFR101:2	91.00	278.50	263.7	2,100	33.11	H	1.231

In Table 6-12 the response parameters of the borehole sections responding to the drilling of KFR102A is shown.

**Table 6-12. Sections responding to the drilling of KFR102A.**

BH-ID	Secup (m)	Seclow (m)	$r_s$ (m)	$dt_L^*$ (s)	Index1 ( $r_s^2/dt_L$ ) ( $m^2/s$ )	Index1 ( $r_s^2/dt_L$ )	T/S ( $m^2/s$ )
KFR04:1	84.09	100.50	244.8	72,420	0.83	L	0.07
KFR04:2	44.09	83.09	254.6	75,420	0.86	L	0.07
KFR05:2	80.15	96.15	281.3	79,320	1.00	L	0.08
KFR07B:1	8.60	21.10	288.0	61,020	1.36	M	0.11
KFR13:1	53.75	76.60	212.9	12,774	3.55	M	0.19
KFR13:2	33.75	52.75	213.8	12,828	3.56	M	0.19
KFR13:3	3.75	32.75	217.5	13,050	3.63	M	0.20
KFR55:2	39.53	47.53	270.8	16,248	4.51	M	0.26
KFR55:3	21.53	38.53	258.8	15,528	4.31	M	0.24
KFR55:4	7.53	20.53	244.7	14,682	4.08	M	0.23
KFR101:1	279.50	341.76	236.7	2,820	19.87	H	0.81
KFR101:2	91.00	278.50	161.6	720	36.27	H	1.21
KFR102B:1	146.00	180.08	99.1	540	18.19	H	0.59
KFR102B:2	128.00	145.00	108.4	1,020	11.52	H	0.40
KFR102B:3	0.00	127.00	156.1	7,020	3.47	M	0.17
KFR103:1	178.00	200.50	181.0	23,220	1.41	M	0.09
KFR103:2	79.00	177.00	169.0	8,820	3.24	M	0.16

In Table 6-13 the response parameters of the borehole sections responding to the drilling of KFR105 is shown.

**Table 6-13. Sections responding to the drilling of KFR105.**

BH-ID	Secup (m)	Seclow (m)	$r_s$ (m)	$dt_L^*$ (s)	Index1 $r^2/t_L$ ( $m^2/s$ )	Index1 ( $r_s^2/dt_L$ )	T/S ( $m^2/s$ )
HFR101:0	8.04	209.30	224.2	438,420	0.11	L	0.011
HFR102:1	28.00	55.04	149.5	50,220	0.45	L	0.026
HFR102:2	0.00	27.00	174.1	860,820	0.04	L	0.004
KFR27:1	110.00	501.64	196.5	82,320	0.47	L	0.030
KFR27:2	47.00	109.00	117.7	10,980	1.26	M	0.054
KFR27:3	0.00	46.00	151.0	24,720	0.92	L	0.046
KFR102A:3	255.00	422.00	264.7	79,620	0.88	L	0.056
KFR102A:4	220.00	254.00	222.5	160,920	0.31	L	0.023
KFR102A:5	214.00	219.00	218.7	85,320	0.56	L	0.036
KFR102A:6	185.00	213.00	216.9	143,580	0.33	L	0.024
KFR102A:7	103.00	184.00	220.8	81,420	0.60	L	0.038
KFR102A:8	0.00	102.00	261.5	81,420	0.84	L	0.054
KFR103:1	178.00	200.50	265.5	288,420	0.24	L	0.022
KFR103:2	79.00	177.00	262.8	58,020	1.19	M	0.071
KFR104:1	333.00	454.57	207.6	455,820	0.09	L	0.010
KFR104:2	98.00	332.00	124.0	273,720	0.06	L	0.005
KFR104:3	0.00	97.00	212.7	300,420	0.15	L	0.014

In Table 6-14 the response parameters of the borehole sections responding to the drilling of KFR106 is shown.

**Table 6-14. Sections responding to the drilling of KFR106.**

BH-ID	Secup (m)	Seclow (m)	$r_s$ (m)	$dt_L^*$ (s)	Index1 ( $r_s^2/dt_L$ ) ( $m^2/s$ )	Index1 ( $r_s^2/dt_L$ )	T/S ( $m^2/s$ )
HFR106	9.0	190.4	118.8	780	18.09	H	0.613
KFR103:1	178.00	200.50	265.1	2,100	33.47	H	1.307
KFR103:2	79.00	177.00	289.8	25,500	3.29	M	0.206
KFR103:3	0.00	78.00	341.4	40,380	2.89	M	0.202

A response matrix of Index 1 for all 6 drillings in this report, including all observation sections investigated is shown in Table 6-15. The classification of the response indices is according to Table 3-1.

The strongest responses, denoted H in Table 6-15, occurred during drilling in HFR106 in observation borehole KFR103:1 and during drilling in KFR27 in observation borehole KFR101:1 and KFR101:2. During the drilling in KFR102A, strong responses occurred in observation borehole KFR101:1, KFR101:2, KFR102B:1 and KFR102B:2. The drilling of KFR106 gave strong responses in observation borehole HFR106 and KFR103:1.

**Table 6-15. Response matrix with Index 1 for the drilling of HFR102, HFR106, KFR27, KFR102A, KFR105 and KFR106.**

Drilling borehole	HFR102	HFR106	KFR27	KFR102A	KFR105	KFR106
Observation borehole	Index 1	Index 1	Index 1	Index 1	Index 1	Index 1
HFR101	No data	No data	No data	N	L	N
HFR102:1	Drilling	N	N	No data	L	N
HFR102:2	Drilling	N	N	N	L	N
HFR105:0	N	No data	No data	No data	No data	No data
HFR105:1	No data	N	N	N	N	N
HFR105:2	No data	N	N	N	N	N
HFR105:3	No data	N	N	N	N	N
HFR105:4	No data	N	N	N	N	N
HFR106	N	Drilling	No data	No data	No data	H
HFR106:1	No data	Drilling	No data	No data	No data	No data
HFR106:2	No data	Drilling	No data	No data	No data	No data
KFR01:1	N	N	N	N	N	N
KFR01:2	N	N	N	N	N	N
KFR02:1	N	M	N	N	N	N
KFR02:2	N	M	N	N	N	N
KFR02:3	N	M	N	N	N	N
KFR02:4	N	M	N	N	N	N
KFR03:1	N	N	N	N	N	N
KFR03:2	N	N	N	N	N	N
KFR03:3	N	N	N	N	N	N
KFR03:4	N	N	N	N	N	N
KFR04:1	N	N	L	L	N	N
KFR04:2	N	N	L	L	N	N
KFR04:3	N	N	L	N	N	N
KFR04:4	N	N	N	N	N	N

Drilling borehole	HFR102	HFR106	KFR27	KFR102A	KFR105	KFR106
Observation borehole	Index 1	Index 1	Index 1	Index 1	Index 1	Index 1
KFR05:1	N	N	N	N	N	N
KFR05:2	N	N	L	L	N	N
KFR05:3	N	N	N	N	N	N
KFR05:4	N	N	N	N	N	N
KFR7A:1	N	N	N	N	N	N
KFR7A:2	N	N	N	N	N	N
KFR7A:3	N	N	N	N	N	N
KFR07B:1	N	N	L	M	N	N
KFR07B:2	N	N	N	N	N	N
KFR08:1	N	N	N	N	N	N
KFR08:2	N	N	N	N	N	N
KFR08:3	N	N	N	N	N	N
KFR09:1	N	N	N	N	N	N
KFR13:1	N	M	L	M	N	N
KFR13:2	N	M	L	M	N	N
KFR13:3	N	M	L	M	N	N
KFR19:1	N	N	N	N	N	N
KFR19:2	N	N	N	N	N	N
KFR19:3	N	N	N	N	N	N
KFR19:4	N	N	N	N	N	N
KFR27:0	N	No data	Drilling	No data	No data	No data
KFR27:1	No data	N	Drilling	No data	L	N
KFR27:2	No data	N	Drilling	No data	M	N
KFR27:3	No data	N	Drilling	No data	L	N
KFR55:1	N	N	N	N	N	N
KFR55:2	N	N	N	M	N	N
KFR55:3	N	N	L	M	N	N
KFR55:4	N	N	L	M	N	N
KFR56	N	N	N	N	N	N
KFR101:1	No data	N	H	H	N	N
KFR101:2	No data	N	H	H	N	N
KFR101:3	No data	N	N	N	N	N
KFR102A:1	No data	N	No data	Drilling	N	N
KFR102A:2	No data	N	No data	Drilling	N	N
KFR102A:3	No data	N	No data	Drilling	L	N
KFR102A:4	No data	N	No data	Drilling	L	N
KFR102A:5	No data	N	No data	Drilling	L	N
KFR102A:6	No data	N	No data	Drilling	L	N
KFR102A:7	No data	N	No data	Drilling	L	N
KFR102A:8	No data	N	No data	Drilling	L	N
KFR102B:1	No data	N	No data	H	N	N
KFR102B:2	No data	N	No data	H	N	N
KFR102B:3	No data	N	No data	M	N	N
KFR103:1	No data	H	No data	M	L	H
KFR103:2	No data	M	No data	M	M	M
KFR103:3	No data	N	No data	N	N	M
KFR104:1	No data	N	No data	No data	L	N
KFR104:2	No data	N	No data	No data	L	N
KFR104:3	No data	N	No data	No data	L	N
KFR105:1	No data	No data	No data	No data	Drilling	N
KFR105:2	No data	No data	No data	No data	Drilling	N
KFR105:3	No data	No data	No data	No data	Drilling	N
KFR105:4	No data	No data	No data	No data	Drilling	N
KFR105:5	No data	No data	No data	No data	Drilling	N
KFR106	No data	No data	No data	No data	No data	Drilling

## 7 References

SKB's (Svensk Kärnbränslehantering AB) publications can be found at [www.skb.se/publications](http://www.skb.se/publications).

**Jönsson S, Harrström J, Ludvigson J-E, Nilsson A-C, 2008.** Site investigation SFR. Hydraulic tests, flow logging and hydrochemical sampling. Boreholes HFR101, HFR102 and HFR105. SKB P-08-87, Svensk Kärnbränslehantering AB.

**Kruseman G P, de Ridder N A, 1991.** Analysis and evaluation of pumping test data. 2nd ed. Wageningen: International Institute for Land Reclamation and Improvement. (ILRI publication 47).

**Ludvigson J-E, Jönsson S, Levén J, 2004.** Forsmark site investigation. Hydraulic evaluation of pumping activities prior to hydro-geochemical sampling in borehole KFM03A – Comparison with results from difference flow logging. SKB P-04-96, Svensk Kärnbränslehantering AB.

**Streltsova T D, 1988.** Well testing in heterogeneous formations. New York: Wiley.

### Drawdown responses and sperical distance to all observation borehole sections in the interference tests.

Pumping/Injection borehole	Observation borehole section	Secup (m)	Seclow (m)	Distance (m)	Drawdown (m)
	KFR08	62.95	104.00	499.8	< 0.1
	KFR08	35.95	61.95	468.6	< 0.1
	KFR08	5.95	34.95	443.2	< 0.1
	KFR09	0.00	80.24	253.8	< 0.1
	KFR13	53.75	76.60	324.2	< 0.1
	KFR13	33.75	52.75	318.8	< 0.1
	KFR13	3.75	32.75	314.3	< 0.1
	KFR19	95.57	110.00	352.7	< 0.1
	KFR19	77.57	94.57	336.2	< 0.1
	KFR19	66.82	76.57	322.0	< 0.1
	KFR19	51.82	65.82	309.3	< 0.1
	KFR27	110.00	501.64	361.5	< 0.1
	KFR27	47.00	109.00	309.5	< 0.1
	KFR27	0.00	46.00	318.0	< 0.1
	KFR55	48.53	61.89	346.4	< 0.1
	KFR55	39.53	47.53	341.8	< 0.1
	KFR55	21.53	38.53	336.8	< 0.1
	KFR55	7.53	20.53	331.5	< 0.1
	KFR56	9.55	81.70	447.3	< 0.1
	KFR101	279.50	341.76	638.9	< 0.1
	KFR101	91.00	278.50	558.9	< 0.1
	KFR101	0.00	90.00	504.0	< 0.1
	KFR102A:1	444.00	600.83	492.8	< 0.1
	KFR102A:2	423.00	443.00	449.6	< 0.1
	KFR102A:3	255.00	422.00	419.8	< 0.1
	KFR102A:4	220.00	254.00	409.1	< 0.1
	KFR102A:5	214.00	219.00	409.8	< 0.1
	KFR102A:6	185.00	213.00	411.2	< 0.1
	KFR102A:7	103.00	184.00	420.5	< 0.1
	KFR102A:8	0.00	102.00	450.7	< 0.1
	KFR102B:1	146.00	180.08	473.5	< 0.1
	KFR102B:2	128.00	145.00	472.4	< 0.1
	KFR102B:3	0.00	127.00	476.6	< 0.1
	KFR103:1	178.00	200.50	489.4	< 0.1
	KFR103:2	79.00	177.00	481.5	< 0.1
	KFR103:3	0.00	78.00	484.9	< 0.1
	KFR104:1	333.00	454.57	315.9	1.82
	KFR104:2	98.00	332.00	142.5	3.82
	KFR104:3	0.00	97.00	69.1	0.82
Injection borehole HFR101	HFR102	0.00	55.40	148.4	< 0.1
	HFR105	0.00	200.50	330.0	< 0.1
	KFR01:1	44.65	62.30	515.9	< 0.1
	KFR01:2	11.15	43.65	503.7	< 0.1
	KFR02:1	137.24	170.30	161.1	< 0.1
	KFR02:2	119.24	136.24	138.8	< 0.1
	KFR02:3	81.24	118.24	116.6	< 0.1
	KFR02:4	43.24	80.24	91.6	1.25
	KFR03:1	81.16	101.60	261.3	< 0.1
	KFR03:2	57.16	80.16	255.6	< 0.1
	KFR03:3	45.16	56.16	252.5	< 0.1
	KFR03:4	5.16	44.16	250.2	< 0.1
	KFR04	84.09	100.50	332.7	< 0.1
	KFR04	44.09	83.09	324.3	< 0.1
	KFR04	28.09	43.09	318.3	< 0.1
	KFR04	5.09	27.09	315.5	< 0.1
	KFR05	97.15	131.00	359.3	< 0.1
	KFR05	80.15	96.15	346.4	< 0.1
	KFR05	57.15	79.15	337.4	< 0.1



Pumping/Injection borehole	Observation borehole section	Secup (m)	Seclow (m)	Distance (m)	Drawdown (m)
	KFR05	12.15	56.15	324.4	< 0.1
	KFR7A	48.11	74.70	464.5	< 0.1
	KFR7A	20.11	47.11	437.5	< 0.1
	KFR7A	2.11	19.11	415.3	< 0.1
	KFR7B	8.60	21.10	409.4	< 0.1
	KFR7B	3.40	7.60	406.2	< 0.1
	KFR08	62.95	104.00	499.8	< 0.1
	KFR08	35.95	61.95	468.6	< 0.1
	KFR08	5.95	34.95	443.2	< 0.1
	KFR09	0.00	80.24	253.8	< 0.1
	KFR13	53.75	76.60	324.2	< 0.1
	KFR13	33.75	52.75	318.8	< 0.1
	KFR13	3.75	32.75	314.3	< 0.1
	KFR19	95.57	110.00	352.7	< 0.1
	KFR19	77.57	94.57	336.2	< 0.1
	KFR19	66.82	76.57	322.0	< 0.1
	KFR19	51.82	65.82	309.3	< 0.1
	KFR27	110.00	501.64	361.5	< 0.1
	KFR27	47.00	109.00	309.5	< 0.1
	KFR27	0.00	46.00	318.0	< 0.1
	KFR55	48.53	61.89	346.4	< 0.1
	KFR55	39.53	47.53	341.8	< 0.1
	KFR55	21.53	38.53	336.8	< 0.1
	KFR55	7.53	20.53	331.5	< 0.1
	KFR56	9.55	81.70	447.3	< 0.1
Injection borehole HFR102	HFR105:0	21.20	200.50	424.2	< 0.1
	KFR01:1	44.65	62.30	643.5	< 0.1
	KFR01:2	11.15	43.65	628.7	< 0.1
	KFR02:1	137.24	170.30	241.5	< 0.1
	KFR02:2	119.24	136.24	218.8	< 0.1
	KFR02:3	81.24	118.24	195.2	< 0.1
	KFR02:4	43.24	80.24	165.4	< 0.1
	KFR03:1	81.16	101.60	233.3	< 0.1
	KFR03:2	57.16	80.16	219.5	< 0.1
	KFR03:3	45.16	56.16	209.6	< 0.1
	KFR03:4	5.16	44.16	197.5	< 0.1
	KFR04:1	84.09	100.50	270.6	< 0.1
	KFR04:2	44.09	83.09	255.6	< 0.1
	KFR04:3	28.09	43.09	243.4	< 0.1
	KFR04:4	5.09	27.09	236.5	< 0.1
	KFR05:1	97.15	131.00	309.1	< 0.1
	KFR05:2	80.15	96.15	289.5	< 0.1
	KFR05:3	57.15	79.15	275.0	< 0.1
	KFR05:4	12.15	56.15	252.2	< 0.1
	KFR7A:1	48.11	74.70	390.0	< 0.1
	KFR7A:2	20.11	47.11	363.1	< 0.1
	KFR7A:3	2.11	19.11	341.0	< 0.1
	KFR7B:1	8.60	21.10	338.2	< 0.1
	KFR7B:2	3.40	7.60	332.8	< 0.1
	KFR08:1	62.95	104.00	419.3	< 0.1
	KFR08:2	35.95	61.95	391.9	< 0.1
	KFR09:1	0.00	80.24	325.8	< 0.1
	KFR13:1	53.75	76.60	264.1	< 0.1
	KFR13:2	33.75	52.75	251.1	< 0.1
	KFR13:3	3.75	32.75	237.9	< 0.1
	KFR19:1	95.57	110.00	268.6	< 0.1
	KFR19:2	77.57	94.57	254.4	< 0.1
	KFR19:3	66.82	76.57	242.4	< 0.1
	KFR19:4	51.82	65.82	231.9	< 0.1
	KFR27	0.00	146.50	190.3	< 0.1
	KFR55:1	48.53	61.89	281.1	< 0.1
	KFR55:2	39.53	47.53	273.3	< 0.1
	KFR55:3	21.53	38.53	264.6	< 0.1
	KFR55:4	7.53	20.53	254.9	< 0.1
	KFR56:1	9.55	81.70	363.1	< 0.1

Linear plots of hydraulic head versus time for responding observation sections together with precipitation, barometric pressure and sea level data.

A2.1 Interference test in KFR105

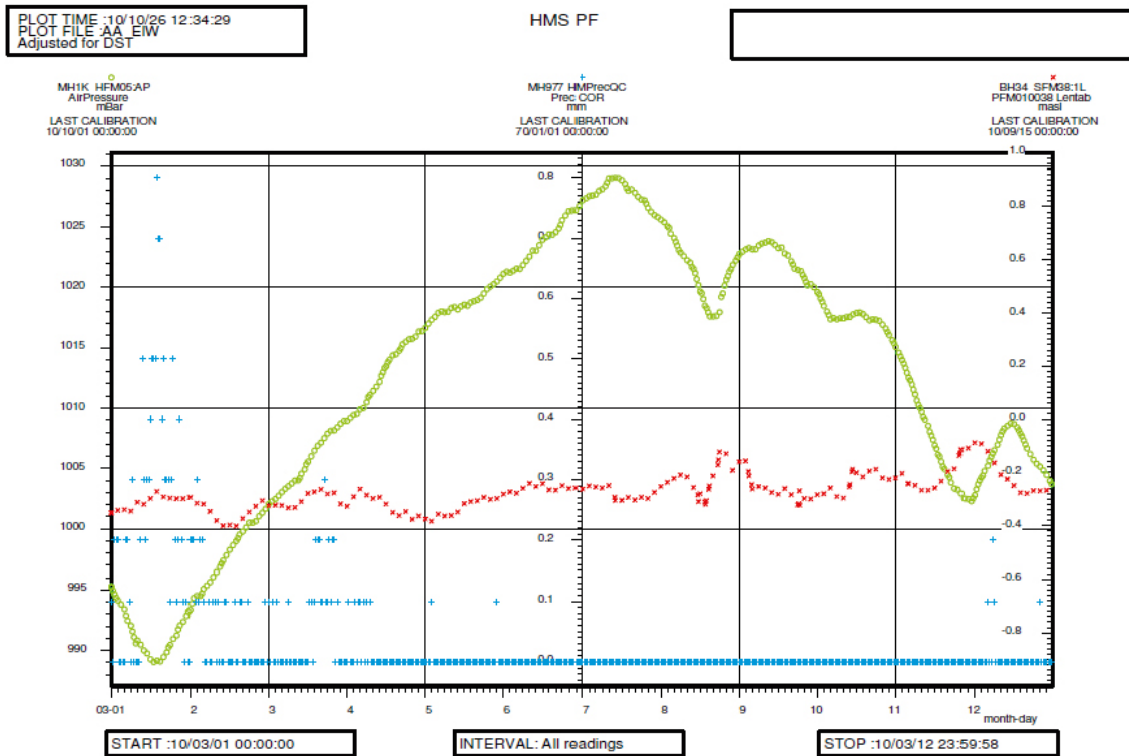


Figure A2-1. Registered air pressure (o), precipitation (+) and sea water level (x) at SFR during the interference test period in KFR105. Each parameter has its own Y-scale.

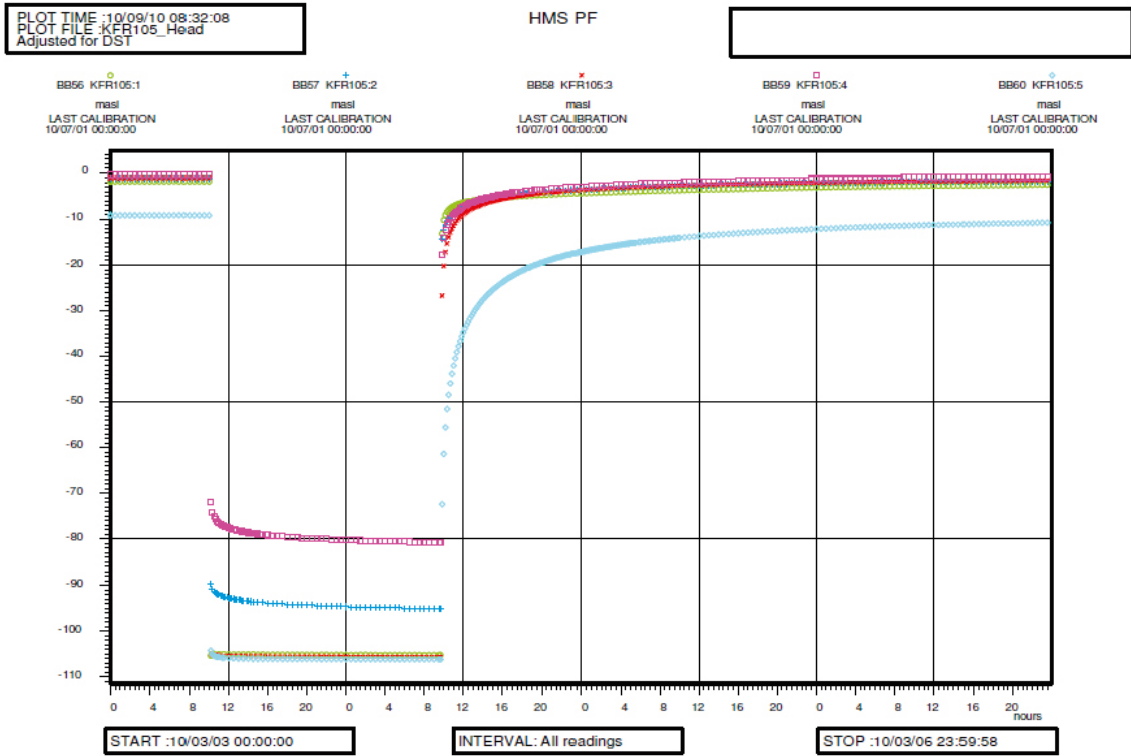


Figure A2-2. Linear plot of observed head versus time in the pumping borehole KFR105 during the interference pumping test in KFR105.

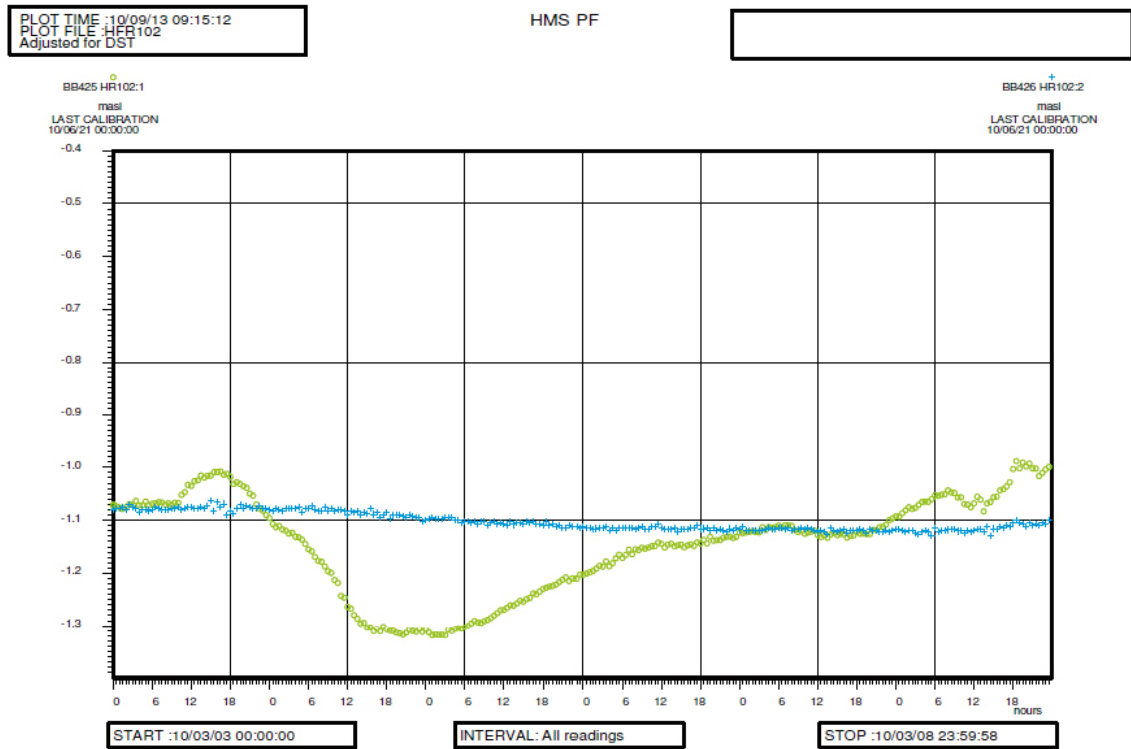


Figure A2-3. Linear plot of observed head versus time in the observation borehole HFR102 during the interference pumping test in KFR105.

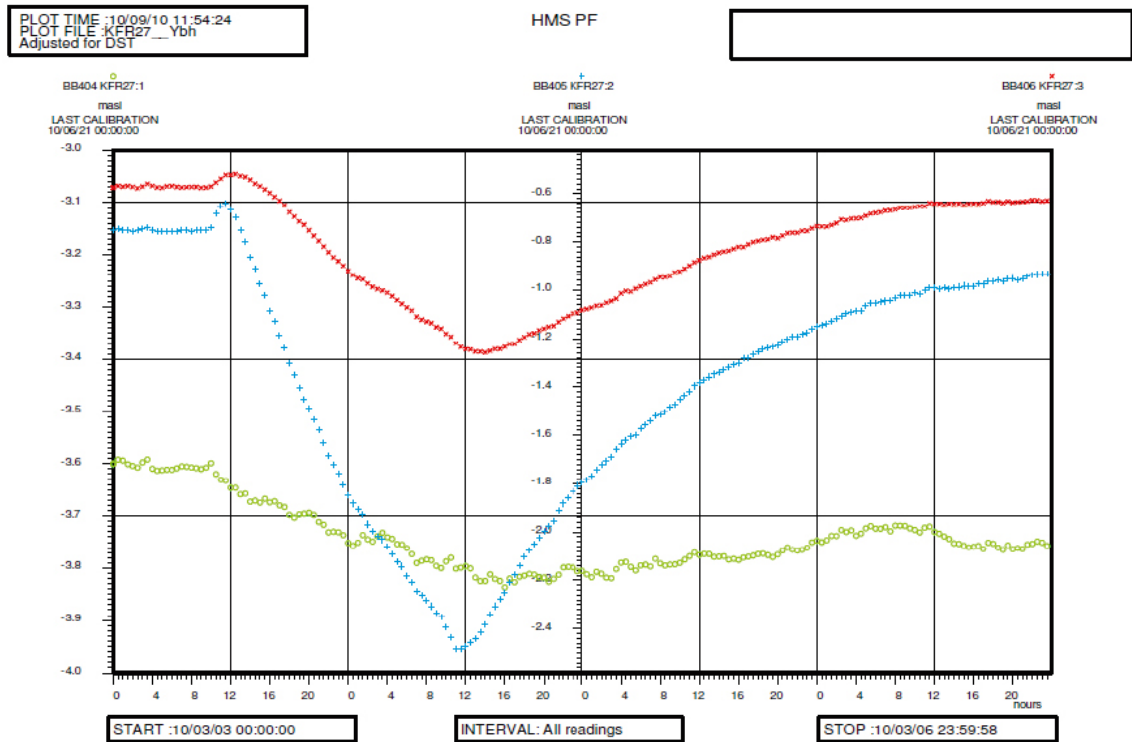


Figure A2-4. Linear plot of observed head versus time in the observation borehole KFR27 during the interference pumping test in KFR105. Each section has its own Y-scale.

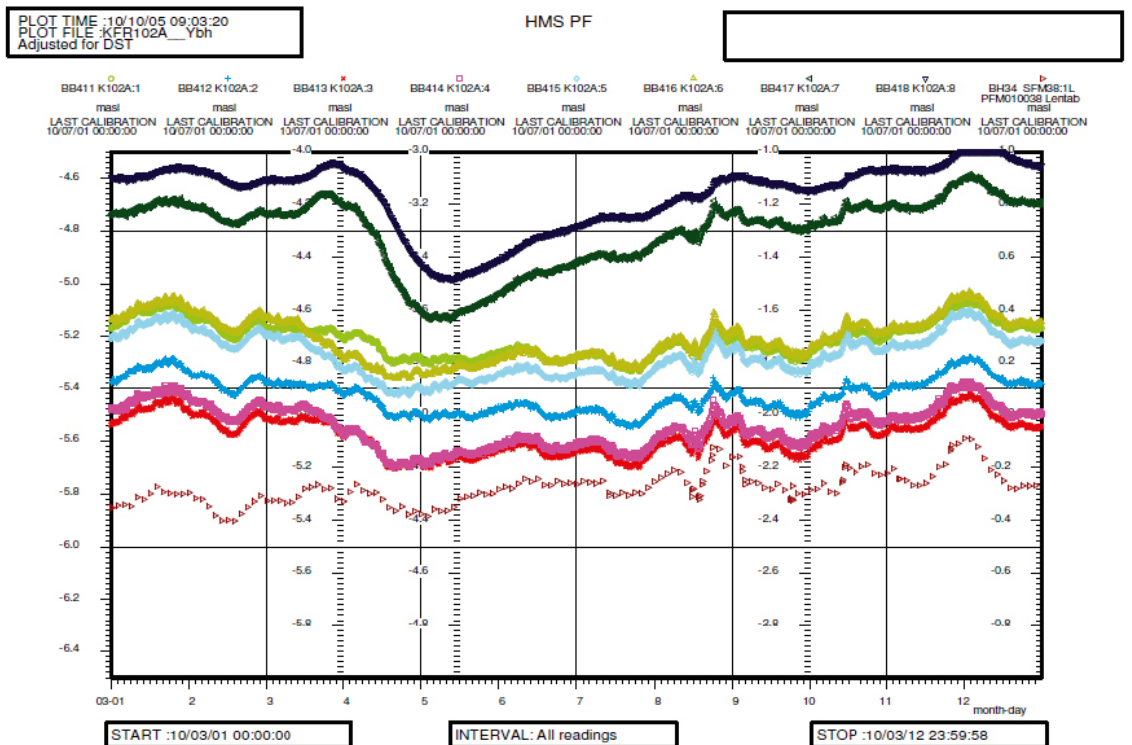


Figure A2-5. Linear plot of observed head versus time in the observation borehole KFR102A together with sea water level (lowest curve) during the interference pumping test in KFR105.

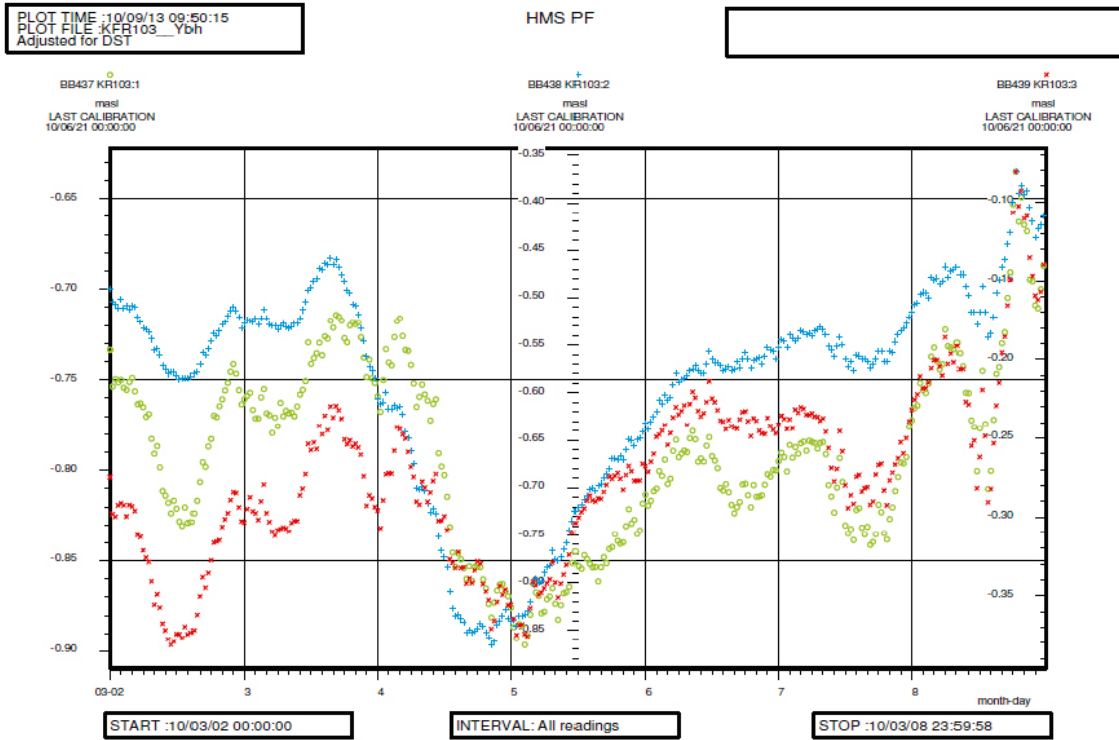


Figure A2-6. Linear plot of observed head versus time in the observation borehole KFR103 during the interference pumping test in KFR105. Each section has its own Y-scale.

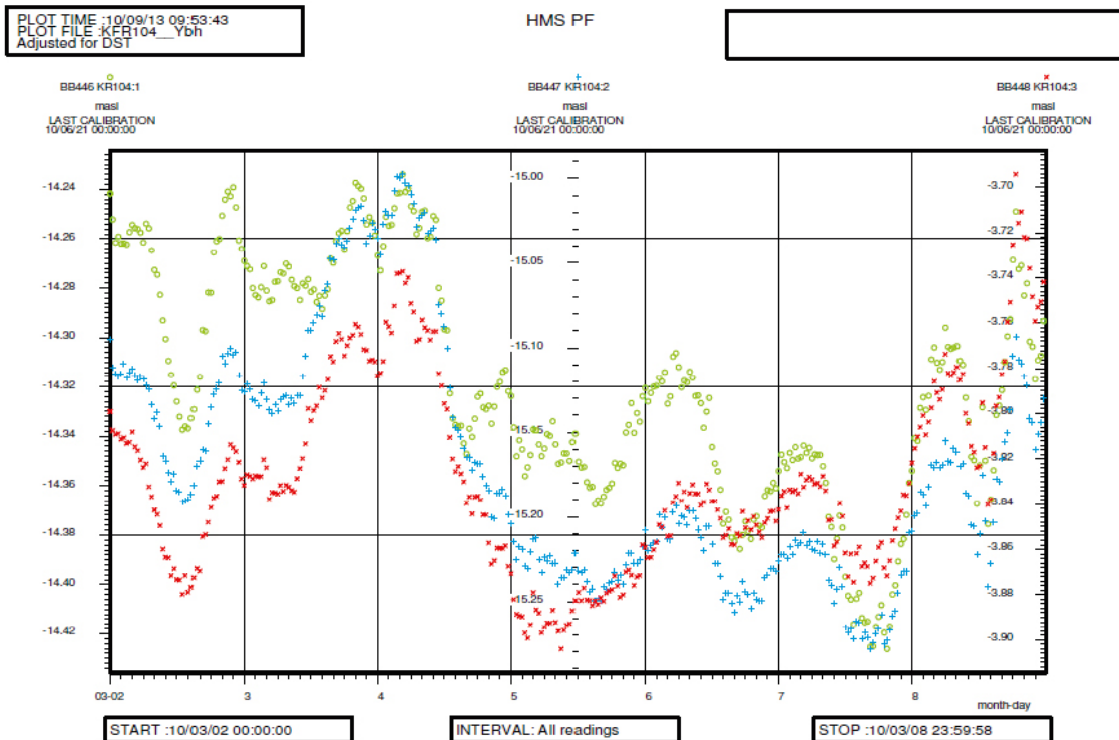
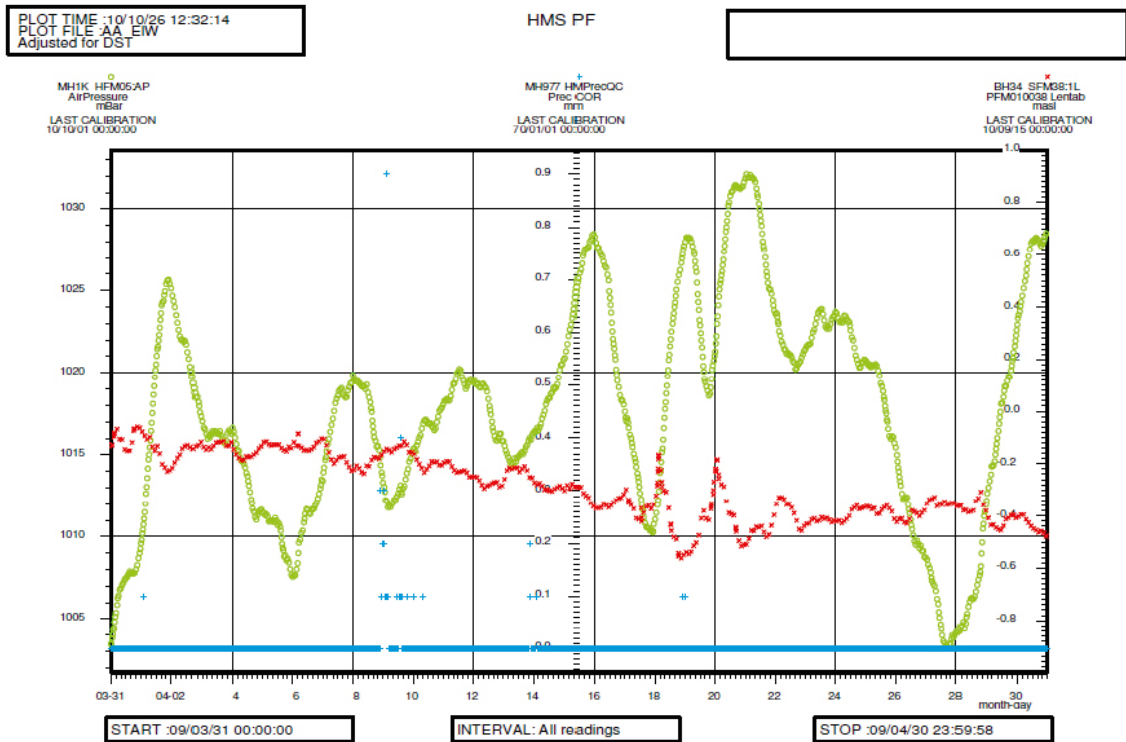
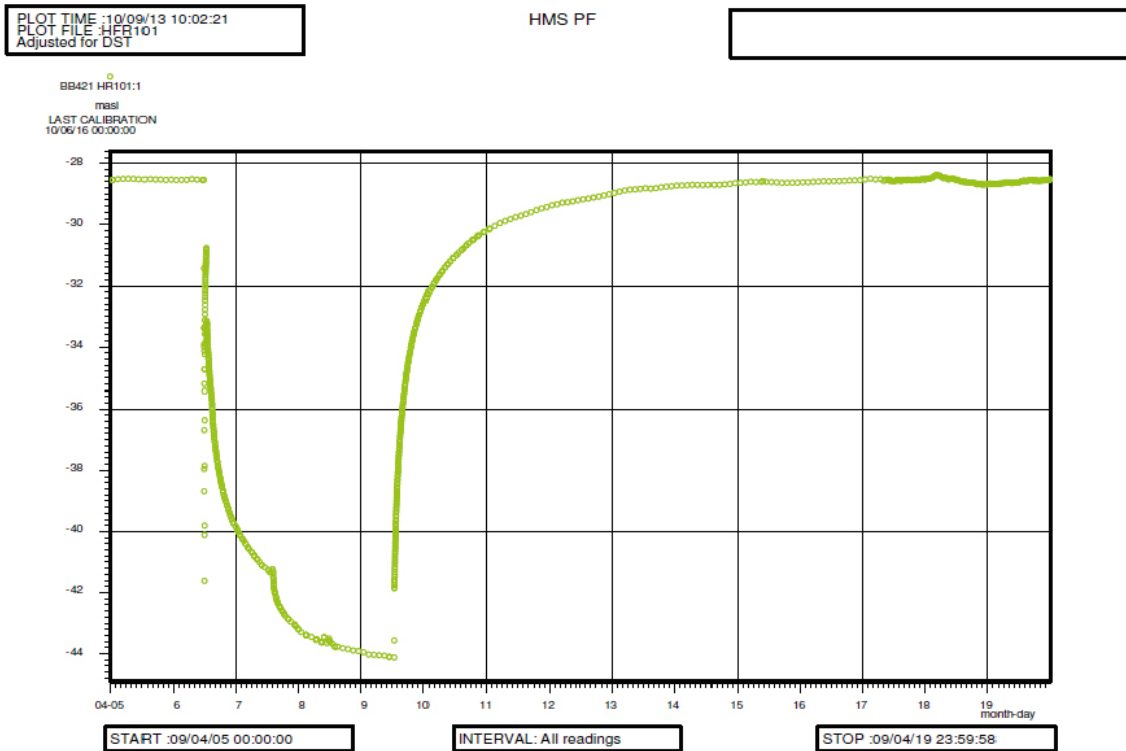


Figure A2-7. Linear plot of observed head versus time in the observation borehole KFR104 during the interference pumping test in KFR105. Each section has its own Y-scale.

## A2.2 Interference pumping test in HFR101



**Figure A2-8.** Registered air pressure (o), precipitation (+) and sea water level (x) at SFR during the interference pumping test period in HFR101. Each parameter has its own Y-scale.



**Figure A2-9.** Linear plot of observed head versus time in the pumping borehole HFR101 during the interference pumping test in HFR101.

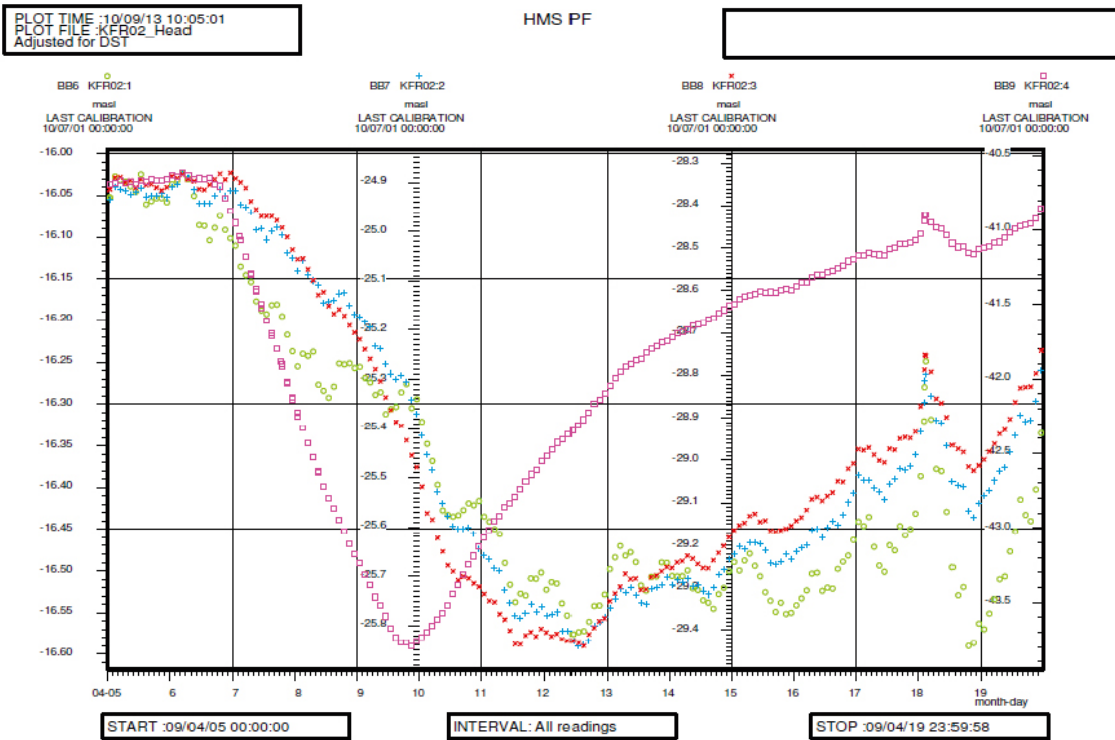


Figure A2-10. Linear plot of observed head versus time in the observation borehole KFR02 during the interference pumping test in HFR101. Each section has its own Y-scale.

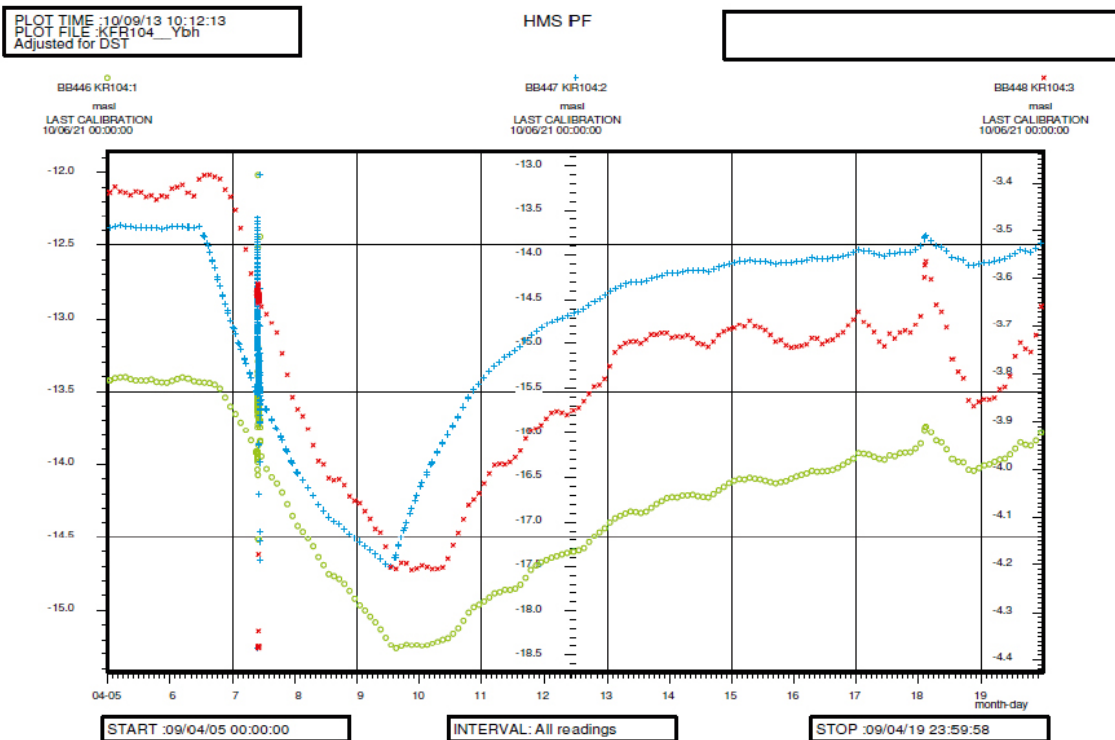


Figure A2-11. Linear plot of observed head versus time in the observation borehole KFR104 during the interference pumping test in HFR101. Each section has its own Y-scale.

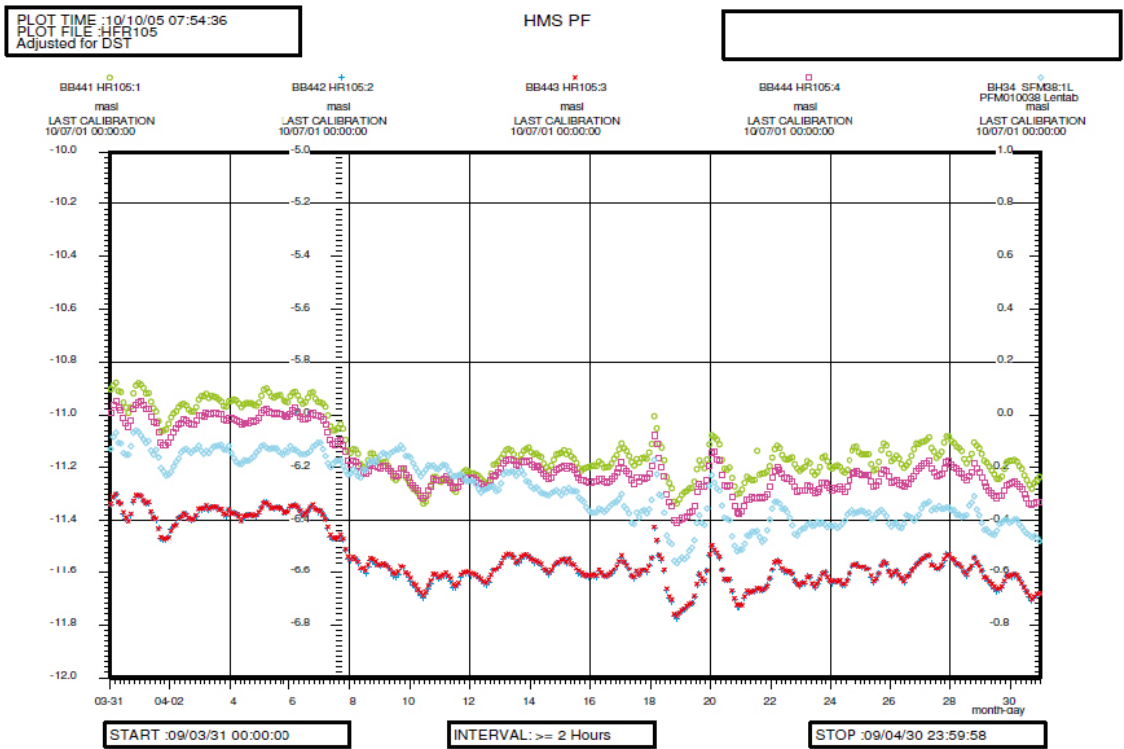


Figure A2-12. Linear plot of observed head versus time in the observation borehole HFR105 together with sea water level during the interference pumping test in HFR101.

### A2.3 Interference injection test in HFR101

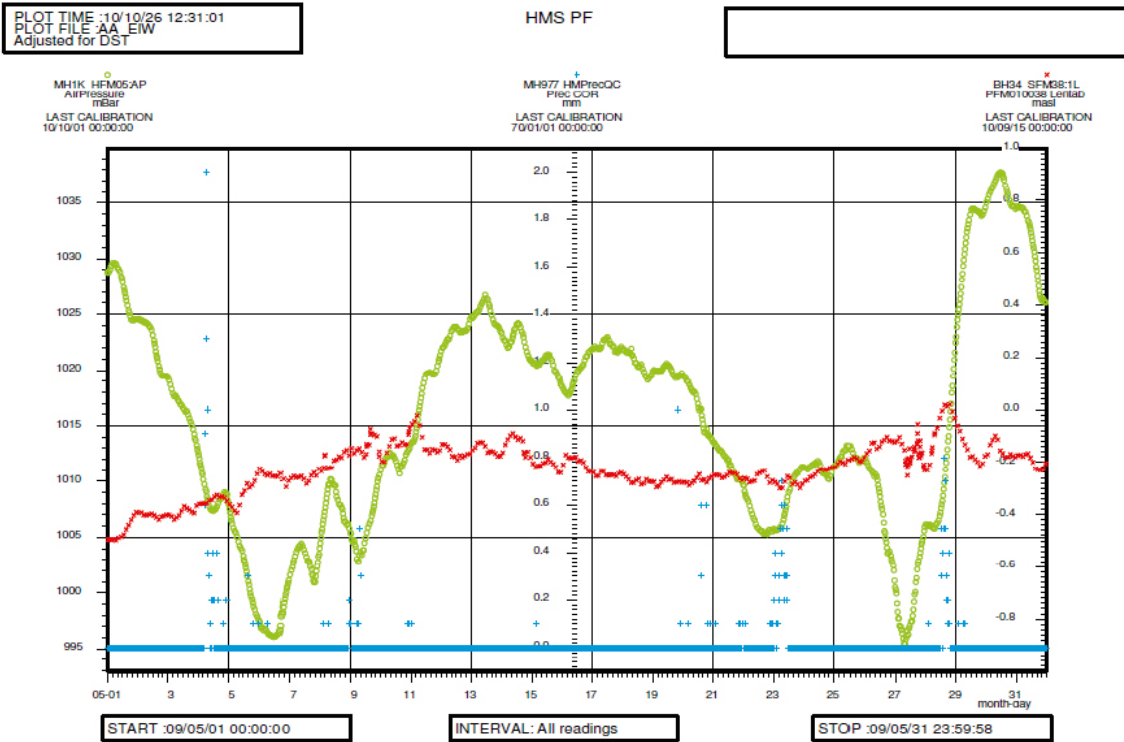


Figure A2-13. Registered air pressure (o), precipitation (+) and sea water level (x) at SFR during the interference injection test period in HFR101. Each section has its own Y-scale.



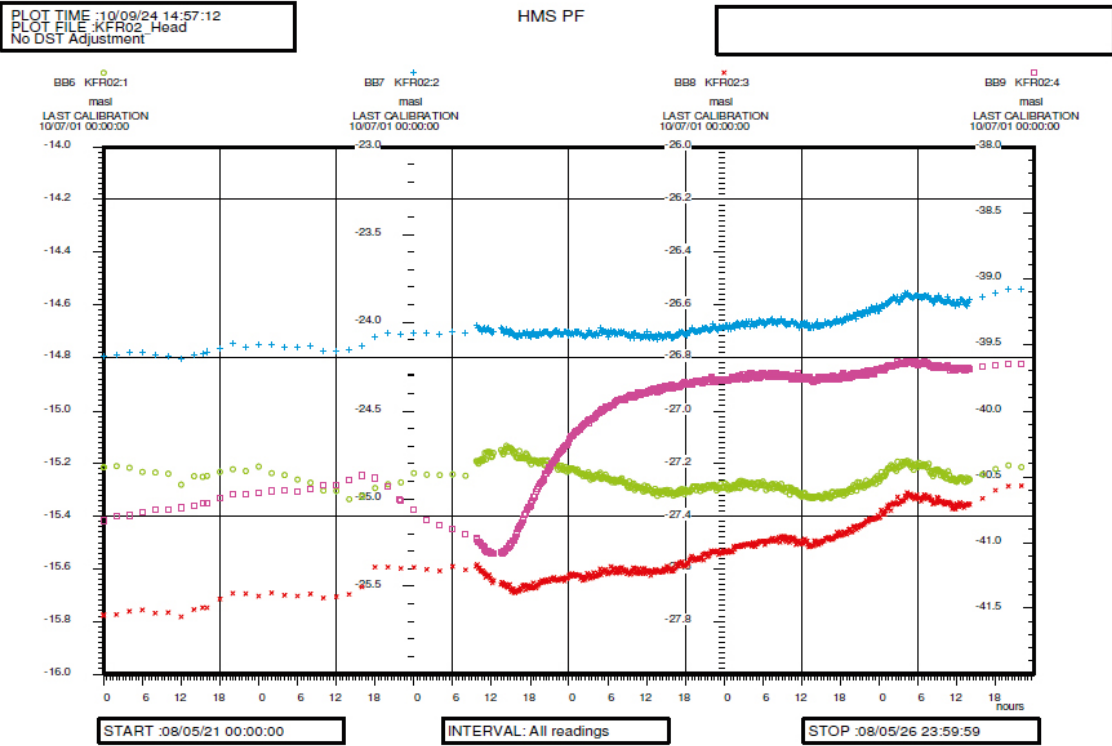


Figure A2-14. Linear plot of observed head versus time in the observation borehole KFR02 during the interference injection test in HFR101. Each section has its own Y-scale.

### A2.4 Interference injection test in HFR102

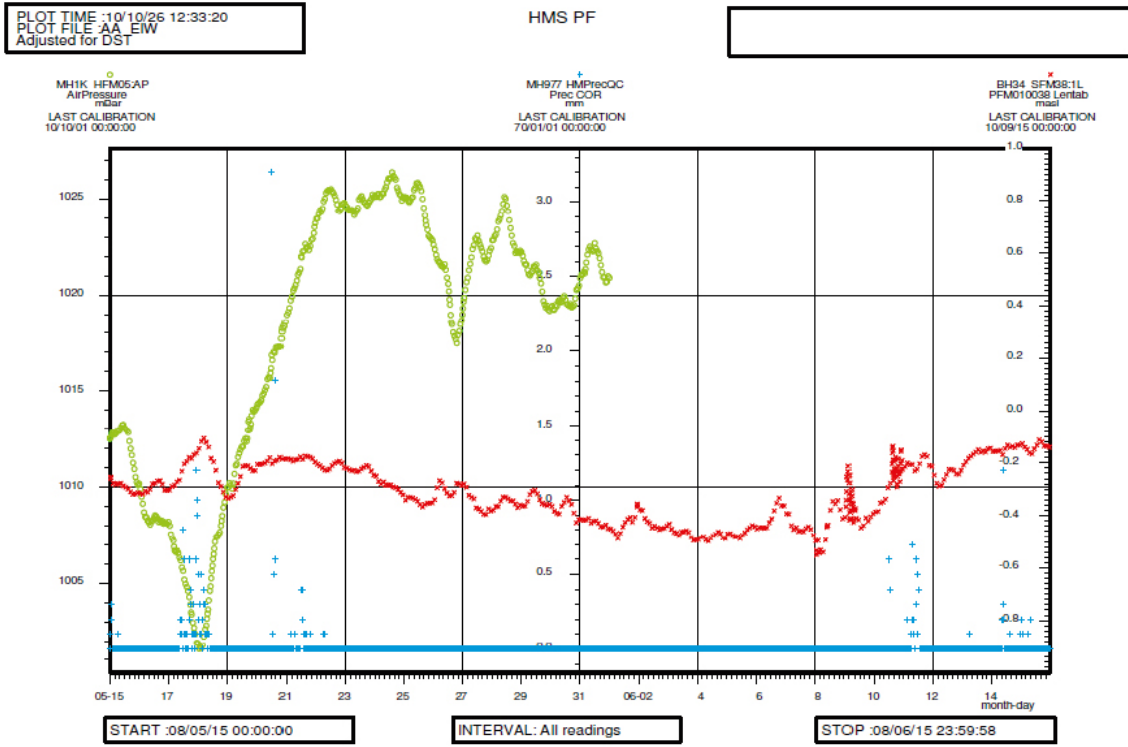


Figure A2-15. Registered air pressure (o), precipitation (+) and sea water level (x) at SFR during the interference injection test period in HFR102. Each parameter has its own Y-scale.



## Hydraulic interference test diagrams

Nomenclature:

$T$  = transmissivity ( $m^2/s$ )

$S$  = storativity (-)

$K_z/K_r$  = ratio of hydraulic conductivities in the vertical and radial direction (set to 1)

$S_w$  = skin factor

$r(w)$  = borehole radius (m)

$b$  = thickness of formation (m)

### A3.1 Interference test in KFR105

Interference test in KFR105, observation borehole section HFR102:1

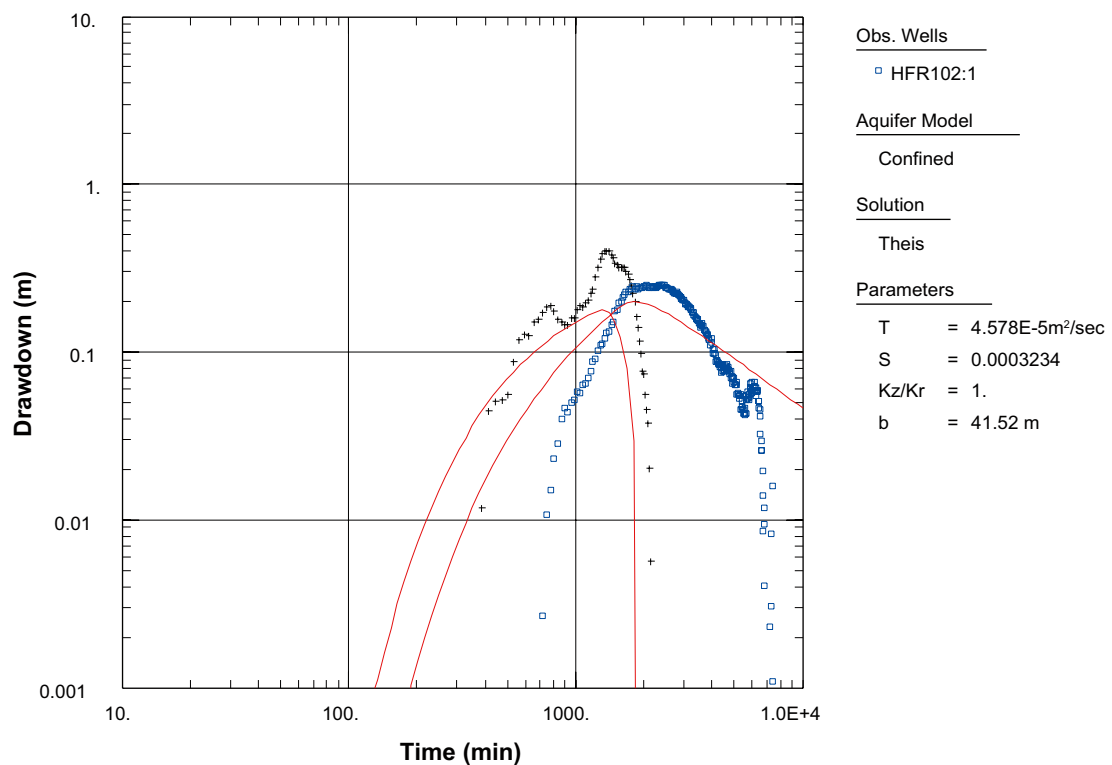
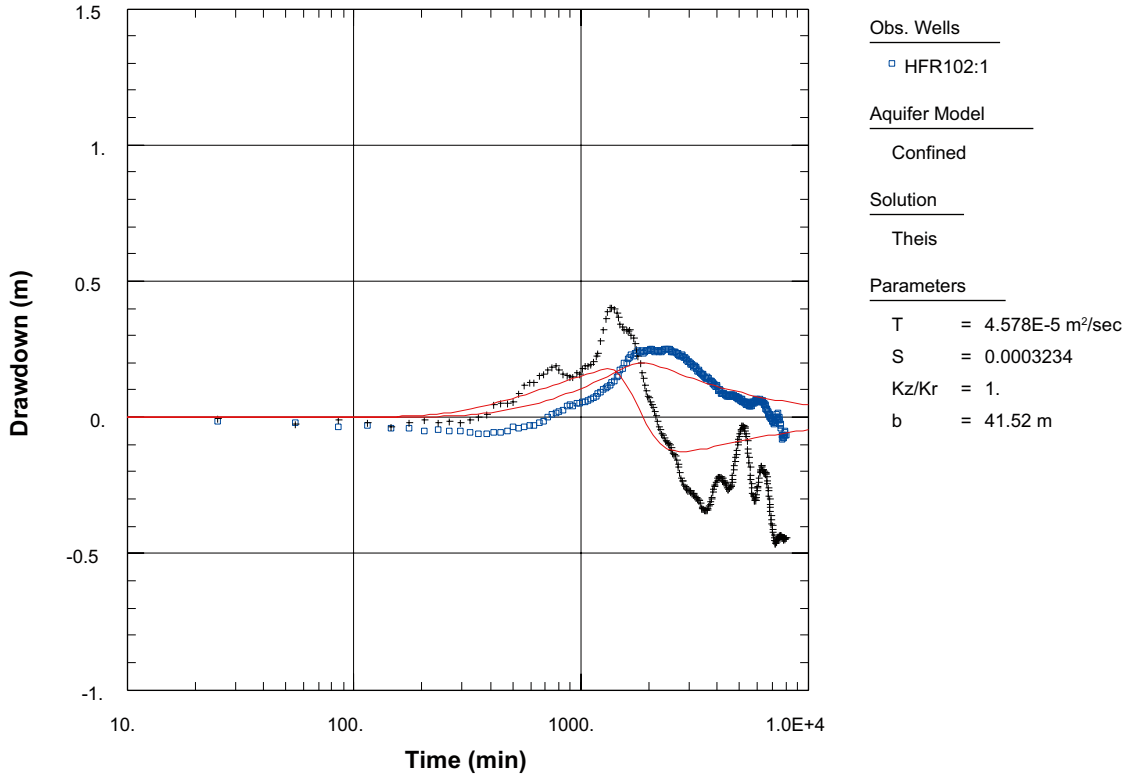


Figure A3-1. Log-log plot of drawdown ( $\square$ ) and drawdown derivative,  $ds/d(\ln t)$  ( $+$ ), versus time in the observation borehole section HFR102:1 during the interference test in KFR105.

**Interference test in KFR105, observation borehole section HFR102:1**



*Figure A3-2. Lin-log plot of drawdown (□) and drawdown derivative,  $ds/d(\ln t)$  (+), versus time in the observation borehole section HFR102:1 during the interference test in KFR105.*

**Interference test in KFR105, observation borehole section KFR27:1**

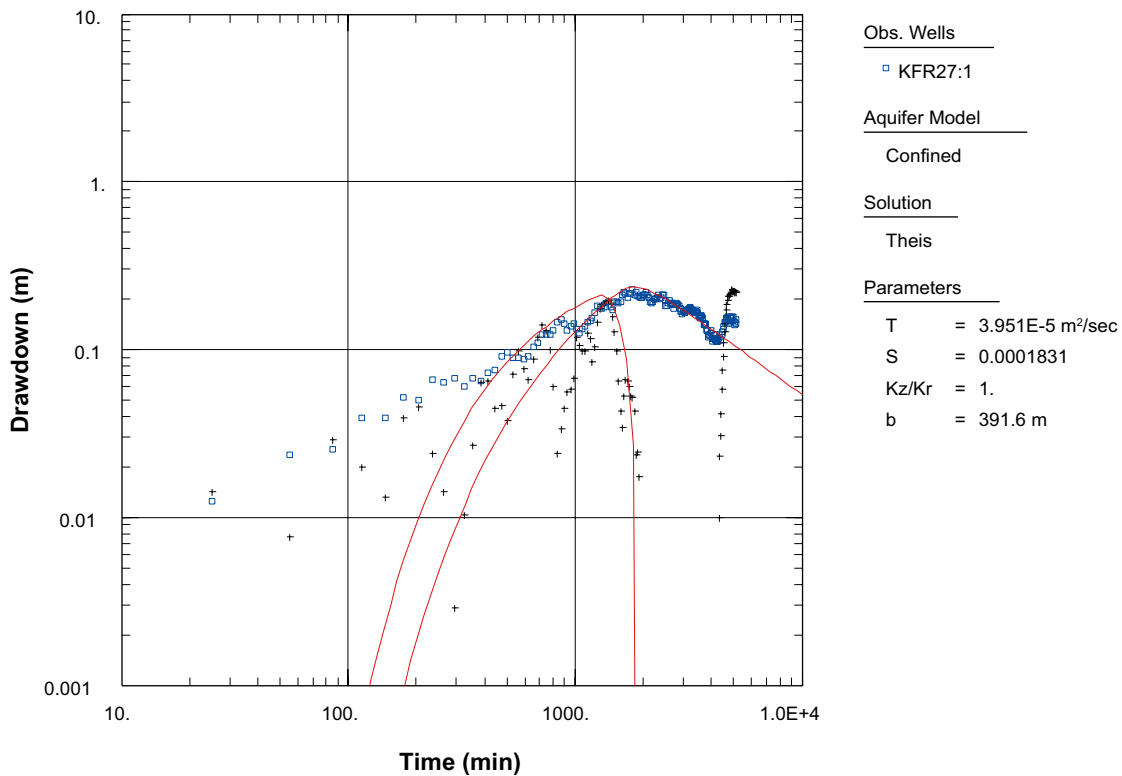


*Figure A3-3. Log-log plot of drawdown (□) and drawdown derivative,  $ds/d(\ln t)$  (+), versus time in the observation borehole section KFR27:1 during the interference test in KFR105.*

**Interference test in KFR105, observation borehole section KFR27:1**

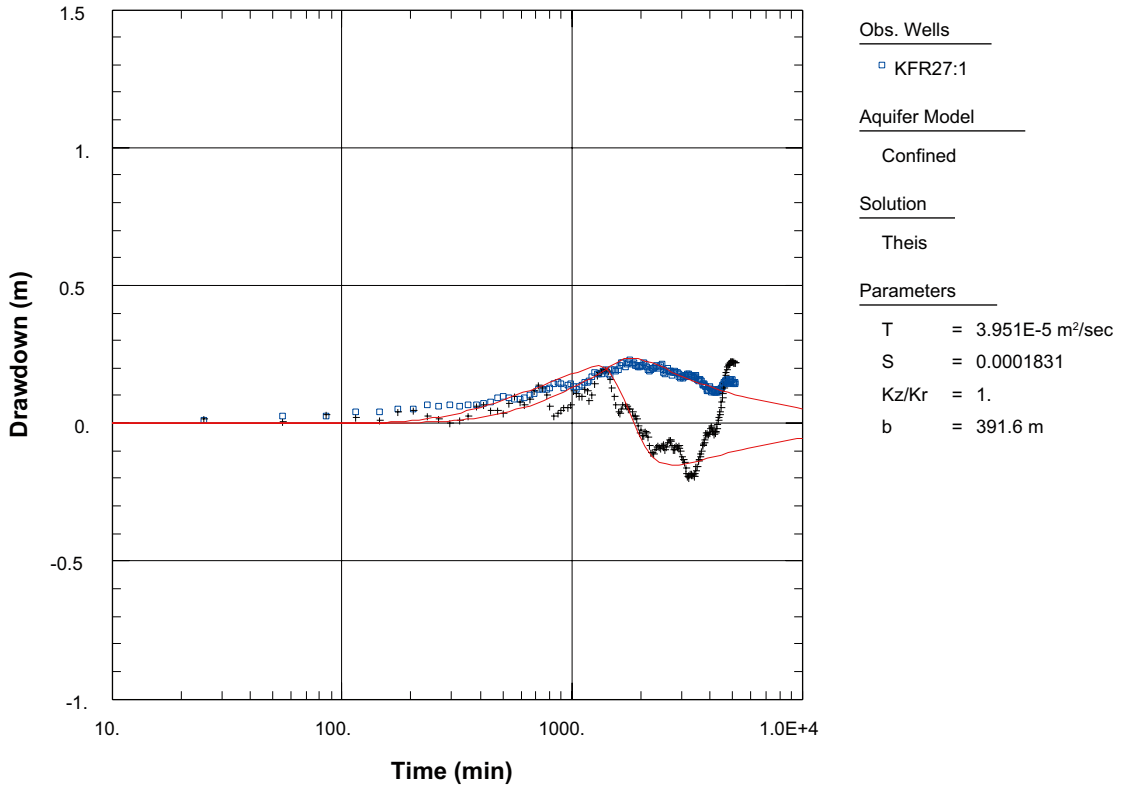


*Figure A3-4. Lin-log plot of drawdown (□) and drawdown derivative,  $ds/d(\ln t)$  (+), versus time in the observation borehole section KFR27:1 during the interference test in KFR105.*

**Interference test in KFR105, observation borehole section KFR27:2**

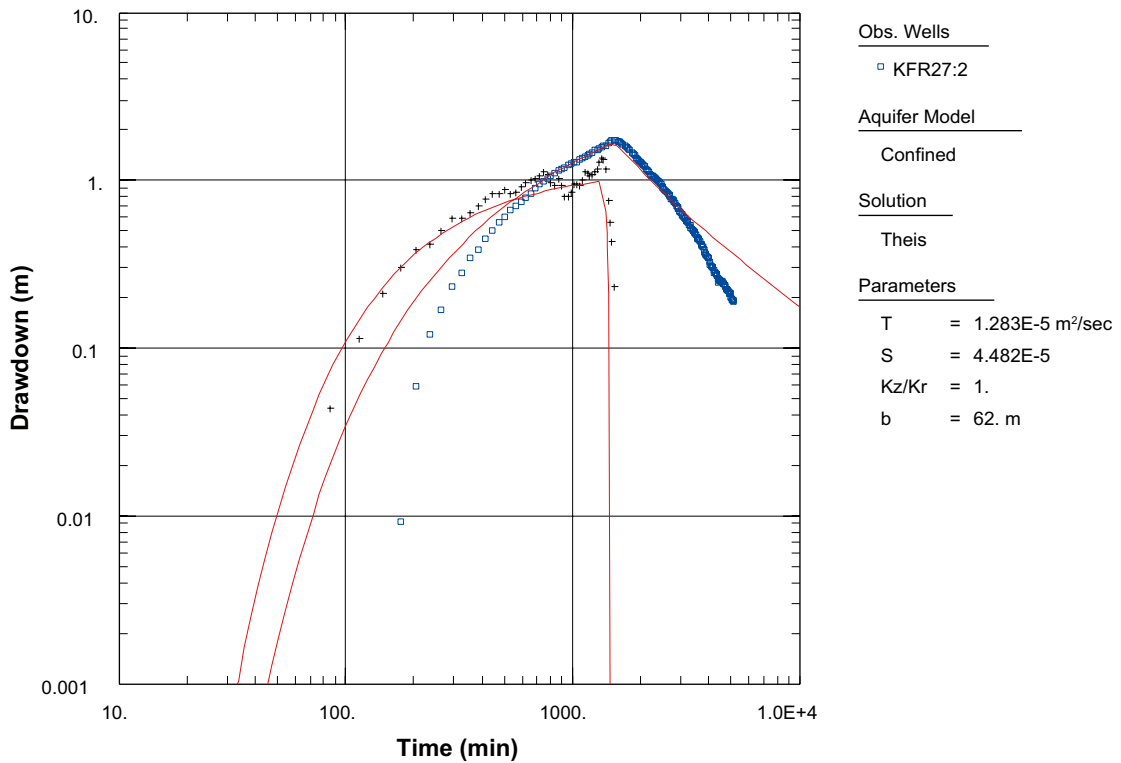


*Figure A3-5. Log-log plot of drawdown (□) and drawdown derivative,  $ds/d(\ln t)$  (+), versus time in the observation borehole section KFR27:2 during the interference test in KFR105.*

Interference test in KFR105, observation borehole section KFR27:2

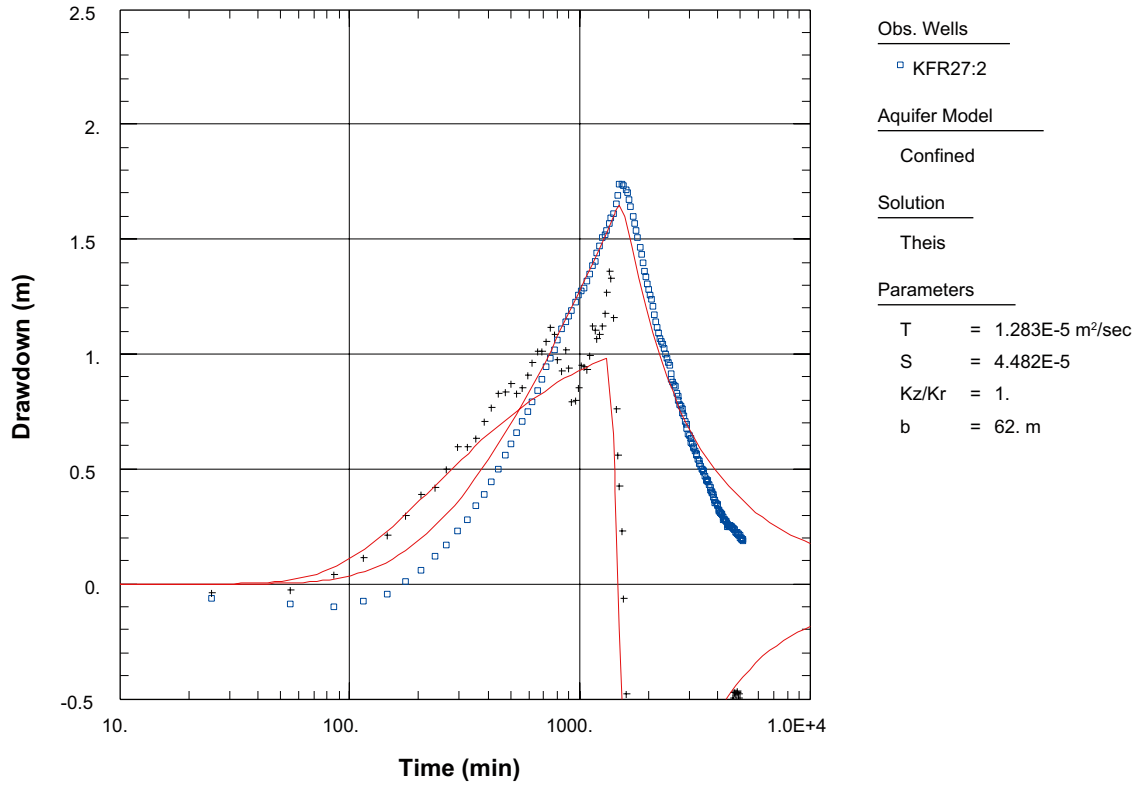


Figure A3-6. Lin-log plot of drawdown (□) and drawdown derivative,  $ds/d(\ln t)$  (+), versus time in the observation borehole section KFR27:2 during the interference test in KFR105.

Interference test in KFR105, observation borehole section KFR27:3

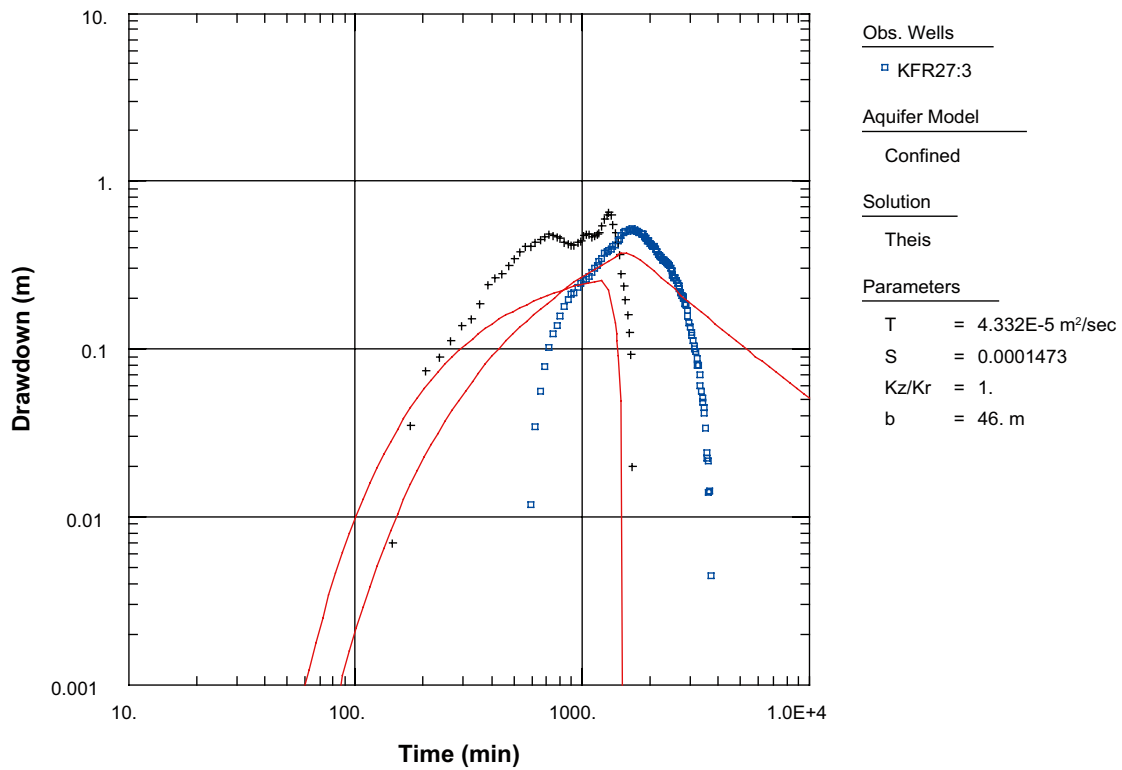
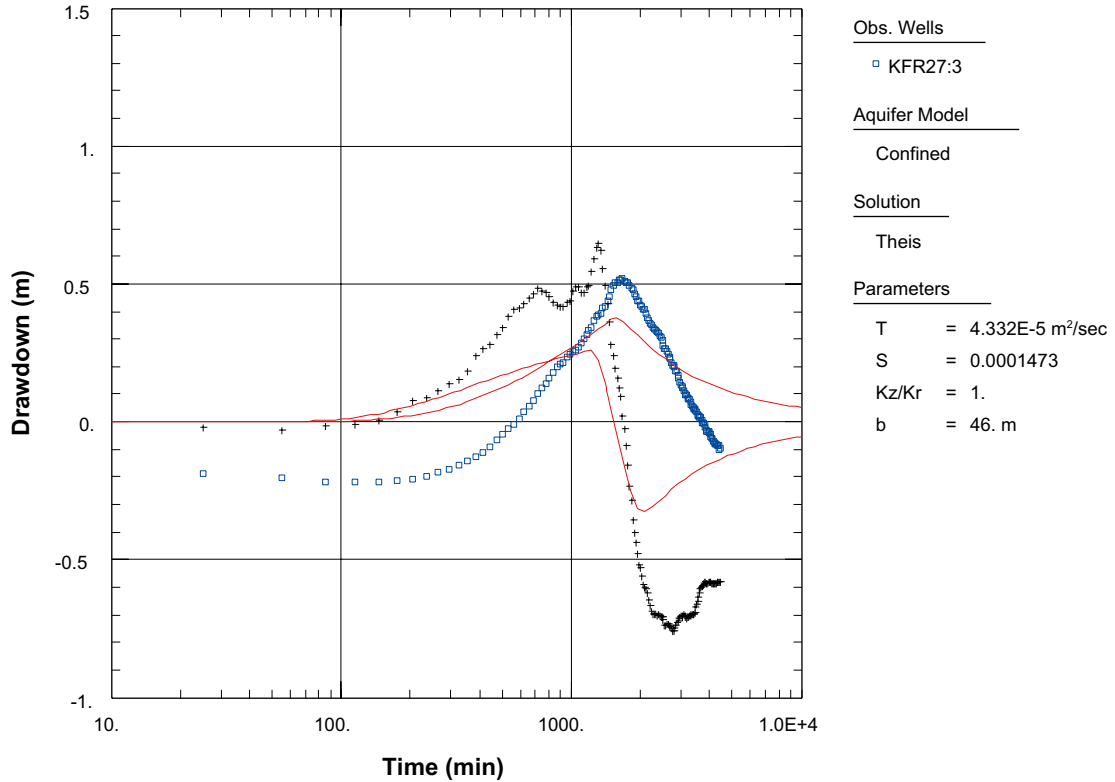


Figure A3-7. Log-log plot of drawdown (□) and drawdown derivative,  $ds/d(\ln t)$  (+), versus time in the observation borehole section KFR27:3 during the interference test in KFR105.

**Interference test in KFR105, observation borehole section KFR27:3**



*Figure A3-8. Lin-log plot of drawdown (□) and drawdown derivative,  $ds/d(\ln t)$  (+), versus time in the observation borehole section KFR27:3 during the interference test in KFR105.*

**Interference test in KFR105, observation borehole section KFR102A:1**

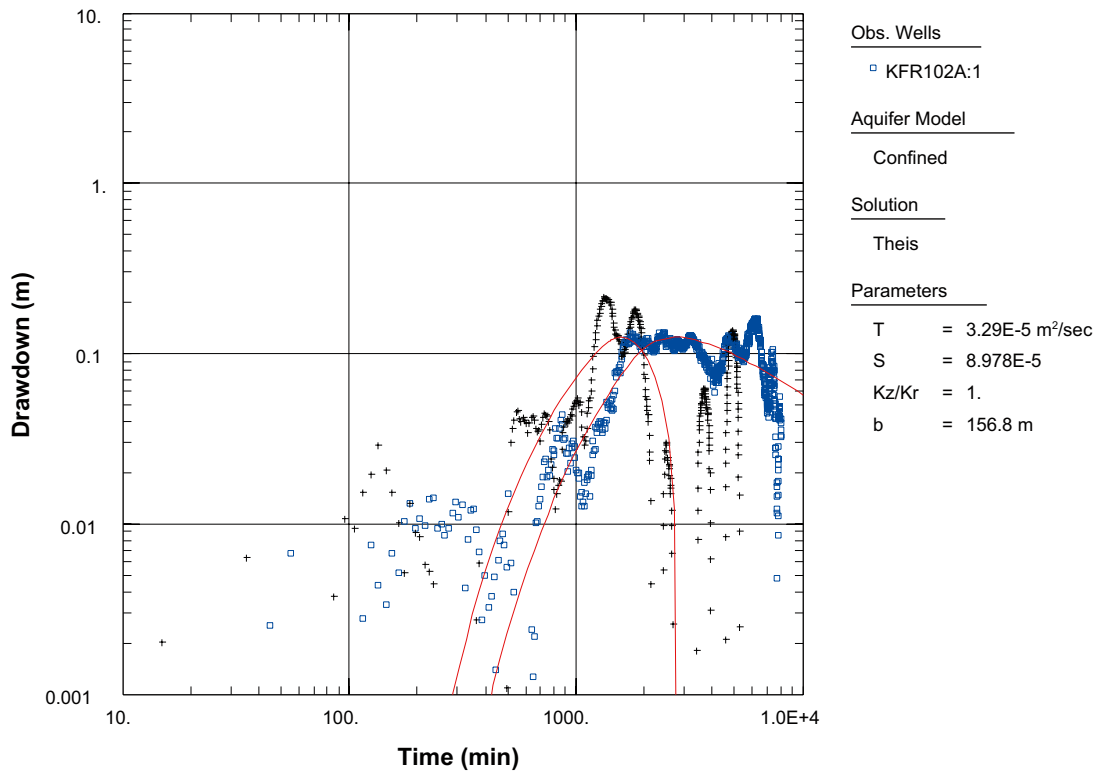


*Figure A3-9. Log-log plot of drawdown (□) and drawdown derivative,  $ds/d(\ln t)$  (+), versus time in the observation borehole section KFR102A:1 during the interference test in KFR105.*

Interference test in KFR105, observation borehole section KFR102A:1

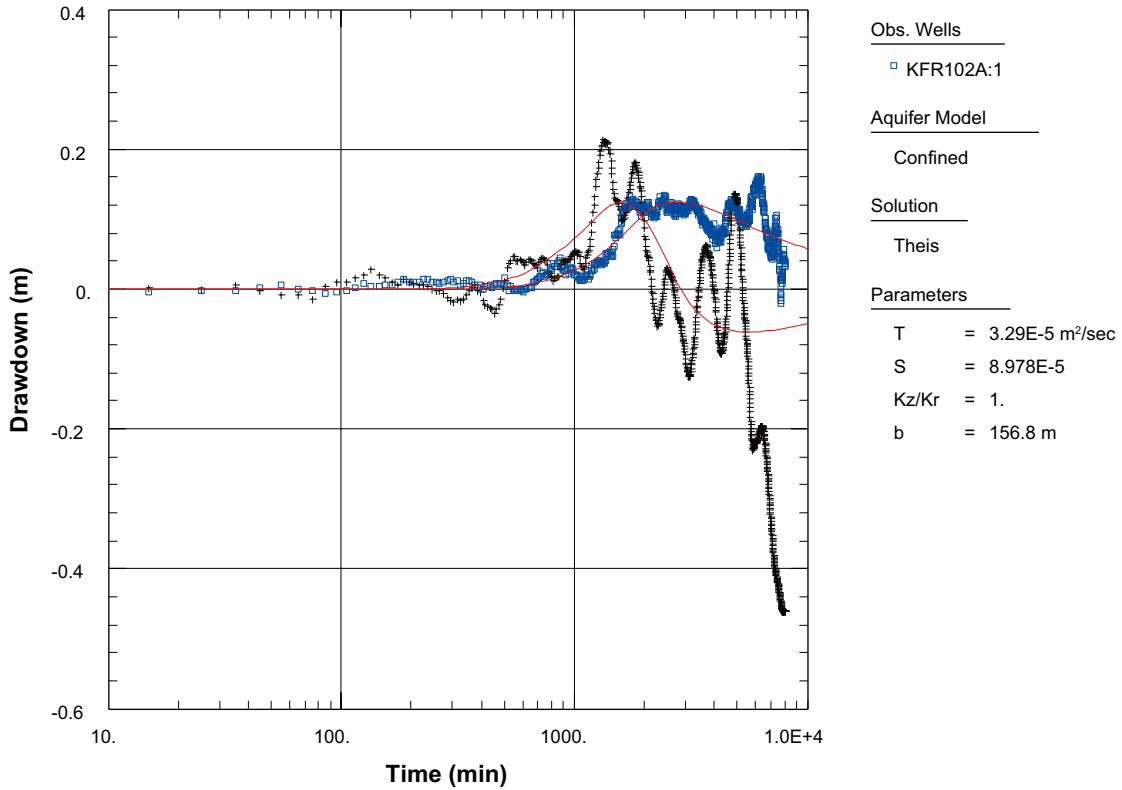


Figure A3-10. Lin-log plot of drawdown (□) and drawdown derivative,  $ds/d(\ln t)$  (+), versus time in the observation borehole section KFR102A:1 during the interference test in KFR105.

Interference test in KFR105, observation borehole section KFR102A:2

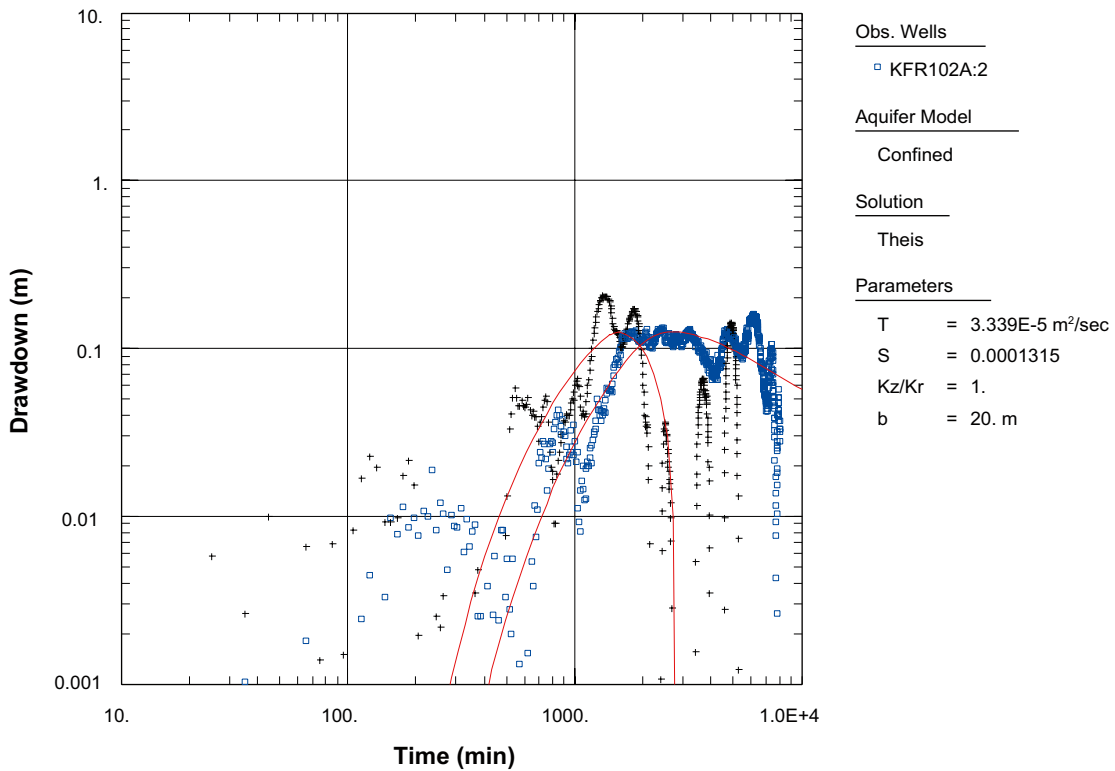
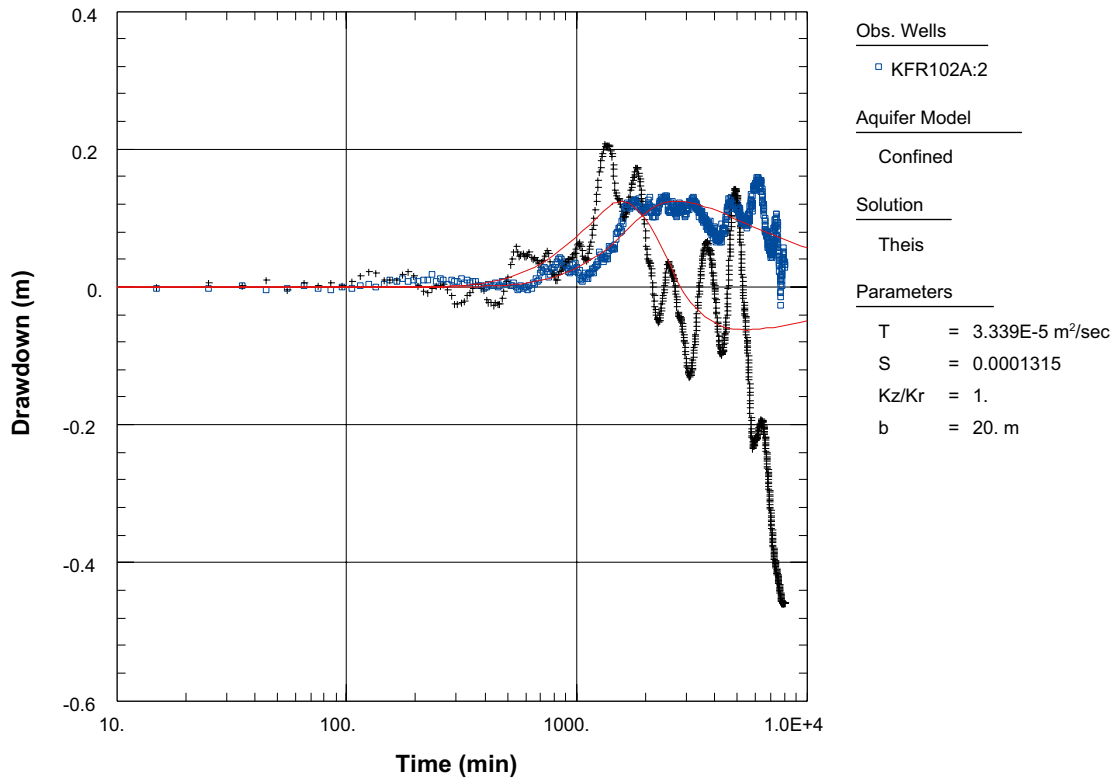


Figure A3-11. Log-log plot of drawdown (□) and drawdown derivative,  $ds/d(\ln t)$  (+), versus time in the observation borehole section KFR102A:2 during the interference test in KFR105.



**Interference test in KFR105, observation borehole section KFR102A:2**



*Figure A3-12. Lin-log plot of drawdown (◻) and drawdown derivative,  $ds/d(\ln t)$  (+), versus time in the observation borehole section KFR102A:2 during the interference test in KFR105.*

**Interference test in KFR105, observation borehole section KFR102A:3**

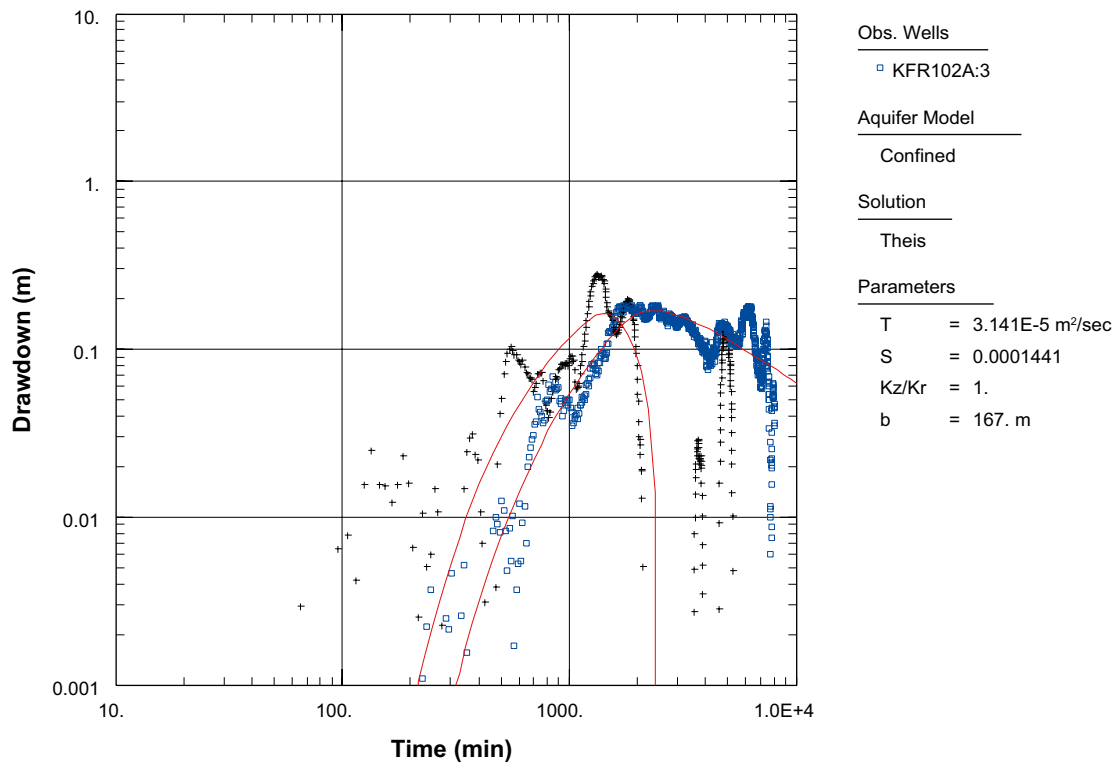


*Figure A3-13. Log-log plot of drawdown (◻) and drawdown derivative,  $ds/d(\ln t)$  (+), versus time in the observation borehole section KFR102A:3 during the interference test in KFR105.*

Interference test in KFR105, observation borehole section KFR102A:3

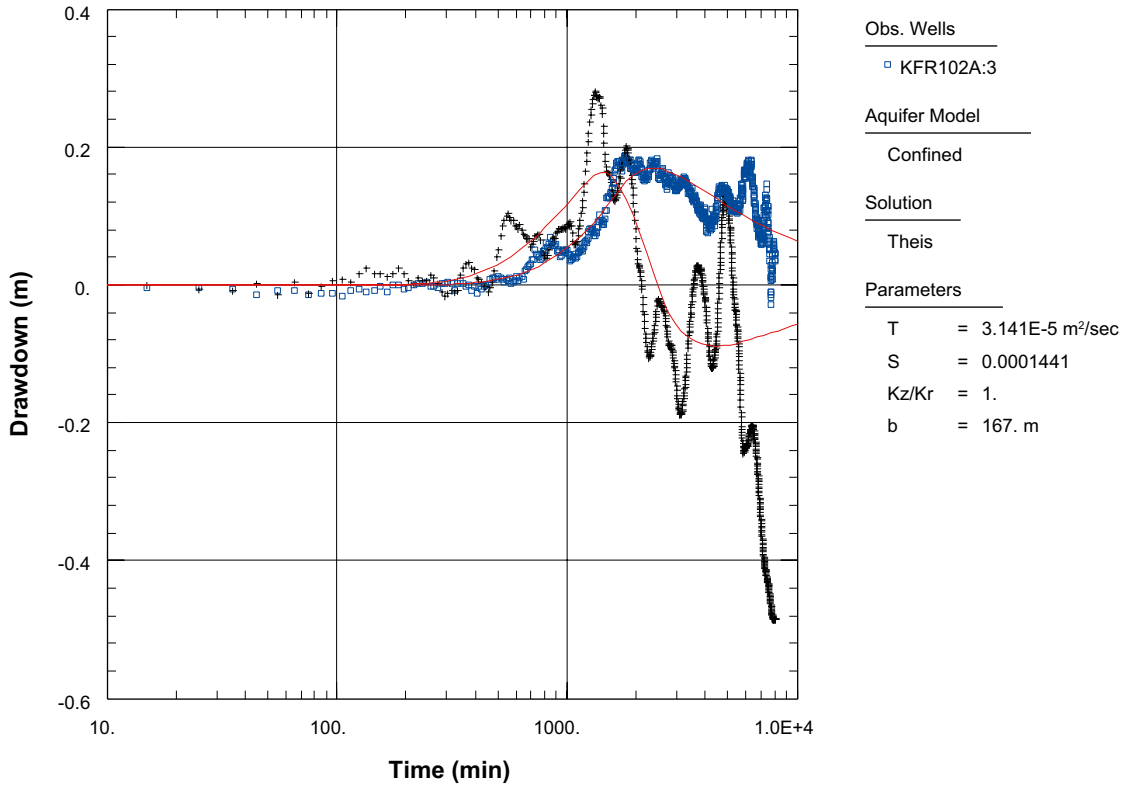


Figure A3-14. Lin-log plot of drawdown (□) and drawdown derivative,  $ds/d(\ln t)$  (+), versus time in the observation borehole section KFR102A:3 during the interference test in KFR105.

Interference test in KFR105, observation borehole section KFR102A:4

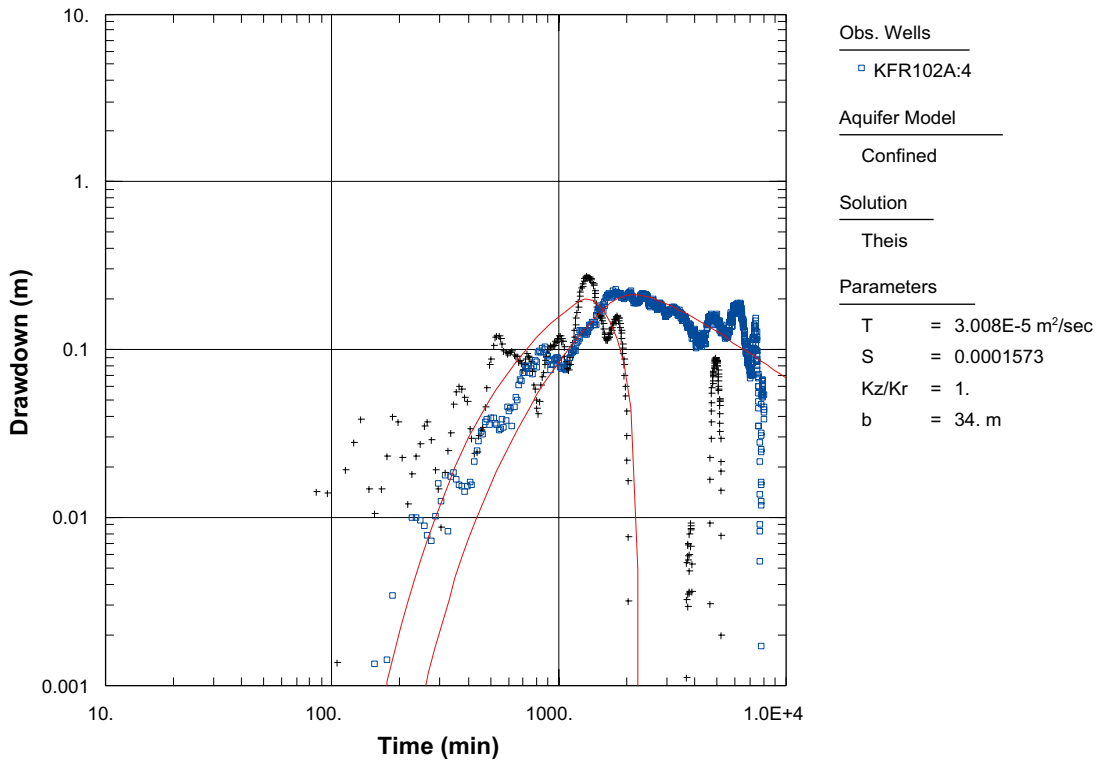
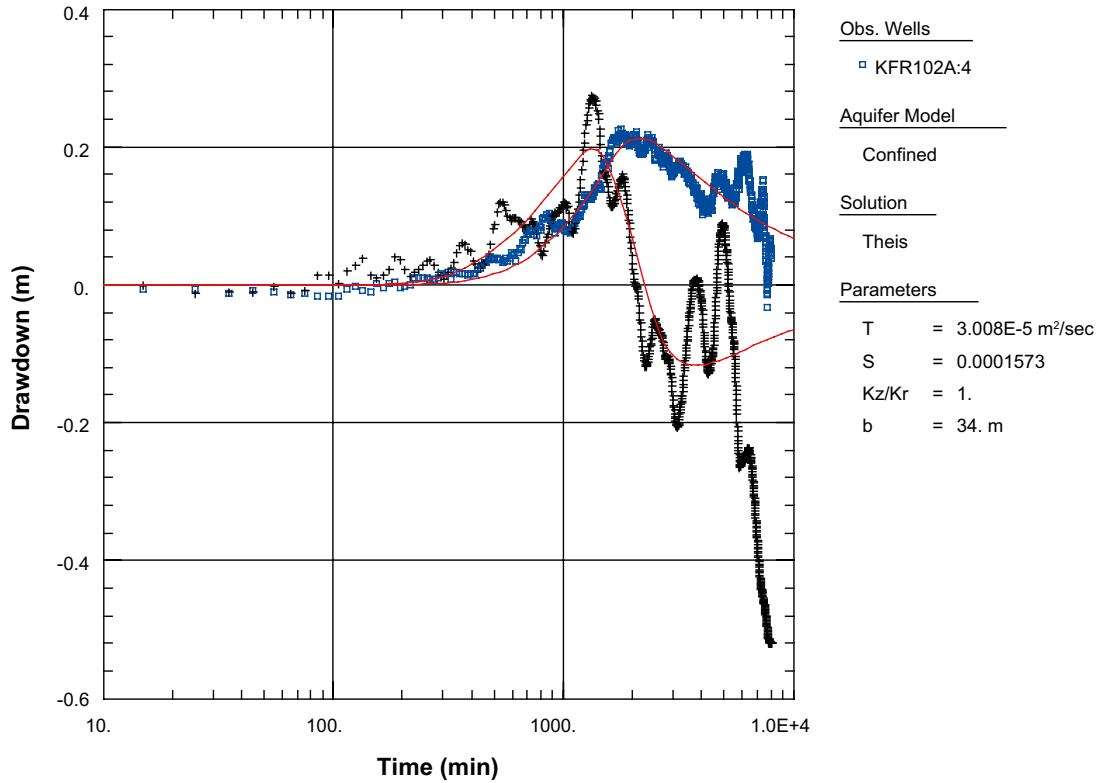


Figure A3-15. Log-log plot of drawdown (□) and drawdown derivative,  $ds/d(\ln t)$  (+), versus time in the observation borehole section KFR102A:4 during the interference test in KFR105.

**Interference test in KFR105, observation borehole section KFR102A:4**



**Figure A3-16.** Lin-log plot of drawdown (□) and drawdown derivative,  $ds/d(\ln t)$  (+), versus time in the observation borehole section KFR102A:4 during the interference test in KFR105.

**Interference test in KFR105, observation borehole section KFR102A:5**

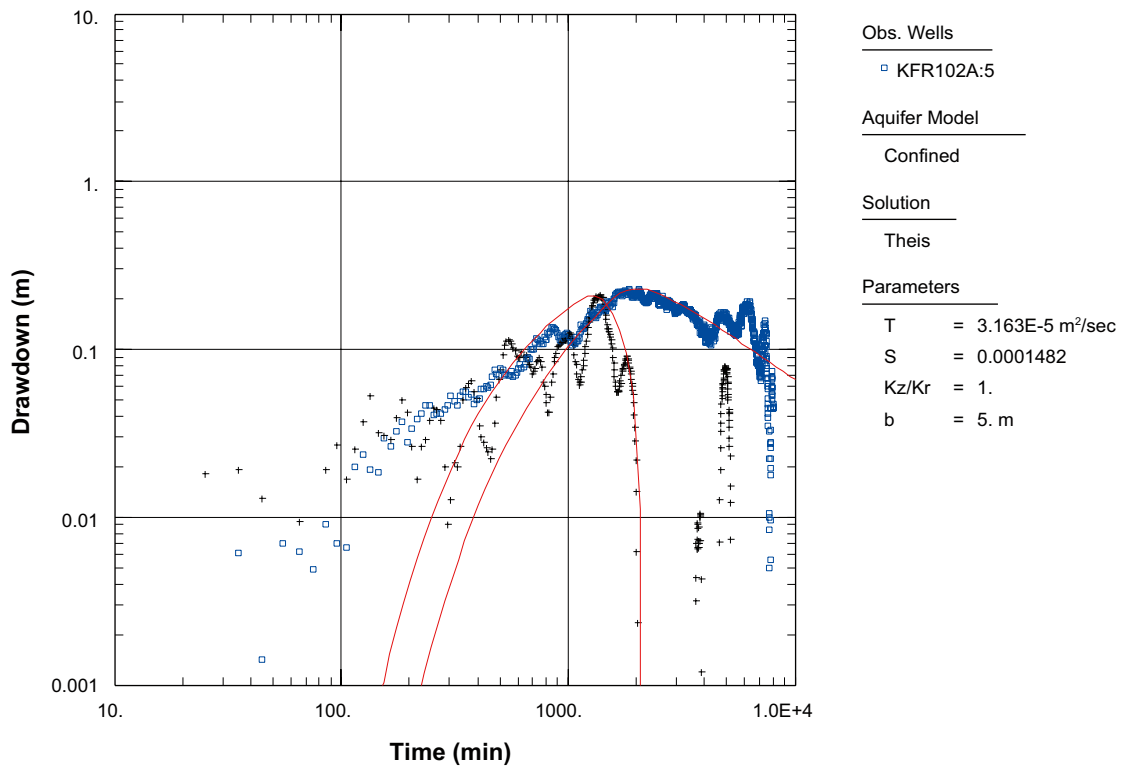


**Figure A3-17.** Log-log plot of drawdown (□) and drawdown derivative,  $ds/d(\ln t)$  (+), versus time in the observation borehole section KFR102A:5 during the interference test in KFR105.

Interference test in KFR105, observation borehole section KFR102A:5

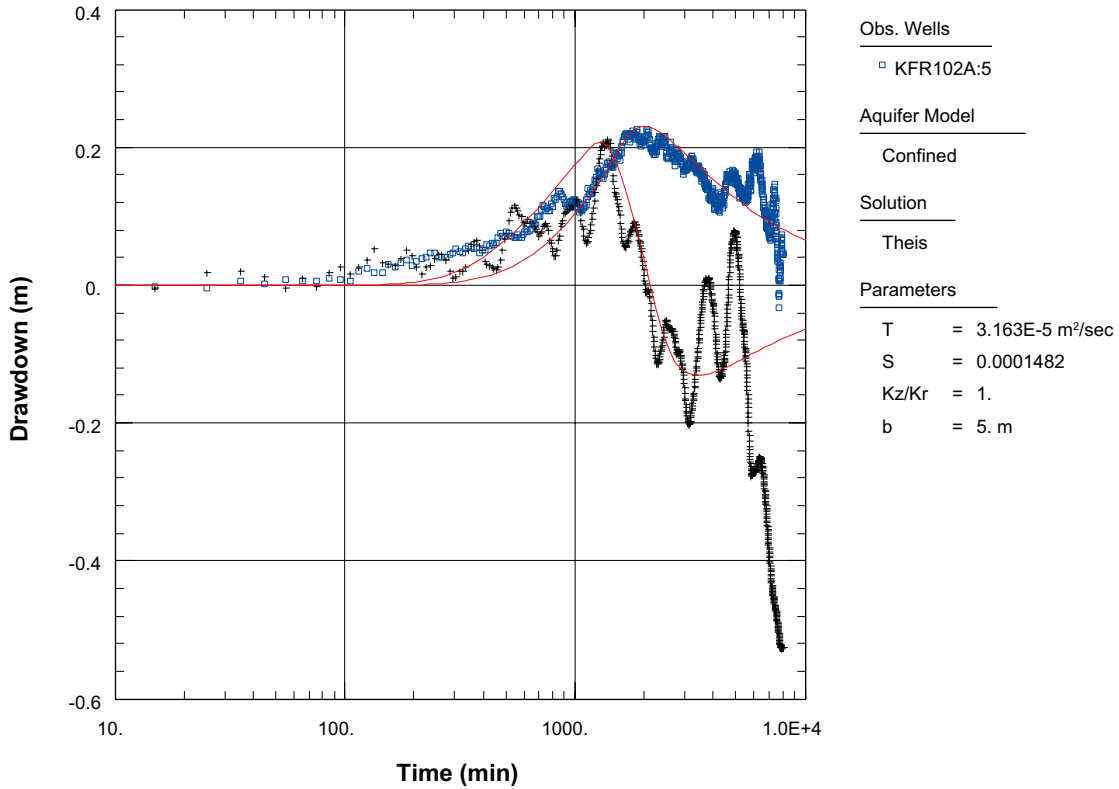


Figure A3-18. Lin-log plot of drawdown (□) and drawdown derivative,  $ds/d(\ln t)$  (+), versus time in the observation borehole section KFR102A:5 during the interference test in KFR105.

Interference test in KFR105, observation borehole section KFR102A:6

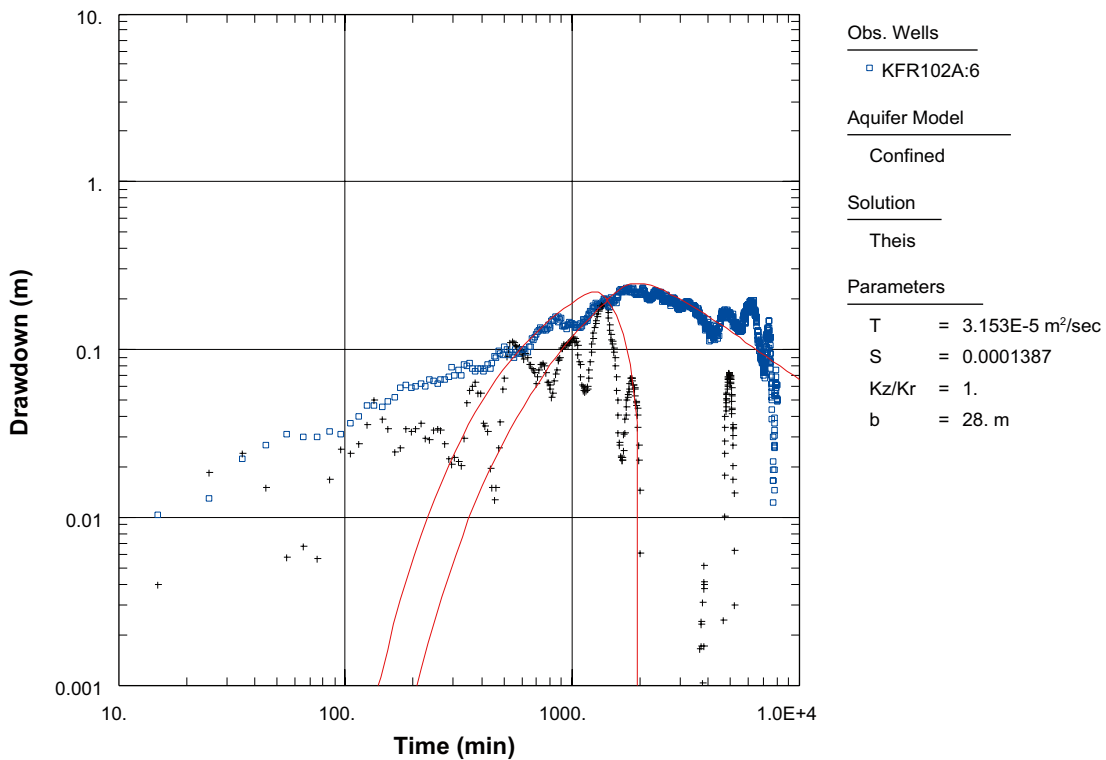
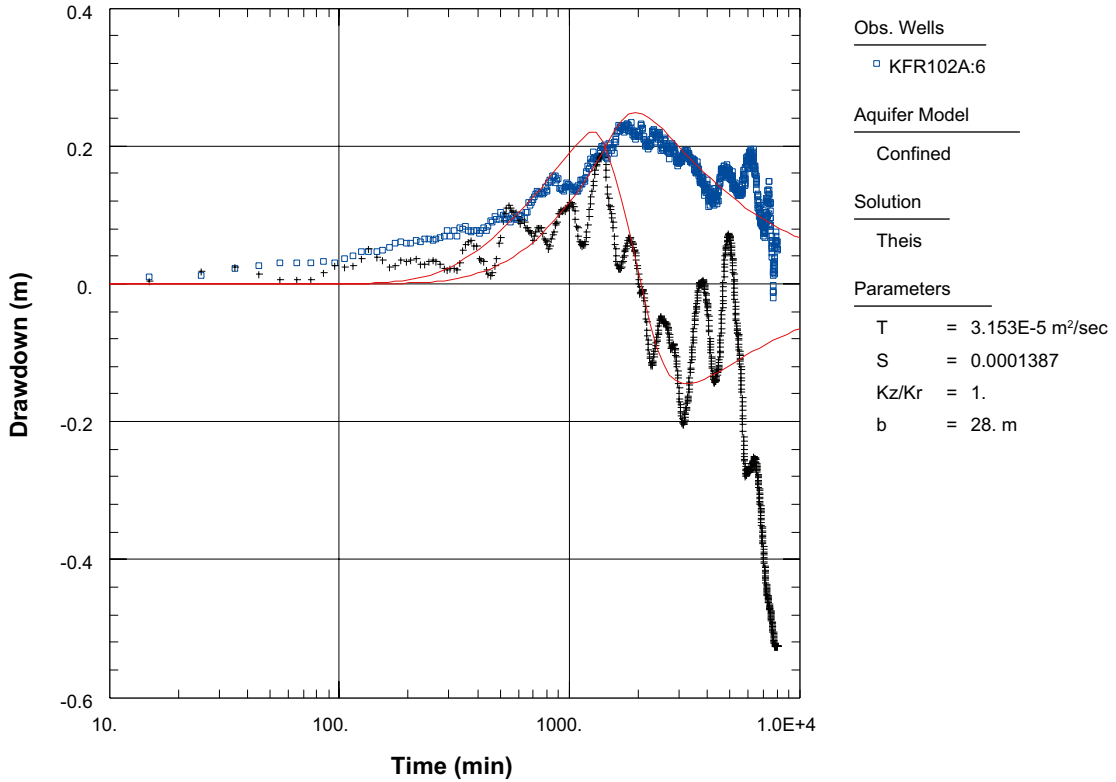


Figure A3-19. Log-log plot of drawdown (□) and drawdown derivative,  $ds/d(\ln t)$  (+), versus time in the observation borehole section KFR102A:6 during the interference test in KFR105.

**Interference test in KFR105, observation borehole section KFR102A:6**



*Figure A3-20. Lin-log plot of drawdown (◻) and drawdown derivative,  $ds/d(\ln t)$  (+), versus time in the observation borehole section KFR102A:6 during the interference test in KFR105.*

**Interference test in KFR105, observation borehole section KFR102A:7**

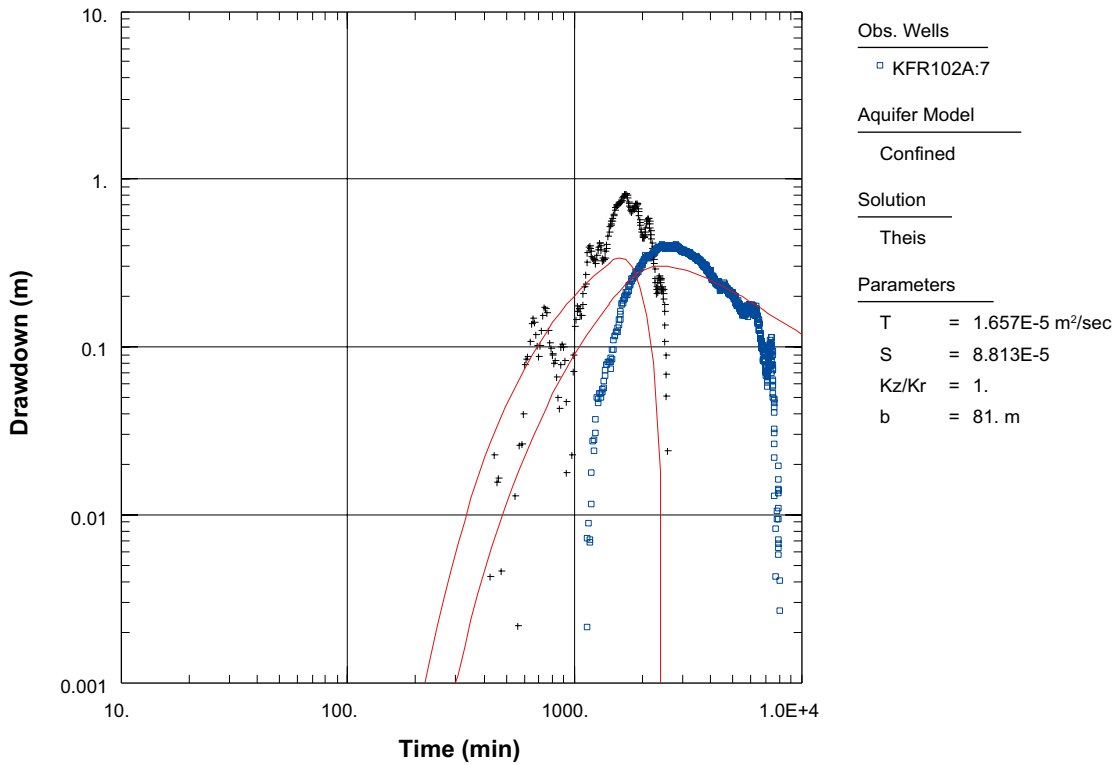


*Figure A3-21. Log-log plot of drawdown (◻) and drawdown derivative,  $ds/d(\ln t)$  (+), versus time in the observation borehole section KFR102A:7 during the interference test in KFR105.*

Interference test in KFR105, observation borehole section KFR102A:7

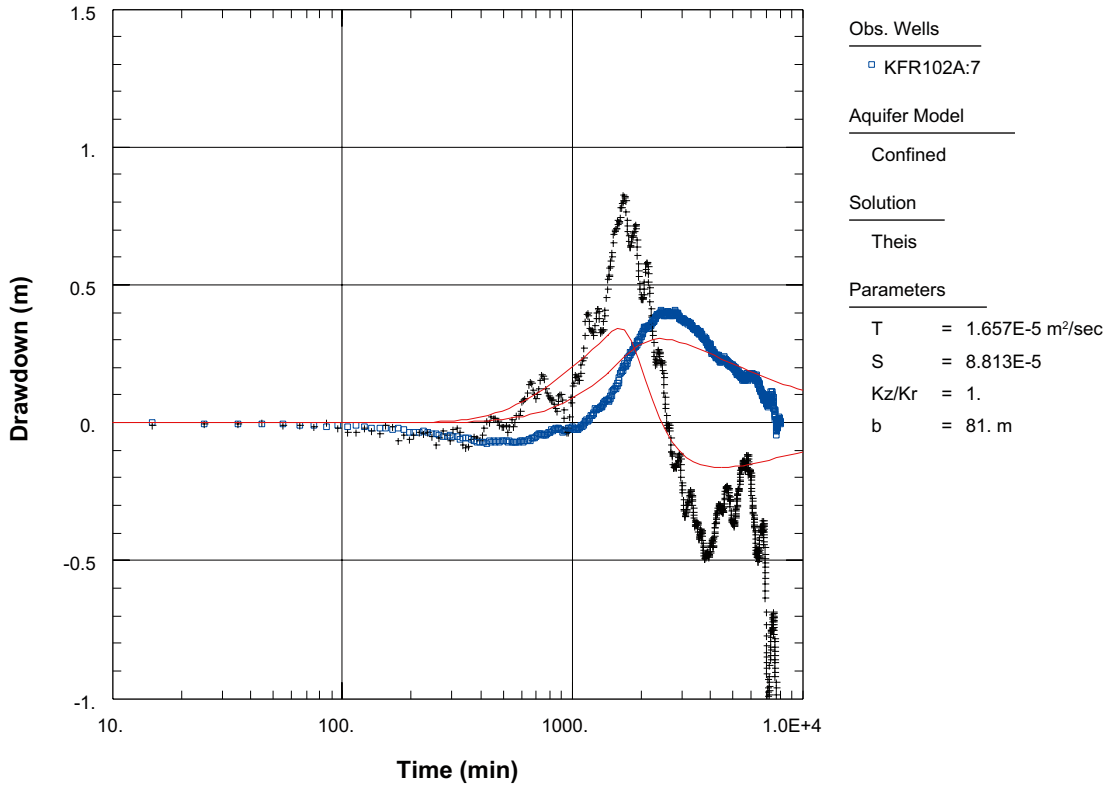


Figure A3-22. Lin-log plot of drawdown (□) and drawdown derivative,  $ds/d(\ln t)$  (+), versus time in the observation borehole section KFR102A:7 during the interference test in KFR105.

Interference test in KFR105, observation borehole section KFR102A:8

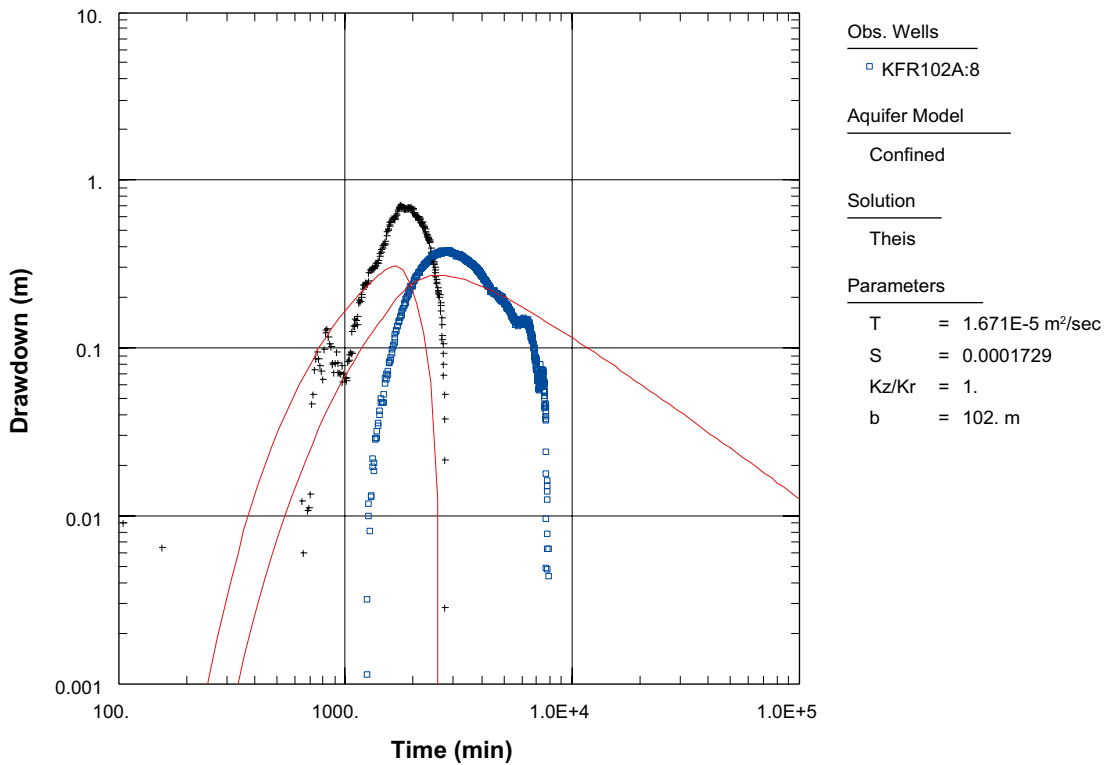
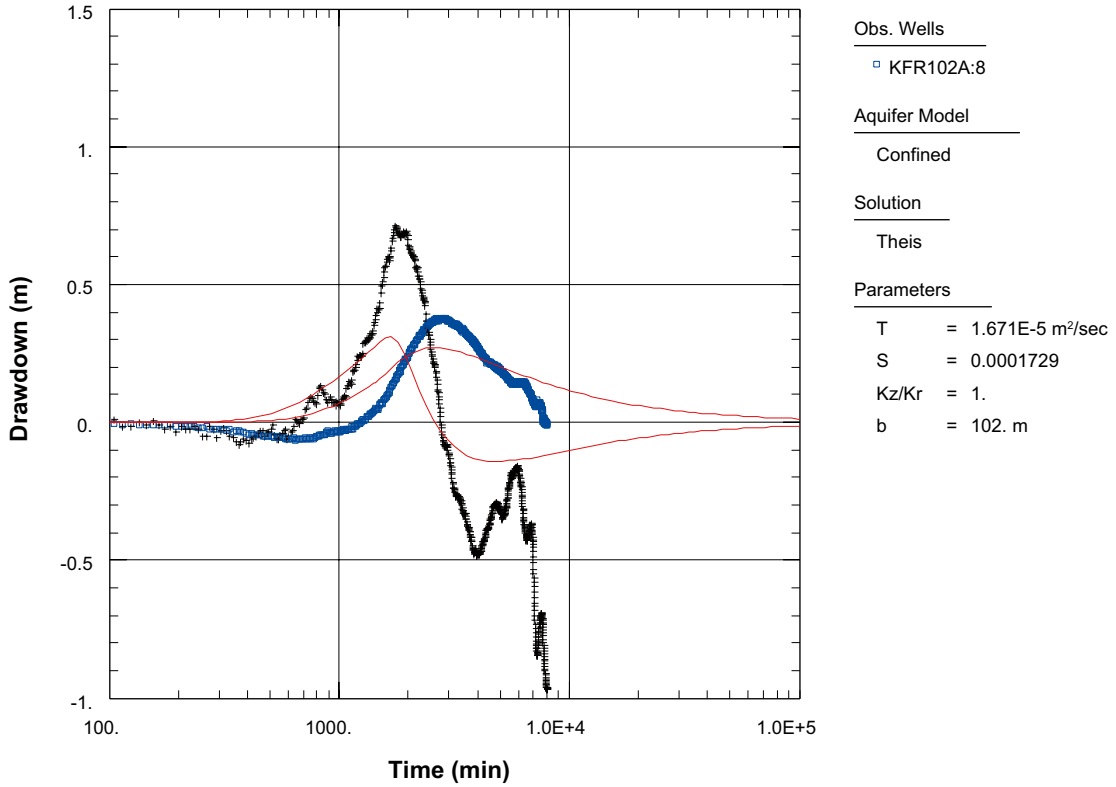


Figure A3-23. Log-log plot of drawdown (□) and drawdown derivative,  $ds/d(\ln t)$  (+), versus time in the observation borehole section KFR102A:8 during the interference test in KFR105.

**Interference test in KFR105, observation borehole section KFR102A:8**



*Figure A3-24. Lin-log plot of drawdown (□) and drawdown derivative,  $ds/d(\ln t)$  (+), versus time in the observation borehole section KFR102A:8 during the interference test in KFR105.*

**Interference test in KFR105, observation borehole section KFR103:2**

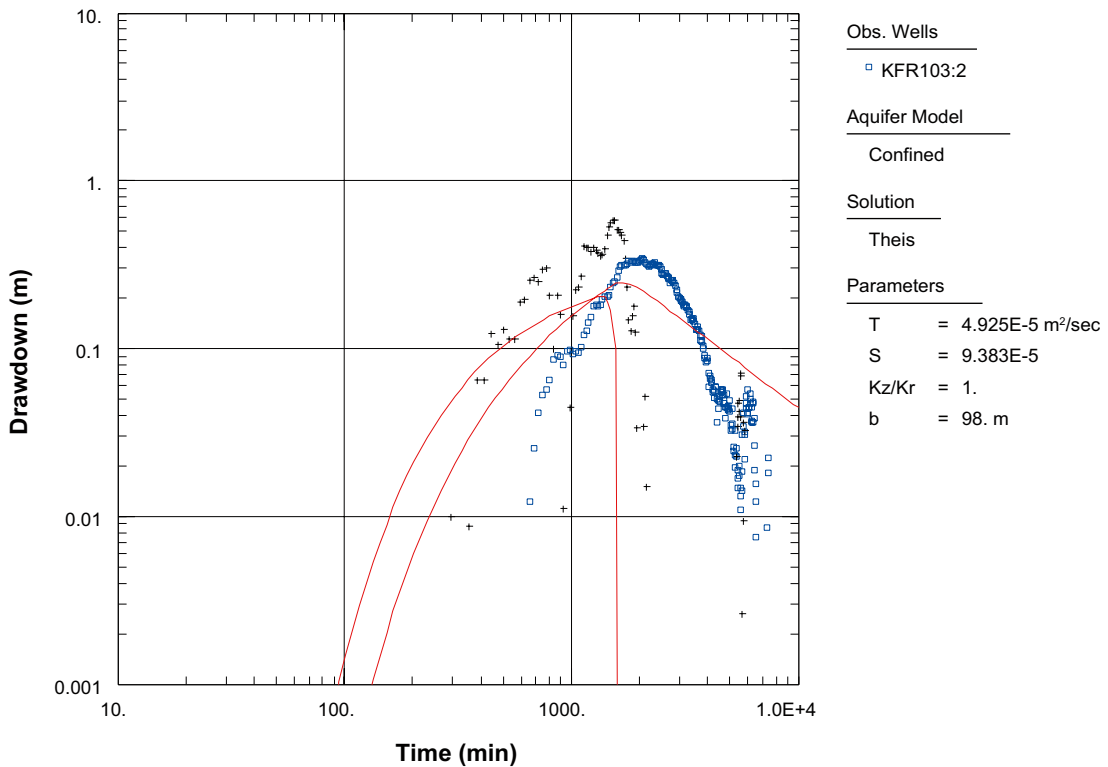


*Figure A3-25. Log-log plot of drawdown (□) and drawdown derivative,  $ds/d(\ln t)$  (+), versus time in the observation borehole section KFR103:2 during the interference test in KFR105.*

Interference test in KFR105, observation borehole section KFR103:2

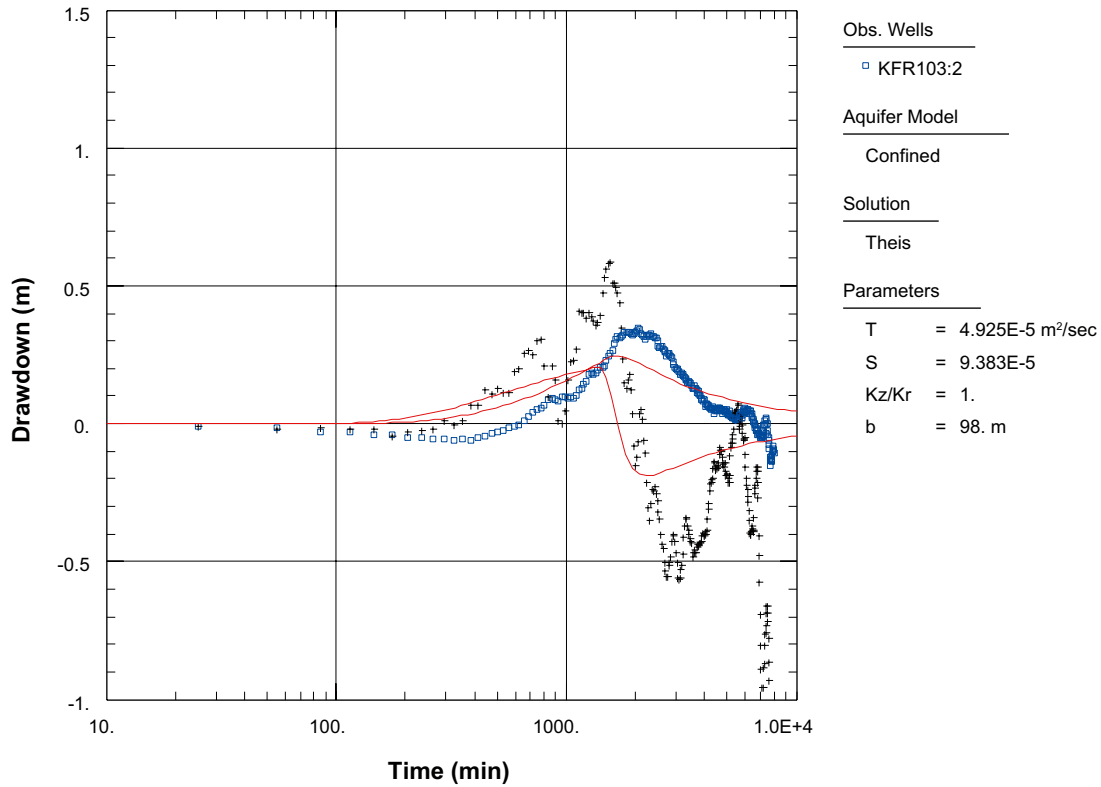


Figure A3-26. Lin-log plot of drawdown (□) and drawdown derivative,  $ds/d(\ln t)$  (+), versus time in the observation borehole section KFR103:2 during the interference test in KFR105.

Interference test in KFR105, observation borehole section KFR104:1

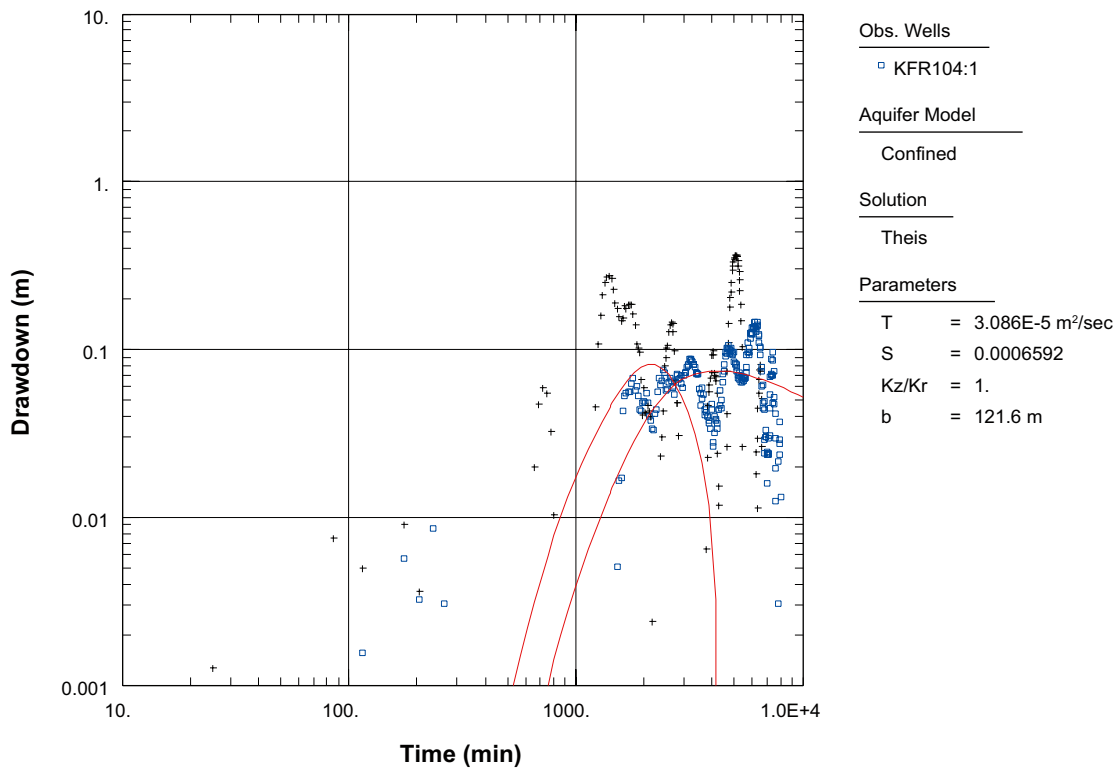
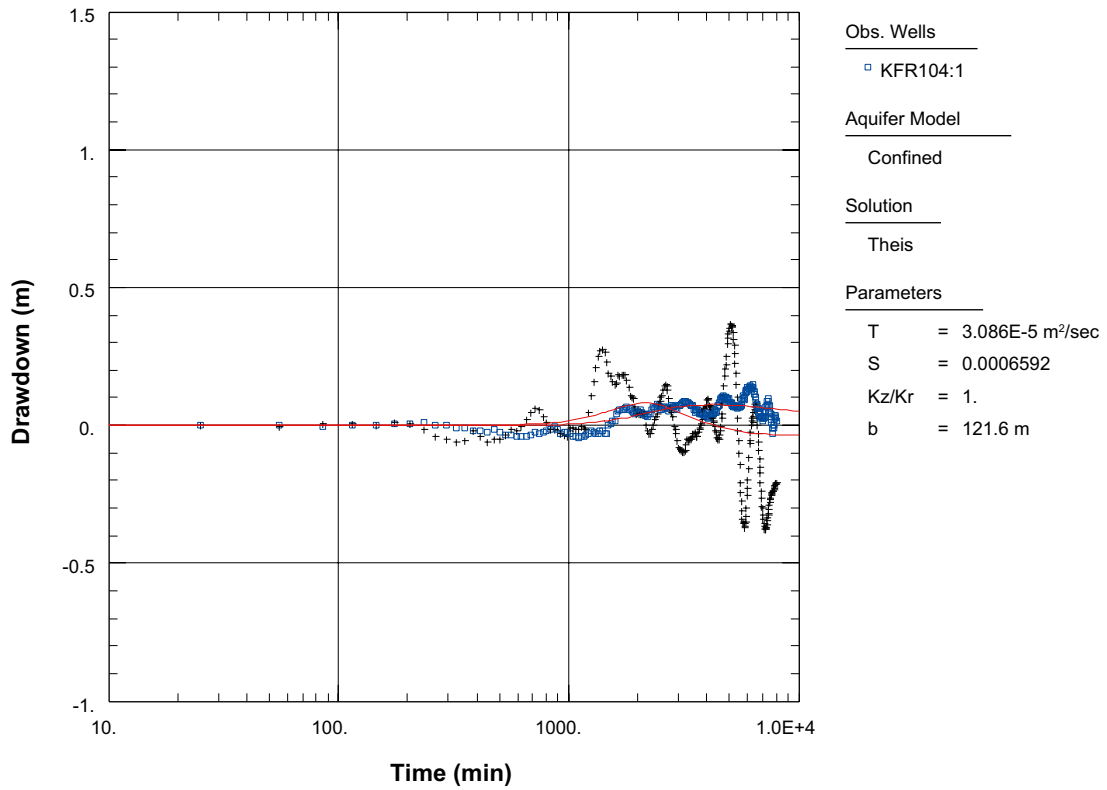


Figure A3-27. Log-log plot of drawdown (□) and drawdown derivative,  $ds/d(\ln t)$  (+), versus time in the observation borehole section KFR104:1 during the interference test in KFR105.



**Interference test in KFR105, observation borehole section KFR104:1**



**Figure A3-28.** Lin-log plot of drawdown (□) and drawdown derivative,  $ds/d(\ln t)$  (+), versus time in the observation borehole section KFR104:1 during the interference test in KFR105.

**Interference test in KFR105, observation borehole section KFR104:2**

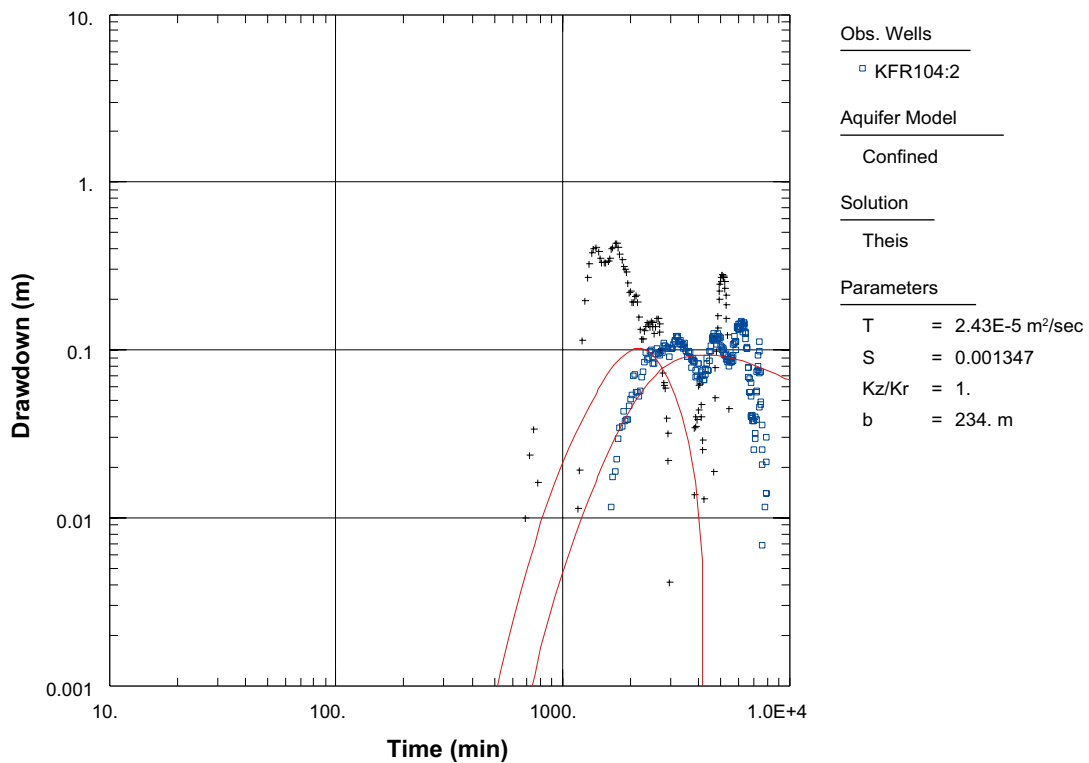


**Figure A3-29.** Log-log plot of drawdown (□) and drawdown derivative,  $ds/d(\ln t)$  (+), versus time in the observation borehole section KFR104:2 during the interference test in KFR105.

**Interference test in KFR105, observation borehole section KFR104:2**

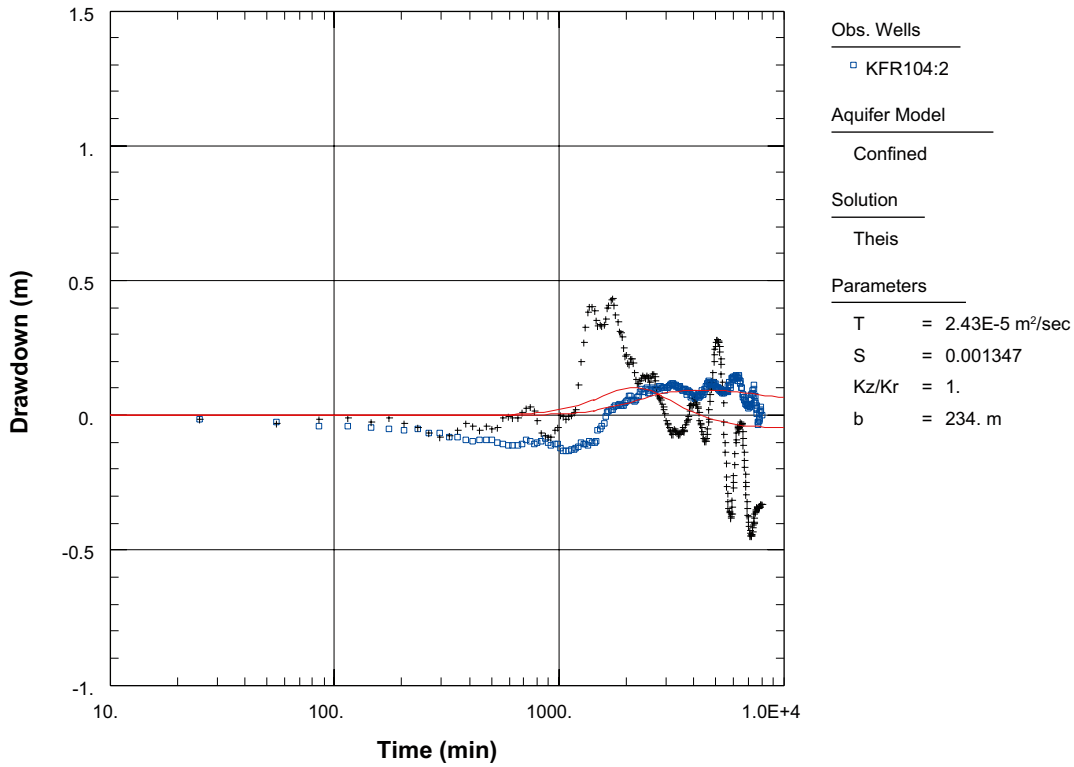


*Figure A3-30. Lin-log plot of drawdown (□) and drawdown derivative,  $ds/d(\ln t)$  (+), versus time in the observation borehole section KFR104:2 during the interference test in KFR105.*

**A3.2 Interference pumping test in HFR101**

**Interference test in HFR101, observation borehole section KFR02:1**

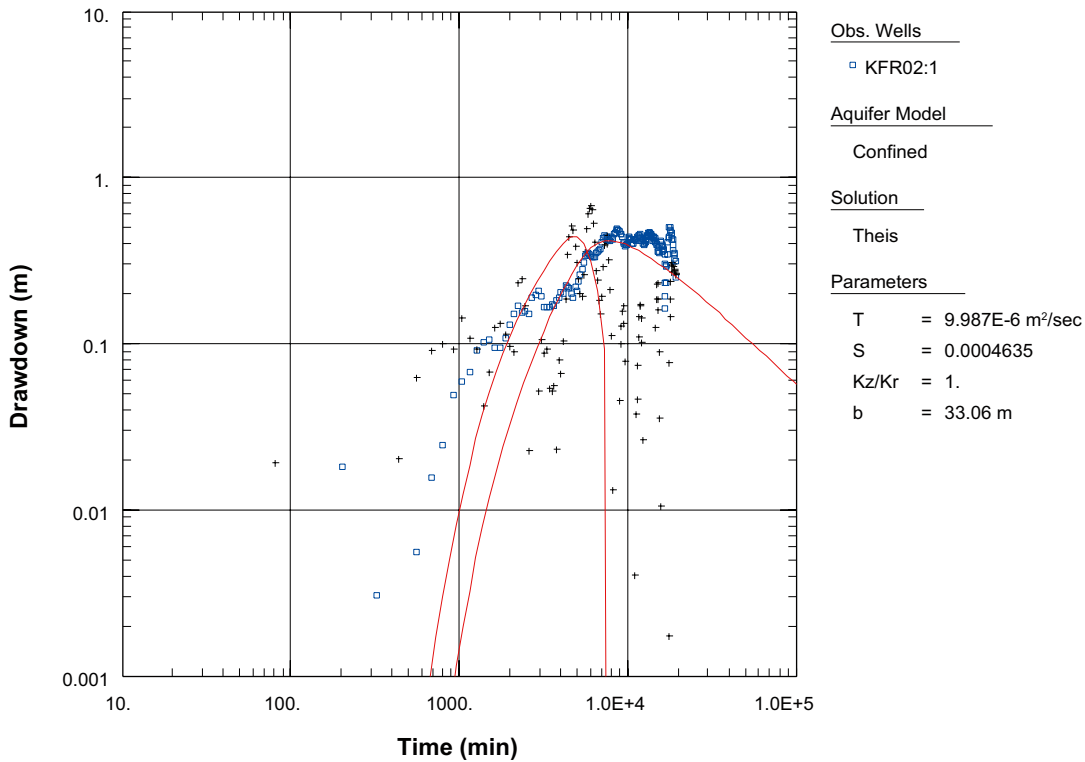


*Figure A3-31. Log-log plot of drawdown (□) and drawdown derivative,  $ds/d(\ln t)$  (+), versus time in the observation borehole section KFR02:1 during the interference pumping test in HFR101.*

**Interference test in HFR101, observation borehole section KFR02:1**

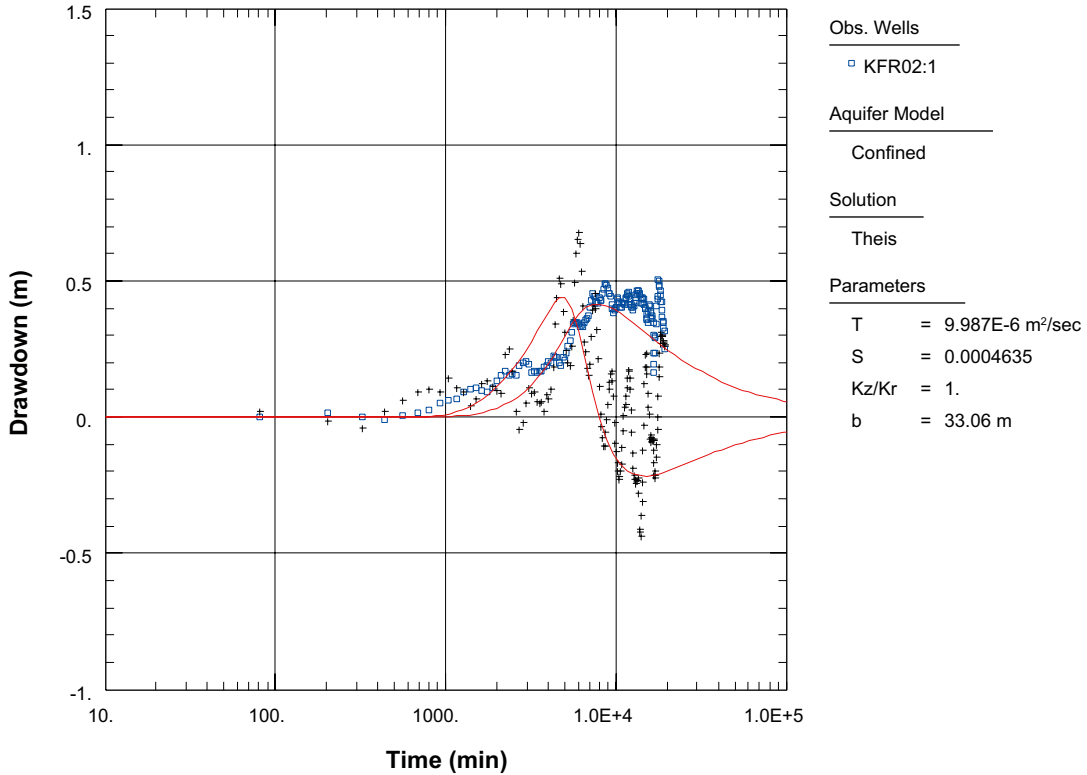


*Figure A3-32. Lin-log plot of drawdown (□) and drawdown derivative,  $ds/d(\ln t)$  (+), versus time in the observation borehole section KFR02:1 during the interference pumping test in HFR101.*

**Interference test in HFR101, observation borehole section KFR02:2**

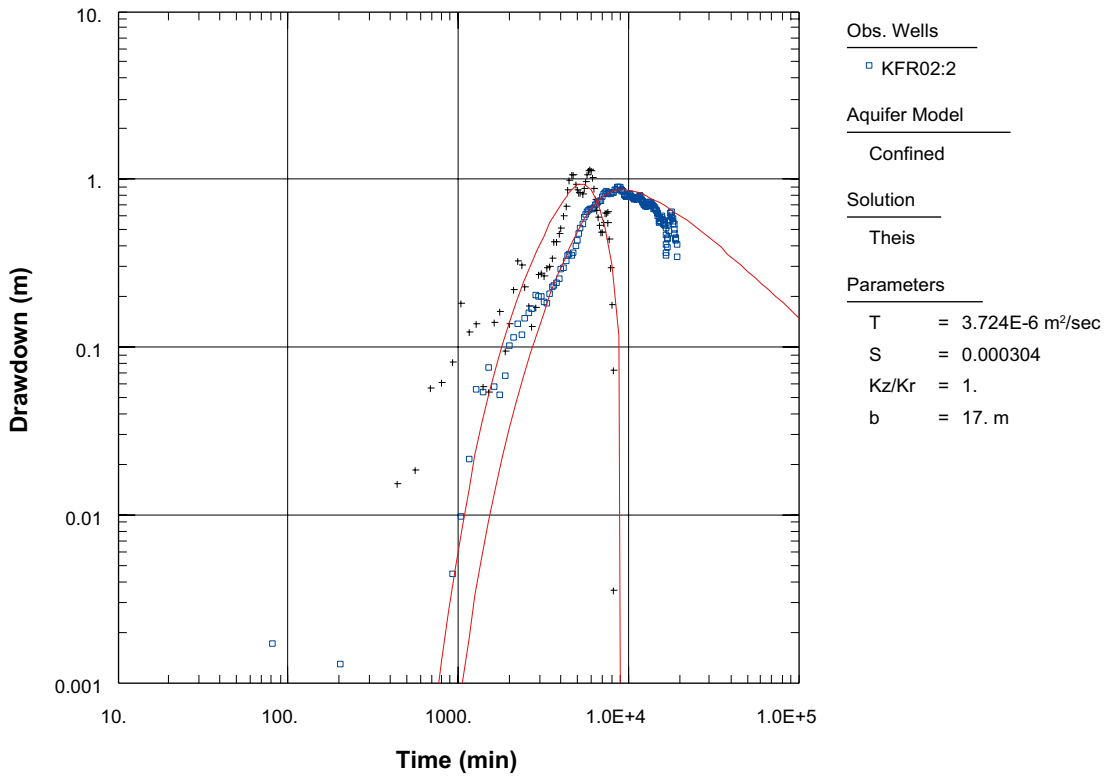


*Figure A3-33. Log-log plot of drawdown (□) and drawdown derivative,  $ds/d(\ln t)$  (+), versus time in the observation borehole section KFR02:2 during the interference pumping test in HFR101.*

Interference test in HFR101, observation borehole section KFR02:2

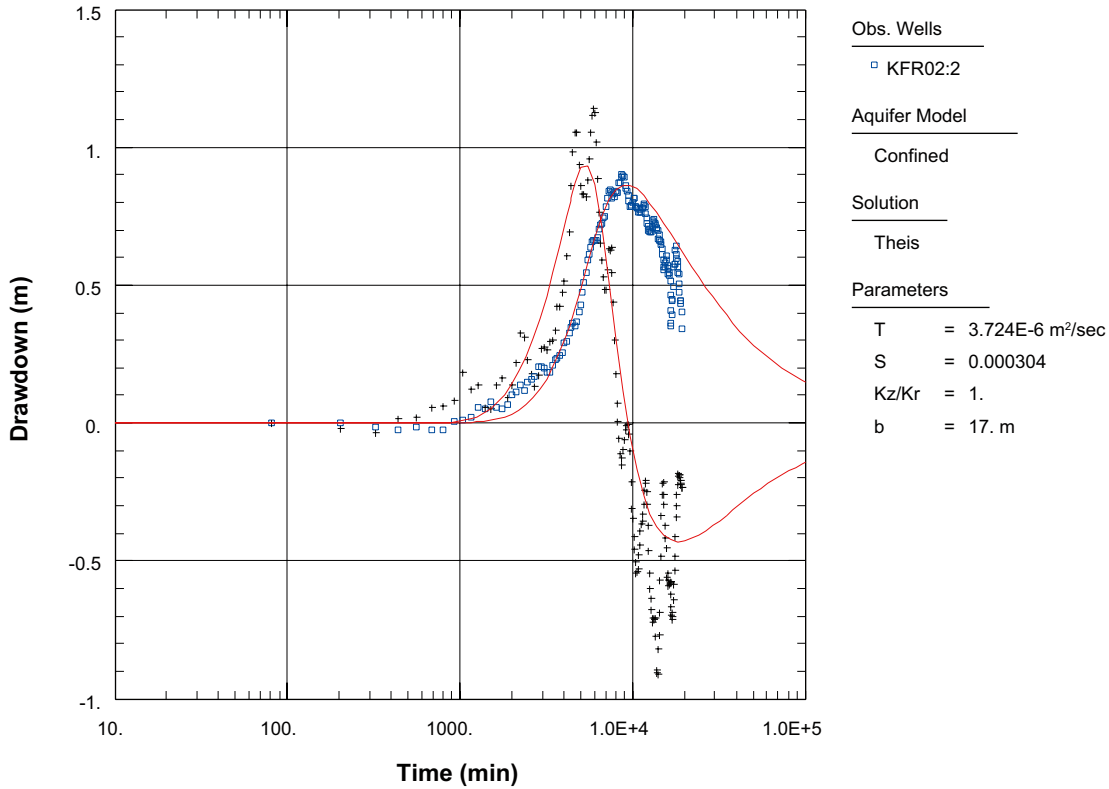


Figure A3-34. Lin-log plot of drawdown (□) and drawdown derivative,  $ds/d(\ln t)$  (+), versus time in the observation borehole section KFR02:2 during the interference pumping test in HFR101.

Interference test in HFR101, observation borehole section KFR02:3

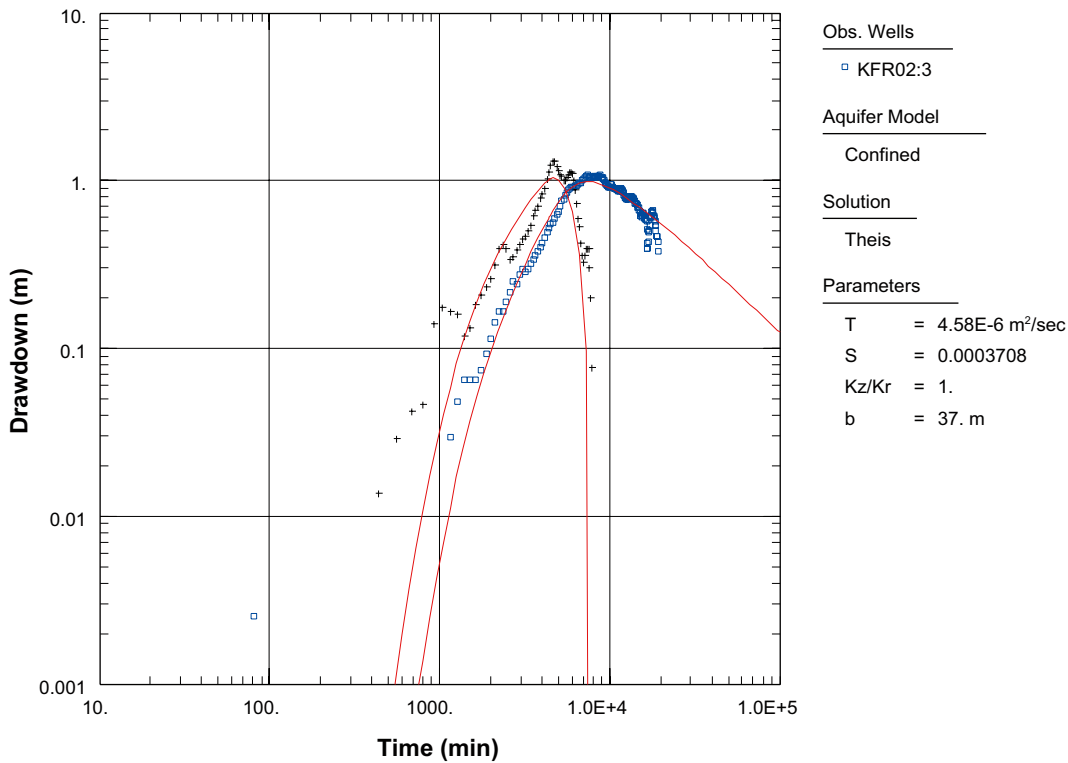
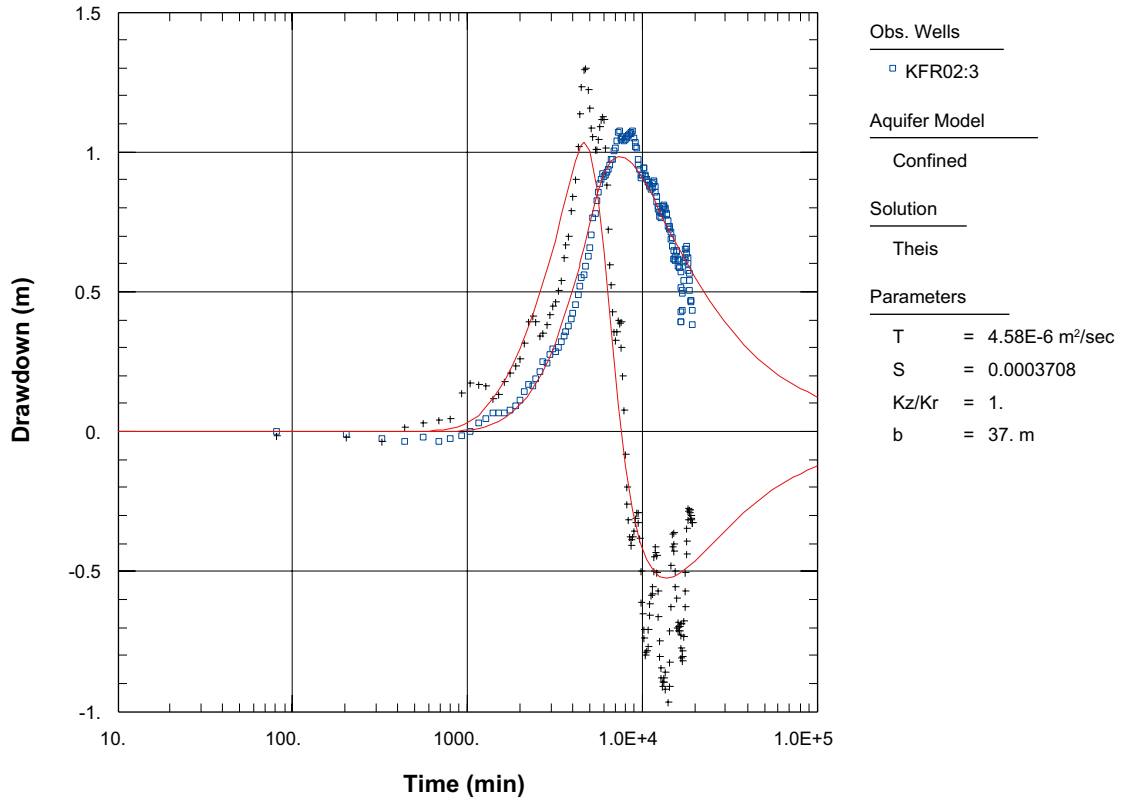


Figure A3-35. Log-log plot of drawdown (□) and drawdown derivative,  $ds/d(\ln t)$  (+), versus time in the observation borehole section KFR02:3 during the interference pumping test in HFR101.

**Interference test in HFR101, observation borehole section KFR02:3**



**Figure A3-36.** Lin-log plot of drawdown (◻) and drawdown derivative,  $ds/d(\ln t)$  (+), versus time in the observation borehole section KFR02:3 during the interference pumping test in HFR101.

**Interference test in HFR101, observation borehole section KFR02:4**

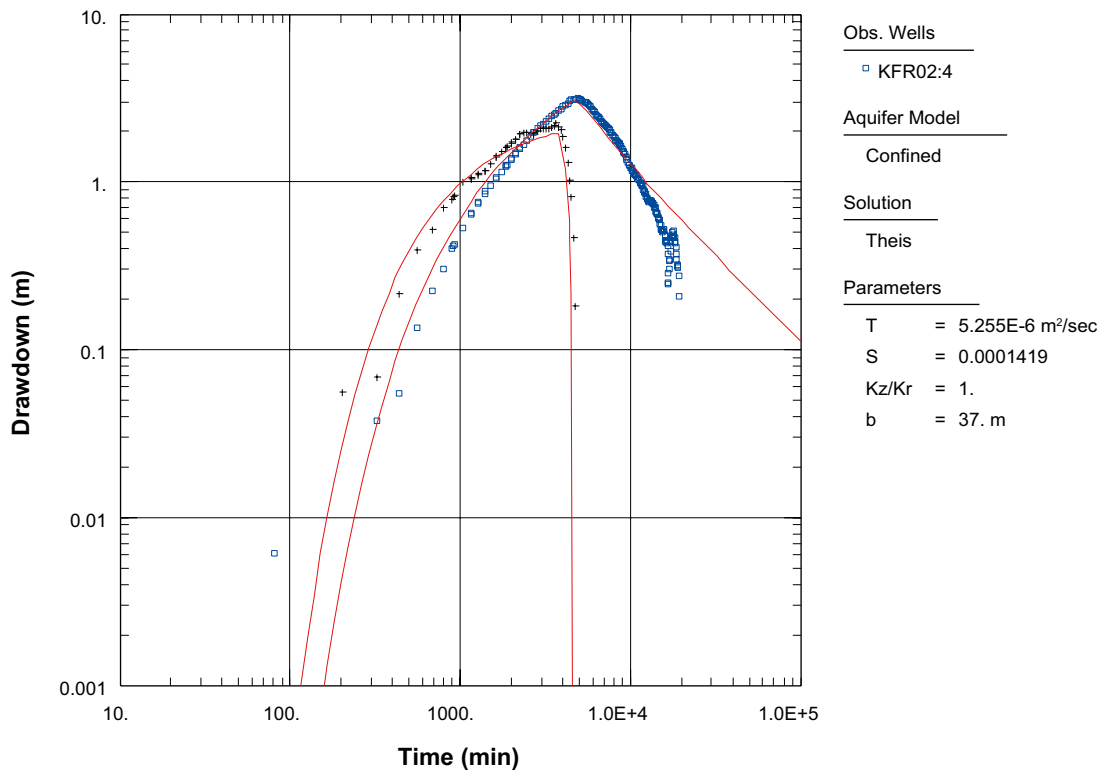


**Figure A3-37.** Log-log plot of drawdown (◻) and drawdown derivative,  $ds/d(\ln t)$  (+), versus time in the observation borehole section KFR02:4 during the interference pumping test in HFR101.

**Interference test in HFR101, observation borehole section KFR02:4**

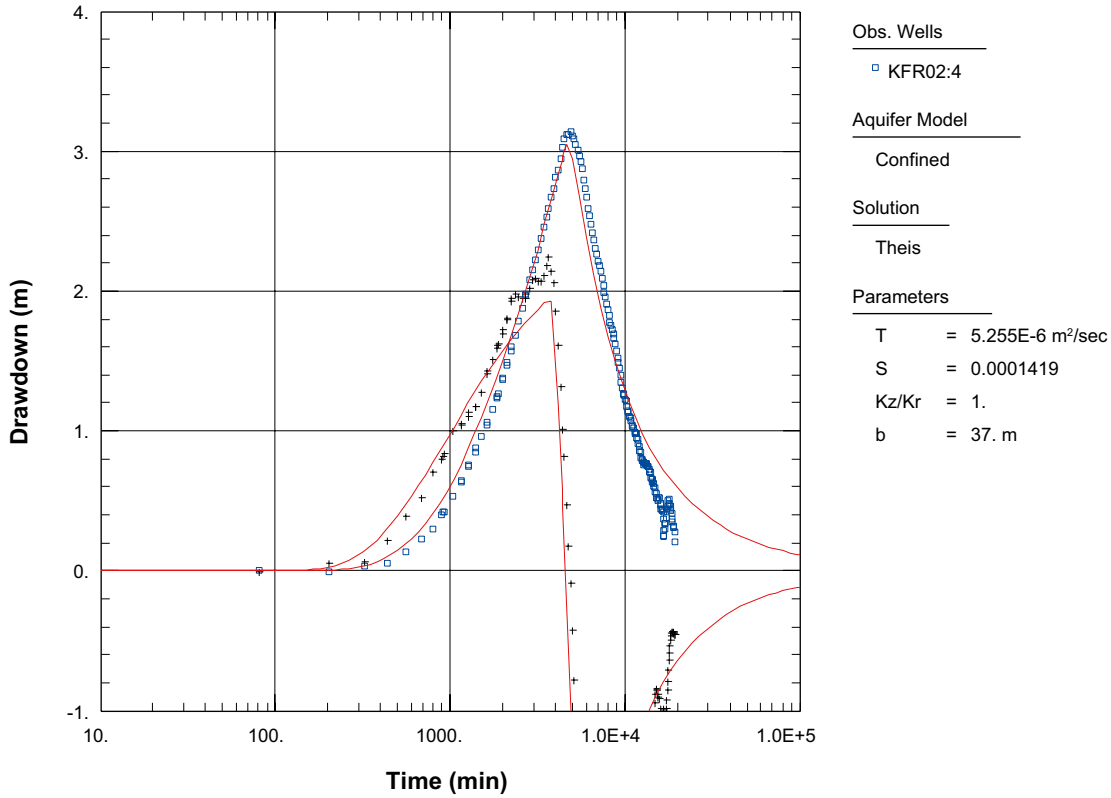


*Figure A3-38. Lin-log plot of drawdown (□) and drawdown derivative,  $ds/d(\ln t)$  (+), versus time in the observation borehole section KFR02:4 during the interference pumping test in HFR101.*

**Interference test in HFR101, observation borehole section KFR104:1**

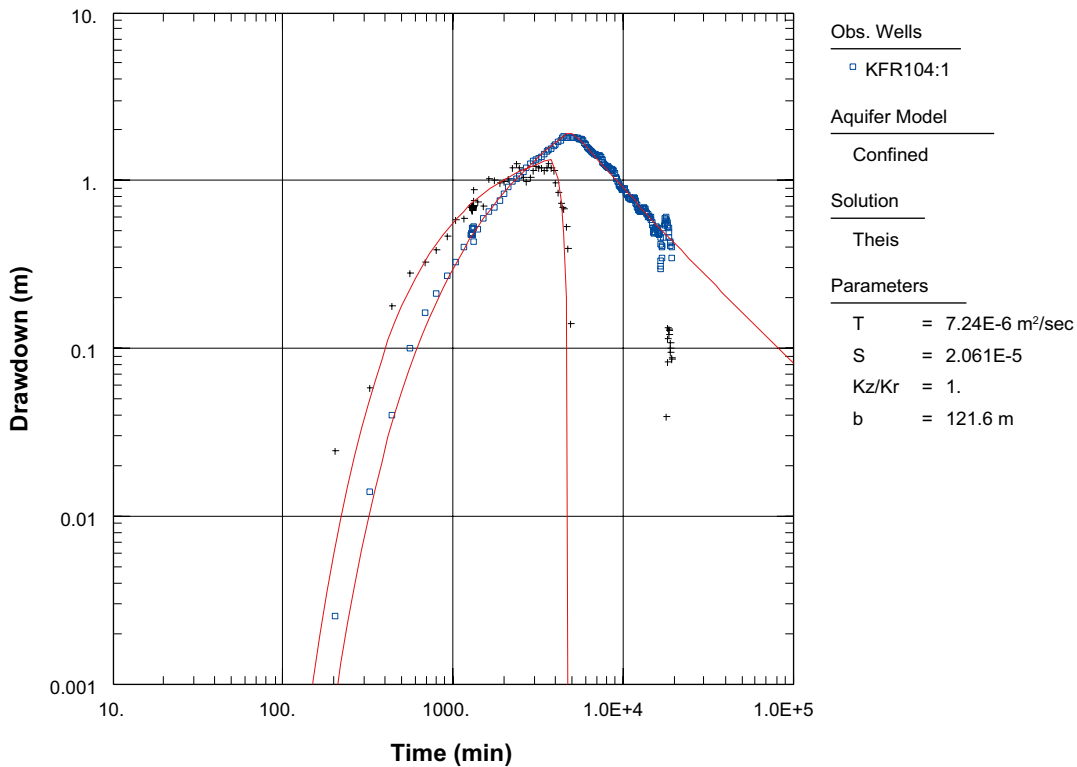


*Figure A3-39. Log-log plot of drawdown (□) and drawdown derivative,  $ds/d(\ln t)$  (+), versus time in the observation borehole section KFR104:1 during the interference pumping test in HFR101.*

**Interference test in HFR101, observation borehole section KFR104:1**

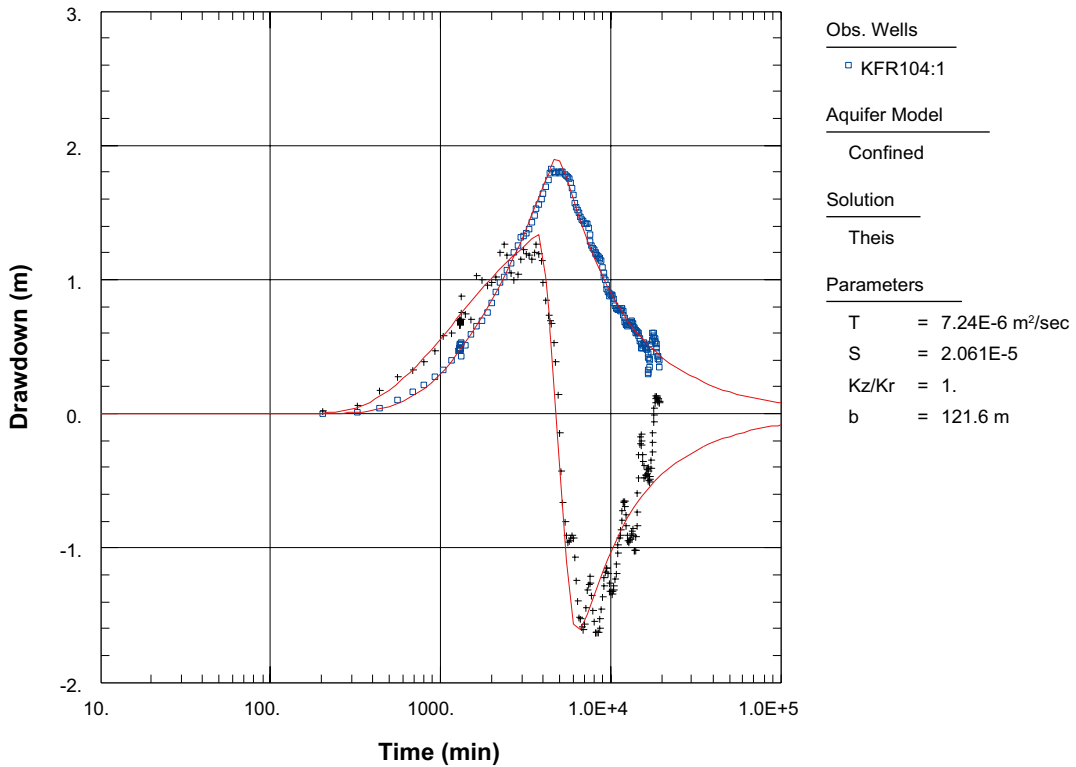


**Figure A3-40.** Lin-log plot of drawdown (□) and drawdown derivative,  $ds/d(\ln t)$  (+), versus time in the observation borehole section KFR104:1 during the interference pumping test in HFR101.

**Interference test in HFR101, observation borehole section KFR104:2**

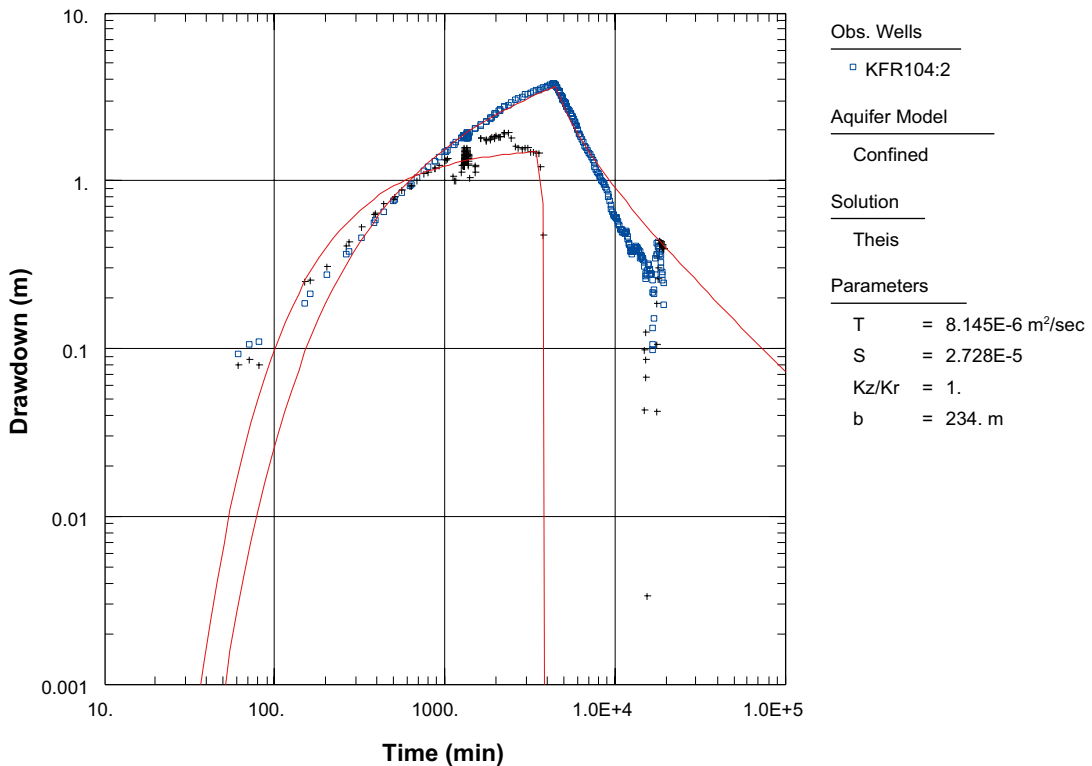


**Figure A3-41.** Log-log plot of drawdown (□) and drawdown derivative,  $ds/d(\ln t)$  (+), versus time in the observation borehole section KFR104:2 during the interference pumping test in HFR101.

**Interference test in HFR101, observation borehole section KFR104:2**

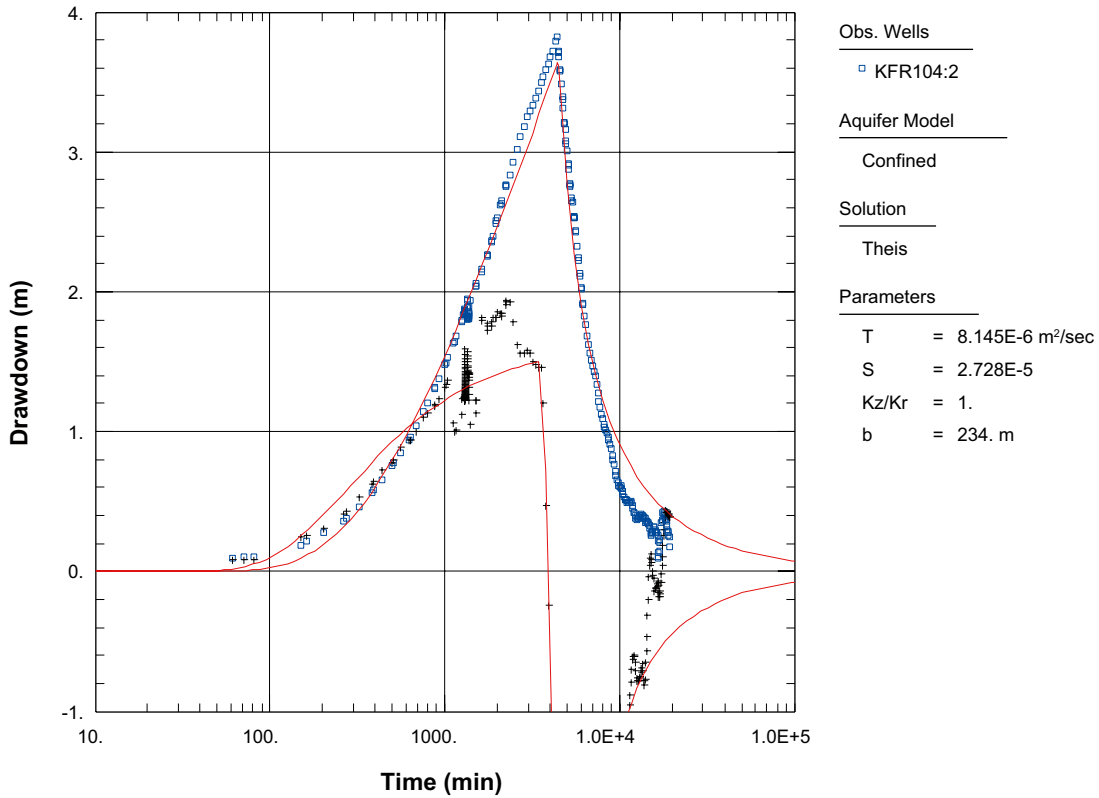


*Figure A3-42. Lin-log plot of drawdown (◻) and drawdown derivative,  $ds/d(\ln t)$  (+), versus time in the observation borehole section KFR104:2 during the interference pumping test in HFR101.*

**Interference test in HFR101, observation borehole section KFR104:3**

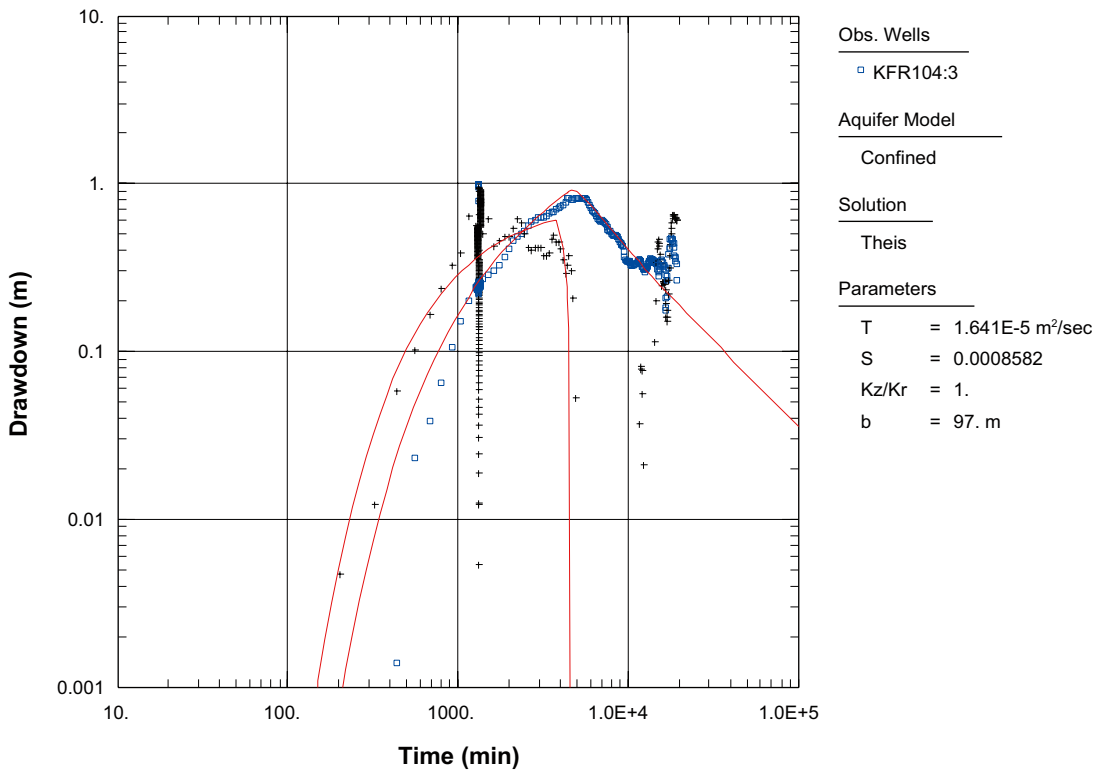


*Figure A3-43. Log-log plot of drawdown (◻) and drawdown derivative,  $ds/d(\ln t)$  (+), versus time in the observation borehole section KFR104:3 during the interference pumping test in HFR101.*



**Interference test in HFR101, observation borehole section KFR104:3**

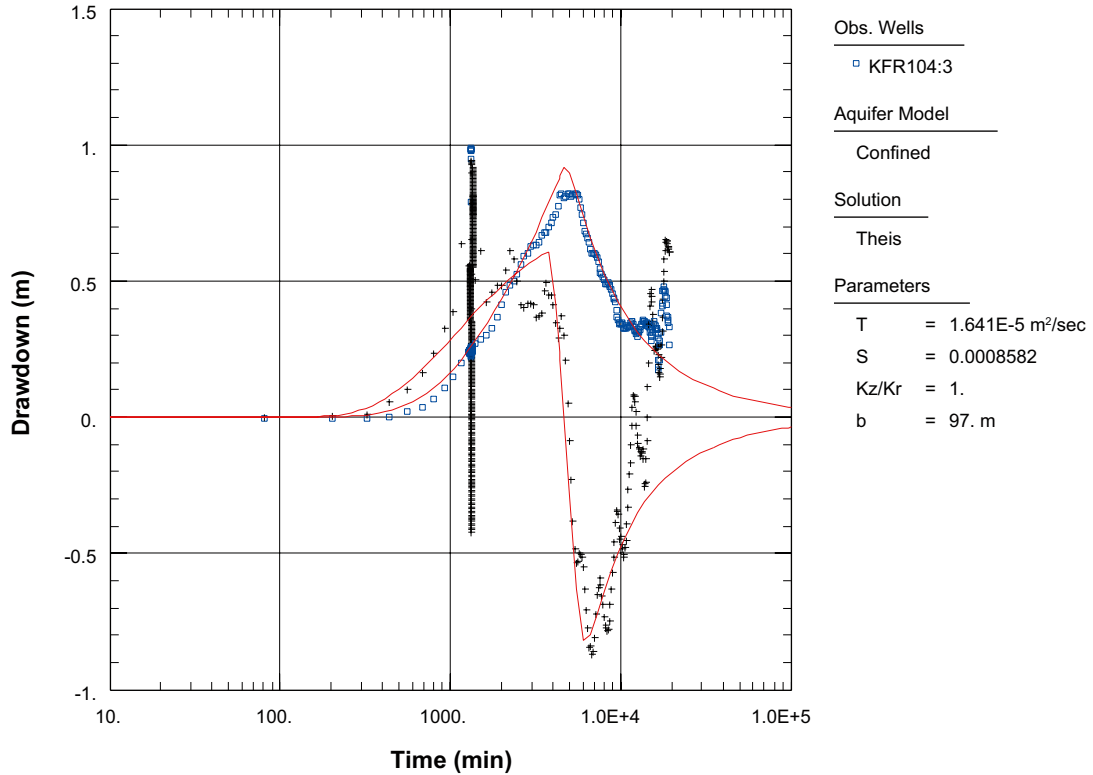


*Figure A3-44. Lin-log plot of drawdown (◻) and drawdown derivative,  $ds/d(\ln t)$  (+), versus time in the observation borehole section KFR104:3 during the interference pumping test in HFR101.*

**Interference pumping test in HFR101, observation borehole section HFR105:1**

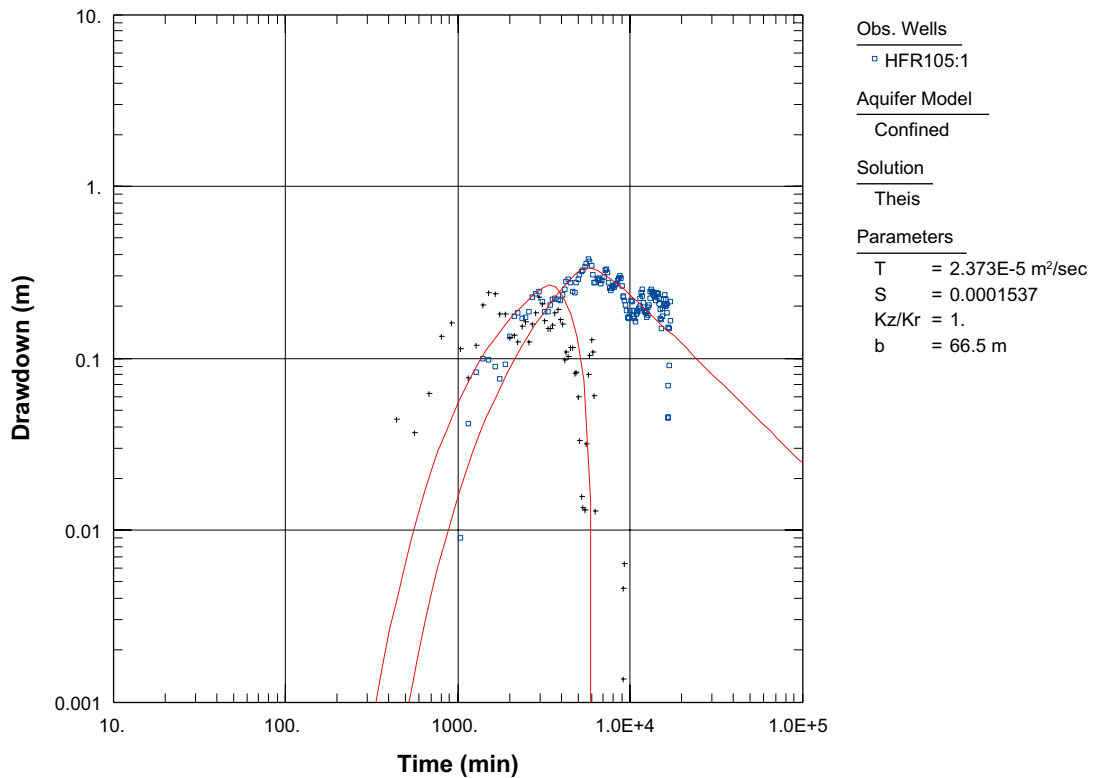


*Figure A3-45. Log-log plot of drawdown (◻) and drawdown derivative,  $ds/d(\ln t)$  (+), versus time in the observation borehole section HFR105:1 during the interference pumping test in HFR101.*

**Interference pumping test in HFR101, observation borehole section HFR105:1**

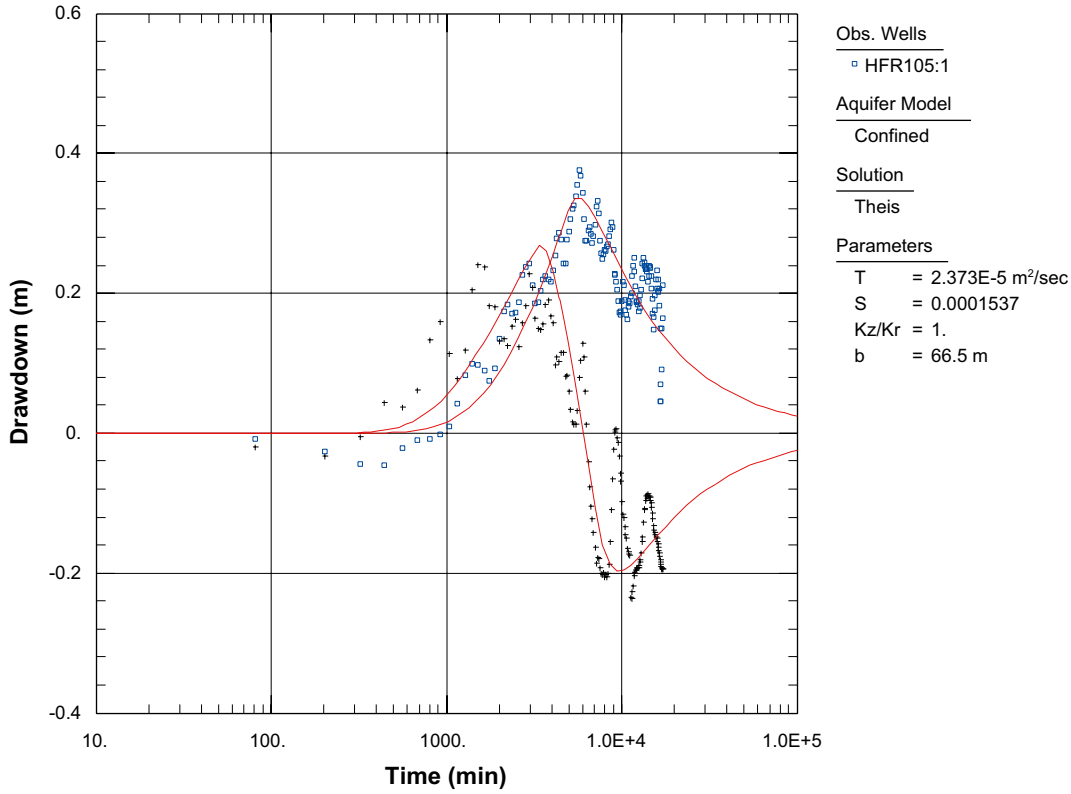


*Figure A3-46. Lin-log plot of drawdown (□) and drawdown derivative,  $ds/d(\ln t)$  (+), versus time in the observation borehole section HFR105:1 during the interference pumping test in HFR101.*

**Interference pumping test in HFR101, observation borehole section HFR105:2**

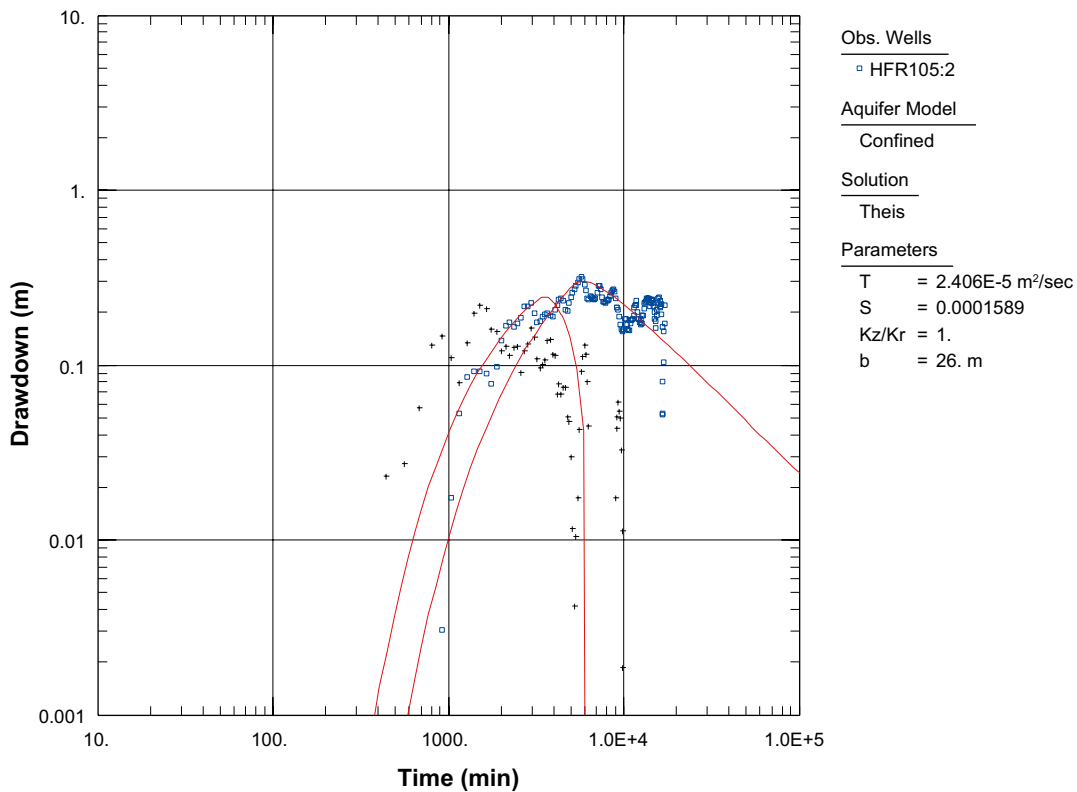


*Figure A3-47. Log-log plot of drawdown (□) and drawdown derivative,  $ds/d(\ln t)$  (+), versus time in the observation borehole section HFR105:2 during the interference pumping test in HFR101.*

**Interference pumping test in HFR101, observation borehole section HFR105:2**

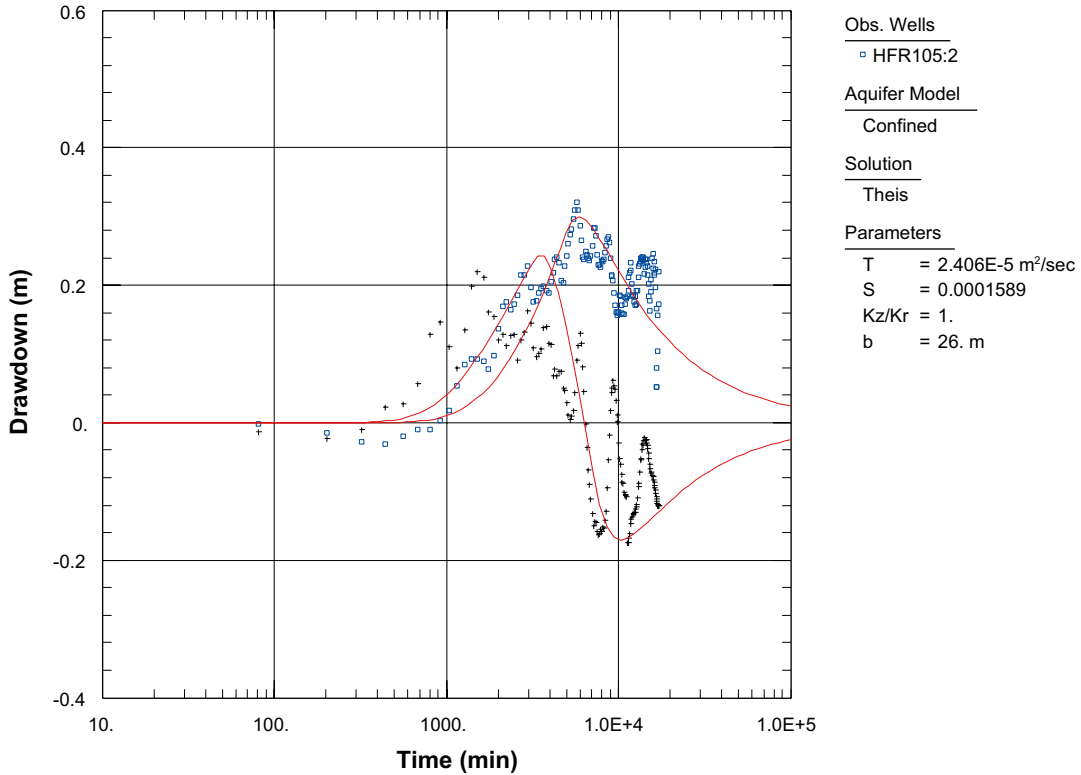


*Figure A3-48. Lin-log plot of drawdown (◻) and drawdown derivative,  $ds/d(\ln t)$  (+), versus time in the observation borehole section HFR105:2 during the interference pumping test in HFR101.*

**Interference pumping test in HFR101, observation borehole section HFR105:3**

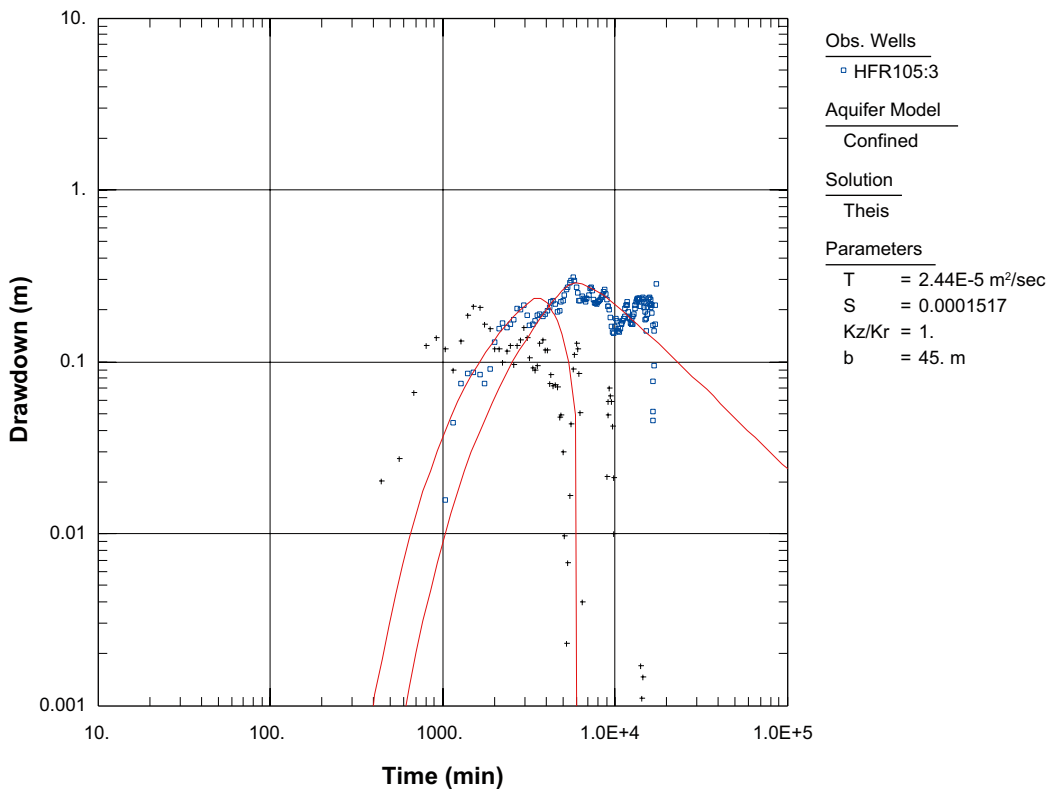


*Figure A3-49. Log-log plot of drawdown (◻) and drawdown derivative,  $ds/d(\ln t)$  (+), versus time in the observation borehole section HFR105:3 during the interference pumping test in HFR101.*

**Interference pumping test in HFR101, observation borehole section HFR105:3**

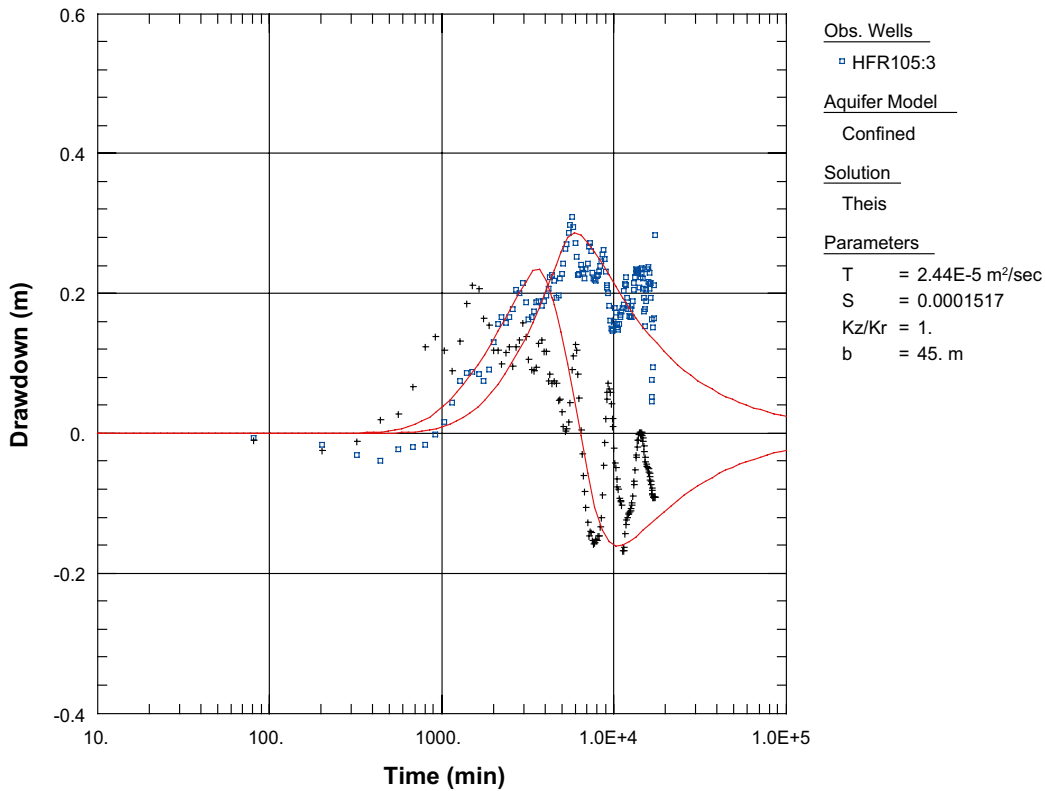


*Figure A3-50. Lin-log plot of drawdown (□) and drawdown derivative,  $ds/d(\ln t)$  (+), versus time in the observation borehole section HFR105:3 during the interference pumping test in HFR101.*

**Interference pumping test in HFR101, observation borehole section HFR105:4**

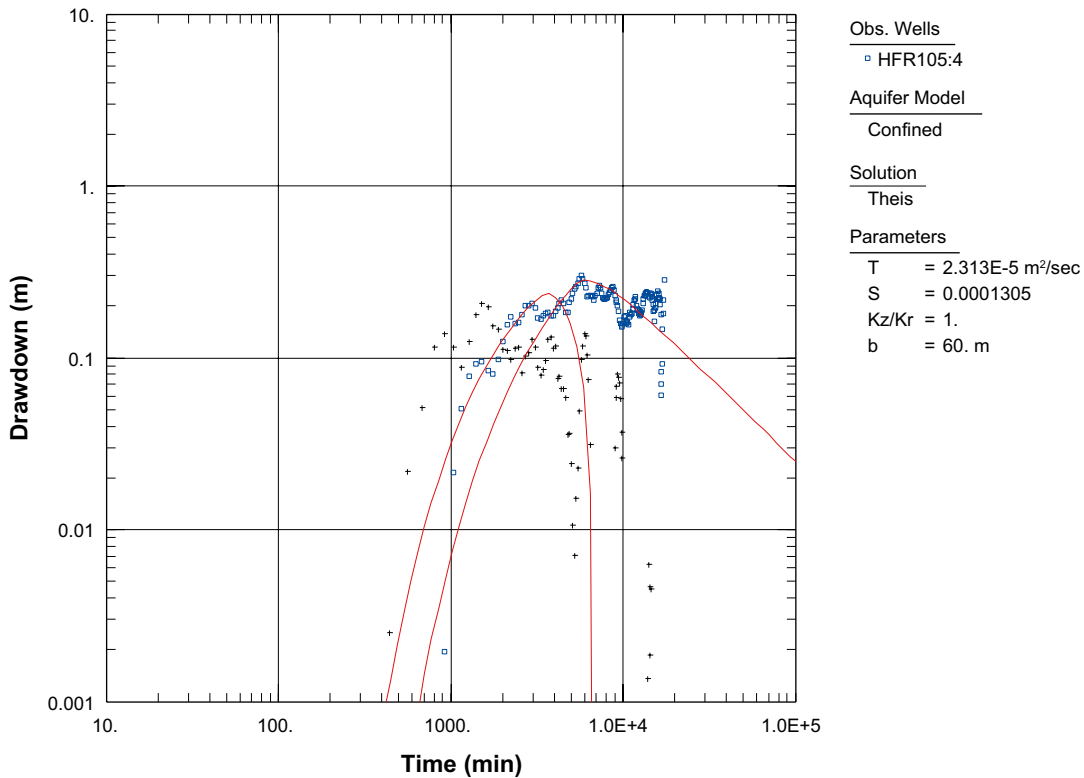


*Figure A3-51. Log-log plot of drawdown (□) and drawdown derivative,  $ds/d(\ln t)$  (+), versus time in the observation borehole section HFR105:4 during the interference pumping test in HFR101.*

**Interference pumping test in HFR101, observation borehole section HFR105:4**

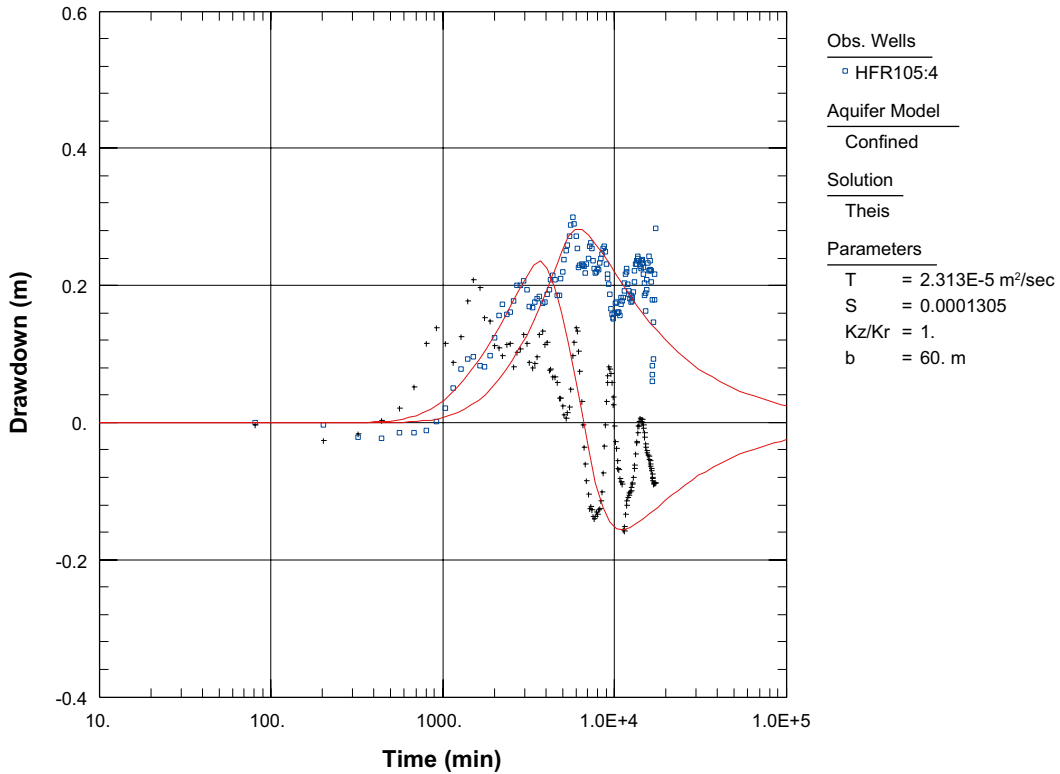


*Figure A3-52. Lin-log plot of drawdown (□) and drawdown derivative,  $ds/d(\ln t)$  (+), versus time in the observation borehole section HFR105:4 during the interference pumping test in HFR101.*

**A3.3 Interference injection test in HFR101**

**Injection test in HFR101, observation borehole section KFR02:4**

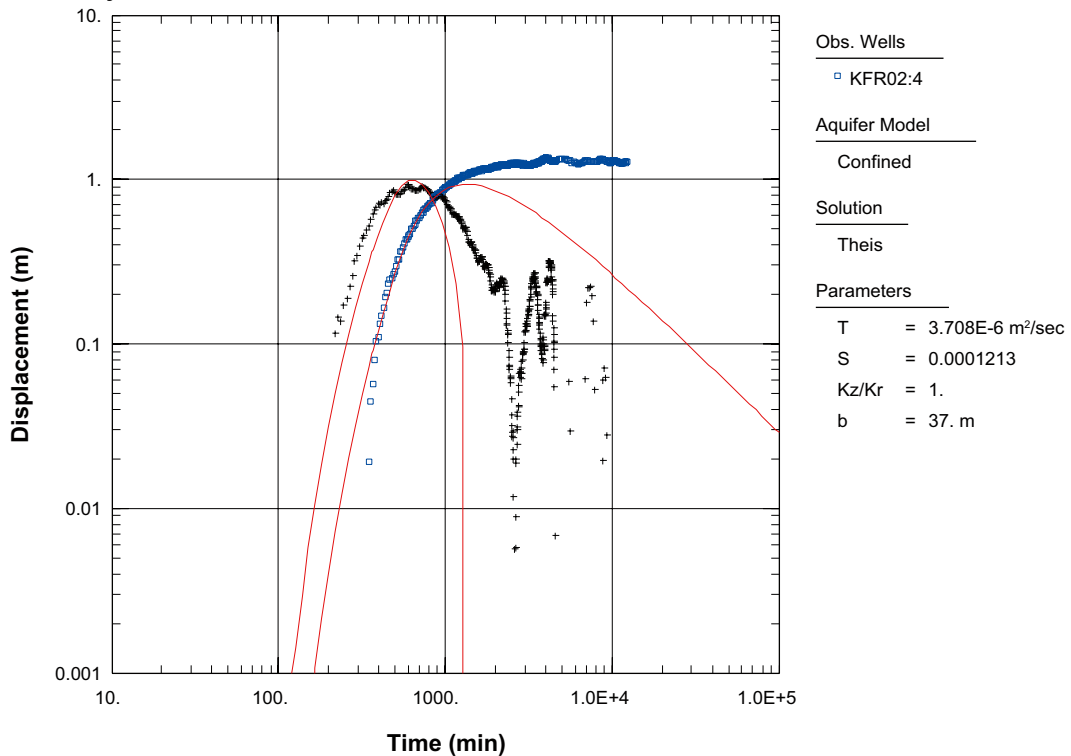


*Figure A3-53. Log-log plot of drawdown (□) and drawdown derivative,  $ds/d(\ln t)$  (+), versus time in the observation borehole section KFR02:4 during the interference injection test in HFR101.*

**Injection test in HFR101, observation borehole section KFR02:4**

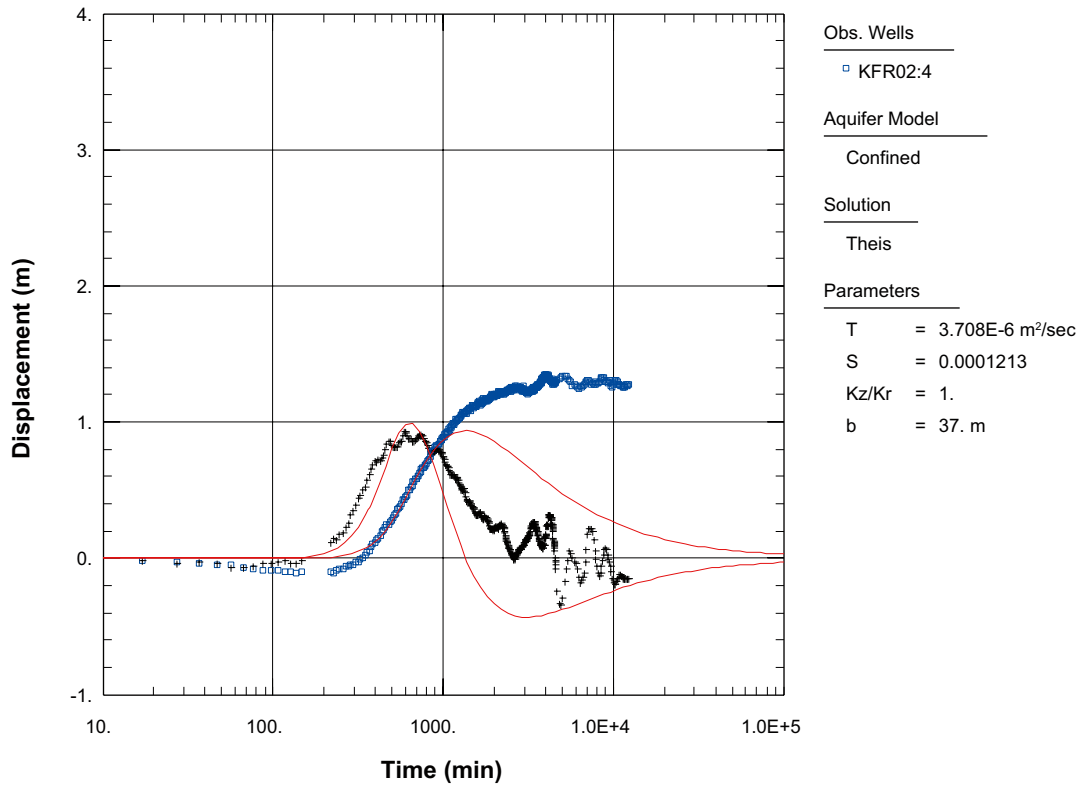


*Figure A3-54. Lin-log plot of drawdown (□) and drawdown derivative,  $ds/d(\ln t)$  (+), versus time in the observation borehole section KFR02:4 during the interference injection test in HFR101.*

### Response index 1 and spherical distance ( $r_s$ ) to all observation borehole sections during drilling

Drilling borehole	Observation borehole	Secup (m)	Seclow (m)	$r_s$ (m)	Index1 $r_s^2/dt_L$ ( $m^2/s$ )
HFR102	HFR105:0	21.20	200.50	424.2	0.00
HFR102	KFR01:1	44.65	62.30	643.5	0.00
HFR102	KFR01:2	11.15	43.65	628.7	0.00
HFR102	KFR02:1	137.24	170.30	241.5	0.00
HFR102	KFR02:2	119.24	136.24	218.8	0.00
HFR102	KFR02:3	81.24	118.24	195.2	0.00
HFR102	KFR02:4	43.24	80.24	165.4	0.00
HFR102	KFR03:1	81.16	101.60	233.3	0.00
HFR102	KFR03:2	57.16	80.16	219.5	0.00
HFR102	KFR03:3	45.16	56.16	209.6	0.00
HFR102	KFR03:4	5.16	44.16	197.5	0.00
HFR102	KFR04:1	84.09	100.50	270.6	0.00
HFR102	KFR04:2	44.09	83.09	255.6	0.00
HFR102	KFR04:3	28.09	43.09	243.4	0.00
HFR102	KFR04:4	5.09	27.09	236.5	0.00
HFR102	KFR05:1	97.15	131.00	309.1	0.00
HFR102	KFR05:2	80.15	96.15	289.5	0.00
HFR102	KFR05:3	57.15	79.15	275.0	0.00
HFR102	KFR05:4	12.15	56.15	252.2	0.00
HFR102	KFR7A:1	48.11	74.70	390.0	0.00
HFR102	KFR7A:2	20.11	47.11	363.1	0.00
HFR102	KFR7A:3	2.11	19.11	341.0	0.00
HFR102	KFR7B:1	8.60	21.10	338.2	0.00
HFR102	KFR7B:2	3.40	7.60	332.8	0.00
HFR102	KFR08:1	62.95	104.00	419.3	0.00
HFR102	KFR08:2	35.95	61.95	391.9	0.00
HFR102	KFR08:3	5.95	34.95	370.1	0.00
HFR102	KFR09:1	0.00	80.24	325.8	0.00
HFR102	KFR13:1	53.75	76.60	264.1	0.00
HFR102	KFR13:2	33.75	52.75	251.1	0.00
HFR102	KFR13:3	3.75	32.75	237.9	0.00
HFR102	KFR19:1	95.57	110.00	268.6	0.00
HFR102	KFR19:2	77.57	94.57	254.4	0.00
HFR102	KFR19:3	66.82	76.57	242.4	0.00
HFR102	KFR19:4	51.82	65.82	231.9	0.00
HFR102	KFR27:0	0.00	146.50	190.3	0.00
HFR102	KFR55:1	48.53	61.89	281.1	0.00
HFR102	KFR55:2	39.53	47.53	273.3	0.00
HFR102	KFR55:3	21.53	38.53	264.6	0.00
HFR102	KFR55:4	7.53	20.53	254.9	0.00
HFR102	KFR56:1	9.55	81.70	363.1	0.00
HFR106	KFR02:1	137.24	170.30	653.3	4.72
HFR106	KFR02:2	119.24	136.24	648.8	4.66
HFR106	KFR02:3	81.24	118.24	645.0	4.42
HFR106	KFR02:4	43.24	80.24	641.9	3.93
HFR106	KFR13:1	53.75	76.60	530.9	3.25
HFR106	KFR13:2	33.75	52.75	528.2	3.35
HFR106	KFR13:3	3.75	32.75	526.2	3.82
HFR106	KFR103:1	178.00	200.50	161.7	25.63
HFR106	KFR103:2	79.00	177.00	173.6	1.56
HFR106	HFR102:1	28.00	55.04	531.1	0.00
HFR106	HFR102:2	0.00	27.00	549.1	0.00
HFR106	HFR105:1	134.00	200.50	785.1	0.00
HFR106	HFR105:2	107.00	133.00	798.4	0.00

Drilling borehole	Observation borehole	Secup (m)	Seclow (m)	$r_s$ (m)	Index1 $r_s^2/dt_L$ (m <sup>2</sup> /s)
HFR106	HFR105:3	61.00	106.00	810.2	0.00
HFR106	HFR105:4	0.00	60.00	831.1	0.00
HFR106	KFR01:1	44.65	62.30	1,078.0	0.00
HFR106	KFR01:2	11.15	43.65	1,067.5	0.00
HFR106	KFR03:1	81.16	101.60	604.3	0.00
HFR106	KFR03:2	57.16	80.16	602.5	0.00
HFR106	KFR03:3	45.16	56.16	601.6	0.00
HFR106	KFR03:4	5.16	44.16	601.3	0.00
HFR106	KFR04:1	84.09	100.50	559.1	0.00
HFR106	KFR04:2	44.09	83.09	563.3	0.00
HFR106	KFR04:3	28.09	43.09	568.9	0.00
HFR106	KFR04:4	5.09	27.09	573.5	0.00
HFR106	KFR05:1	97.15	131.00	601.4	0.00
HFR106	KFR05:2	80.15	96.15	594.1	0.00
HFR106	KFR05:3	57.15	79.15	589.1	0.00
HFR106	KFR05:4	12.15	56.15	582.3	0.00
HFR106	KFR7A:1	48.11	74.70	622.9	0.00
HFR106	KFR7A:2	20.11	47.11	608.3	0.00
HFR106	KFR7A:3	2.11	19.11	596.9	0.00
HFR106	KFR7B:1	8.60	21.10	591.5	0.00
HFR106	KFR7B:2	3.40	7.60	589.6	0.00
HFR106	KFR08:1	62.95	104.00	651.5	0.00
HFR106	KFR08:2	35.95	61.95	652.7	0.00
HFR106	KFR08:3	5.95	34.95	655.0	0.00
HFR106	KFR09:1	0.00	80.24	843.9	0.00
HFR106	KFR19:1	95.57	110.00	601.7	0.00
HFR106	KFR19:2	77.57	94.57	600.1	0.00
HFR106	KFR19:3	66.82	76.57	599.1	0.00
HFR106	KFR19:4	51.82	65.82	598.6	0.00
HFR106	KFR27:1	110.00	501.64	405.9	0.00
HFR106	KFR27:2	47.00	109.00	353.1	0.00
HFR106	KFR27:3	0.00	46.00	363.5	0.00
HFR106	KFR55:1	48.53	61.89	589.3	0.00
HFR106	KFR55:2	39.53	47.53	578.2	0.00
HFR106	KFR55:3	21.53	38.53	565.4	0.00
HFR106	KFR55:4	7.53	20.53	550.3	0.00
HFR106	KFR56:1	9.55	81.70	631.6	0.00
HFR106	KFR101:1	279.50	341.76	348.4	0.00
HFR106	KFR101:2	91.00	278.50	270.9	0.00
HFR106	KFR101:3	0.00	90.00	240.2	0.00
HFR106	KFR102A:1	444.00	600.83	576.0	0.00
HFR106	KFR102A:2	423.00	443.00	495.9	0.00
HFR106	KFR102A:3	255.00	422.00	416.1	0.00
HFR106	KFR102A:4	220.00	254.00	340.4	0.00
HFR106	KFR102A:5	214.00	219.00	327.0	0.00
HFR106	KFR102A:6	185.00	213.00	316.2	0.00
HFR106	KFR102A:7	103.00	184.00	286.7	0.00
HFR106	KFR102A:8	0.00	102.00	258.1	0.00
HFR106	KFR102B:1	146.00	180.08	313.6	0.00
HFR106	KFR102B:2	128.00	145.00	298.3	0.00
HFR106	KFR102B:3	0.00	127.00	266.2	0.00
HFR106	KFR103:3	0.00	78.00	221.1	0.00
HFR106	KFR104:1	333.00	454.57	481.5	0.00
HFR106	KFR104:2	98.00	332.00	532.0	0.00
HFR106	KFR104:3	0.00	97.00	616.6	0.00
HFR106	KFR106:0	0.00	300.13	119.2	0.00
KFR27	KFR04:1	84.09	100.50	249.4	0.59
KFR27	KFR04:2	44.09	83.09	257.3	0.62
KFR27	KFR04:3	28.09	43.09	267.7	0.62
KFR27	KFR05:2	80.15	96.15	287.5	0.73
KFR27	KFR07B:1	8.60	21.10	317.5	0.84



Drilling borehole	Observation borehole	Secup (m)	Seclow (m)	$r_s$ (m)	Index1 $r_s^2/dt_L$ (m <sup>2</sup> /s)
KFR27	KFR13:1	53.75	76.60	213.4	0.46
KFR27	KFR13:2	33.75	52.75	214.6	0.45
KFR27	KFR13:3	3.75	32.75	218.6	0.46
KFR27	KFR55:3	21.53	38.53	266.6	0.64
KFR27	KFR55:4	7.53	20.53	252.2	0.41
KFR27	KFR101:1	279.50	341.76	340.6	33.34
KFR27	KFR101:2	91.00	278.50	263.7	33.11
KFR27	HFR102:1	28.00	55.04	237.8	0
KFR27	HFR102:2	0.00	27.00	264.7	0
KFR27	HFR105:1	134.00	200.50	528.5	0
KFR27	HFR105:2	107.00	133.00	551.4	0
KFR27	HFR105:3	61.00	106.00	571.0	0
KFR27	HFR105:4	0.00	60.00	603.7	0
KFR27	KFR01:1	44.65	62.30	804.6	0
KFR27	KFR01:2	11.15	43.65	795.3	0
KFR27	KFR02:1	137.24	170.30	297.1	0
KFR27	KFR02:2	119.24	136.24	293.9	0
KFR27	KFR02:3	81.24	118.24	292.9	0
KFR27	KFR02:4	43.24	80.24	295.9	0
KFR27	KFR03:1	81.16	101.60	264.5	0
KFR27	KFR03:2	57.16	80.16	266.8	0
KFR27	KFR03.3	45.16	56.16	269.9	0
KFR27	KFR03:4	5.16	44.16	276.5	0
KFR27	KFR04:4	5.09	27.09	276.4	0
KFR27	KFR05:1	97.15	131.00	293.6	0
KFR27	KFR05:3	57.15	79.15	284.4	0
KFR27	KFR05:4	12.15	56.15	282.2	0
KFR27	KFR7A:1	48.11	74.70	371.1	0
KFR27	KFR7A:2	20.11	47.11	347.3	0
KFR27	KFR7A:3	2.11	19.11	328.0	0
KFR27	KFR07B:2	3.40	7.60	316.6	0
KFR27	KFR08:1	62.95	104.00	417.0	0
KFR27	KFR08:2	35.95	61.95	403.1	0
KFR27	KFR08:3	5.95	34.95	393.6	0
KFR27	KFR09:1	0.00	80.24	503.7	0
KFR27	KFR19:1	95.57	110.00	324.2	0
KFR27	KFR19:2	77.57	94.57	315.7	0
KFR27	KFR19:3	66.82	76.57	308.8	0
KFR27	KFR19:4	51.82	65.82	303.1	0
KFR27	KFR55:1	48.53	61.89	289.5	0
KFR27	KFR55:2	39.53	47.53	278.8	0
KFR27	KFR56:1	9.55	81.70	384.5	0
KFR27	KFR101:3	0.00	90.00	248.0	0
KFR102A	KFR04:1	84.09	100.50	244.8	0.83
KFR102A	KFR04:2	44.09	83.09	254.6	0.86
KFR102A	KFR05:2	80.15	96.15	281.3	1.00
KFR102A	KFR07B:1	8.60	21.10	288.0	1.36
KFR102A	KFR13:1	53.75	76.60	212.9	3.55
KFR102A	KFR13:2	33.75	52.75	213.8	3.56
KFR102A	KFR13:3	3.75	32.75	217.5	3.63
KFR102A	KFR55:2	39.53	47.53	270.8	4.51
KFR102A	KFR55:3	21.53	38.53	258.8	4.31
KFR102A	KFR55:4	7.53	20.53	244.7	4.08
KFR102A	KFR101:1	279.50	341.76	236.7	19.87
KFR102A	KFR101:2	91.00	278.50	161.6	36.27
KFR102A	KFR102B:1	146.00	180.08	99.1	18.19
KFR102A	KFR102B:2	128.00	145.00	108.4	11.52
KFR102A	KFR102B:3	0.00	127.00	156.1	3.47
KFR102A	KFR103:1	178.00	200.50	181.0	1.41
KFR102A	KFR103:2	79.00	177.00	169.0	3.24
KFR102A	HFR101:0	8.04	209.30	410.5	0

Drilling borehole	Observation borehole	Secup (m)	Seclow (m)	$r_s$ (m)	Index1 $r_s^2/dt_L$ (m <sup>2</sup> /s)
KFR102A	HFR102:2	0.00	27.00	333.4	0
KFR102A	HFR105:1	134.00	200.50	634.4	0
KFR102A	HFR105:2	107.00	133.00	656.4	0
KFR102A	HFR105:3	61.00	106.00	675.0	0
KFR102A	HFR105:4	0.00	60.00	706.1	0
KFR102A	KFR01:1	44.65	62.30	906.9	0
KFR102A	KFR01:2	11.15	43.65	897.0	0
KFR102A	KFR02:1	137.24	170.30	376.0	0
KFR102A	KFR02:2	119.24	136.24	373.2	0
KFR102A	KFR02:3	81.24	118.24	372.2	0
KFR102A	KFR02:4	43.24	80.24	374.2	0
KFR102A	KFR03:1	81.16	101.60	293.2	0
KFR102A	KFR03:2	57.16	80.16	295.0	0
KFR102A	KFR03:3	45.16	56.16	297.7	0
KFR102A	KFR03:4	5.16	44.16	303.4	0
KFR102A	KFR04:3	28.09	43.09	266.9	0
KFR102A	KFR04:4	5.09	27.09	276.7	0
KFR102A	KFR05:1	97.15	131.00	285.4	0
KFR102A	KFR05:3	57.15	79.15	279.8	0
KFR102A	KFR05:4	12.15	56.15	280.4	0
KFR102A	KFR7A:1	48.11	74.70	330.7	0
KFR102A	KFR7A:2	20.11	47.11	311.8	0
KFR102A	KFR7A:3	2.11	19.11	297.3	0
KFR102A	KFR07B:2	3.40	7.60	287.6	0
KFR102A	KFR08:1	62.95	104.00	372.7	0
KFR102A	KFR08:2	35.95	61.95	367.3	0
KFR102A	KFR08:3	5.95	34.95	365.2	0
KFR102A	KFR09:1	0.00	80.24	563.0	0
KFR102A	KFR19:1	95.57	110.00	315.3	0
KFR102A	KFR19:2	77.57	94.57	311.9	0
KFR102A	KFR19:3	66.82	76.57	309.7	0
KFR102A	KFR19:4	51.82	65.82	308.3	0
KFR102A	KFR55:1	48.53	61.89	281.4	0
KFR102A	KFR56	9.55	81.70	351.2	0
KFR102A	KFR101:3	0.00	90.00	184.6	0
KFR102A	KFR103:3	0.00	78.00	190.5	0
KFR105	HFR101:0	8.04	209.30	224.2	0.11
KFR105	HFR102:1	28.00	55.04	149.5	0.45
KFR105	HFR102:2	0.00	27.00	174.1	0.04
KFR105	KFR27:1	110.00	501.64	196.5	0.47
KFR105	KFR27:2	47.00	109.00	117.7	1.26
KFR105	KFR27:3	0.00	46.00	151.0	0.92
KFR105	KFR102A:3	255.00	422.00	264.7	0.88
KFR105	KFR102A:4	220.00	254.00	222.5	0.31
KFR105	KFR102A:5	214.00	219.00	218.7	0.56
KFR105	KFR102A:6	185.00	213.00	216.9	0.33
KFR105	KFR102A:7	103.00	184.00	220.8	0.60
KFR105	KFR102A:8	0.00	102.00	261.5	0.84
KFR105	KFR103:1	178.00	200.50	265.5	0.24
KFR105	KFR103:2	79.00	177.00	262.8	1.19
KFR105	KFR104:1	333.00	454.57	207.6	0.09
KFR105	KFR104:2	98.00	332.00	124.0	0.06
KFR105	KFR104:3	0.00	97.00	212.7	0.15
KFR105	HFR105:1	134.00	200.50	423.7	0
KFR105	HFR105:2	107.00	133.00	442.0	0
KFR105	HFR105:3	61.00	106.00	458.9	0
KFR105	HFR105:4	0.00	60.00	488.7	0
KFR105	KFR01:1	44.65	62.30	698.0	0
KFR105	KFR01:2	11.15	43.65	687.2	0
KFR105	KFR02:1	137.24	170.30	252.6	0
KFR105	KFR02:2	119.24	136.24	242.4	0

Drilling borehole	Observation borehole	Secup (m)	Seclow (m)	$r_s$ (m)	Index1 $r_s^2/dt_L$ (m <sup>2</sup> /s)
KFR105	KFR02:3	81.24	118.24	234.2	0
KFR105	KFR02:4	43.24	80.24	228.2	0
KFR105	KFR03:1	81.16	101.60	268.5	0
KFR105	KFR03:2	57.16	80.16	265.7	0
KFR105	KFR03.3	45.16	56.16	264.9	0
KFR105	KFR03:4	5.16	44.16	265.8	0
KFR105	KFR04:1	84.09	100.50	285.6	0
KFR105	KFR04:2	44.09	83.09	284.7	0
KFR105	KFR04:3	28.09	43.09	286.6	0
KFR105	KFR04:4	5.09	27.09	289.5	0
KFR105	KFR05:1	97.15	131.00	330.5	0
KFR105	KFR05:2	80.15	96.15	318.8	0
KFR105	KFR05:3	57.15	79.15	310.9	0
KFR105	KFR05:4	12.15	56.15	300.1	0
KFR105	KFR7A:1	48.11	74.70	420.3	0
KFR105	KFR7A:2	20.11	47.11	393.5	0
KFR105	KFR7A:3	2.11	19.11	371.4	0
KFR105	KFR7B:1	8.60	21.10	363.1	0
KFR105	KFR7B:2	3.40	7.60	360.4	0
KFR105	KFR08:1	62.95	104.00	461.8	0
KFR105	KFR08:2	35.95	61.95	440.9	0
KFR105	KFR08:3	5.95	34.95	425.1	0
KFR105	KFR09:1	0.00	80.24	441.5	0
KFR105	KFR13:1	53.75	76.60	257.8	0
KFR105	KFR13:2	33.75	52.75	253.6	0
KFR105	KFR13:3	3.75	32.75	251.2	0
KFR105	KFR19:1	95.57	110.00	336.2	0
KFR105	KFR19:2	77.57	94.57	323.8	0
KFR105	KFR19:3	66.82	76.57	313.5	0
KFR105	KFR19:4	51.82	65.82	304.6	0
KFR105	KFR55:1	48.53	61.89	317.7	0
KFR105	KFR55:2	39.53	47.53	307.5	0
KFR105	KFR55:3	21.53	38.53	295.9	0
KFR105	KFR55:4	7.53	20.53	282.4	0
KFR105	KFR56:1	9.55	81.70	417.1	0
KFR105	KFR101:1	279.50	341.76	454.0	0
KFR105	KFR101:2	91.00	278.50	364.0	0
KFR105	KFR101:3	0.00	90.00	309.2	0
KFR105	KFR102A:1	444.00	600.83	399.3	0
KFR105	KFR102A:2	423.00	443.00	327.9	0
KFR105	KFR102B:1	146.00	180.08	290.6	0
KFR105	KFR102B:2	128.00	145.00	286.0	0
KFR105	KFR102B:3	0.00	127.00	285.8	0
KFR105	KFR103:3	0.00	78.00	284.5	0
KFR106	HFR106	9.0	190.4	118.8	18.09
KFR106	HFR106:1	50.0	190.4	118.2	—
KFR106	HFR106:2	9.03	49.00	147.6	—
KFR106	KFR103:1	178.00	200.50	265.1	33.47
KFR106	KFR103:2	79.00	177.00	289.8	3.29
KFR106	KFR103:3	0.00	78.00	341.4	2.89
KFR106	HFR101:0	8.04	209.30	740.1	0
KFR106	HFR102:1	28.00	55.04	637.8	0
KFR106	HFR102:2	0.00	27.00	655.7	0
KFR106	HFR105:1	134.00	200.50	851.4	0
KFR106	HFR105:2	107.00	133.00	864.6	0
KFR106	HFR105:3	61.00	106.00	876.2	0
KFR106	HFR105:4	0.00	60.00	896.5	0
KFR106	KFR01:1	44.65	62.30	1,147.5	0
KFR106	KFR01:2	11.15	43.65	1,138.2	0
KFR106	KFR02:1	137.24	170.30	750.1	0
KFR106	KFR02:2	119.24	136.24	747.2	0

Drilling borehole	Observation borehole	Secup (m)	Seclow (m)	$r_s$ (m)	Index1 $r_s^2/dt_L$ (m <sup>2</sup> /s)
KFR106	KFR02:3	81.24	118.24	745.2	0
KFR106	KFR02:4	43.24	80.24	744.0	0
KFR106	KFR03:1	81.16	101.60	715.7	0
KFR106	KFR03:2	57.16	80.16	715.1	0
KFR106	KFR03:3	45.16	56.16	715.1	0
KFR106	KFR03:4	5.16	44.16	716.0	0
KFR106	KFR04:1	84.09	100.50	673.1	0
KFR106	KFR04:2	44.09	83.09	678.9	0
KFR106	KFR04:3	28.09	43.09	685.7	0
KFR106	KFR04:4	5.09	27.09	691.0	0
KFR106	KFR05:1	97.15	131.00	714.8	0
KFR106	KFR05:2	80.15	96.15	708.8	0
KFR106	KFR05:3	57.15	79.15	704.8	0
KFR106	KFR05:4	12.15	56.15	699.3	0
KFR106	KFR7A:1	48.11	74.70	739.1	0
KFR106	KFR7A:2	20.11	47.11	724.8	0
KFR106	KFR7A:3	2.11	19.11	713.6	0
KFR106	KFR7B:1	8.60	21.10	707.5	0
KFR106	KFR7B:2	3.40	7.60	706.0	0
KFR106	KFR08:1	62.95	104.00	768.9	0
KFR106	KFR08:2	35.95	61.95	770.7	0
KFR106	KFR08:3	5.95	34.95	773.4	0
KFR106	KFR09:1	0.00	80.24	952.3	0
KFR106	KFR13:1	53.75	76.60	642.8	0
KFR106	KFR13:2	33.75	52.75	641.7	0
KFR106	KFR13:3	3.75	32.75	641.3	0
KFR106	KFR19:1	95.57	110.00	721.0	0
KFR106	KFR19:2	77.57	94.57	719.0	0
KFR106	KFR19:3	66.82	76.57	717.7	0
KFR106	KFR19:4	51.82	65.82	716.7	0
KFR106	KFR27:1	110.00	501.64	492.7	0
KFR106	KFR27:2	47.00	109.00	464.8	0
KFR106	KFR27:3	0.00	46.00	476.5	0
KFR106	KFR55:1	48.53	61.89	705.4	0
KFR106	KFR55:2	39.53	47.53	694.4	0
KFR106	KFR55:3	21.53	38.53	681.7	0
KFR106	KFR55:4	7.53	20.53	666.6	0
KFR106	KFR56:1	9.55	81.70	750.8	0
KFR106	KFR101:1	279.50	341.76	436.7	0
KFR106	KFR101:2	91.00	278.50	379.7	0
KFR106	KFR101:3	0.00	90.00	360.8	0
KFR106	KFR102A:1	444.00	600.83	655.0	0
KFR106	KFR102A:2	423.00	443.00	581.8	0
KFR106	KFR102A:3	255.00	422.00	511.1	0
KFR106	KFR102A:4	220.00	254.00	446.7	0
KFR106	KFR102A:5	214.00	219.00	435.7	0
KFR106	KFR102A:6	185.00	213.00	426.8	0
KFR106	KFR102A:7	103.00	184.00	402.9	0
KFR106	KFR102A:8	0.00	102.00	378.7	0
KFR106	KFR102B:1	146.00	180.08	429.7	0
KFR106	KFR102B:2	128.00	145.00	416.4	0
KFR106	KFR102B:3	0.00	127.00	387.2	0
KFR106	KFR104:1	333.00	454.57	547.1	0
KFR106	KFR104:2	98.00	332.00	621.2	0
KFR106	KFR104:3	0.00	97.00	717.4	0
KFR106	KFR105:1	265.00	303.00	473.1	0
KFR106	KFR105:2	170.00	264.00	488.6	0
KFR106	KFR105:3	138.00	169.00	510.6	0
KFR106	KFR105:4	120.00	137.00	521.1	0
KFR106	KFR105:5	4.00	119.00	553.4	0

Linear plots of hydraulic head versus time for responding sections during drilling together with precipitation, barometric pressure and sea level data.

A5.1 Percussion drilling of HFR102

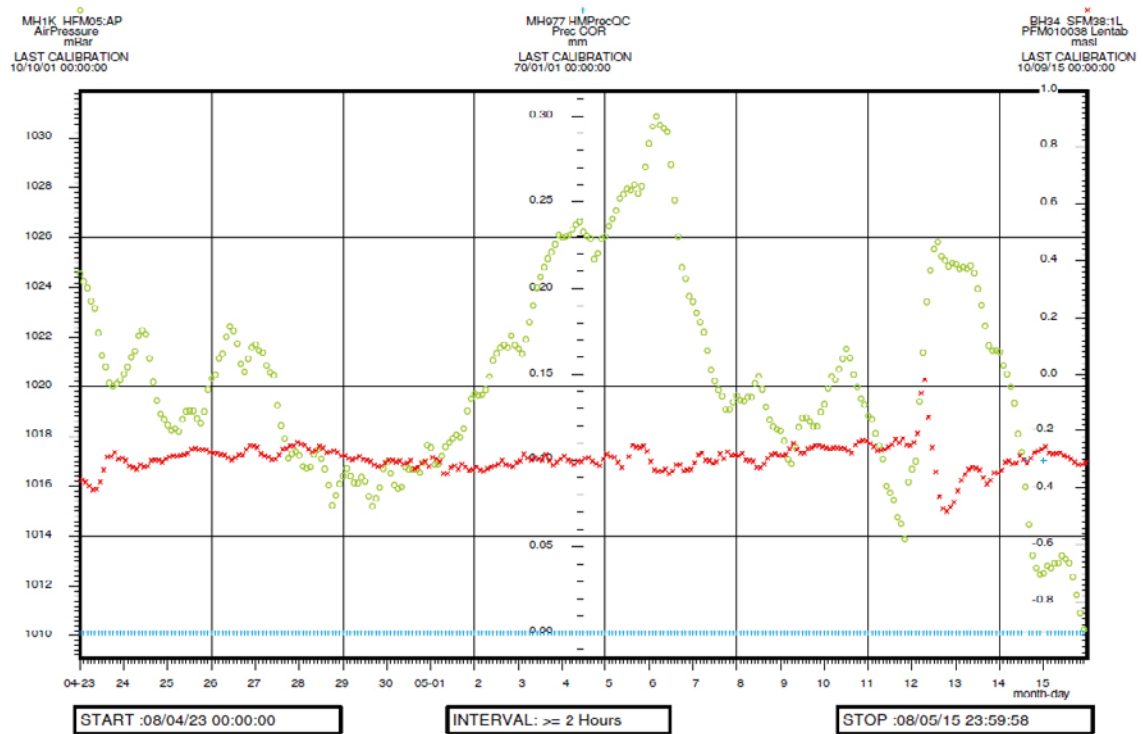


Figure A5-1. Registered air pressure (o), precipitation (+) and sea water level (x) at SFR during the drilling of HFR102. Each parameter has its own Y-scale.

## A5.2 Percussion drilling of HFR106

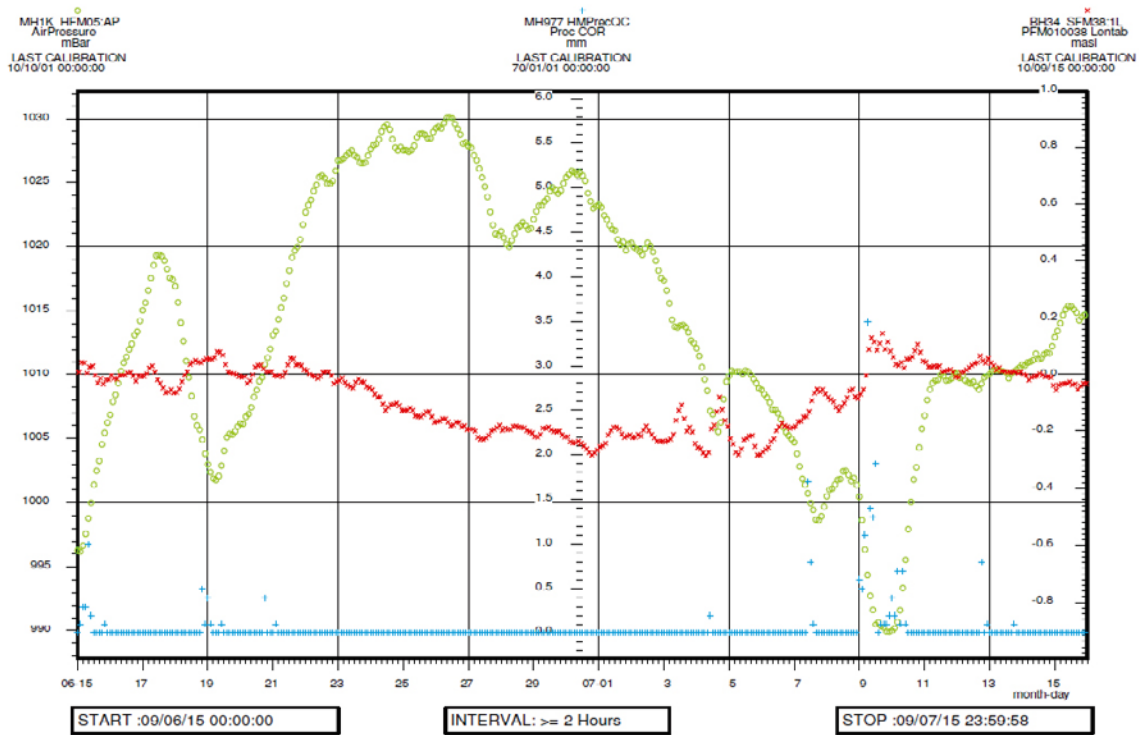


Figure A5-2. Registered air pressure (o), precipitation (+) and sea water level (x) at SFR during the drilling of HFR106. Each parameter has its own Y-scale.

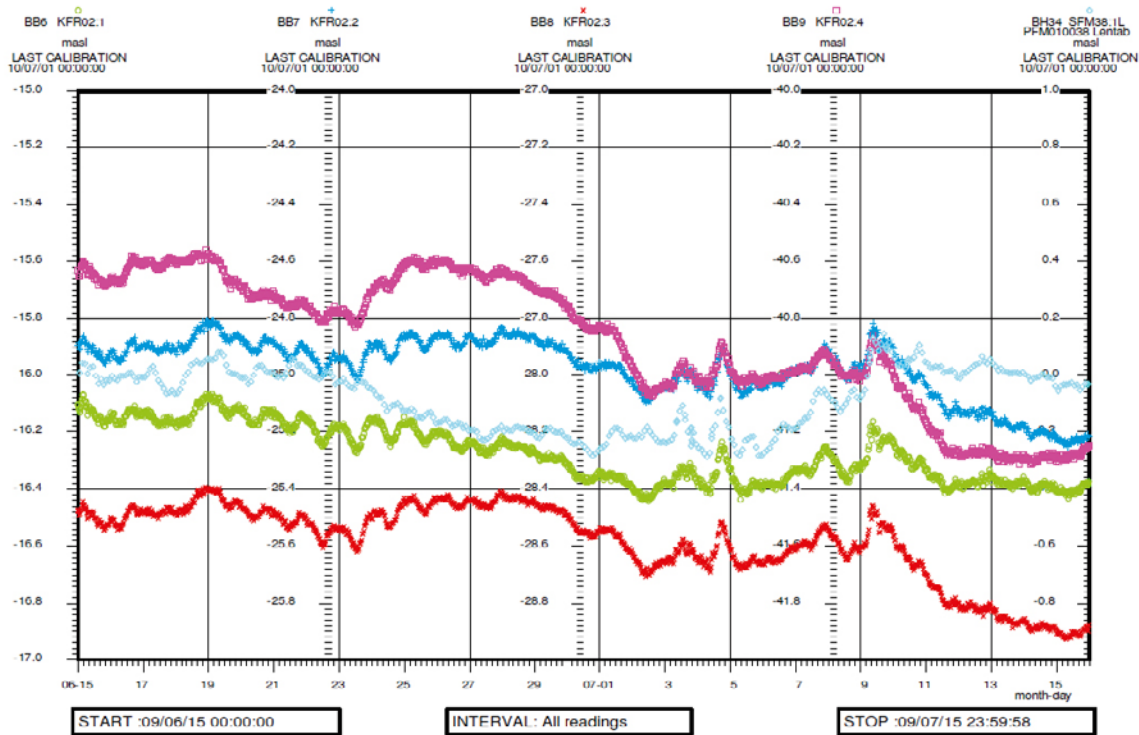


Figure A5-3. Linear plot of observed head versus time in the observation borehole KFR02 together with sea water level during the drilling of HFR106.

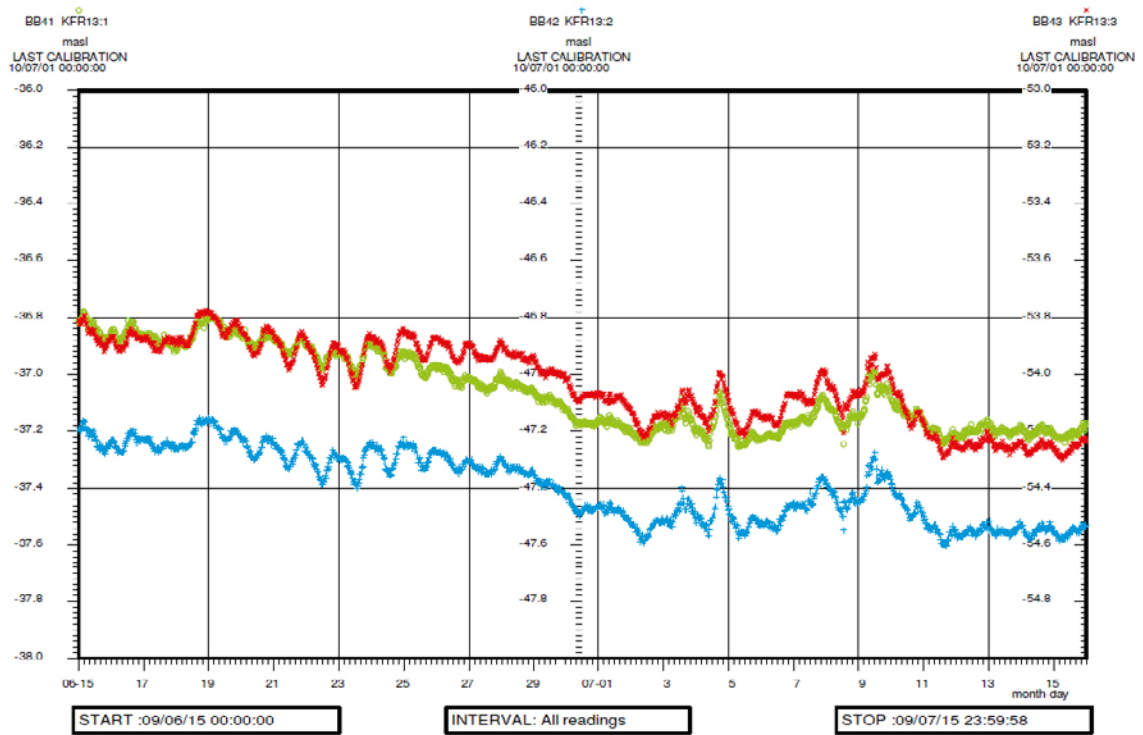


Figure A5-4. Linear plot of observed head versus time in the observation borehole KFR13 during the drilling of HFR106.

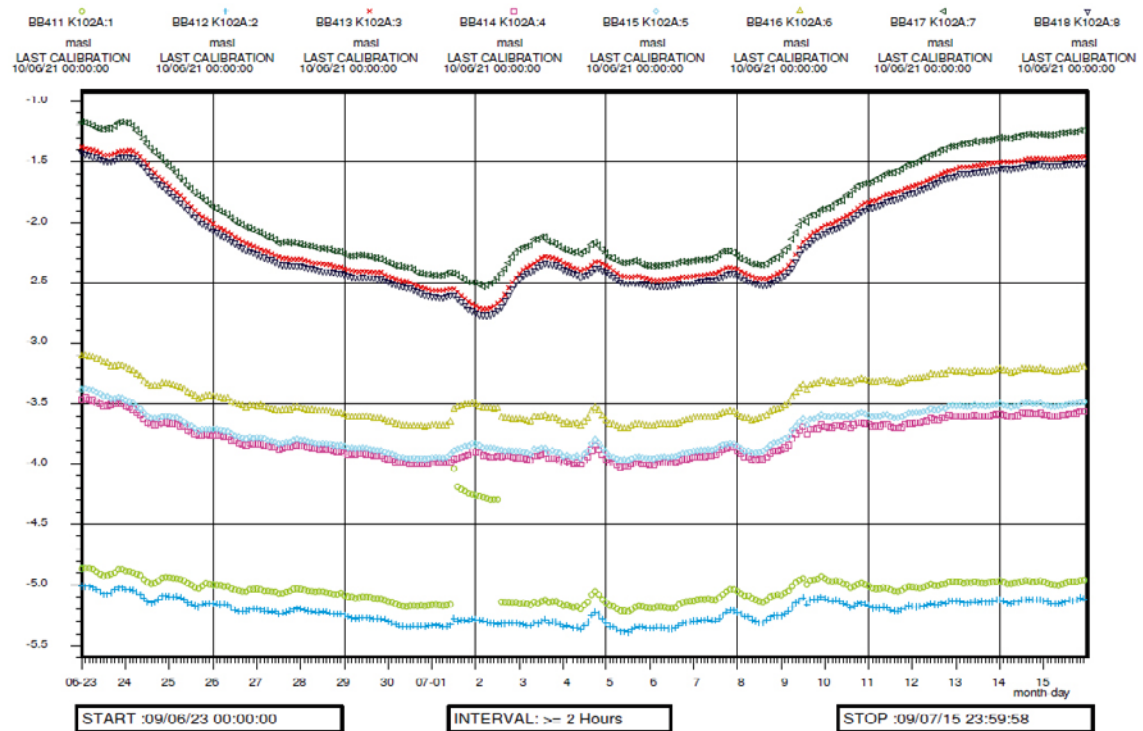


Figure A5-5. Linear plot of observed head versus time in the observation borehole KFR102A during the drilling of HFR106. Sections 3, 7 and 8 show a response while sections 1, 2, 4, 5 and 6 are unaffected.

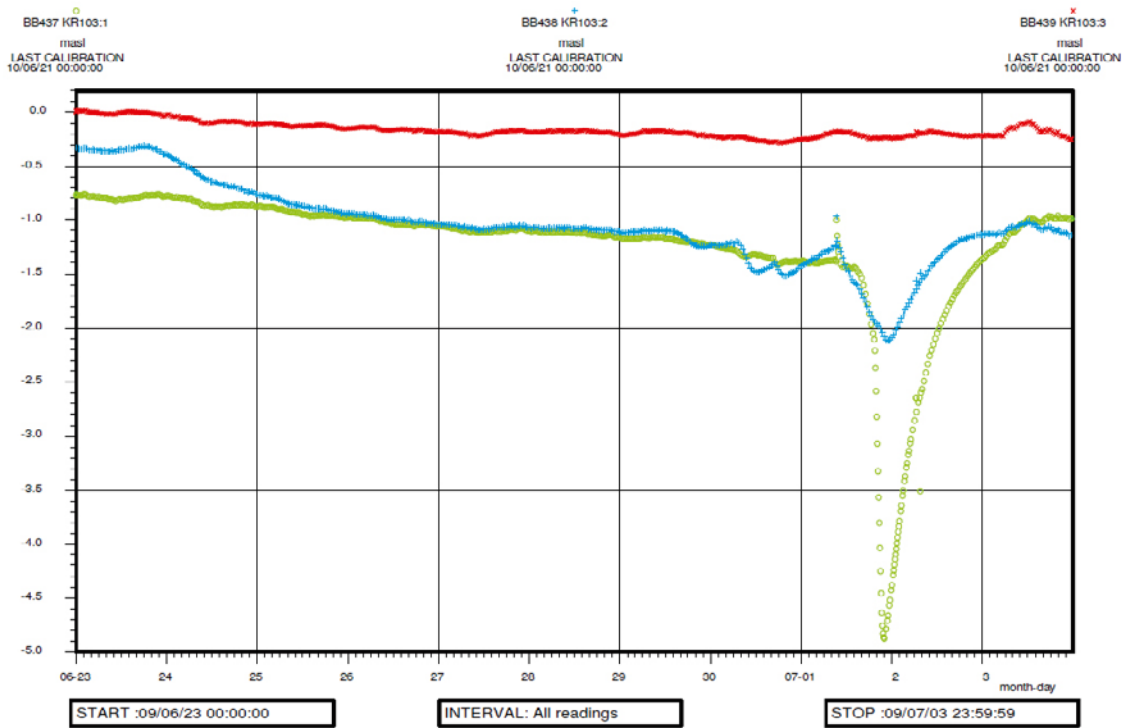


Figure A5-6. Linear plot of observed head versus time in the observation borehole KFR103 during the drilling of HFR106. Sections 1 and 2 show a response while section 3 is unaffected.

### A5.3 Core drilling of KFR27

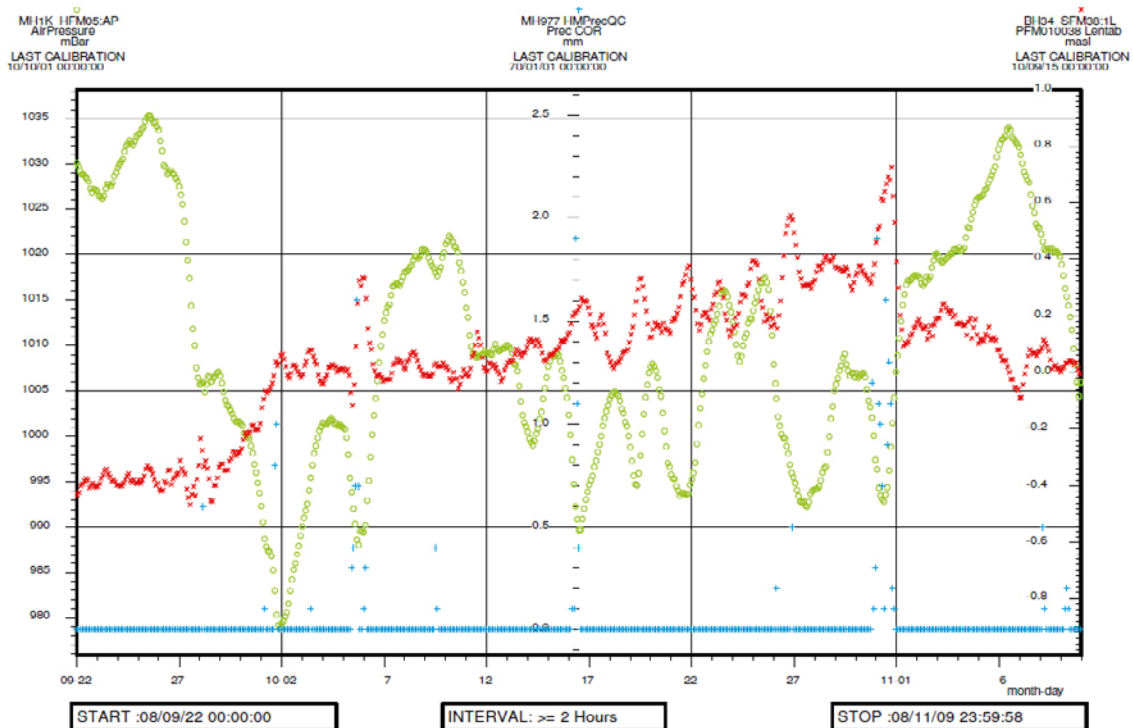


Figure A5-7. Registered air pressure (o), precipitation (+) and sea water level (x) at SFR during the drilling of KFR27. Each parameter has its own Y-scale.



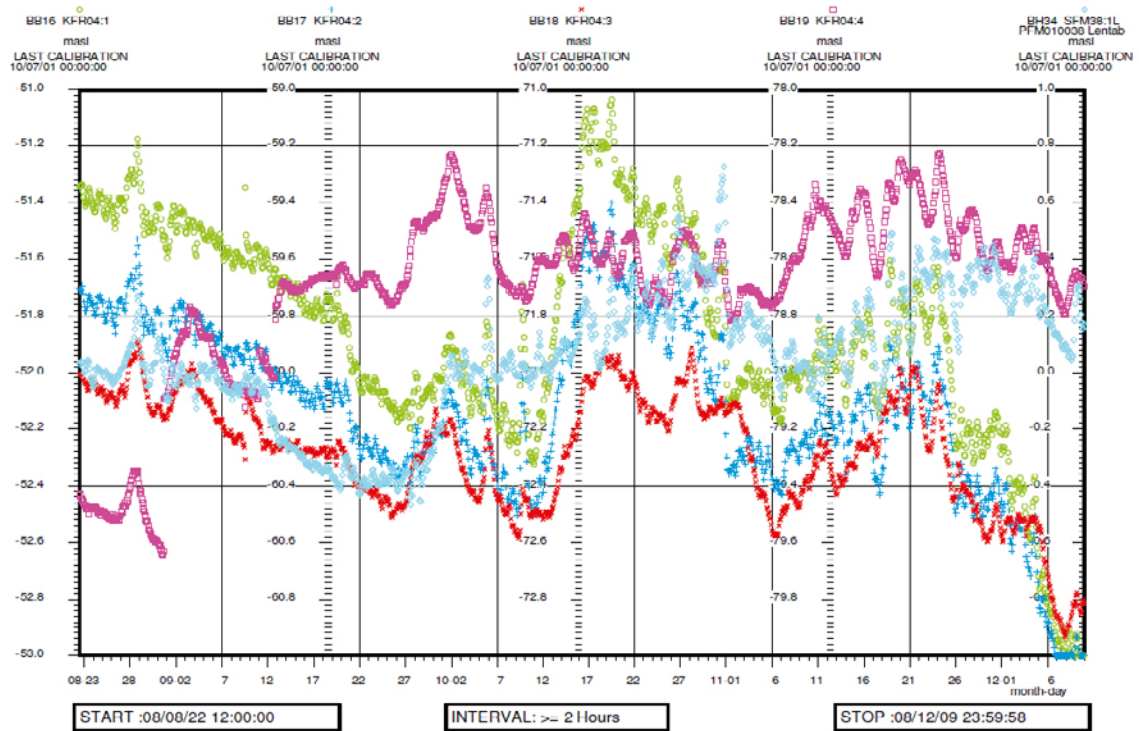


Figure A5-8. Linear plot of observed head versus time in the observation borehole KFR04 together with sea water level during the drilling of KFR27. Sections 1,2 and 3 show a response while section 4 is unaffected.

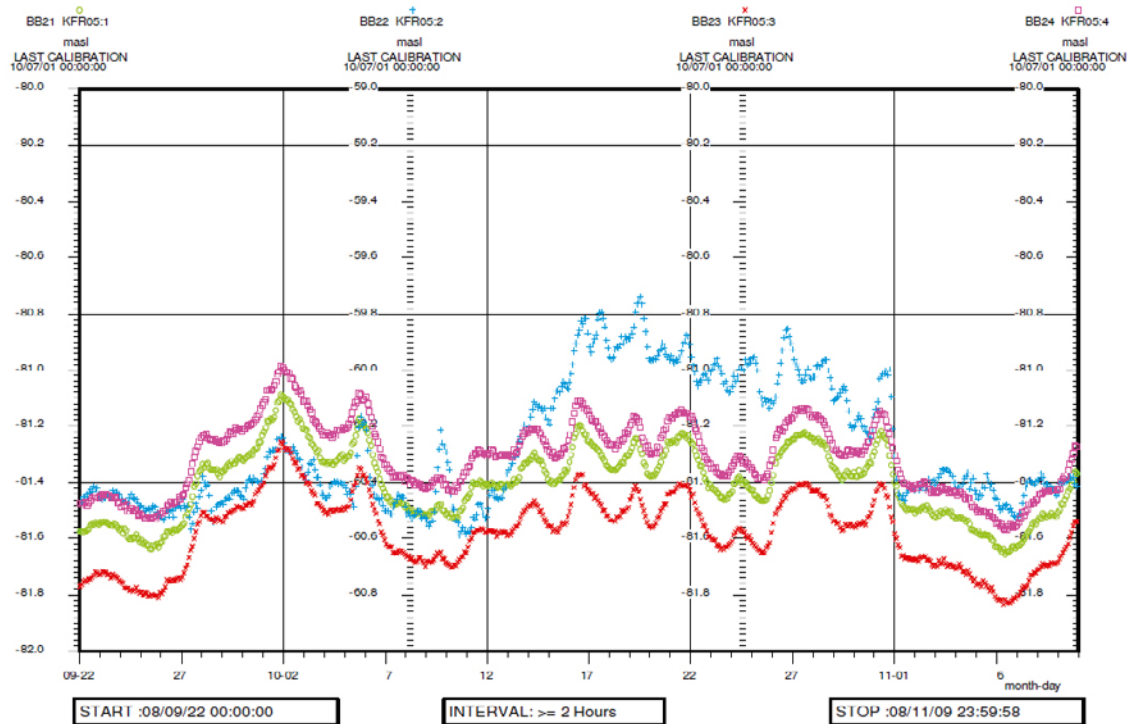


Figure A5-9. Linear plot of observed head versus time in the observation borehole KFR05 during the drilling of KFR27. Section 2 shows a response while sections 1, 3 and 4 are unaffected.

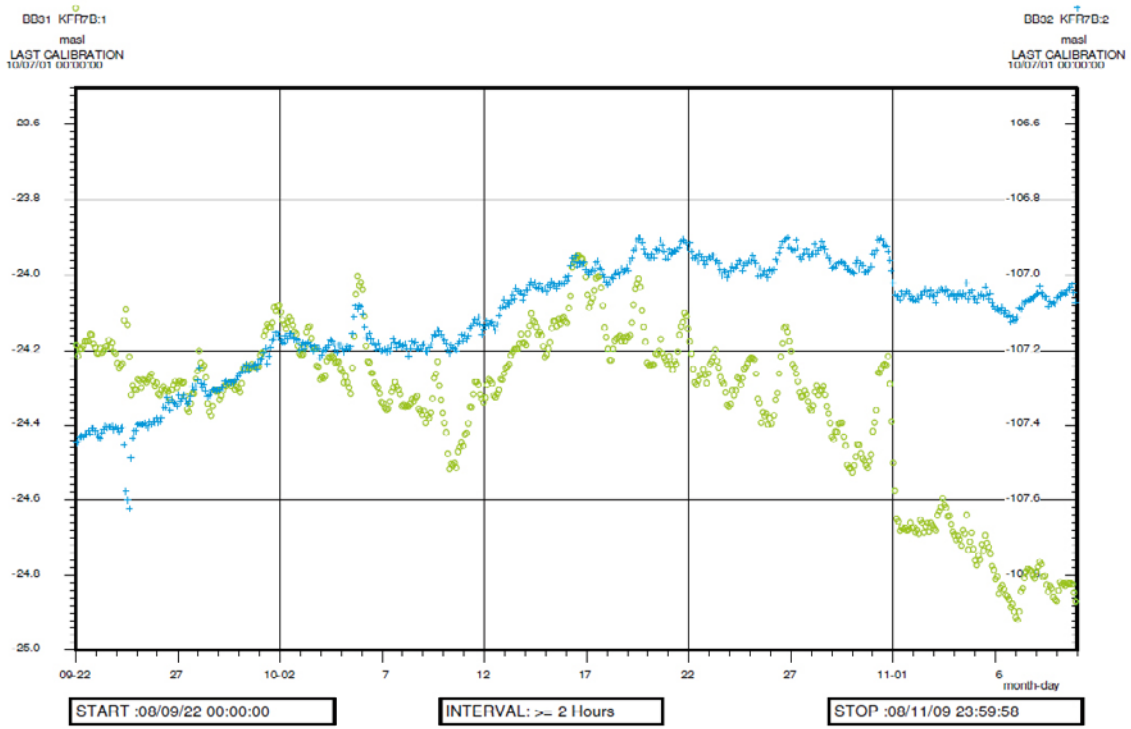


Figure A5-10. Linear plot of observed head versus time in the observation borehole KFR7B during the drilling of KFR27. Section 1 shows a response while section 2 is unaffected.

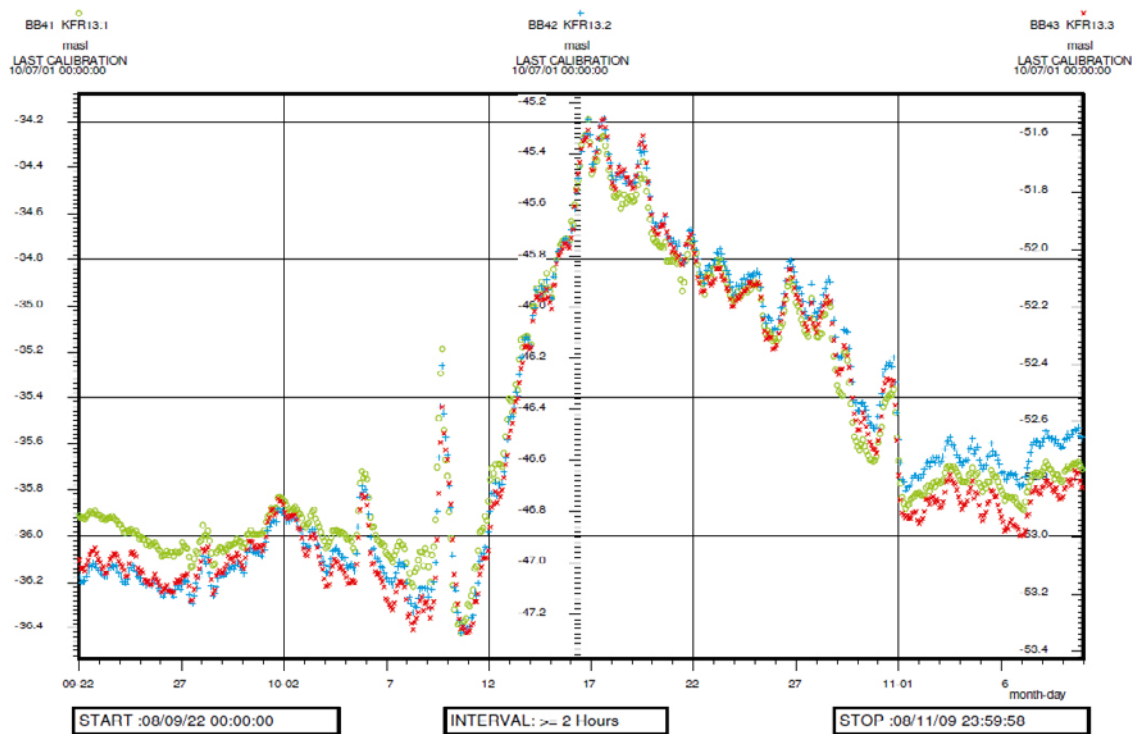
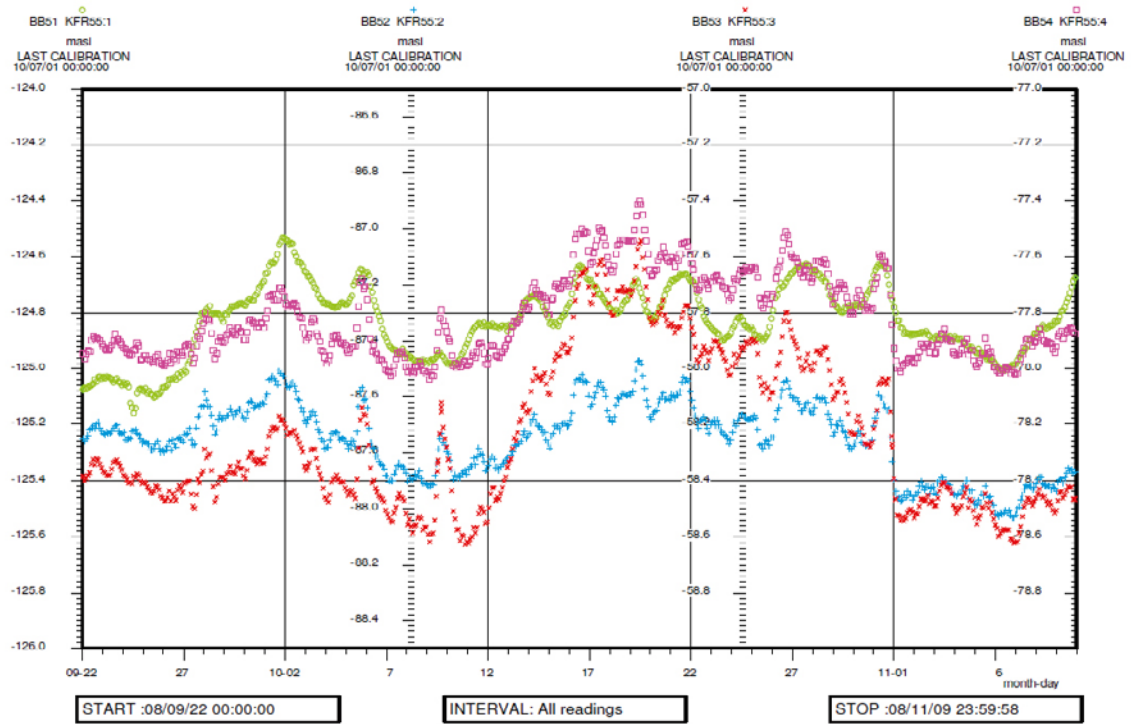
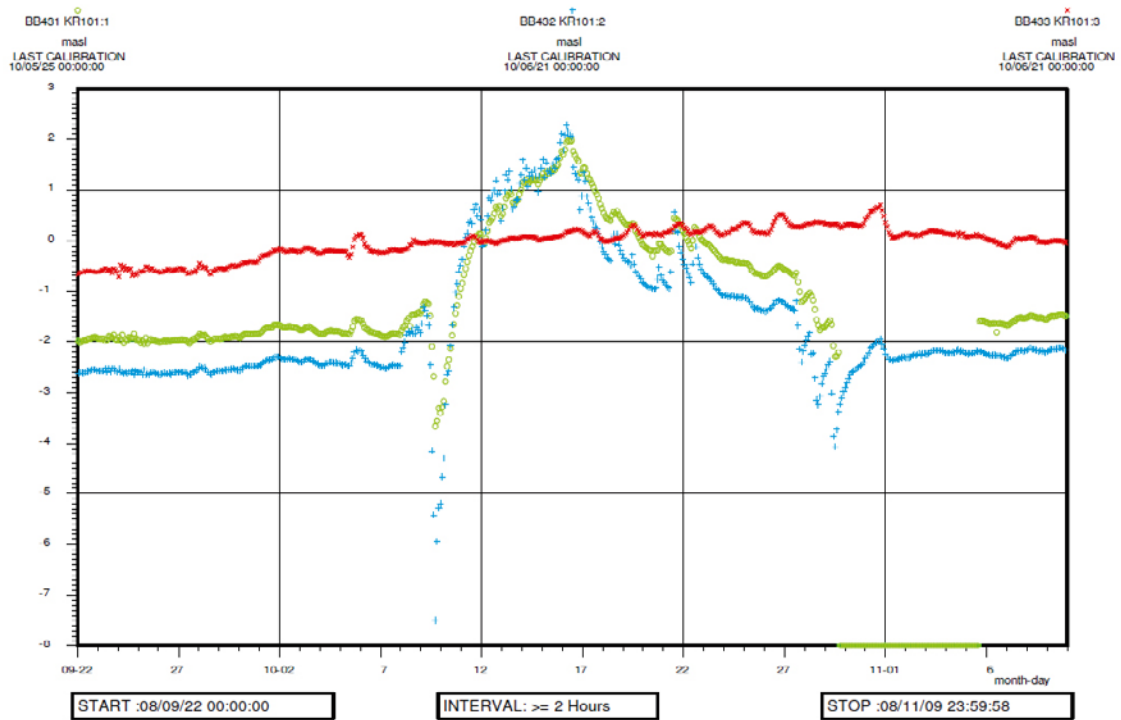


Figure A5-11. Linear plot of observed head versus time in the observation borehole KFR13 during the drilling of KFR27.



**Figure A5-12.** Linear plot of observed head versus time in the observation borehole KFR55 during the drilling of KFR27. Sections 3 and 4 show a response while sections 1 and 2 are unaffected.



**Figure A5-13.** Linear plot of observed head versus time in the observation borehole KFR101 during the drilling of KFR27. Sections 1 and 2 show a response while section 3 is unaffected.

## A5.4 Core drilling of KFR102A

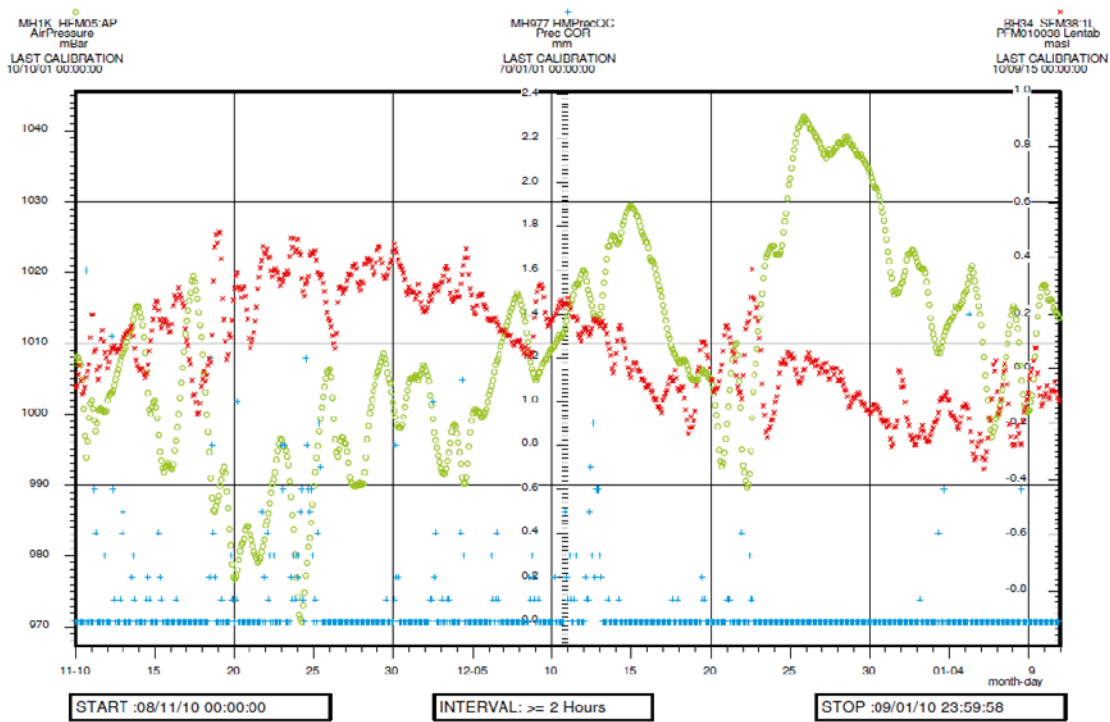


Figure A5-14. Registered air pressure (o), precipitation (+) and sea water level (x) at SFR during the drilling of KFR102A. Each parameter has its own Y-scale.

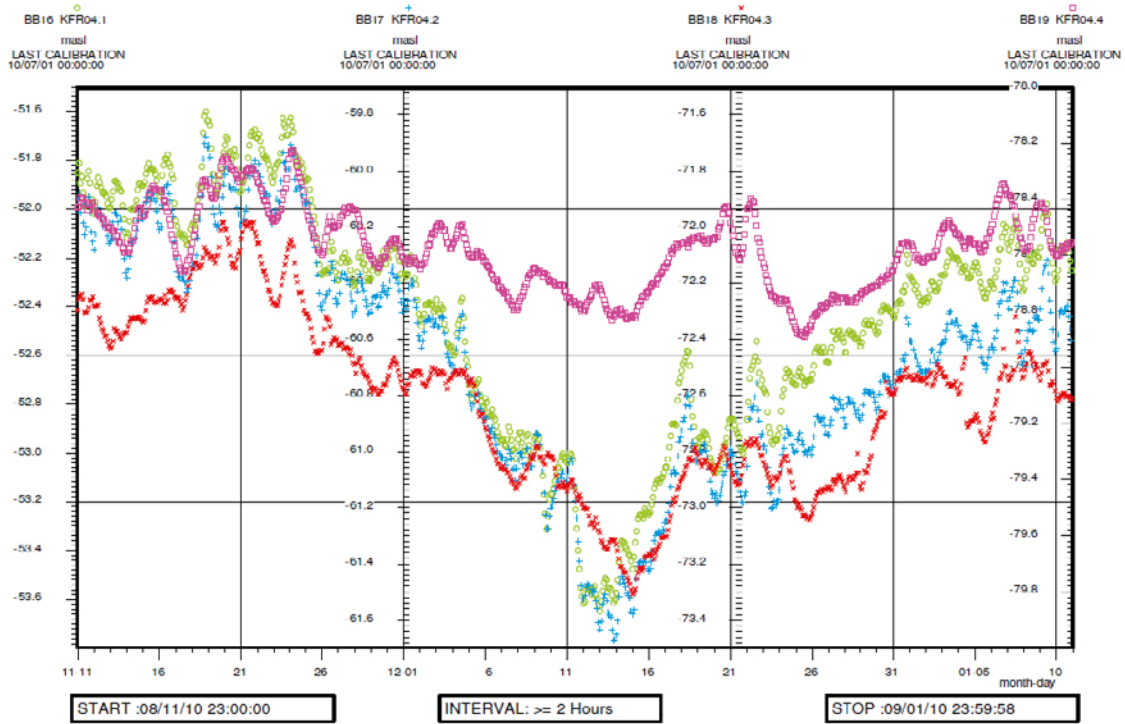
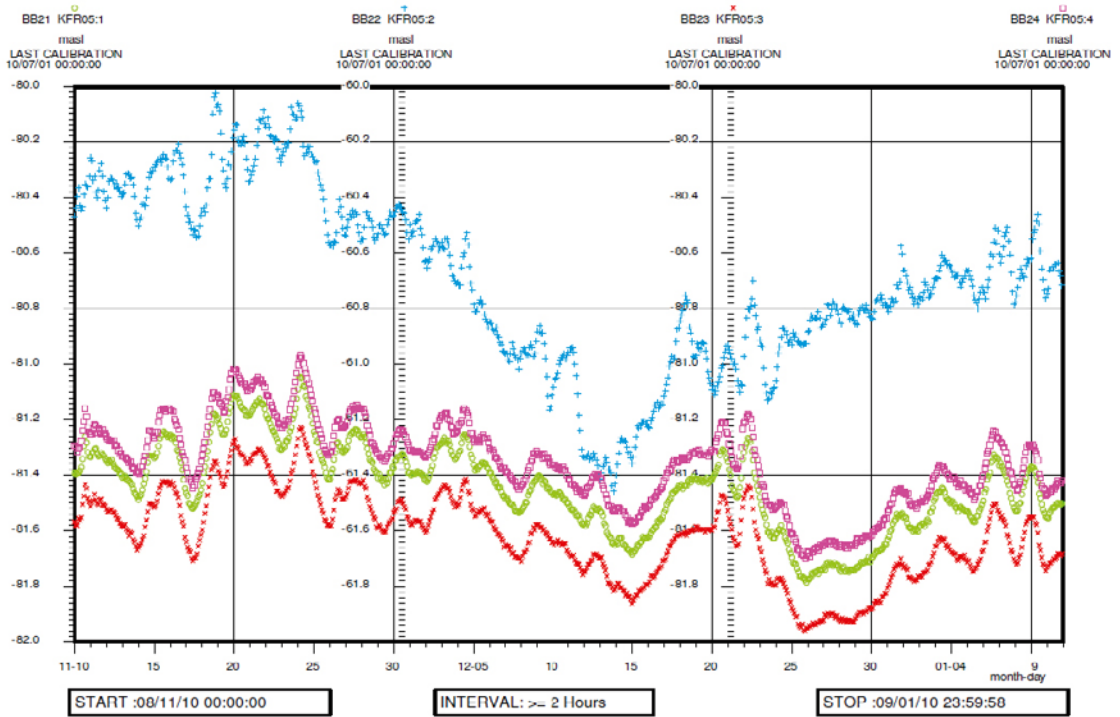
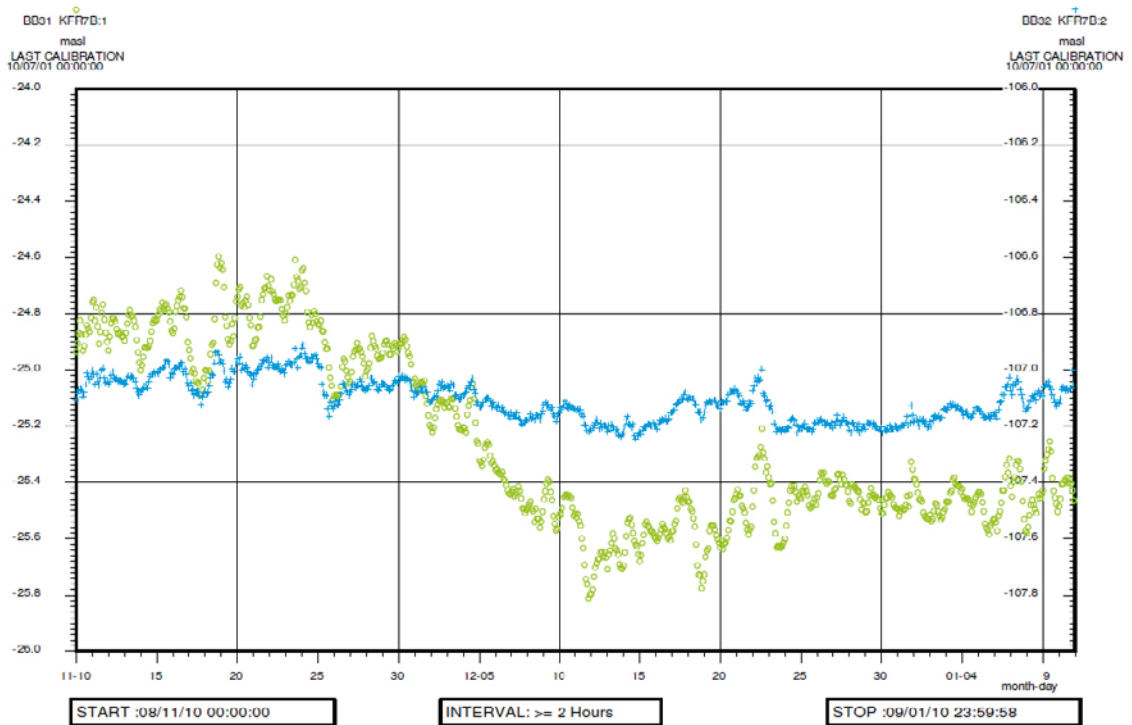


Figure A5-15. Linear plot of observed head versus time in the observation borehole KFR04 during the drilling of KFR102A. Sections 1 and 2 show a response while sections 3 and 4 are unaffected.



**Figure A5-16.** Linear plot of observed head versus time in the observation borehole KFR05 during the drilling of KFR102A. Section 2 shows a response while sections 1, 3 and 4 are unaffected.



**Figure A5-17.** Linear plot of observed head versus time in the observation borehole KFR7B during the drilling of KFR102A. Section 1 shows a response while section 2 is unaffected.

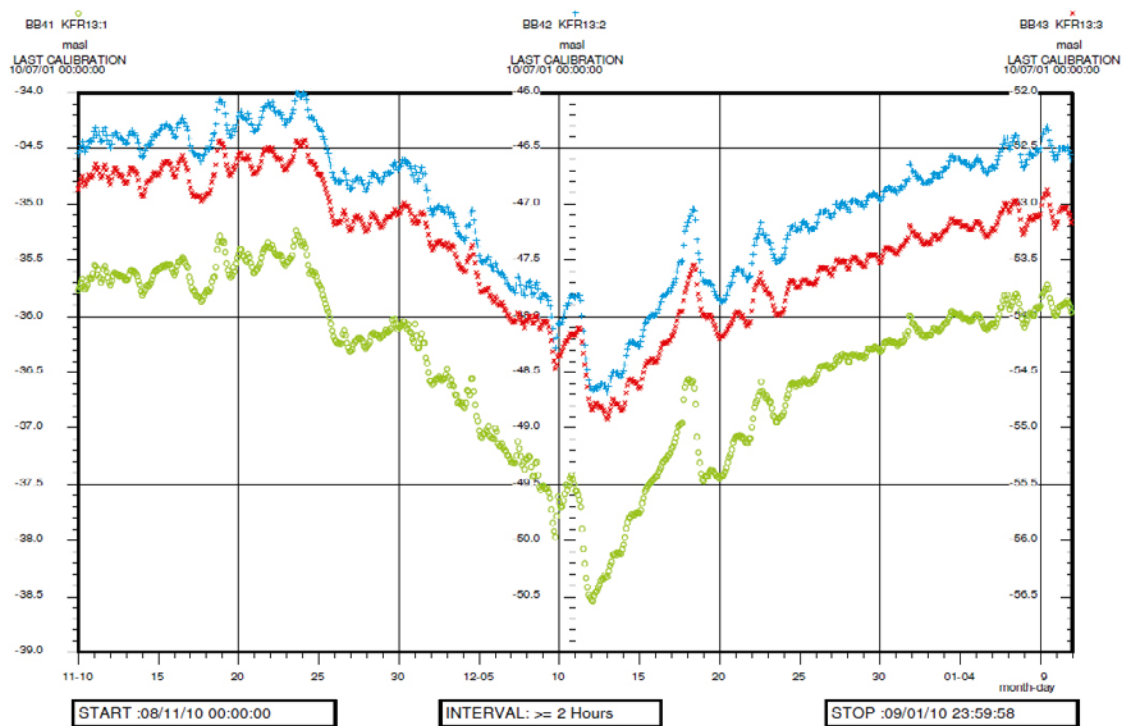


Figure A5-18. Linear plot of observed head versus time in the observation borehole KFR13 during the drilling of KFR102A.

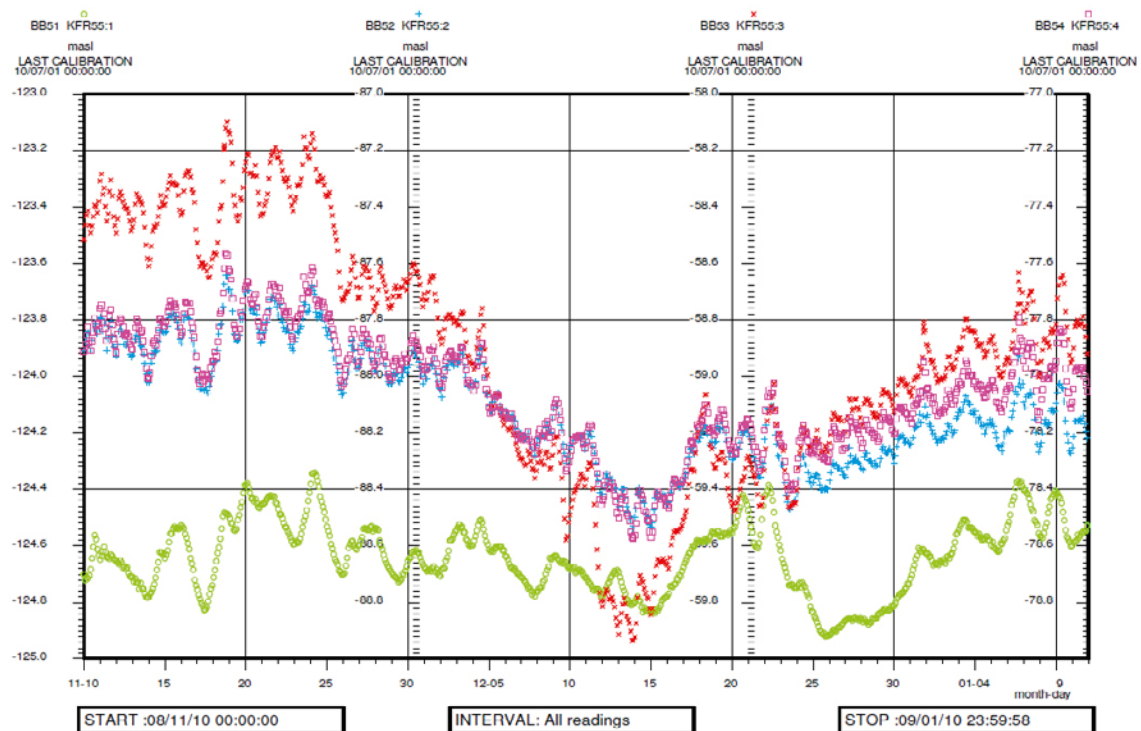
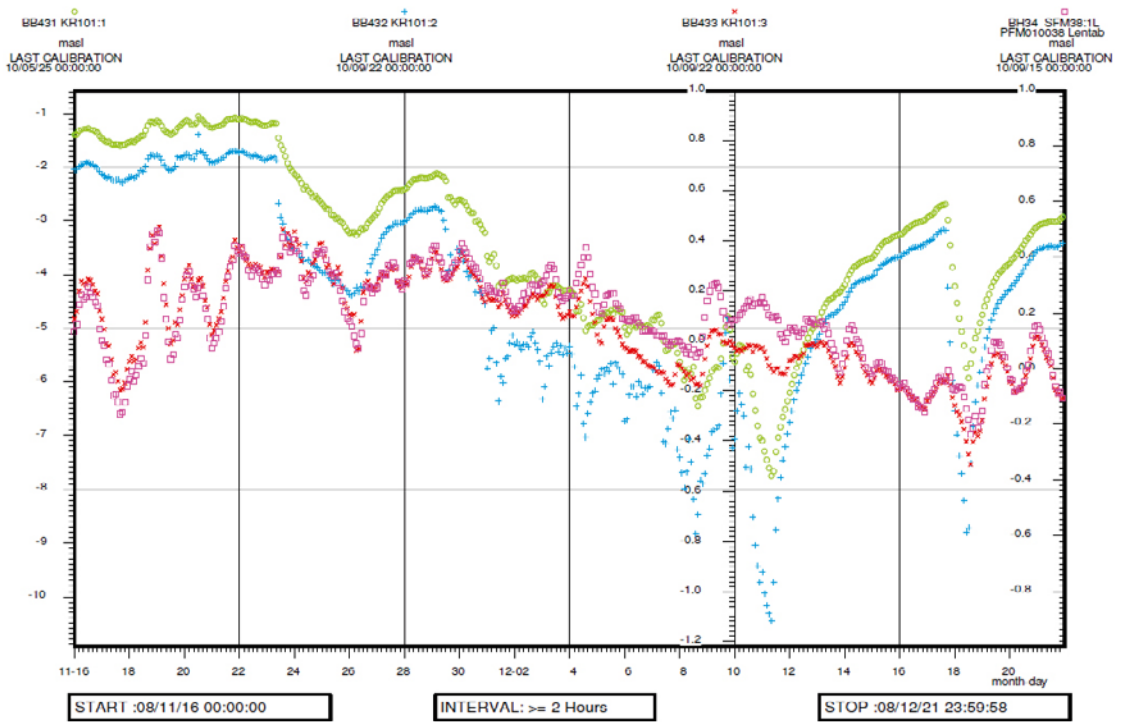
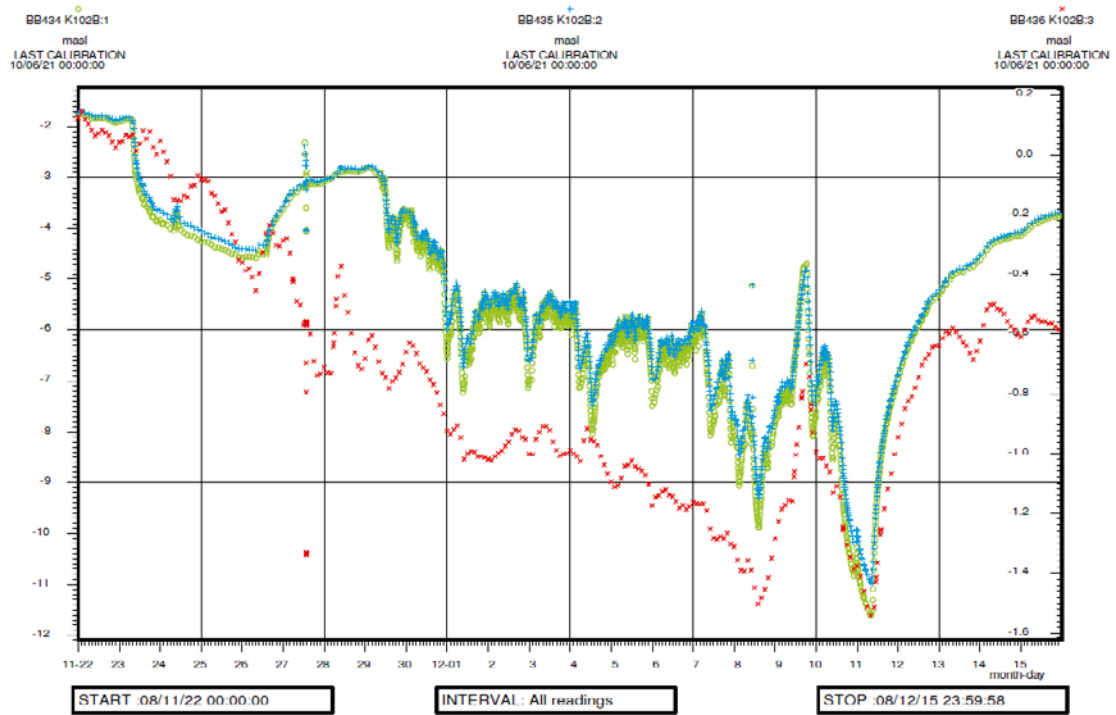


Figure A5-19. Linear plot of observed head versus time in the observation borehole KFR55 during the drilling of KFR102A. Sections 2, 3 and 4 show a response while section 1 is unaffected.



**Figure A5-20.** Linear plot of observed head versus time in the observation borehole KFR101 together with sea level during the drilling of KFR102A. Sections 1 and 2 show a response while section 3 is unaffected.



**Figure A5-21.** Linear plot of observed head versus time in the observation borehole KFR102B during the drilling of KFR102A.

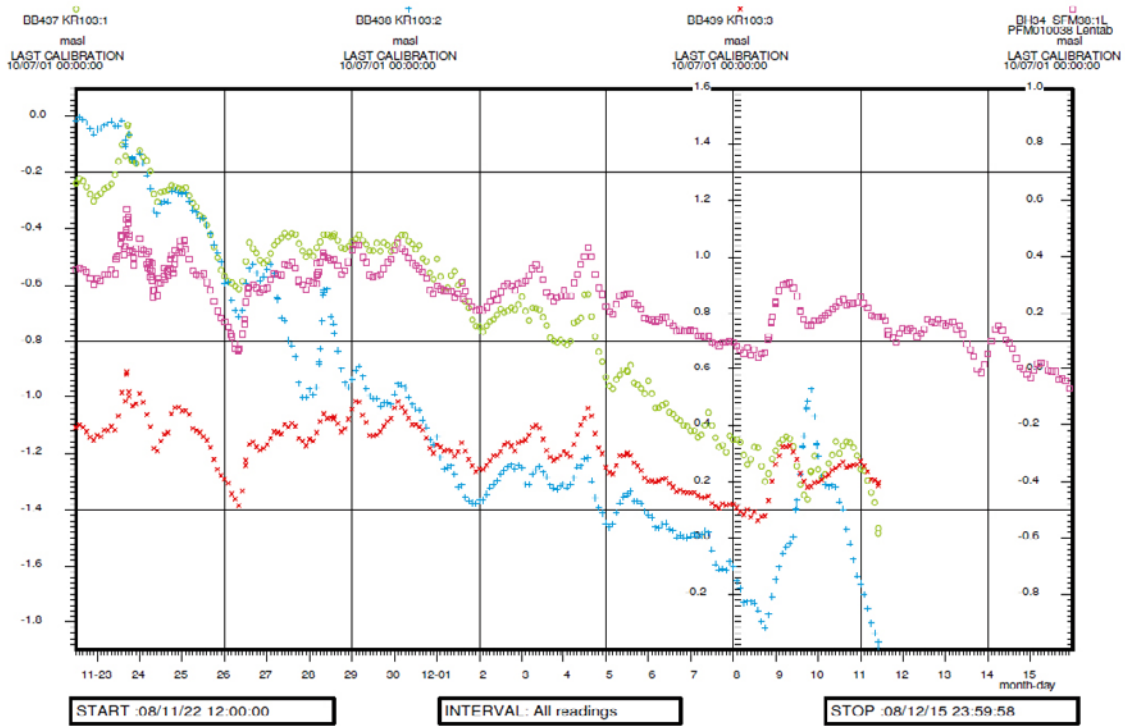


Figure A5-22. Linear plot of observed head versus time in the observation borehole KFR103 together with sea level during the drilling of KFR102A. Sections 1 and 2 show a response while section 3 is unaffected.

### A5.5 Core drilling of KFR105

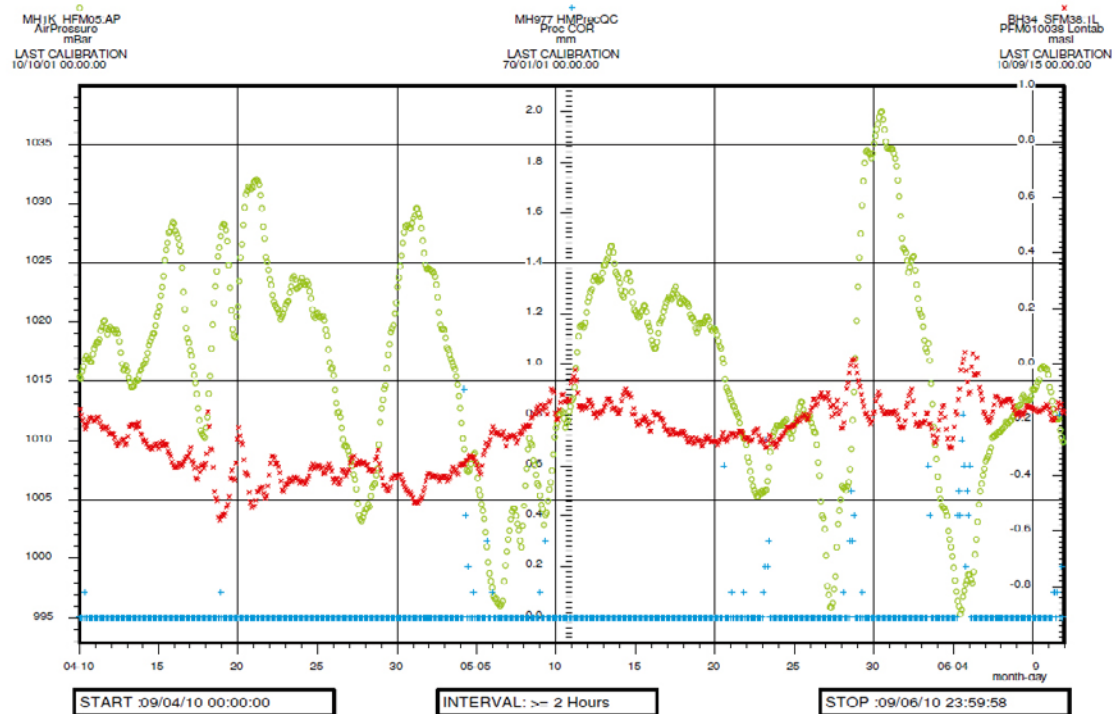
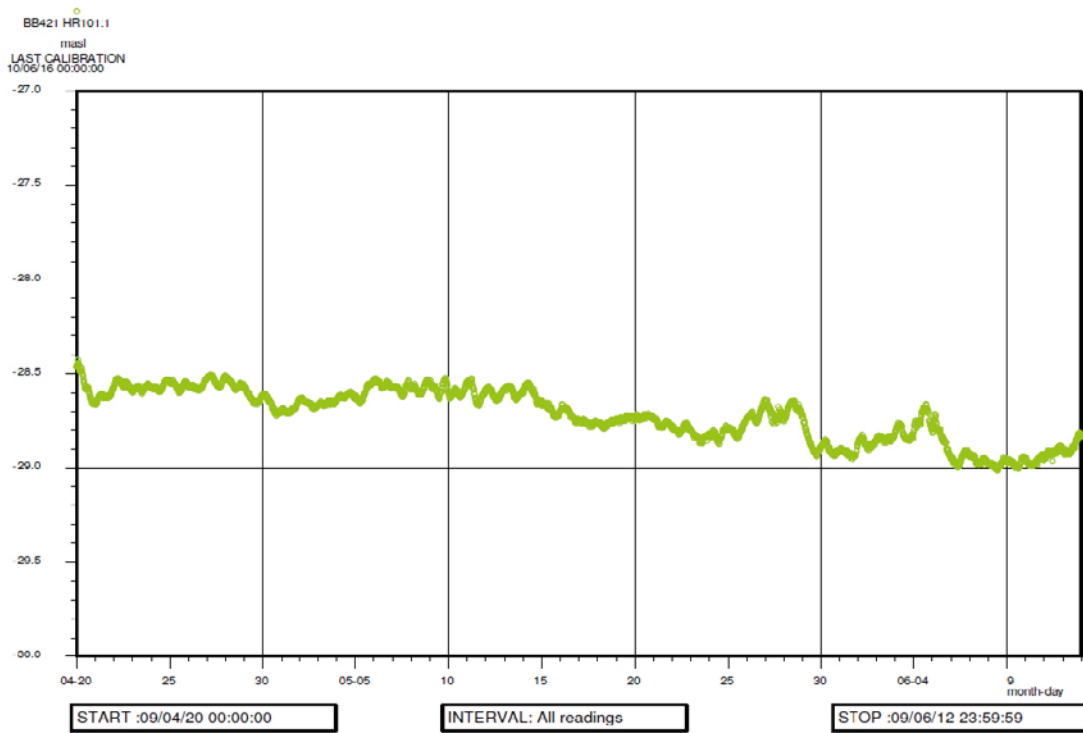
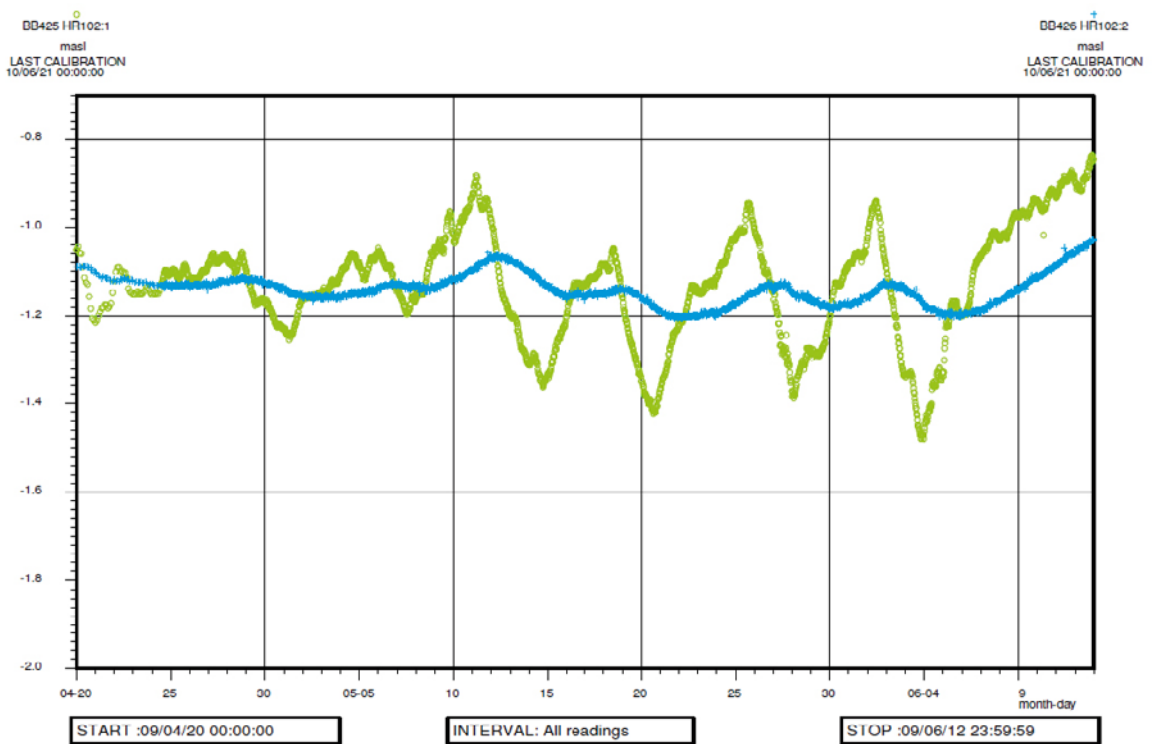


Figure A5-23. Registered air pressure (o), precipitation (+) and sea water level (x) at SFR during the drilling of KFR105. Each parameter has its own Y-scale.





**Figure A5-24.** Linear plot of observed head versus time in the observation borehole HFR101 during the drilling of KFR105.



**Figure A5-25.** Linear plot of observed head versus time in the observation borehole HFR102 during the drilling of KFR105.

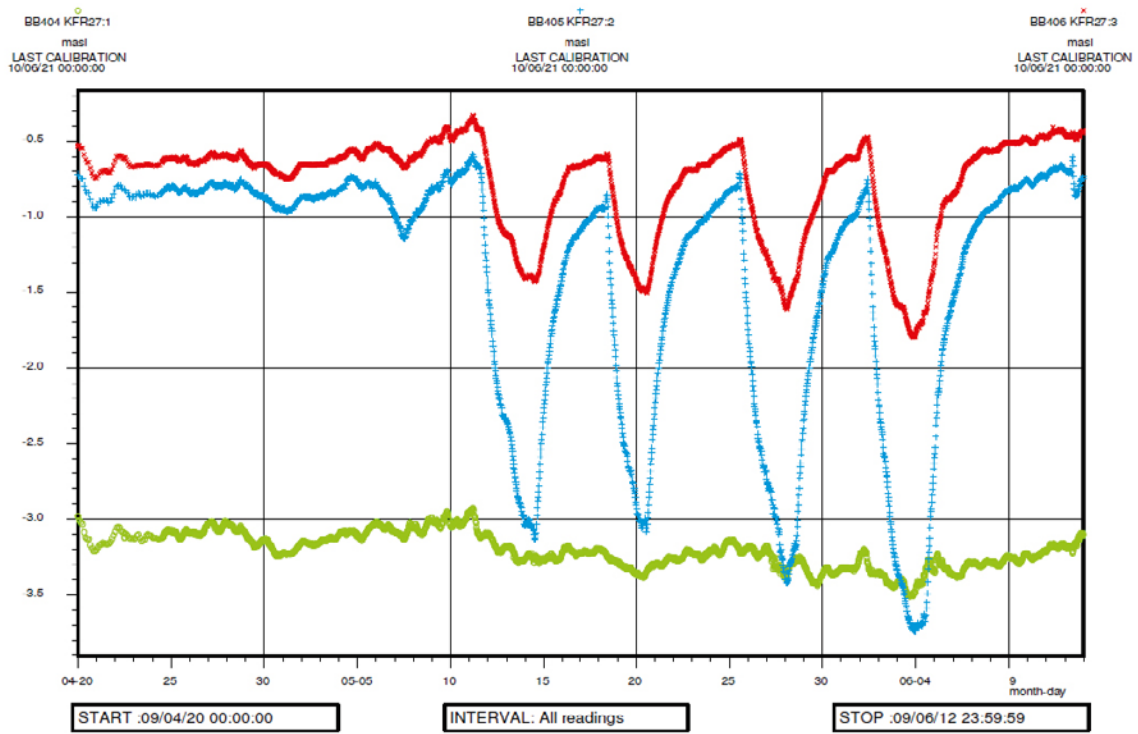


Figure A5-26. Linear plot of observed head versus time in the observation borehole KFR27 during the drilling of KFR105.

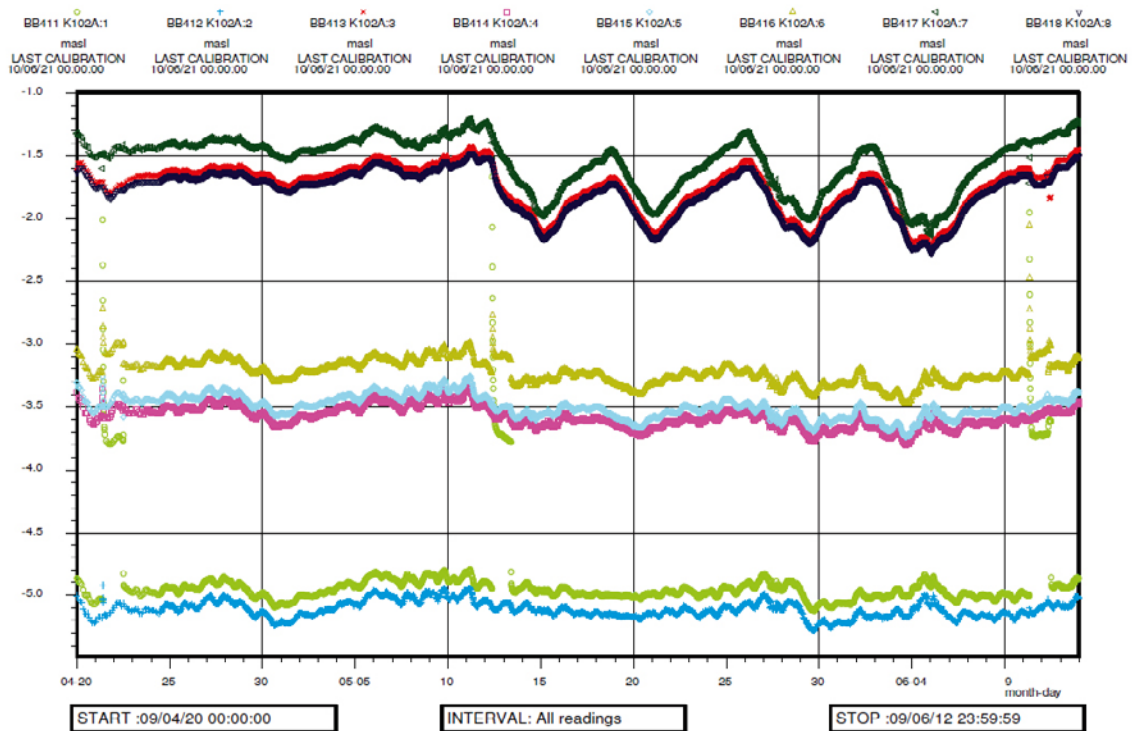
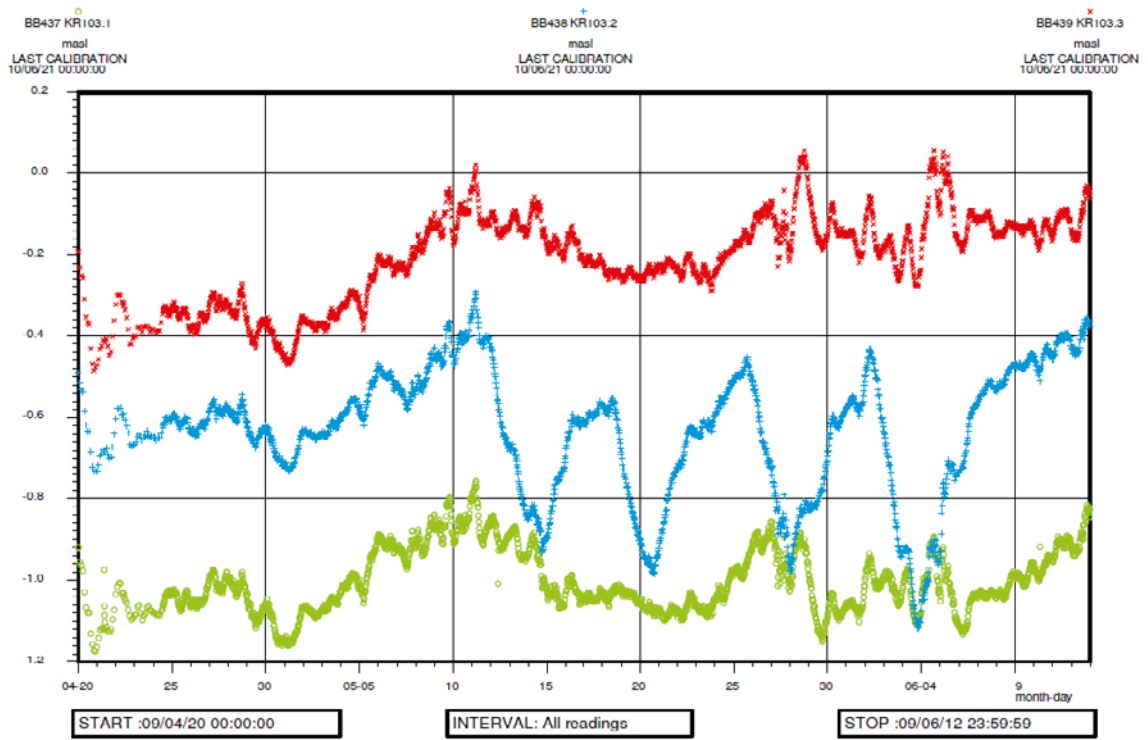
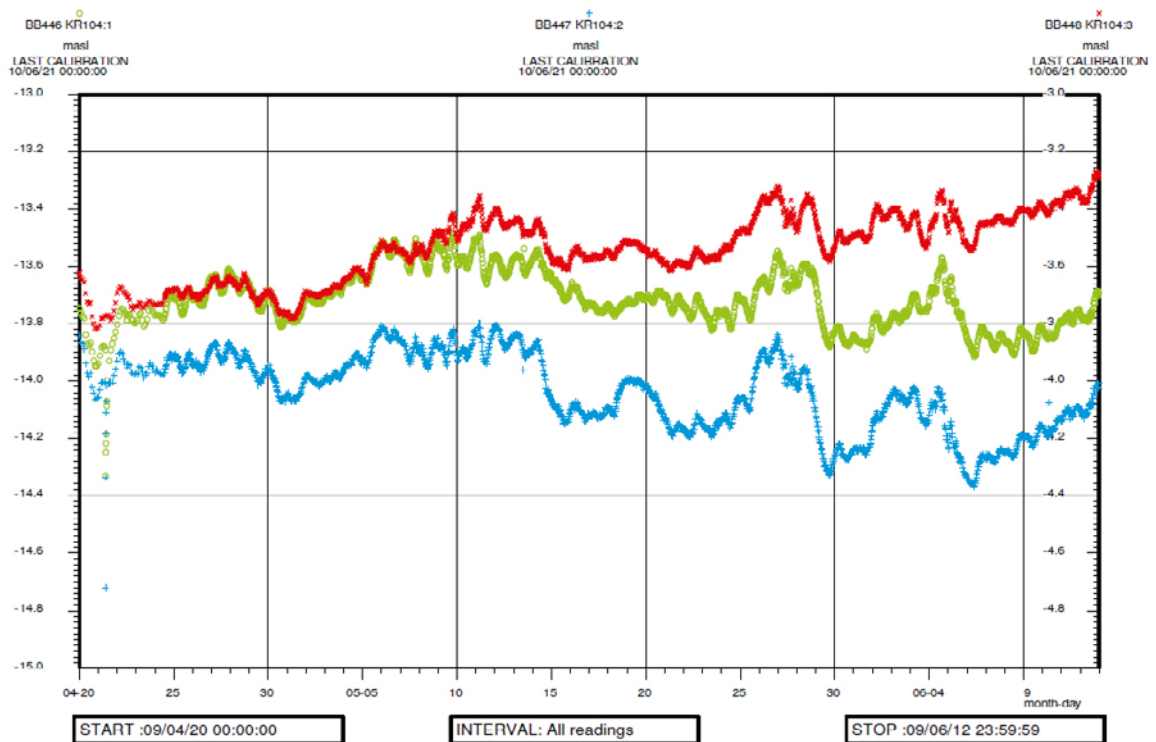


Figure A5-27. Linear plot of observed head versus time in the observation borehole KFR102A during the drilling of KFR105. Sections 3, 4, 5, 6, 7 and 8 are responding while sections 1 and 2 are unaffected.



**Figure A5-28.** Linear plot of observed head versus time in the observation borehole KFR103 during the drilling of KFR105. Sections 1 and 2 are responding while section 3 is unaffected.



**Figure A5-29.** Linear plot of observed head versus time in the observation borehole KFR104 during the drilling of KFR105.

## A5.6 Core drilling of KFR106

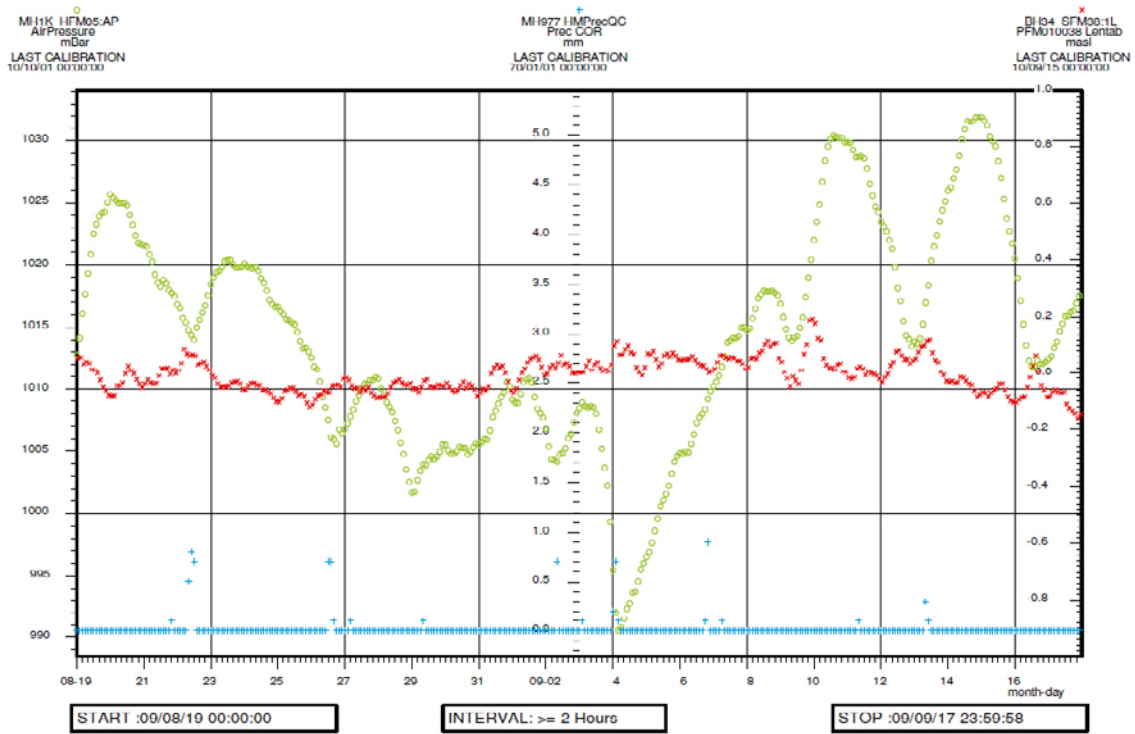


Figure A5-30. Registered air pressure (o), precipitation (+) and sea water level (x) at SFR during the drilling of KFR106. Each parameter has its own Y-scale.

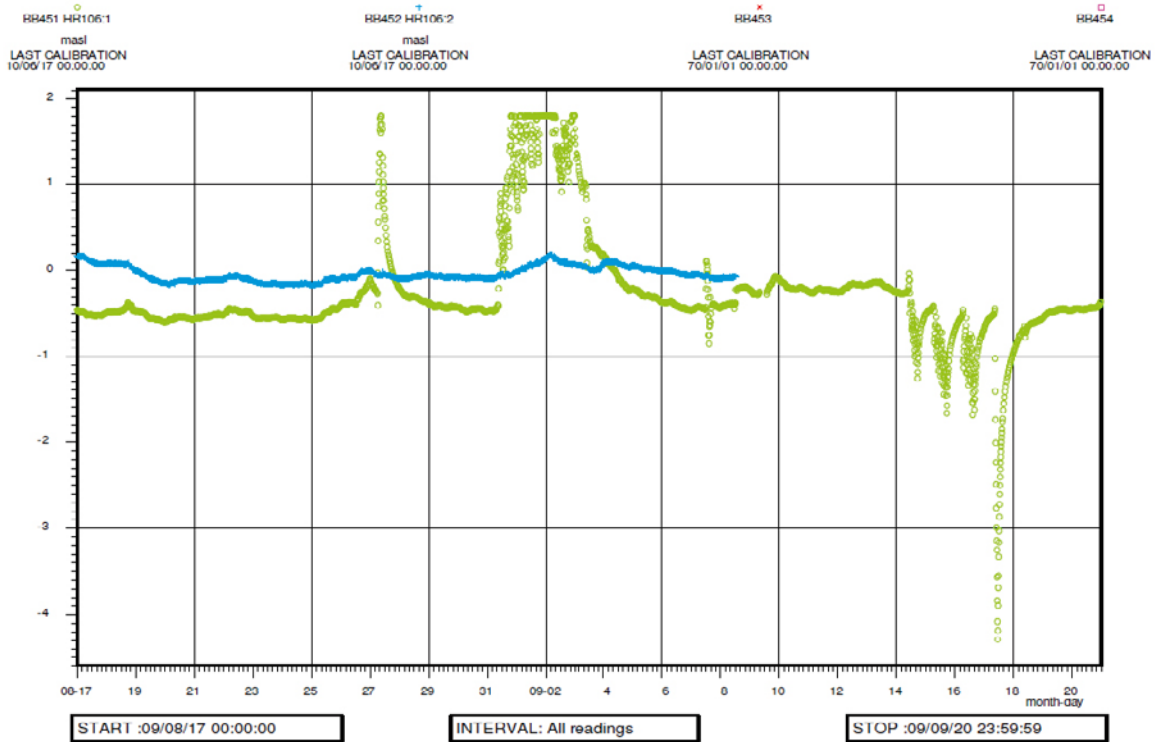
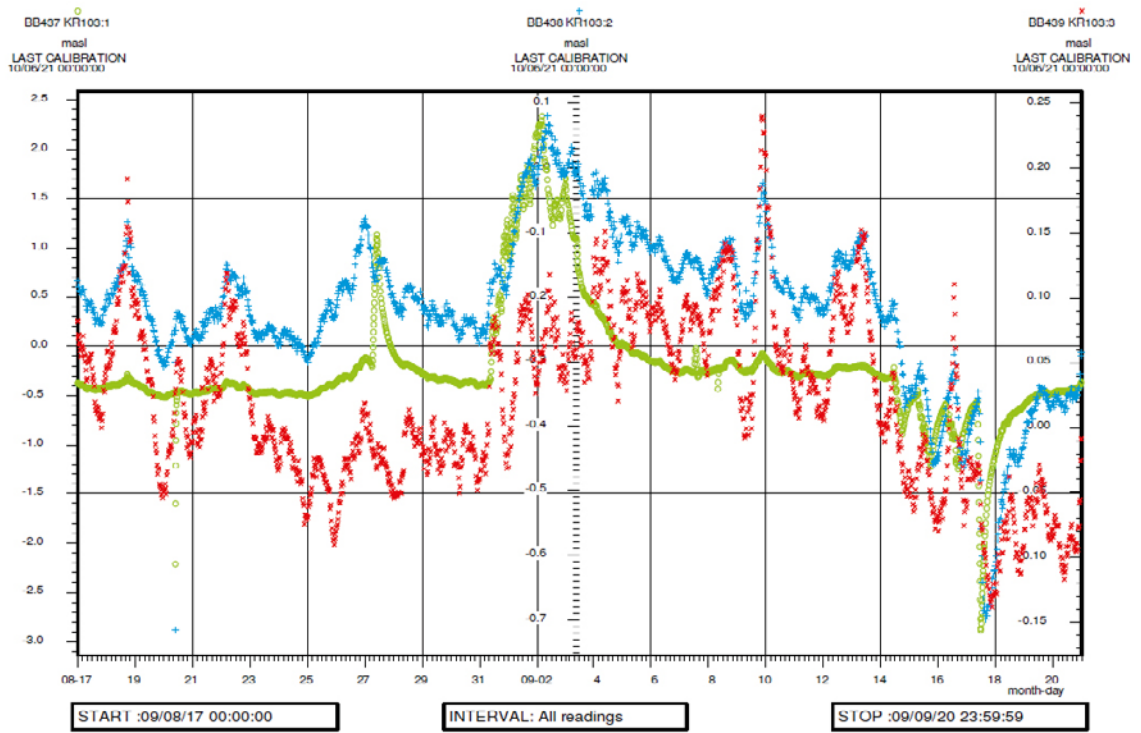


Figure A5-31. Linear plot of observed head versus time in the observation borehole HFR106 during the drilling of KFR106. The packers are removed from the borehole between the drilling period and the nitrogen lifting.



*Figure A5-32. Linear plot of observed head versus time in the observation borehole KFR103 during the drilling of KFR106.*